Norwegian University of Life Sciences
Faculty of Biosciences
Department of Plant Sciences

Philosophiae Doctor (PhD)
Thesis 2023:64

Evolution of flowering adaptations in temperate grasses

Evolusjon av blomstringstilpassingar i tempererte gras

Martin Paliocha

Evolution of flowering adaptations in temperate grasses

Evolusjon av blomstringstilpassingar i tempererte gras

Philosophiae Doctor (PhD) Thesis

Martin Paliocha

Norwegian University of Life Sciences
Faculty of Biosciences
Department of Plant Sciences

Ås
2023

Thesis 2023:64
ISSN 1894-6402
ISBN 978-82-575-2093-9

Gress!

~ Bård Tufte Johansen

Supervisors

Main Supervisor

Siri Fjellheim
Professor, dr. scient.
Faculty of Biosciences
Department of Plant Sciences
Norwegian University of Life Sciences

Co-Supervisors

Jill Christine Preston
Professor, PhD
College of Agriculture and Life Sciences
Department of Plant Biology
The University of Vermont, Burlington, USA

Torgeir Rhodén Hvidsten
Professor, PhD
Faculty of Chemistry,
Biotechnology and Food Science
Norwegian University of Life Sciences

Marian Schubert
Researcher, PhD
Faculty of Biosciences
Department of Plant Sciences
Norwegian University of Life Sciences

Kathrine Frey Frøslie
Associate Professor, PhD
Faculty of Chemistry,
Biotechnology and Food Science
Norwegian University of Life Sciences

Evaluation Committee

Committee Coordinator

Simen Rød Sandve
Professor, PhD
Faculty of Biosciences
Department of Animal and Aquacultural Sciences
Norwegian University of Life Sciences

External Evaluators

Angelica Lindlöf
Senior Lecturer, PhD
School of Bioscience
University of Skövde
Sweden

Kathleen Greenham
Assistant Professor, PhD
College of Biological Sciences
Department of Plant and Microbial Biology
University of Minnesota, Saint Paul, USA

Acknowledgements

Long time ago, in an empire far, far away a guy with a beard, no pants, and a terrible view on women infamously posited that the whole is greater than the sum of its parts. In case of my thesis, the exact opposite applies. This PhD project has been a collective effort in every thinkable aspect and the product of copious encounters with a lot of wonderful people and their manifold contributions throughout its unfolding. I am immensely thankful to all of you who consider themselves a part it. Yes–you, too!

I want to express my deepest gratitude to my main supervisor Siri Fjellheim. Though I regard you one of the brightest accomplishments of evolution, I am not sure if you fully comprehend the amount admiration I have for your capabilities as scientist, supervisor, teacher, psychologist, motivator, and friend. Thank you for sharing immeasurable amounts of enthusiasm, inspiration, and patience that made this endeavour possible. I am well aware that my maintenance has been quite demanding at times, and I do not take any of your support for granted–either it manifested in the form of your usual scientific excellence, dedicated leadership, effective pep-talks, or colossal amounts of tinned fish. I could never have foreseen any of this when our paths crossed fexactly one decade ago. Takk, *sjef*!

I am equally thankful to my brilliant team of co-supervisors with whom I had the joy to collaborate with. A huge Dankeschön to Marian for answering all sorts of unhinged questions at unspeakable times and being a steadfast supplier of oddly specific tools for the assembly of transcriptomes, furniture, or bicycles. It has been deeply comforting to share my inherent frustration over constantly falling behind every single project, side quest, or self-imposed deadline with you. Moreover, I want to thank my evo-devo mastermind Jill for the constant provision of excellent feedback on slightly less excellent bits of incomprehensible text, vague results, and confusing figures. It has been tremendously refreshing to work with you and I look genuinely forward to continue to expand the massive amount of fascinating knowledge you and Siri *et al.* have accumulated over the past years. Likewise, I am grateful to Torgeir for being at hand whenever my analytical skills reached their limit and encouraging me to move into increasingly more extreme niches within the of convoluted realm of bioinformatics, statistics, and headaches. Functional data analysis would not have been possible without the help and visualisation skills of my favourite statistician Kathrine. Thank you for being supportive and enthusiastic at all times. Your contagious excitement about our work has been an essential component of my scientific progress and mental well-being throughout the past years, although I may have appeared to do my very best to balance your and Siri's enthusiasm by being doubtful, self-deprecating, and negative most of the time.

No words can adequately express the depth of gratitude I owe to the past and present members of the Fjellheim research group. You are the reason I enjoy going to work and I

would not have been able to write a single line of code without your tremendous support. Special thanks to my work wife Camilla Lorange Lindberg. This PhD is also, in part, your accomplishment. Thanks to your emotional, scientific, and culinary support, along with your humor that rivals that of a six-year-old (and myself), the typical academic rollercoaster of a PhD has often felt more like frolicking in a field of daisies and other fructan accumulators. Thanks to Ane Charlotte Hjertaas for deep talks about the regulation of genes, emotions, and mortgages and to Felix Hernandez Nohr for assistance with the inflection of Latin verbs and introducing me to good blends of tea. Shoutout to Darshan and Sylvia for all the cumbersome labwork you did in connection with the paper we do not want to mention by its name, although it turned out almost as cool as you. I am also extremely thankful to the Department of Plant Sciences for providing a good working environment full of kind and quirky nerds. Yes, I mean you Anja, Tanya, Siv, Franz, Liv, Sondre, Signe, Øyvind, Crystal, Morten, Gry, Sara, Sheona, Min, Odd Arne, Sahameh, Rómulo, Mallik, Akhil, Anne Guri, Åshild *et al*. Special thanks Stefano Zanotto, who has been instrumental in destigmatising the consumption of plain sugar at times when our misery and despair were equally bottomless as void of our snack drawers. Thank you for dragging me out of the office to enjoy life at the beach or on the bicycle seat. Big thanks to Anna, Mara, Elena, Kari and Nini for excellent administrative support throughout this PhD, we are lucky to have you around! Also, I want to thank everyone who let me teach in all sorts of courses ranging from taxonomic botany to theoretical statistics. I am also grateful to my union Norsk Tjenestemannslag (NTL) for supporting both me and all other colleagues equally.

Gossiping about the ongoing events at NMBU would have lacked its charm without Kristina Severine Rudskjær Stenløkk. You are a great professional scientist and even greater friend–and your humour is equally refreshing as the beer you brew, albeit substantially darker. I also want to thank my favourite wandering herb almanac Line Lieblein Røsæg for sharing the frustrations of fruitless labwork and initiating long and disproportionate lunch breaks in the park. Speaking of lunch breaks: thanks to all the other people at CIGENE who still remember me for providing a second home, memorable Christmas parties, and awkward encounters in the restroom.

Huge thanks to my non-work friends and family for patiently tolerating and supporting me even at my worst, although most of you do not have the slightest idea about what I am working with. Just like me sometimes. Special thanks to Pernille for reminding me that the wonders of life extend beyond the obscurities of genes and grasses. Approaching and crossing the finish line would have certainly felt less meaningful without you.

Eg er attende,

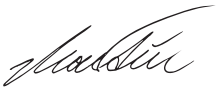

Arendal, 10th August MMXXIII

Contents

List of Papers

I Independent recruitment of *FRUITFULL*-like transcription factors in the convergent origins of vernalization-responsive grass flowering

Paliocha M, Schubert M, Preston JC & Fjellheim S

Molecular Phylogenetics and Evolution, 2023, 179: 107678.

doi:10.1016/j.ympev.2022.107678

II Major niche transitions in Pooideae correlate with variation in photoperiodic flowering and evolution of CCT domain genes

Fjellheim S, Young DA, **Paliocha M**, Johnsen SS, Schubert M & Preston JC

Journal of Experimental Botany, 2022, 73 (12): 4079–4093.

doi:10.1093/jxb/erac149

III Modulation of diurnal gene expression under contrasting photoperiods in the early-diverging Pooideae grass *Melica ciliata*

Paliocha M, Schubert M, Aunbakk NB, Hvidsten TR, Preston JC, Frøslie KF & Fjellheim S

Manuscript, 2023.

IV Comparative transcriptomics and evolution of photoperiod-mediated flowering in temperate grasses

Paliocha M, Schubert M, Frøslie KF, Preston JC, Hvidsten TR & Fjellheim S

Manuscript, 2023.

Abstract

Grasses (Poaceae) represent an unparalleled evolutionary success story and are particularly well adapted to the environmental challenges posed by temperate habitats. Crucial to their evolutionary success in temperate ecosystems is their ability to align phenological events coordinating growth and reproduction with predictable, seasonal variations in temperature and daylength. However, only a few subfamilies of grasses have spread to temperate niches, a biogeographic bias that renders grasses a good system for comparative analyses of physiological and phenological traits that facilitate adaptive radiations in temperate habitats. The work presented in this thesis identified and characterised molecular mechanisms that determine the rules for seasonal flowering, driving one of the most successful adaptive radiations among flowering plants.

Many temperate grasses synchronise flowering with favourable conditions within the relatively short growing season through a two-step process. First, prolonged cold exposure enhances their ability to flower, a process known as vernalisation. Transition from vegetative to reproductive growth is then further accelerated by long photoperiod in spring. This warrants the subsequent emergence inflorescences under suitable environmental conditions, timed to utilise a limited growing season. This development is controlled by interlocked genetic networks that integrate mechanisms for sensing cold, photoperiod, and timing.

In this doctoral project, I examined the evolutionary history of adaptations to temperate climates in various subfamilies of grasses and potential implications for shifts between biological niches from their original tropical to increasingly temperate habitats. The research was focused on mechanisms that control flowering in model and temperate cereal species to investigate whether these are conserved within and between Pooideae and other temperate subfamilies. I employed a wide range of methodological approaches, such as growth experiments, phylogenetic reconstruction, comparative transcriptomics, and functional data analysis for these purposes. The results indicate that a portion of the genetic basis for adaptation to long photoperiods evolved early within the Pooideae subfamily, and that vernalization responses have arisen multiple times in different subfamilies through a parallel evolutionary process. Nevertheless, it was demonstrated that many of the investigated genetic processes had undergone extensive lineage-specific evolution, and that minor changes in how these genes are regulated in response to external cues are sufficient to promote transitions between habitats with different demands for physiological and phenological adaptations such as floral onset, especially within the early-diverging Pooideae lineage Stipeae.

Samandrag

Gras (Poaceae) er ein evolusjonær suksesshistorie utan like og særleg godt tillempa dei miljømessige utfordringane tempererte habitat byr på. Utslagsgjevande for grasa sin evolusjonære framgang i tempererte økosystem er deira evne til å høve fenologiske hendingar som samordnar vekst og formeiring med føreseielege, årstidsbundne variasjonar i temperatur og daglengd. Likevel har berre nokre få underfamiliar av gras spreidd seg til tempererte nisjar, ei biogeografisk skeivfordeling som gjer grasfamilien til eit godt døme for samanliknande analyse av fysiologiske og fenologiske trekk som fremjar adaptive radiasjonar i tempererte habitat. Arbeidet lagt fram i denne avhandlinga identifiserte og karakteriserte molekylære mekanismar som fastset reglane for årstidsbunden blomstring, noko som driv ei av dei mest suksessrike adaptive radiasjonane blant blomsterplanter.

Mange tempererte planter samkøyrer blomstring med gunstige tilhøve i den høvesvis korte vekstsesongen gjennom ein to-stegsprosess. Fyrst aukar langvarig kulde evna til å blomstre i ein prosess som kallast vernalisering. Overgangen frå vegetativ til reproduktiv vekst vert ytterlegare framskunda av lang fotoperiode på våren. Dette tryggjar påfølgjande framvekst av blomsterstand under høvelege forhold, tidsnok til å nytte seg av ein tidsavgrensa vekstsesong. Denne utviklinga styrast av samanvovne genetiske nettverk som knyter saman mekanismar for sansing av kulde, fotoperiode og tidtaking.

I dette doktorgradsprosjektet undersøkte eg den evolusjonære historia til tilpassingar til tempererte klima i ulike underfamiliar av gras og mogelege fylgjer for skift mellom biologiske nisjar frå deira opphavleg tropiske til stadig meir tempererte habitat. Forskinga vart retta mot mekanismar som styrer blomstring i modell- og tempererte kornartar for å undersøkje om desse er konservert innanfor og mellom Pooideae og andre tempererte underfamiliar. Eg nytta eit breitt register av metodologiske tilnærmingar slik som vekstforsøk, fylogenetisk rekonstruksjon, samanliknande transkriptomikk og funksjonell data-analyse til desse føremål. Resultata peiker mot at ein del av det genetiske grunnlaget for tilpassing til lang fotoperiode utvikla seg tidleg i Pooideae-underfamilien og at vernaliseringsrespons har oppstått fleire gongar i ulike underfamiliar av gras gjennom ein parallell evolusjonær prosess. Likevel vart det vist at mange av dei undersøkte genetiske prosessane hadde gjennomgått omfattande linjespesifikk evolusjon og at små endringar i korleis desse gen regulerast av og i høve til ytre påverknadar er tilstrekkelege til å fremje overgang mellom habitat med ulike krav til fysiologiske og fenologiske tilpassingar slik som blomstringstid, særleg i den tidlegskilde Pooideae-linja Stipeae.

Synopsis

1.1 Life at high latitudes

Plants are not particularly gifted in moving. A direct implication of this simple fact is that plants are unable to escape unfavourable conditions by changing location. This limitation inflicts strong selective pressure on traits warranting appropriate environmental adaptation. Plants have consequently evolved a vast arsenal of mechanisms allowing them to anticipate, endure or escape environmental conditions unfavourable to survival and reproduction (Bradshaw, 1965; King & Heide, 2009; Preston & Sandve, 2013). In temperate zones, the occurrence of seasons creates a complex environment for flowering plants. The defining feature of temperate seasons is the periodic fluctuation of temperature and daylength throughout the year. Alternating seasons limit the timeframe for plant growth and reproduction to a relatively short growing period during spring and summer. Restricted opportunities for individual survival and fecundity confound evolutionary success in these regions and require the alignment of developmental events with seasons (Junttila, 1996; Amasino, 2010; Körner, 2016).

Flowering time is a critical life-history trait, as it marks the transition from vegetative to reproductive growth and is essential for seed set, dispersal, gene flow, and ultimately, evolutionary success (Andrés & Coupland, 2012). Early flowering may expose reproductive tissue to potentially harmful cold spells during early spring, whereas late flowering prevents seed set before the arrival of winter (Gaudinier & Blackman, 2020). Timely, but flexible onset of reproduction is therefore essential in seasonal environments (Murfet, 1977; Bäurle & Dean, 2006). Posing an arduous obstacle for plant life, winters are commonly avoided through cessation and subsequent onset of vegetative and reproductive growth interposed by a period of dormancy when conditions are at its harshest (Junttila, 1996). Perennial and winter-annual plants coordinate this development by sensing changes in their environment, like periodic fluctuations in temperature and photoperiod, and their coincidence with endogenous signals (Bernier, 1988; Poethig, 1990). Fine-tuning of flowering time allows temperate plants to capitalise on limited growing periods and ensure reproductive success despite the challenges imposed by the seasonal constraints of their temperate habitats.

1.2 Temperate grasses

The evolutionary success of grasses (Poaceae) is difficult to understate. Grasses are one of the largest angiosperm families with over eleven thousand recognised species (Gallaher *et al.*, 2022; Soreng *et al.*, 2022). Like most other angiosperms, grasses evolved in the tropics (Bremer, 2002; Bouchenak-Khelladi *et al.*, 2010). Extant grasses, however, are found in almost every terrestrial habitat and grasslands cover almost a quarter of the world's land area (Shantz, 1954; Strömberg, 2011), demonstrating their exceptional capacity to adapt to a vast range of environments. Global grass distribution ranges from the rainforests and savannas of the equatorial tropics to the harsh environments of the Arctic and Antarctic, occupying habitats from coastal marshes to mountain ecosystems (Strömberg, 2011). Contrary to many other cosmopolitan vascular plant lineages, grass diversity is not greatest in their tropical areas of origin. Instead, species richness in Poaceae follows a shallow poleward cline with peaks at mid- and high latitudes and is positively associated with continentality and topographic heterogeneity (Tzvelev, 1989; Kreft & Jetz, 2007; Visser *et al.*, 2014).

Grasses are divided into two major lineages, named BOP and PACMAD (Fig. 1A), according to the subfamilies they harbour (Cotton *et al.*, 2015; Soreng *et al.*, 2015, 2017). Notable examples of PACMAD grasses are crops of tropical and subtropical origin such as maize (*Zea mays*), sorghum (*Sorghum bicolor*), and millets (several genera and species). Famous BOP grasses include rice (*Oryza sativa*), bamboos (Bambusoideae), and many temperate cereals and forages such as wheat (*Triticum aestivum*), barley (*Hordeum vulgare*), rye (Secale cereale), oat (*Avena sativa*), timothy (*Phleum pratense*), fescues and ryegrasses (*Festuca* and *Lolium*). Pooideae are the most diverse grass subfamily with ~4,120 recognised species organised in 15 tribes (Soreng *et al.*, 2022). Pooideae are further divided into the agronomically important, monophyletic core-Pooideae and numerous early-diverging lineages (Davis & Soreng, 1993; Schubert *et al.*, 2019b; Zhang *et al.*, 2022). Almost all temperate cereals are confined to core-Pooideae, while the model species *Brachypodium distachyon* is the most prominent member of early-diverging lineages (Soreng *et al.*, 2022).

Contradicting their ostensible diversity and evolutionary success, only few grass lineages have significantly dispersed into temperate areas. Most notably, Pooideae are successful in cool, seasonal habitats of the northern hemisphere where they constitute most the grass

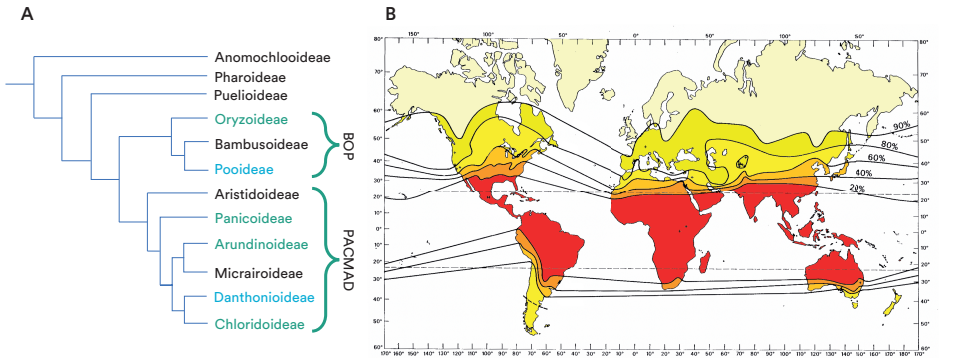

Figure 1 | A) Simplified phylogeny of the Poaceae describing the relationship of different grass subfamilies according to Soreng *et al.* (2017). Coloured clades were targeted in this thesis, blue clades specify subfamilies commonly considered temperate. **B)** Latitudinal diversity gradient of Pooideae represented as the relative percentage of Pooideae taxa within the overall grass flora. Regions depicted in red denote a low proportion of Pooideae; yellow regions indicate a high proportion of Pooideae. Redrawn and modified from Hartley (1973).

flora (Fig. 1B; Hartley, 1973; Cross, 1980), whereas southern temperate grass assemblages are characterised by the subfamily Danthonioideae and austral Pooideae species (Linder *et al.*, 2010; Visser *et al.*, 2014). Lineage-specific climatic specialisations are also reported from other grass subfamilies such as Chloridoideae and Aristidoideae, which are predominantly found in arid environments (Edwards & Smith, 2010; Visser *et al.*, 2012, 2014). These biogeographic patterns imply that successful adaptation to the peculiarities of temperate climates is confined to specific clades, making grasses an interesting system for the comparative study of physiological and developmental innovations that provide fitness advantages and drive plant radiations towards peak altitudes and latitudes on global scales.

1.3 Dual induction of flowering

One of the pivotal traits rendering grasses particularly successful in temperate habitats is their ability to couple flowering to temperature and photoperiod, a mechanism ensuring the adequate timing of reproductive onset when conditions are most favourable (Heide, 1994; King & Heide, 2009). Due to their socio-economic, agricultural, and ecological significance in temperate climates, this process is particularly well-studied in Pooideae (Heide, 1994). In many temperate grasses, attainment of floral competency is promoted by long-lasting cold, a process called vernalisation (Purvis, 1934; Chouard, 1960). Vegetative to reproductive phase change, culm elongation, and the development of inflorescences is then further

promoted by long days (Heide, 1994). This two-stage flowering induction ensures that flowering occurs early enough to culminate in successful seed set before the end of the growing season while simultaneously preventing the emergence of sensitive floral tissue during unpredictable conditions in early spring (Fjellheim *et al.*, 2014). Endogenous and environmental signals are commonly sensed in leaves and converge at the floral integrator *FLOWERING LOCUS T* (*FT*), which confers the florigen signal (Evans, 1971; Turck *et al.*, 2008; Amasino, 2010; Pin & Nilsson, 2012). Moving through the phloem, FT is then translocated to the shoot apex where it ultimately alters the developmental fate of the shoot apical meristem (SAM) from vegetative to reproductive (Zeevaart, 2008). Dual induction of flowering prompted by vernalisation and photoperiod involves considerable crosstalk between the light- and temperature-sensitive modules of the floral pathway (Lindlöf, 2010), providing great flexibility to the timing of reproductive onset (Fig. 2). Vernalisation and photoperiod can also act interchangeably (Woods *et al.*, 2019), thus providing secondary flowering mechanisms that can be relied upon under more ambiguous environmental circumstances.

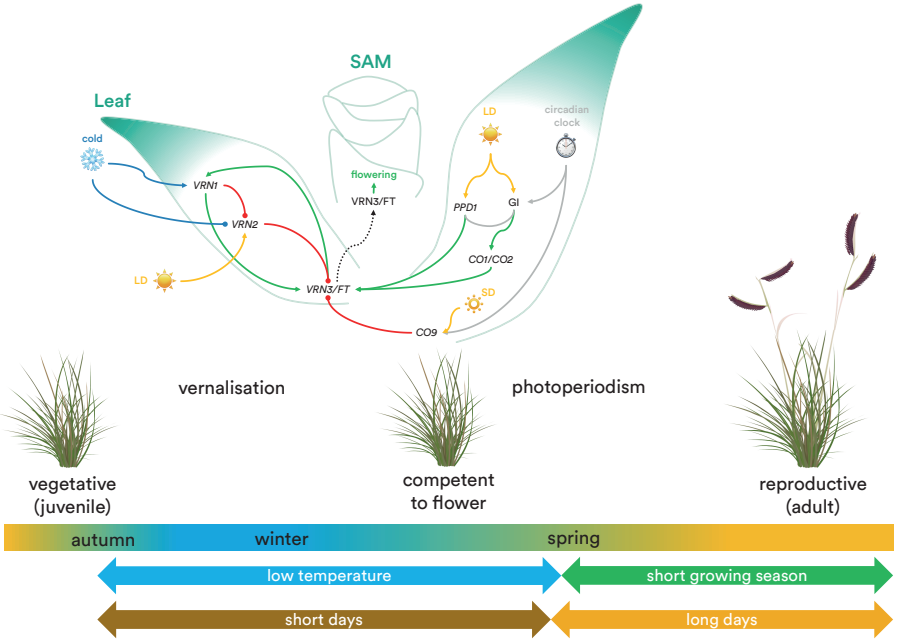

Figure 2 | Consensus model of dual flowering induction in temperate grasses (Pooideae) by vernalisation and photoperiod. Simplified flowering pathway according to Bouché *et al.* (2017) and Preston & Fjellheim (2020).

1.3.1 Vernalisation response

The phenomenon of induced or significantly accelerated flowering by long-lasting cold is called vernalisation response (McKinney, 1940; Chouard, 1960). Due to its agricultural significance, vernalisation has been extensively studied in cereal crops and forage grasses (Gaßner, 1918; Purvis, 1934), many of which belong to the temperate subfamily Pooideae (Ream *et al.*, 2012). The consensus model for grass vernalisation outlined in winter wheat, barley, and *B. distachyon* revolves around the interaction and mutual feedback of three central genes called *VERNALIZATION 1–3* (Trevaskis *et al.*, 2007; Dennis & Peacock, 2009; Greenup *et al.*, 2009; Bouché *et al.*, 2017). Prior to the onset of winter, expression of the *FT*-orthologue *VERNALIZATION 3* (*VRN3*) is repressed by the CCT domain-containing transcription factor VRN2, which prevents premature flowering during autumnal growth (Trevaskis *et al.*, 2006; Hemming *et al.*, 2008). Low temperatures induce histone modifications at the *VRN1* locus that gradually increase its transcription during winter (Distelfeld *et al.*, 2009; Oliver *et al.*, 2009, 2013; Deng *et al.*, 2015). *VRN1* encodes a *FRUITFULL*-like (*FUL*-like) transcription factor that functions as a repressor of *VRN2* (Deng *et al.*, 2015), thereby relieving the repression of *FT*-like *VRN3* that ultimately establishes reproductive competence at the SAM. Inflorescence initiation and emergence is then further enhanced by long photoperiods in spring through *PHOTOPERIOD 1* (*PPD1*), a pseudo-response regulator promoting the expression of grass florigen *VRN3* (Turner *et al.*, 2005; Hemming *et al.*, 2008; Sasani *et al.*, 2009).

Vernalisation-cued flowering is common among Pooideae and believed to be one of the major traits enabling their radiation in temperate zones (Preston & Kellogg, 2008; Preston & Sandve, 2013; McKeown *et al.*, 2016; Zhong *et al.*, 2018). Phylogenetic reconstruction of vernalisation responsiveness in temperate grasses indicates that acquisition of *VRN1*-mediated flowering happened early in the evolutionary trajectory of Pooideae, which originated approximately 61–77 Mya (McKeown *et al.*, 2016; Schubert *et al.*, 2019b). This implies that ancestral Pooideae lineages had already developed some level of adaptation to temperate seasonality prior to the global cooling following the Paleocene–Eocene thermal maximum (~55.5 Mya; Bowen *et al.*, 2015; Schubert *et al.*, 2019b). Further diversification and range expansion of Pooideae during the consequent intensification of global seasonality and spread of temperate biomes suggests that vernalisation responsiveness provided a significant

adaptive advantage in colonising these novel habitats (McKeown *et al.*, 2016; Schubert *et al.*, 2019b; Preston & Fjellheim, 2020). Multiple rounds of whole-genome and tandem duplications have contributed to the expansion *FUL*-like transcription factors in grasses (Gaut, 2002; Preston & Kellogg, 2006; McKain *et al.*, 2016; Zhang *et al.*, 2022). Apart from *VRN1* (*FUL1*), its closest paralogue *FUL2*, has also been reported to undergo upregulation by cold, indicating an innate propensity of cold-induced transcription of these important developmental regulators (Gocal *et al.*, 2001; Petersen *et al.*, 2004; Ergon *et al.*, 2013; Li *et al.*, 2016). Paralogues of *VRN1* (collectively referred to as *FUL*-like) are redundantly involved in flower development and meristem identity in numerous grass species, suggesting of partial functional conservation (Preston & Kellogg, 2006, 2007, 2008; Preston *et al.*, 2009; Kinjo *et al.*, 2012; Li *et al.*, 2016, 2019; McKeown *et al.*, 2016; Yang *et al.*, 2021; Zhang *et al.*, 2022). This raises the hypothesis of whether expansion of other grass lineages found in temperate zones (like Danthonioideae) was facilitated by similar phenological adaptations, possibly involving co-option of different *FUL*-like paralogues into the vernalisation pathway.

1.3.2 Photoperiodic flowering

Temperate grass flowering is, in general, induced or accelerated by long days heralding the onset of spring (Heide, 1994; Colasanti & Coneva, 2009). Essential to the photoperiodic flowering pathway in temperate cereals are the CCT domain genes *PPD1*, *CONSTANS 1* (*CO1*), *CO2*, CO9 and its paralogue *VRN2*, which induce or repress transcription of *VRN3*/*FT* when daylength exceeds or falls below a certain threshold (Laurie *et al.*, 1995; Turner *et al.*, 2005; Kikuchi *et al.*, 2011; Shaw *et al.*, 2012). Expression of many CCT domain genes follows distinct diurnal rhythms, indicating their central role in linking the photoperiodic flowering pathway to the circadian clock (Campoli & von Korff, 2014; Fjellheim *et al.*, 2014). The circadian clock is the internal time-keeping system responsible for the maintenance of rhythmic gene expression and a key component of the photoperiodic flowering pathway as it generates endogenous signals imperative to the integration of exogenous light cues (Song *et al.*, 2015).

Due to its involvement in many facets of plant physiology and development, the core circadian oscillator is subject strong selective pressure for optimal timing and therefore remarkably conserved among plants (Michael *et al.*, 2003; Dodd *et al.*, 2005; Greenham &

McClung, 2015). Consequently, much of the circadian clock model outlined in *Arabidopsis thaliana* is transferable to grasses (Cao *et al.*, 2021). The circadian clock is a sophisticated gene network consisting of interlocking regulatory loops that reach peak activity during different periods of the day (Hsu & Harmer, 2014). Stable diurnal rhythmicity of circadian clock components is achieved through mutual feedback and environmental entrainment (Millar, 2004; Harmer, 2009). Starting at dusk, *CIRCADIAN CLOCK ASSOCIATED 1* (*CCA1*) and *LATE ELONGATED HYPOCOTYL* (*LHY*) are transcriptionally activated. LHY and CCA1 interact and sequentially activate *PSEUDO-RESPONSE REGULATOR 9* (*PRR9*), *PRR7*, and *PRR5* which jointly repress *LHY* and *CCA1* alongside *REVEILLE 8* (*RVE8*). This, in turn, triggers the activity of evening-phased genes such as *TIMING OF CAB EXPRESSION 1* (*TOC1*), *LUX ARRYTHMO* (*LUX*), and *EARLY FLOWERING 4* (*ELF4*), which are initially repressed by LHY and CCA1 (Hsu & Harmer, 2014). Together with evening-phased ELF3, LUX and ELF4 collectively form the evening complex (EC) that inhibits the transcription of *PRR7* and *PRR9*. Furthermore, TOC1 also represses *PRR7* and *PRR9* as well as *LHY* and *CCA1*. This link leads to reciprocal regulation between the morning loop and evening complex (EC) genes results in diurnal expression of clock output genes, such as *GIGANTEA* (*GI*). GI acts a critical node linking multiple pathways to clock oscillations through protein-level interactions, including CCT domain genes mediating photoperiodic flowering and the circadian clock itself (Bendix *et al.*, 2015; Li & Xu, 2017).

Oscillations generated by the plant circadian clock modulate sensitivity to photic conditions, which is important for the recognition of different daylengths (Johansson & Staiger, 2014). Light-induced initiation of flowering in photoperiod-sensitive plants requires the coincidence of endogenous circadian clock signals and specific daylength configurations (Imaizumi & Kay, 2006; Song *et al.*, 2015). These light signals are perceived by photoreceptors such as PHYTOCHROME (PHY) A–C, and CRYPTOCHROMEs (CRYs) that undergo reversible conversions between non-functional and functional forms in response to the absorption of specific wavelengths (Lin, 2000; Mathews, 2010; Gao *et al.*, 2019). The photoreceptor *PHYC* is central in the context of daylength-dependent grass flowering, as it acts as a flowering promoter under inductive LDs in temperate grasses like *B. distachyon* and barley (Nishida *et al.*, 2013; Chen *et al.*, 2014; Woods *et al.*, 2014; Raissig & Woods, 2022). The ratio of red (R) and far-red light (FR) is responsible for the conversion of phytochromes between their biologically active (PHY_{FR}) and inactive (PHY_{R}) states (Quail, 2002). Phyto-

chromes are activated upon absorption of red light, which initiates a signalling cascade leading to altered gene expression through protein interactions with active PHY_{FR} molecules, often entailing interactions between different activated PHYs (Quail, 2002). Under FR-rich conditions like dusk and night, influence of active PHYs is reduced through gradual conversion into their PHY_R state (Quail, 2002). Phytochrome changeover thus provides vital information about the relative lengths of day and night (Borthwick & Hendricks, 1960). In *B. distachyon*, $PHYC_{FR}$ interacts with the EC component ELF3 (Gao *et al.*, 2019; Bouché *et al.*, 2022; Woods *et al.*, 2023). Hence, reversion rates of activated $PHYC_{FR}$ are suggested to play an important role in sensing night length thus linking the perception of light to signals produced by the circadian clock (Gao *et al.*, 2019). Information about relative day- and night-length is also communicated directly into the photoperiodic flowering pathway by PHYC-mediated transcription of *PPD1*, *CO*-like, and *VRN3/FT* (Woods *et al.*, 2014; Raissig & Woods, 2022).

Comparative analyses between LD- and SD-grasses have revealed that species-specific diurnal expression of CCT domain genes involved in photoperiodic flowering is further determined by their interaction at the protein level (Preston & Fjellheim, 2020). For instance, wheat VRN2 is a floral repressor that suppresses transcription of *VRN3/FT* through its interaction with NUCLEAR FACTOR-Y (NF-Y) proteins. However, flower-promoting CO2 competes with VRN2 in the formation of NF-Y complexes, thereby counteracting its repressive function and introducing flexibility to the regulation of flowering in wheat (Li *et al.*, 2011). In the SD-plant rice, this relationship is reversed. There, the rice orthologue of VRN2 called GRAIN NUMBER, PLANT HEIGHT, AND HEADING DATE 7 (GHD7) alters the role of the rice CO-orthologue HD1a under LDs from promotion to repression of flowering, thereby delaying reproduction under non-inductive photoperiods (Okada et al., 2017; Herath, 2019). These interactions are further modified by PHYs and GI, adding yet another layer of light- and circadian clock-interference to the photoperiodic flowering pathway (Hong *et al.*, 2010; Itoh *et al.*, 2010; Woods *et al.*, 2014; Zheng *et al.*, 2019). Another interesting CCT gene component of the photoperiodic flowering pathway in barley is the *VRN2* paralogue *CO9*. Both *VRN2* and *CO9* are floral repressors, however expression of *VRN2* is promoted LDs whereas its sister *CO9* is activated by SDs (Kikuchi *et al.*, 2011; Monteagudo *et al.*, 2019). Expression of CCT domain genes relative to daylength is thus instrumental in orchestrating the photoperiodic flowering response. It remains to be

tested whether the suppression of flowering under SDs mediated by *CO9* is a barley-specific outcome of domestication or a broader phenomenon with implications for the adaptive radiation of Pooideae in areas where suppression of SD flowering is beneficial.

Expansion and regulatory diversification of CCT domain genes has played a crucial role in the domestication of both SD crops like sorghum, maize, rice, and LD cereals such as barley and wheat in non-native regions (Cockram *et al.*, 2007, 2012; Higgins *et al.*, 2010), highlighting their importance in adaptation to habitats with different photoperiodic flowering requirements. Epistatic interactions between CCT genes and their interference with the circadian clock supports the coordination of flowering time with environmental cues on varying timescales, thereby contributing to the adaptability and success of grasses in a wide range of challenging habitats.

1.4 Niche transitions and adaptive grass evolution

The evolution of grasses is intimately tied to habitat transitions (Preston & Fjellheim, 2020). Grasses likely originated in the understories or margins of tropical Gondwanan forests during the middle or Late Cretaceous (Bouchenak-Khelladi *et al.*, 2010; Christin *et al.*, 2014; Gallaher *et al.*, 2019; Schubert *et al.*, 2019b). During subsequent global cooling throughout the Paleogene, numerous grass lineages appeared in emerging temperate niches (Schubert *et al.*, 2019b; Gallaher *et al.*, 2022). Ancestral Pooideae likely evolved in a cold microhabitat with episodic frost in nascent Eurasian orogenies ~61–77 Mya within an otherwise warm, aseasonal global climate (Schubert *et al.*, 2019b). Following the emergence of Pooideae, global temperatures plummeted even further and dropped abruptly during the Eocene–Oligocene transition, a drastic event augmenting seasonality on global scales (Veizer *et al.*, 2000; Zachos *et al.*, 2001; Schubert *et al.*, 2019b). Temperate biome expansion during the remainder of the Cenozoic gradually favoured the diversification and range expansion of grasses, establishing them as one of the dominant life forms at from middle to high latitudes (Strömberg, 2011; Schubert *et al.*, 2019b).

Low temperatures are the most immediate stress encountered in contact with temperate climates (Körner, 2016). The remarkable resilience of Pooideae grasses to long- and short-term cold is attributed to the successive attainment of numerous physiological and developmental traits conferring stress endurance and avoidance (Zhong *et al.*, 2018; Preston

& Fjellheim, 2020; Schubert *et al.*, 2020). Comparative evolutionary studies have identified substantial expansions of gene families linked to low-temperature adaptations, such as tolerance to freezing, dehydration, and cold acclimation (Sandve & Fjellheim, 2010; Li *et al.*, 2012; Vigeland *et al.*, 2013; Schubert *et al.*, 2019a). Molecular dating indicates that these gene family expansions and functional changes enhancing cold tolerance align with pivotal paleoclimatic events during Pooideae evolution, which in turn coincide with sub-familial radiations within core- and early-diverging lineages (Schubert *et al.*, 2019b, 2020; Preston & Fjellheim, 2020; Zhang *et al.*, 2022). Similar trends of coinciding adaptive trait evolution and radiation are observed in the evolution of life-cycle adaptations, like the growth rates and life-history strategies (Lindberg *et al.*, 2020), and modifications within the flowering pathway (Woods *et al.*, 2016; McKeown *et al.*, 2016, 2017). For instance, ancestral reconstruction of vernalisation responsiveness across Pooideae suggests an early origin of cold-promoted flowering through a conserved pathway centred around *VRN1* and *VRN3* (McKeown *et al.*, 2016). This is regarded a major step in the adaptive evolution of Pooideae that proved broader benefits during the subsequent increase in global seasonality and facilitated their rapid poleward expansion (McKeown *et al.*, 2016; Preston & Fjellheim, 2020). At the intersection of the vernalisation and photoperiodic flowering pathways, a regulatory novelty involving the cold-repression of *VRN2* by *VRN1* is exclusive to the core-Pooideae, although their individual roles seem to be conserved across the entire subfamily (Woods *et al.*, 2016). This implies that autumnal repression of flowering triggered by LDs is an ancient adaptive strategy that fostered a more recent diversification through the fine-tuning of interactions among its molecular constituents (Preston & Fjellheim, 2020).

1.5 Objectives

The principal objective of the research presented in this thesis was to investigate the molecular and evolutionary mechanisms underpinning seasonal adaptations in response to vernalisation (Paper I) and photoperiod (Paper II–IV) in various temperate grass lineages. Paper I, II, & IV specifically focused on flowering time, while we addressed broader aspects of photoperiod adaptations in Paper III from a chronobiological perspective.

In Paper I, we investigated if vernalisation responsiveness is present in temperate grass lineages beyond Pooideae and examine whether the molecular machinery behind cold-

induced flowering is conserved across grasses or evolved independently in different subfamilies through lineage-specific co-option of paralogous transcription factors.

In PAPER II, we reconstructed the evolutionary history of photoperiodic flowering responses in Pooideae grasses and tested the hypothesis that flowering in response to LDs originated early in the evolutionary history of Pooideae and aided their transition from ancestral tropical to temperate habitats. Additionally, we studied diurnal expression of central photoperiod genes in species with opposite photoperiodic flowering responses to elucidate the molecular mechanisms underlying transitions between LD- and SD-flowering.

In PAPER III, the aim was to study temporal organisation of diurnal gene expression under contrasting photoperiods and conduct an exploratory analysis of the global transcriptomic response to daylength changes in the early-diverging Pooideae grass *Melica ciliata* using functional data analysis.

In PAPER IV, we compared the diurnal transcriptomes of two closely related temperate grasses identified as SD- and LD-responsive in PAPER II. Using the same statistical framework as in PAPER III, we compare the systemic responses to LDs and SDs in the Stipeae species *Nassella pubiflora* and *Oloptum miliaceum* to elucidate the genetic basis of reversion of photoperiodic flowering strategies and establish a model system for the evolution of daylength-mediated flowering time in undomesticated cereal crop-relatives.

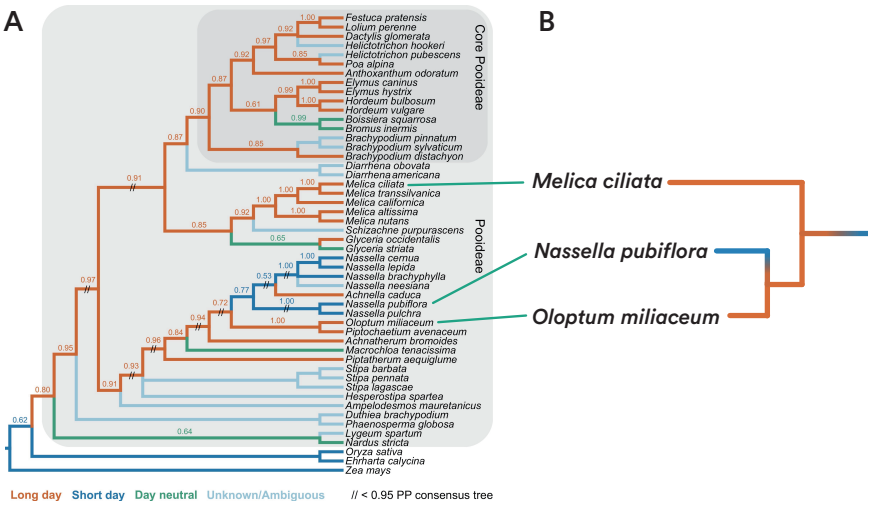

Figure 3 | A) Bayesian consensus tree for the focal grass species in PAPER II, including their realised and ancestral photoperiodic flowering strategies inferred in PAPER II. **B)** Target species for comparative (flowering) gene expression analyses in PAPER II–IV from early-diverging Pooideae tribes.

1.6 Methods in brief

Data analysed during this PhD project was generated in growth experiments where selected grass species were grown under controlled conditions. During these growth experiments, we varied selected environmental parameters to assess the relative effects of sustained cold (vernalisation) and daylength (photoperiod) on flowering time and collected samples of leaf tissue for subsequent gene expression and phylogenetic analyses.

Gene expression data form the foundation of the work presented in this thesis. Transcriptional activity was quantified using RT-qPCR for single genes (PAPER I & II), and RNA-sequencing for global gene expression (PAPER III & IV). To study the evolution of central flowering genes and their regulation, we employed a variety of phylogenetic methods. We reconstructed the evolutionary history of central vernalisation and photoperiodic flowering genes using Bayesian tree inference in PAPER I & II and carried out an ancestral state reconstruction to infer the evolutionary history of photoperiodic flowering in PAPER II (Fig. 3A). Furthermore, we used tools relying on phylogenetic inferences to develop an orthology-based annotation pipeline for the reference-free transcriptome assemblies generated in conjunction with PAPER III & IV.

As both vernalisation and photoperiodic flowering are temporally regulated biological processes, time course expression data formed the foundation of all gene expression analyses carried out in the presented work (PAPER I–IV). Depending on the research hypotheses and biological process in question, we examined gene expression at different resolutions, ranging from weeks (PAPER I), days (PAPER II), to hours (PAPER III–IV). Dense transcriptome sampling of the early-diverging Pooideae species *Melica ciliata*, *Nassella pubiflora*, and *Oloptum miliaceum* (Fig. 3B) over the course of a 24-h period enabled us to employ functional principal components analysis (FPCA). We used the information provided by FPCA for the explorative (PAPER III) and comparative (PAPER IV) analysis of rhythmic gene expression. This allowed us to develop different classification approaches and examine the impact of daylength on diurnal gene regulation in PAPER III and identify candidate genes responsible for opposite photoperiodic flowering strategies in early-diverging Pooideae in PAPER IV.

Materials and methods are further outlined in the respective PAPER*s.*

1.7 Paper summaries and pivotal results

1.7.1 Vernalisation response in PACMAD grasses

PAPER I. Adequate onset of flowering after winter is crucial for plant survival. Many plants have therefore evolved the ability to utilise periods of prolonged cold as flowering signal. Such induction or acceleration of reproductive growth is called vernalisation. Due to its agronomic importance, the molecular basis of vernalisation-mediated flowering has been extensively studied in economically significant species and lineages, such as Pooideae grasses. Although much of the core flowering network is conserved across angiosperms, multiple molecular pathways of vernalisation acting upon flowering genes have evolved. Here, we characterised vernalisation responsiveness in the PACMAD clade of the grass family to investigate whether flowering adaptations to prolonged cold are present in temperate grass lineages other than Pooideae and if the underlying molecular mechanism perceiving long-lasting cold parallels the model established in Pooideae or evolved independently.

Through a common-garden experiment under controlled conditions, we surveyed flowering time in response to vernalisation in 12 populations from seven temperate PACMAD species. We detected significantly cold-accelerated flowering in all species, suggesting that vernalisation response is a widespread trait in the grass family. Nevertheless, we also found substantial intraspecific variation between the vernalisation responses of different populations, demonstrating that sensitivity to prolonged cold is a quantitative trait considerably influenced by local adaptation.

To further investigate how vernalisation is perceived in PACMAD grasses, we identified orthologues of the cold-responsive vernalisation gene *VRN1* and its closest paralogue *FUL2* through phylogenetic analysis and confirmed the diversity of *FUL*-like genes in PACMAD and other grass taxa as well as their complex evolutionary history shaped by whole-genome and tandem duplications. Subsequent gene expression analysis revealed a significant increase in *VRN1* and *FUL2* transcription in some cold-treated species. In the Arundinoideae grass *Molinia caerulea*, a significant increase in *FUL2* expression was detected following eight weeks of cold while the transcription of *VRN1* remained low, suggesting that vernalisation response might be conveyed by *FUL2* in this species. In *Danthonia decumbens*, however, both *VRN1* and *FUL2* were upregulated, indicating that *FUL*-like genes might

have a natural tendency to cold-induced transcription and somewhat redundant functions in some species. Gene expression patterns in *Bouteloua gracilis* (Chloridoideae) and *Themeda triandra* (Panicoideae) did not support the recruitment of *VRN1* or *FUL2* into the vernalisation pathway, though both species were flowering significantly faster in response to vernalisation. This suggests the presence of multiple vernalisation pathways, possibly involving more distant paralogues of *VRN1* and *FUL2* in these grass species.

We show that vernalisation-mediated flowering is a common phenomenon in temperate PACMAD grasses that likely involves differential neofunctionalisation of *FUL*-like paralogues. Our findings contribute to the understanding of vernalisation responses in grasses and offer a basis for future functional characterisation of *VRN1* and *FUL2* to fully untie their elusive roles in flowering time evolution across the grass family.

1.7.2 Evolution of photoperiodic flowering in Pooideae

PAPER II. Flowering is triggered by different cues, depending on what ensures most adequate onset of reproduction in the current environmental context. Members of the temperate grass subfamily Pooideae are particularly well-adapted to temperate seasonality. Consequently, flowering is triggered by long days to coordinate reproduction with the onset of spring in most Pooideae. However, grasses evolved in the tropics where short day-flowering or day-neutrality is most beneficial. This suggests that LD-flowering is an adaptive strategy that evolved early in the Pooideae and facilitated their radiation into seasonal habitats. We tested this hypothesis by identifying photoperiodic flowering types through a growth experiment in a representative sample of Pooideae species, followed by ancestral state reconstruction, and expression analyses of central photoperiodic flowering genes.

Screening photoperiodic flowering behaviour in 47 Pooideae identified 21 LD species, five SD species, and five day-neutral species. Phylogenetic inference of daylength-mediated flowering in Pooideae revealed that the most recent common Pooideae ancestor likely flowered under LDs. This situates the attainment LD-flowering in Pooideae between their origin during the Late Cretaceous–Paleocene (~67 Mya) and the expansion of seasonal climates following the Eocene–Oligocene transition (~34 Mya). Moreover, we identified a secondary transition from ancestral LD- to SD-flowering in the genus *Nassella* which is a relatively recent Pooideae radiation native to neotropical montane habitats. This suggests that

Pooideae have an innate ability to evolve flowering adaptations to both long and short photoperiods which, in turn, facilitate the conquest of novel habitats.

To understand the mechanisms of secondary reversion to SD-flowering, we studied the expression of genes known to convey photoperiodic flowering in domesticated Pooideae within early-diverging species with opposite flowering strategies. Specifically, we compared the expression of the photoreceptor *PHYC* and the CCT genes *PPD1*, *CO1*, *VRN2* and its paralogue *CO9* in the SD species *Nassella pubiflora* with LD-responsive *Melica ciliata* and *Oloptum miliaceum*. To investigate role of *CO9* across Poaceae, we also characterised its diurnal expression in the SD-responsive Oryzoideae species *Ehrharta calycina*.

Expression profiles of *PHYC* and *PPD1* advocated for the retention of their roles as floral accelerators under LDs, despite repeated transitions between different flowering strategies in early-diverging Pooideae. Photoperiod did not significantly affect the transcription of *PHYC* in *Melica*, *Nassella*, and *Oloptum*. Peak activity of *PHYC* after dusk in all species, however, was congruent with its expression in barley, suggesting that conveyance of photoperiod sensitivity *per se* is conserved across both LD- and SD-responsive taxa. Peak abundance of *PPD1* aligned with the light phase in both photoperiods and was consistently more elevated under LDs than SDs in LD-flowering *M. ciliata* and *O. miliaceum,* indicative of its functional conservation in LD-responsive species. Contrary to LD-flowering Pooideae, photoperiod had a significant effect on the expression of *N. pubiflora CO1* with generally higher expression in SDs than LDs, supporting its role as flowering promoter under the absence of PPD1 such as in wheat and barley.

Transcriptional profiling of *VRN2* supported its role as LD-repressor of flowering, as its expression was similarly promoted by LDs in *N. pubiflora* and *M. ciliata*. Diurnal expression of *O. miliaceum VRN2* deviated considerably from its closest orthologue in *Nassella*, though this was likely caused by transcript abundance falling below the threshold of detection. Diurnal transcription of the *VRN2*-paralogue *CO9* on the other hand, was conserved between closely related *N. pubiflora* and *O. miliaceum*, with significantly increased expression during early morning in LD and a night peak in SD. Since we further demonstrate that CO9 is degraded in the dark, shifted *CO9* transcription in LD may prevent the interaction with VRN2 that attenuates flowering in *N. pubiflora*, thereby promoting the onset of reproductive growth under SDs. Our data suggests a possible functional shift where *VRN2* may have supplanted the role of *CO9* as transcriptional repressor under SDs in LD-

flowering taxa, implying that the LD response in *O. miliaceum* might be secondary.

Here, we demonstrate the diversity of photoperiodic flowering networks in temperate grasses and reveal that differential shifts of diurnal CCT gene expression are associated with the evolution of opposite flowering strategies and major niche transitions.

1.7.3 Diurnal gene regulation in *Melica ciliata*

PAPER III. Photoperiod has considerable impact on gene regulation in plants. Here, we investigated the temporal gene expression patterns in the grass species *Melica ciliata* under opposite photoperiods simulating LDs and SDs. Due to its interesting phylogenetic placement within Pooideae as a sister clade to the agronomically important core-Pooideae, *M. ciliata* holds particular significance for comparative gene expression studies in temperate grasses. Understanding how different daylengths influence global transcriptome dynamics in *M. ciliata* is valuable for eliciting the mechanisms of photoperiodic regulation of biological processes in undomesticated crop relatives.

We grew *M. ciliata* plants under contrasting LD and SD conditions and employed FPCA to deconstruct the temporal variation arising from diurnal gene expression to discern the primary transcriptomic responses to contrasting photoperiods and investigate how gene expression is coordinated under opposite photoperiods. We revealed that differences in overall gene expression level accounted for most diurnal variation. Standardisation of expression curves accentuated diurnal fluctuations and highlighted distinct, photoperiod-specific gene expression patterns. Diurnal rhythmicity of most transcripts was influenced by photoperiod, signifying the severe effect of daylength changes on overall gene expression. Diurnal behaviour of rhythmically expressed genes varied significantly between the two photoperiods. Expression inclines and declines were confined to specific times of the day, with different associations observed in LDs and SDs, indicating the presence of multiple modes and mechanisms of photoperiod perception. Furthermore, we identified associations between specific gene expression patterns and specific biological processes, like responses to stress, reproduction, and circadian rhythm using gene ontology (GO) enrichment analysis.

Overall, the study provides insights into the regulation of diurnal gene expression and enhances our understanding of how plants adapt to different day lengths. Furthermore, we demonstrate that FPCA offers a handy framework for the comparative exploration of

temporal gene expression dynamics and hypothesis generation in longitudinal *de novo* transcriptomes, paving way for further analyses targeting photoperiodic gene regulation in non-model grass species.

1.7.4 Recurrent evolution of photoperiodism in Stipeae

PAPER IV. As demonstrated in PAPER II, early-diverging Pooideae from the tribe Stipeae provide an appealing study system for the recurrent evolution of photoperiodic flowering strategies. In this study, we extended the line of investigation from PAPER II and considered the interspecific diurnal transcriptome dynamics of SD-responsive *Nassella pubiflora* and LD-responsive *Oloptum miliaceum* to clarify the evolution flowering time in this system.

Aided by functional data analysis, we designed a comparative transcriptomic approach to exhaustively detect divergent diurnal expression between species under LDs and SDs and identify candidate genes putatively involved in generating opposite daylength-mediated flowering strategies in Stipeae grasses. We confirmed the presence of opposite photoperiodic flowering behaviours in Stipeae, with significantly hastened flowering of *O. miliaceum* under LDs and SD-accelerated flowering under in *N. pubiflora*. To explore the underlying mechanisms of these flowering responses, we outlined genome-wide transcriptional activity with FPCA, a method allowing us to capture the most essential temporal features of global gene expression under LDs and SDs in both species. Despite their opposite flowering behaviours, we observed prominent conservation of diurnal gene regulation between *O. miliaceum* and *N. pubiflora*. Temporal variation in LD and SD gene expression adhered to analogous fundamental diurnal patterns in both species. Species-specific differences were mainly caused by variations in the timing of peak and trough expression. Most circadian clock gene orthologues identified in *N. pubiflora* and *O. miliaceum* responded similarly to photoperiod changes, indicating that the entrainment of circadian clock genes by photoperiod is generally conserved.

Using FPCA scores to construct a proxy measure for regulatory divergence, we identified two sets of genes with discrepant LD and SD expression between *Nassella* and *Oloptum*. Regulatory divergence under LDs was primarily restricted to basic processes, as evidenced by the presence of GO terms related to different aspects of metabolism. Interspecific diurnal divergence under SDs was associated with genes involved in flower development and

light-signalling, suggesting the presence of divergent photoperiod processing mechanisms in the flowering pathways of *O. miliaceum* and *N. pubiflora*. Closer examination revealed regulatory divergence of flowering-time genes, such as a *FT*-like antagonist of florigen, an orthologue of a response-regulator central in rice that is yet uncharacterised in Pooideae, as well as the circadian clock component *ELF3*. These play essential roles in the floral transition and photoperiodic flowering pathways in domesticated and model grasses and are potential contributors to the opposite flowering strategies in the Stipeae species *N. pubiflora* and *O. miliaceum*.

In this study, we demonstrate that the evolution of flowering time in Pooideae is closely tied to differential diurnal expression of relatively few genes that transmit daylength cues into developmental and signalling pathways and provide insight into the molecular basis of reversible flowering strategies associated with habitat transitions in grasses.

1.8 Discussion and future perspectives

Macroevolutionary processes rarely involve shifts from tropical to temperate biomes (Donoghue, 2008), stressing the formidable challenges plants need surmount to accomplish this step. General scarcity of this phenomenon across different grass subfamilies is indicative of the substantial challenges posed by environmental filtering, wherein the unique selective forces of temperate niches permit only lineages with highly specialised adaptations to leap out of their ancestral areas of origin (Schubert *et al.*, 2020). Phenological adjustments like the timely onset of flowering are pivotal in this context. Range expansions in grasses have been previously linked to flowering gene evolution (Preston & Fjellheim, 2020), indicating that novel connections between core floral regulators accelerate radiations of grasses into seasonal niches. However, detailed features of the dual flowering response have been primarily elucidated from variations in domesticated species and are not necessarily transferable to the adaptive innovations aiding the global conquest of increasingly demanding habitats by their untamed relatives. This thesis offers new perspectives on these particular aspects.

1.8.1 Lineage-specific flowering adaptations in grasses

Emerging early in the evolution of Pooideae, vernalisation and LD-flowering conferred significant advantages, facilitating their swift colonisation of emerging temperate biomes

(Schubert *et al.*, 2019b; Preston & Fjellheim, 2020). Due to their old age relative to other grass lineages, Pooideae managed to seize the most accessible temperate niches by the time other grass subfamilies ventured forth (Pirie *et al.*, 2009; Linder *et al.*, 2013; Gallaher *et al.*, 2022). This may have prompted these later lineages to develop more specialised adaptations tailored to thrive in niches climatically or geographically distinct from those already occupied by Pooideae (in particular core-Pooideae), such as montane or continental habitats at lower latitudes outside the Palearctic (Linder *et al.*, 2013; Humphreys & Linder, 2013; Pardo *et al.*, 2020; Pardo & VanBuren, 2021; Gallaher *et al.*, 2022). Stipeae are the most diverse early-diverging Pooideae tribe and principally found in steppes and highlands across the neotropic, nearctic, and palearctic realms (Hamasha *et al.*, 2012; Romaschenko *et al.*, 2012; Cialdella *et al.*, 2014). Considering their age, current geographic distribution, and flowering characteristics, we posit that the occurrence of Stipeae as a whole (PAPER II) and *N. pubiflora* in particular (PAPER IV) in neotropical highlands might be the result of a secondary shift from more seasonal, nearctic, open habitats into montane neotropical niches with analogous demands to stress acclimation, but not photoperiodism (PAPER II & IV). Transition from ancestral LD- to SD-flowering, driven by regulatory innovations in diurnal expression patterns of central flowering genes (PAPER II & IV), may have aided the southward migration of Stipeae along the mountain ridges of the Americas (PAPER II). This may also partially explain the diversity in vernalisation mechanisms in temperate PACMAD species (PAPER I), which may be the result of parallel evolution within a later wave of grass migrations into temperate niches, following their initial colonisation by Pooideae.

1.8.2 Modes of flowering-time gene evolution

A recurring pattern evident in the presented findings is that flexible flowering responses confer an evolutionary advantage promoting the diversification of certain grass lineages in seasonally fluctuating habitats. The ability to fine-tune floral onset in response to environmental cues can be attributed to the expansion and functional diversification of essential gene families, such as *FUL*-like (PAPER I), CCT domain genes (PAPER II), and likely also *FT*-like genes (PAPER IV), which play pivotal roles in the control of floral transition and adaptation (Colasanti & Coneva, 2009). Collectively, the presented work provides evidence that radiations of different grass lineages on global scales match the expansion and functional

diversification of these gene families on a molecular level.

Maintenance of a certain degree of functional redundancy within the floral network is pivotal for its adjustment and rewiring (Albert *et al.*, 2002; De Smet & Van de Peer, 2012). This kind of variation enables the simultaneous lability and conservation of regulators within the same genetic network underlying a specific trait (Abouheif & Wray, 2002; Moczek *et al.*, 2011). Stable functional redundancy offers adaptive flexibility which, in turn, facilitates the effective adjustment of flowering-time to diverse light and temperature conditions (Blackman *et al.*, 2011; Gaudinier & Blackman, 2020). Common for these sources of flowering-time diversity is the recruitment of close paralogues of a central floral regulator into an existing pathway. Importance of a gene for individual fitness is believed to be a principal constraint of sequence evolution (Kimura & Ohta, 1974). Master regulators situated at central nodes within a regulatory network are often involved in a multitude of biological processes and therefore subject to balancing selection due to such pleiotropic trade-offs. This may explain why we detect regulatory divergence only in more peripheral genes of the floral pathway between closely related species (PAPER IV), or paralogues of more central regulators (PAPER I & II).

Gene duplications can alleviate these selective constraints by initially producing an entirely redundant copy, which grants the opportunity to either undergo complete innovation (neofunctionalisation) of one paralogue or partial preservation (subfunctionalisation) of function in both duplicates (Force *et al.*, 1999; Lynch & Conery, 2000). *FUL*-like, CCT genes, and *FT*-like paralogues are prolific within grass genomes and participate in diverse developmental and physiological processes (Cockram *et al.*, 2012; Bennett & Dixon, 2021; Zhang *et al.*, 2022), thus offering developmental toolkits for the evolution of adaptive traits through the aforementioned mechanisms (Preston *et al.*, 2011).

Molecular mechanisms of vernalisation responsiveness in temperate PACMAD grasses (PAPER I) uncovered the differential neofunctionalisation of cold-responsive *FUL*-like paralogues relative to their Pooideae counterparts. Ancestrally, transcription factors of the *FUL*-like gene family primarily act as determinants of floral whorl identity in the SAMs of both *Arabidopsis* and grasses (Litt & Irish, 2003; Preston & Kellogg, 2007; Preston *et al.*, 2009), implying that cold-responsiveness of *FUL*-paralogues is a derived trait. Further promotion of this regulatory novelty could have been facilitated by the relaxation of selective constraints on one of its copies following a gene duplication event, under circumstances

were floral promotion by long-term cold yielded fitness benefits. Recruitment of the closest orthologue of Pooideae *VRN1* into the vernalisation pathway of *M. caerulea* suggests neofunctionalisation of a *FUL*-like paralogue which might have been instrumental in facilitating the spread of this species into seasonal niches. Similar evolution of flowering-genes in PAPER II further suggests the generalisability of this mode of adaptive innovation. Given paralogous relationship between *VRN2* and *CO9*, it is plausible that these genes underwent duplication followed by divergence in function to accommodate different photoperiodic flowering strategies. The expression patterns suggest that *VRN2*, initially a LD-repressor of flowering (Woods *et al.*, 2016), might have taken on a novel role under short day (SD) conditions in *O. miliaceum*, potentially replacing the function of *CO9*. This shift could represent a case of subfunctionalisation, where duplicated CCT genes specialise in different regulatory roles within the photoperiodic flowering pathway. On the other hand, *CO9* may have acquired a new role in promoting flowering under SD conditions in *N. pubiflora*, possibly through a novel protein interaction hastening the deterioration of CO9 proteins under LDs, but not in SDs. This suggests a scenario of neofunctionalisation, the novel function involves a shift in diurnal *CO9* regulation influencing the coincidence with other genes that regulate its degradation. Irrespective of the exact evolutionary process, our results indicate a dynamic interplay between the proliferation of CCT domain genes, discrepant expression between paralogues, and functional innovation through novel interactions with other flowering-time genes (PAPER II). This interplay plays a crucial role in shaping the photoperiodic flowering pathways of temperate grasses.

Allelic variation in flowering-time loci is the source of considerable variation in domesticated grasses and the model species *B. distachyon* (Woods *et al.*, 2017; Bettgenhaeuser *et al.*, 2017; Fernández-Calleja *et al.*, 2021). This variation has played a crucial role in precise enhancement of flowering-time and other economic traits across latitudinal gradients and climatic extremes in cultivated crops (Koo *et al.*, 2013; Göransson *et al.*, 2019; Han *et al.*, 2023; Zhao *et al.*, 2023). Geographic origin also plays a substantial role in phasing of gene expression and even central rhythmic processes such as the circadian clock are documented to vary considerably between populations (de Montaigu *et al.*, 2015; de Montaigu & Coupland, 2017; Oravec & Greenham, 2022). Especially allelic variation within the circadian clock has been demonstrated to exert significant influence on flowering time, highlighting the crucial role that genetic diversity even within the most central regulatory mechanisms

plays in shaping the timing of developmental events (Lee *et al.*, 2022; Maeda & Nakamichi, 2022). Mindful of the potential pitfalls associated with genetically heterogenous grass germplasm, we aimed to mitigate within-species or population variations through biological replicates and refraining from pooling any RNA or DNA samples in all of our experiments (PAPER I–IV). However, it is advisable to approach the findings of cross-species analyses investigating diurnal expression shifts in wild species (PAPER II–IV) with a degree of caution given that divergence of periodic processes might be amplified by distinct evolutionary histories.

1.8.3 Shedding light on clock ticks and timely blooms

Historically, two models have been developed for the endogenous time-keeping mechanisms in plants. The hourglass model suggests that an internal photoperiodic clock measures the duration of light and dark periods, with critical night length triggering flowering (Borthwick & Hendricks, 1960). On the other hand, the external coincidence model proposes that flowering occurs when an external cue (like dawn or dusk) coincides with an internal physiological state, such as the expression level of circadian clock output genes or the abundance of their protein products (Pittendrigh, 1960; Pittendrigh & Minis, 1964; Sawa *et al.*, 2008). Both models entail the perception of light by photoreceptors at the beginning of the light-signalling cascade and are not necessarily mutually exclusive and partially redundant. However, the hourglass and coincidence models serve as valuable frameworks for distinguishing the relative significance of different photosensory systems among different plant taxa and understanding the biological timing mechanisms they entail.

A recent hypothesis suggests that the hourglass model might be of greater significance in temperate grasses (Raissig & Woods, 2022). In *B. distachyon*, barley and wheat, the phytochromes *PHYC* and *PHYB* emerge as increasingly more pivotal components of photoperiodic flowering pathway (Woods *et al.*, 2014, 2023; Pearce *et al.*, 2016; Kippes *et al.*, 2020; Bouché *et al.*, 2022; Alvarez *et al.*, 2023). Generally, our findings from PAPER III & IV lend support to this hypothesis by revealing the presence of multiple photosensory systems in *M. ciliata* (PAPER III) and Stipeae (PAPER IV), though somewhat contradicted by the absence of significant effects of photoperiod on *PHYC* in PAPER II. Variation in the light-perceiving layer of the floral pathway yields an extensive array of potential molecular configurations

through the interplay between photoreceptors, flowering-time genes, and interacting co-factors (such as PIFs; Pham *et al.*, 2017). This intricate network forms a dynamic system adept at integrating a multitude of environmental cues crucial for precise flowering regulation (PAPER III & IV). Interaction among light-sensing, time-keeping, and signal-transducing modules within the flowering network of temperate grasses remains partially understood, and determining their respective roles in various species presents an exciting avenue for future research.

Under natural conditions, both light and temperature vary over the course of a day. An important caveat of our research targeting photoperiod responses is the omission of temperature variations in our experimental design. Rhythmic processes in plants, such as stomatal opening, leaf movements, and growth are temperature-dependent and modulated by the integration of both photoperiod and ambient temperature through the circadian clock (Yakir *et al.*, 2007; Hotta *et al.*, 2013). For instance, temperature changes are the foremost cue sustaining circadian oscillations in the transcriptome of *B. distachyon* and required for the precise timing of gene expression and numerous developmental processes throughout the day (MacKinnon *et al.*, 2020). Likewise, in *Arabidopsis*, the expression of florigen *FT* significantly diverges from laboratory reports under natural conditions, a discrepancy arising from distinct stabilisation of CO governed by both temperature and light-sensitive regulators such as phytochromes and *ELF3* (Song *et al.*, 2018). Refining growth parameters to replicate natural plant responses more precisely has significant potential for advancing our understanding of diurnally regulated processes such as seasonal flowering responses.

An inherent challenge in gene expression studies is that transcript abundance alone is insufficient to predict protein levels accurately (Gygi *et al.*, 1999). Rhythms, whether within the floral network or other processes, are sustained through the interaction of genes at the protein level and subject to considerable post-translational regulation (*e.g.*, PAPER II). Transcriptome data therefore illuminate only a part of the regulatory interferences necessary to sustain time-dependent processes in plants (Seaton *et al.*, 2018; Mehta *et al.*, 2021). Integration of proteome and transcriptome data holds great promise for the elucidation of the precise mechanisms by which floral regulators orchestrate the intricate symphony of floral onset and other time-dependent processes.

1.9 Functional gene expression analysis

Many aspects of plant biology display time-dependent characteristics and follow predictable oscillatory patterns (Somers, 1999). Gathering data over a given time interval provides a natural means of approximating reoccurring temporal changes in biological systems. The fundamental unit of in time-course expression studies are gene expression profiles. Due to practical limitations, these profiles are usually comprised of point-measurements, which can be approximated by curves if collected densely enough. Representing such continuous processes as functions rather than discrete samples allows precise analysis of dynamic fluctuations over time (Leng & Müller, 2005). Functional data analysis (FDA) is a framework specifically developed for the statistical analysis of random samples composed of continuous functions, enabling the study of complex biological processes in their most natural form of representation (Ramsay & Silverman, 2005; Shang, 2014).

Methodological approaches based on FDA have been extensively explored in gene expression data analysis, yielding notable advancements in various contexts. For instance, microarray analyses leveraging FPCA for the detection of rhythmic gene expression have displayed increased statistical power when contrasted with traditional methodologies such as linear model-based approaches (Leng & Müller, 2005; Song *et al.*, 2007, 2008; Liu & Yang, 2009; Wu & Wu, 2013). Moreover, these techniques have proved valuable in the analysis of sequencing data, particularly in the decomposition of variation in DNA-binding protein coverage profiles, presenting a novel avenue for dissecting intricate genomic interactions (Madrigal & Krajewski, 2015). Beyond genomics, functional analyses have also demonstrated efficacy in plant phenotyping. Extraction of shared patterns from growth curves in sorghum demonstrates the versatility of FPCA-based approaches in resolving temporal dynamics of biological processes (Miao *et al.*, 2020).

To the best of my knowledge, we deliver the first application of FPCA-based transcriptome profiling for the explorative analysis of rhythmic gene expression (Paper III) and cross-species transcriptomics (Paper IV). Conventional methods for analysing rhythmic gene expression often require extensive sampling across multiple cycles to understand the interplay between phase and period (Bar-Joseph, 2004; Li *et al.*, 2015; Wu *et al.*, 2016; Hughes *et al.*, 2017). While our approach did not allow for precise numerical evaluation of these fundamental wavelet aspects, it retains its value in qualitatively assessing period and

phase with clear biological interpretability (PAPER III & IV). This is particularly useful in situations where the need for biological replicates limits the ability to cover multiple periods with sufficient density (PAPER III & IV).

Promising extensions of our initial attempts of FPCA-based characterisation of transcriptome data (PAPER III & IV) include the application of more sophisticated techniques for classifying FPCA scores, such as discriminant analysis, hierarchical models, logistic regression, or support vector machines (Leng & Müller, 2005; Hong & Li, 2006; Song *et al.*, 2008; Liu & Yang, 2009; Wu & Wu, 2013). Precision and recall in FDA-based analysis have been further enhanced by successfully incorporating a noise component into the classification of time-dependent gene expression using functional single-value decomposition (Bar-Joseph *et al.*, 2012). Another intriguing FDA technique capable of distinguishing phase and amplitude in periodic functions is curve registration (Ramsay & Li, 1998), a method effectively employed to detect desynchronised gene expression during floral transition in *Brassica rapa* (Calderwood *et al.*, 2021).

Lack of standardised nomenclature, outdated software tools, and the prevalence of more established methodologies collectively impede the adoption of FDA-based approaches within the emerging landscape of extensive gene expression datasets. Despite its potential to be the most intuitive analytical avenue for longitudinal and cyclical biological data (PAPER III & IV), application of FDA in genomics is occasional. This useful framework deserves greater advocacy and promotion, especially among biologists less accustomed to rigorous mathematical and statistical techniques. Efforts to bridge this gap and make FDA more accessible to researchers with varying quantitative backgrounds are necessary for harnessing its full potential in for the analysis of longitudinal, time-dependent data gathered in grasses and other vegetables.

1.10 References

Abouheif E, Wray GA. **2002**. Evolution of the gene network underlying wing polyphenism in ants. *Science* **297**: 249–252.

Albert VA, Oppenheimer DG, Lindqvist C. **2002**. Pleiotropy, redundancy and the evolution of flowers. *Trends in Plant Science* **7**: 297–301.

Alvarez MA, Li C, Lin H, Joe A, Padilla M, Woods DP, Dubcovsky J. **2023**. *EARLY FLOWERING 3* interactions with *PHYTOCHROME B* and *PHOTOPERIOD1* are critical for the photoperiodic regulation of wheat heading time. *PLOS Genetics* **19**: e1010655.

Amasino R. **2010**. Seasonal and developmental timing of flowering. *The Plant Journal* **61**: 1001–1013.

Andrés F, Coupland G. **2012**. The genetic basis of flowering responses to seasonal cues. *Nature Reviews Genetics* **13**: 627–639.

Bar-Joseph Z. **2004**. Analyzing time series gene expression data. *Bioinformatics* **20**: 2493–2503.

Bar-Joseph Z, Gitter A, Simon I. **2012**. Studying and modelling dynamic biological processes using time-series gene expression data. *Nature Reviews Genetics* **13**: 552–564.

Bäurle I, Dean C. **2006**. The timing of developmental transitions in plants. *Cell* **125**: 655–664.

Bendix C, Marshall CM, Harmon FG. **2015**. Circadian clock genes universally control key agricultural traits. *Molecular Plant* **8**: 1135–1152.

Bennett T, Dixon LE. **2021**. Asymmetric expansions of *FT* and *TFL1* lineages characterize differential evolution of the EuPEBP family in the major angiosperm lineages. *BMC Biology* **19**: 181.

Bernier G. **1988**. The control of floral evocation and morphogenesis. *Annual Review of Plant Physiology and Plant Molecular Biology* **39**: 175–219.

Bettgenhaeuser J, Corke FM, Opanowicz M, Green P, Hernández-Pinzón I, Doonan JH, Moscou MJ. **2017**. Natural variation in *Brachypodium* links vernalization and flowering time loci as major flowering determinants. *Plant Physiology* **173**: 256–268.

Blackman BK, Michaels SD, Rieseberg LH. **2011**. Connecting the sun to flowering in sunflower adaptation. *Molecular Ecology* **20**: 3503–3512.

Borthwick HA, Hendricks SB. **1960**. Photoperiodism in plants. *Science* **132**: 1223–1228.

Bouché F, Woods DP, Amasino R. **2017**. Winter memory throughout the plant kingdom: different paths to flowering. *Plant Physiology* **173**: 27–35.

Bouché F, Woods DP, Linden J, Li W, Mayer KS, Amasino RM, Périlleux C. **2022**. *EARLY FLOWERING 3* and photoperiod sensing in *Brachypodium distachyon*. *Frontiers in Plant Science* **12**: 769194.

Bouchenak-Khelladi Y, Verboom GA, Savolainen V, Hodkinson TR. **2010**. Biogeography of the grasses (Poaceae): a phylogenetic approach to reveal evolutionary history in geographical space and geological time. *Botanical Journal of the Linnean Society* **162**: 543–557.

Bowen GJ, Maibauer BJ, Kraus MJ, Röhl U, Westerhold T, Steimke A, Gingerich PD, Wing SL, Clyde WC. **2015**. Two massive, rapid releases of carbon during the onset of the Palaeocene–Eocene thermal maximum. *Nature Geoscience* **8**: 44–47.

Bradshaw AD. **1965**. Evolutionary significance of phenotypic plasticity in plants. *Advances in Genetics* **13**: 115–155.

Bremer K. **2002**. Gondwanan evolution of the grass alliance of families (Poales). *Evolution* **56**: 1374–1387.

Calderwood A, Hepworth J, Woodhouse S, Bilham L, Jones DM, Tudor E, Ali M, Dean C, Wells R, Irwin JA, *et al.* **2021**. Comparative transcriptomics reveals desynchronisation of gene expression during the floral transition between *Arabidopsis* and *Brassica rapa* cultivars. *Quantitative Plant Biology* **2**: 1–13.

Campoli C, von Korff M. **2014**. Genetic control of reproductive development in temperate cereals. *Advances in Botanical Research* **72**: 131–158.

Cao S, Luo X, Xu D, Tian X, Song J, Xia X, Chu C, He Z. **2021**. Genetic architecture underlying light and temperature mediated flowering in *Arabidopsis*, rice, and temperate cereals. *New Phytologist* **230**: 1731–1745.

Chen A, Li C, Hu W, Lau MY, Lin H, Rockwell NC, Martin SS, Jernstedt JA, Lagarias JC, Dubcovsky J. **2014**. PHYTOCHROME C plays a major role in the acceleration of wheat flowering under long-day photoperiod. *Proceedings of the National Academy of Sciences of the United States of America* **111**: 10037–10044.

Chouard P. **1960**. Vernalization and its relations to dormancy. *Annual Review of Plant Physiology* **11**: 191–238.

Christin P-A, Spriggs EL, Osborne CP, Strömberg CAE, Salamin N, Edwards EJ. **2014**. Molecular dating, evolutionary rates, and the age of the grasses. *Systematic Biology* **63**: 153–165.

Cialdella AM, Sede SM, Romaschenko K, Peterson PM, Soreng RJ, Zuloaga FO, Morrone O. **2014**. Phylogeny of *Nassella* (Stipeae, Pooideae, Poaceae) based on analyses of chloroplast and nuclear ribosomal DNA and morphology. *Systematic Botany* **39**: 814–828.

Cockram J, Jones H, Leigh FJ, O'Sullivan D, Powell W, Laurie DA, Greenland AJ. **2007**. Control of flowering time in temperate cereals: genes, domestication, and sustainable productivity. *Journal of Experimental Botany* **58**: 1231–1244.

Cockram J, Thiel T, Steuernagel B, Stein N, Taudien S, Bailey PC, O'Sullivan DM. **2012**. Genome dynamics explain the evolution of flowering time CCT domain gene families in the Poaceae. *PLOS One* **7**: e45307.

Colasanti J, Coneva V. **2009**. Mechanisms of floral induction in grasses: something borrowed, something new. *Plant Physiology* **149**: 56–62.

Cotton JL, Wysocki WP, Clark LG, Kelchner SA, Pires JC, Edger PP, Mayfield-Jones D, Duvall MR. **2015**. Resolving deep relationships of PACMAD grasses: a phylogenomic approach. *BMC Plant Biology* **15**: 178.

Cross RA. **1980**. Distribution of sub-families of Gramineae in the Old World. *Kew Bulletin* **35**: 279–289.

Davis JI, Soreng RJ. **1993**. Phylogenetic structure in the grass family (Poaceae) as inferred from chloroplast DNA restriction site variation. *American Journal of Botany* **80**: 1444–1454.

de Montaigu A, Coupland G. **2017**. The timing of *GIGANTEA* expression during day/night cycles varies with the geographical origin of *Arabidopsis* accessions. *Plant Signaling & Behavior* **12**: e1342026.

de Montaigu A, Giakountis A, Rubin M, Tóth R, Cremer F, Sokolova V, Porri A, Reymond M, Weinig C, Coupland G. **2015**. Natural diversity in daily rhythms of gene expression contributes to phenotypic variation. *Proceedings of the National Academy of Sciences of the United States of America* **112**: 905–910.

Deng W, Casao MC, Wang P, Sato K, Hayes PM, Finnegan EJ, Trevaskis B. **2015**. Direct links between the vernalization response and other key traits of cereal crops. *Nature Communications* **6**: 5882.

Dennis ES, Peacock WJ. **2009**. Vernalization in cereals. *Journal of Biology* **8**: 57.

De Smet R, Van de Peer Y. **2012**. Redundancy and rewiring of genetic networks following genome-wide duplication events. *Current Opinion in Plant Biology* **15**: 168–176.

Distelfeld A, Li C, Dubcovsky J. **2009**. Regulation of flowering in temperate cereals. *Current Opinion in Plant Biology* **12**: 178–184.

Dodd AN, Salathia N, Hall A, Kévei E, Tóth R, Nagy F, Hibberd JM, Millar AJ, Webb AAR. **2005**. Plant circadian clocks increase photosynthesis, growth, survival, and competitive advantage. *Science* **309**: 630–633.

Donoghue MJ. **2008**. A phylogenetic perspective on the distribution of plant diversity. *Proceedings of the National Academy of Sciences of the United States of America* **105**: 11549–11555.

Edwards EJ, Smith SA. **2010**. Phylogenetic analyses reveal the shady history of C_4 grasses. *Proceedings of the National Academy of Sciences of the United States of America* **107**: 2532–2537.

Ergon Å, Hamland H, Rognli OA. **2013**. Differential expression of *VRN1* and other MADS-box genes in *Festuca pratensis* selections with different vernalization requirements. *Biologia Plantarum* **57**: 245–254.

Evans LT. **1971**. Flower induction and the florigen concept. *Annual Review of Plant Physiology* **22**: 365–394.

Fernández-Calleja M, Casas AM, Igartua E. 2021. Major flowering time genes of barley: allelic diversity, effects, and comparison with wheat. *Theoretical and Applied Genetics* **134**: 1867–1897.

Fjellheim S, Boden S, Trevaskis B. 2014. The role of seasonal flowering responses in adaptation of grasses to temperate climates. *Frontiers in Plant Science* **5**: 431.

Force A, Lynch M, Pickett FB, Amores A, Yan Y, Postlethwait J. 1999. Preservation of duplicate genes by complementary, degenerative mutations. *Genetics* **151**: 1531–1545.

Gallaher TJ, Adams DC, Attigala L, Burke SV, Craine JM, Duvall MR, Klahs PC, Sherratt E, Wysocki WP, Clark LG. 2019. Leaf shape and size track habitat transitions across forest–grassland boundaries in the grass family (Poaceae). *Evolution* **73**: 927–946.

Gallaher TJ, Peterson PM, Soreng RJ, Zuloaga FO, Li D, Clark LG, Tyrrell CD, Welker CAD, Kellogg EA, Teisher JK. 2022. Grasses through space and time: An overview of the biogeographical and macroevolutionary history of Poaceae. *Journal of Systematics and Evolution* **60**: 522–569.

Gao M, Geng F, Klose C, Staudt A-M, Huang H, Nguyen D, Lan H, Mockler TC, Nusinow DA, Hiltbrunner A, *et al.* 2019. Phytochromes measure photoperiod in *Brachypodium*. *bioRxiv*: 697169.

Gaßner G. 1918. Beiträge zur physiologischen Charakteristik sommer- und winterannueller Gewächse, insbesondere der Getreidepflanzen. *Zeitschrift für Botanik* **10**: 417–480.

Gaudinier A, Blackman BK. 2020. Evolutionary processes from the perspective of flowering time diversity. *New Phytologist* **225**: 1883–1898.

Gaut BS. 2002. Evolutionary dynamics of grass genomes. *New Phytologist* **154**: 15–28.

Gocal GFW, King RW, Blundell CA, Schwartz OM, Andersen CH, Weigel D. 2001. Evolution of floral meristem identity genes. Analysis of *Lolium temulentum* genes related to *APETALA1* and *LEAFY* of *Arabidopsis*. *Plant Physiology* **125**: 1788–1801.

Göransson M, Hallsson JH, Lillemo M, Orabi J, Backes G, Jahoor A, Hermannsson J, Christerson T, Tuvesson S, Gertsson B, *et al.* 2019. Ideal allele combinations for the adaptation of spring barley to northern latitudes. *Frontiers in Plant Science* **10**: 542.

Greenham K, McClung CR. 2015. Integrating circadian dynamics with physiological processes in plants. *Nature Reviews Genetics* **16**: 598–610.

Greenup A, Peacock WJ, Dennis ES, Trevaskis B. 2009. The molecular biology of seasonal flowering-responses in Arabidopsis and the cereals. *Annals of Botany* **103**: 1165–1172.

Gygi SP, Rochon Y, Franza BR, Aebersold R. 1999. Correlation between protein and mRNA abundance in yeast. *Molecular and Cellular Biology* **19**: 1720–1730.

Hamasha HR, von Hagen KB, Röser M. 2012. *Stipa* (Poaceae) and allies in the Old World: molecular phylogenetics realigns genus circumscription and gives evidence on the origin of American and Australian lineages. *Plant Systematics and Evolution* **298**: 351–367.

Han Z, Lei X, Sha H, liu J, Zhang C, Wang J, Zheng H, Zou D, Fang J. 2023. Adaptation to high latitudes through a novel allele of *Hd3a* strongly promoting heading date in rice. *Theoretical and Applied Genetics* **136**: 141.

Harmer SL. 2009. The circadian system in higher plants. *Annual Review of Plant Biology* **60**: 357–377.

Hartley W. 1973. Studies on the origin, evolution, and distribution of the Gramineae. V. The subfamily Festucoideae. *Australian Journal of Botany* **21**: 201–234.

Heide OM. 1994. Control of flowering and reproduction in temperate grasses. *New Phytologist* **128**: 347–362.

Hemming MN, Peacock WJ, Dennis ES, Trevaskis B. 2008. Low-temperature and daylength cues are integrated to regulate *FLOWERING LOCUS T* in barley. *Plant Physiology* **147**: 355–366.

Higgins JA, Bailey PC, Laurie DA. 2010. Comparative genomics of flowering time pathways using *Brachypodium distachyon* as a model for the temperate grasses. *PLOS One* **5**: e10065.

Hong S-Y, Lee S, Seo PJ, Yang M-S, Park C-M. 2010. Identification and molecular characterization of a *Brachypodium distachyon GIGANTEA* gene: functional conservation in monocot and dicot plants. *Plant Molecular Biology* **72**: 485–497.

Hong F, Li H. 2006. Functional hierarchical models for identifying genes with different time-course expression profiles. *Biometrics* **62**: 534–544.

Hotta CT, Nishiyama MY, Souza GM. 2013. Circadian rhythms of sense and antisense transcription in sugarcane, a highly polyploid crop. *PLOS One* **8**: e71847.

Hsu PY, Harmer SL. 2014. Wheels within wheels: the plant circadian system. *Trends in Plant Science* **19**: 240–249.

Hughes ME, Abruzzi KC, Allada R, Anafi R, Arpat AB, Asher G, Baldi P, Bekker C de, Bell-Pedersen D, Blau J, *et al.* 2017. Guidelines for genome-scale analysis of biological rhythms. *Journal of Biological Rhythms* **32**: 380–393.

Humphreys AM, Linder HP. 2013. Evidence for recent evolution of cold tolerance in grasses suggests current distribution is not limited by (low) temperature. *New Phytologist* **198**: 1261–1273.

Imaizumi T, Kay SA. 2006. Photoperiodic control of flowering: not only by coincidence. *Trends in Plant Science* **11**: 550–558.

Itoh H, Nonoue Y, Yano M, Izawa T. 2010. A pair of floral regulators sets critical day length for *Hd3a* florigen expression in rice. *Nature Genetics* **42**: 635–638.

Johansson M, Staiger D. 2014. Time to flower: interplay between photoperiod and the circadian clock. *Journal of Experimental Botany* **66**: 719–730.

Junttila O. 1996. Plant adaptation to temperature and photoperiod. *Agricultural and Food Science* **5**: 251–260.

Kikuchi R, Kawahigashi H, Oshima M, Ando T, Handa H. 2011. The differential expression of *HvCO9*, a member of the *CONSTANS*-like gene family, contributes to the control of flowering under short-day conditions in barley. *Journal of Experimental Botany* **63**: 773–84.

Kimura M, Ohta T. 1974. On some principles governing molecular evolution. *Proceedings of the National Academy of Sciences of the United States of America* **71**: 2848–2852.

King RW, Heide OM. 2009. Seasonal flowering and evolution: the heritage from Charles Darwin. *Functional Plant Biology* **36**: 1027–1036.

Kinjo H, Shitsukawa N, Takumi S, Murai K. 2012. Diversification of three *APETALA1/FRUITFULL*-like genes in wheat. *Molecular Genetics and Genomics* **287**: 283–294.

Kippes N, VanGessel C, Hamilton J, Akpinar A, Budak H, Dubcovsky J, Pearce S. 2020. Effect of *phyB* and *phyC* loss-of-function mutations on the wheat transcriptome under short and long day photoperiods. *BMC Plant Biology* **20**: 297.

Koo B-H, Yoo S-C, Park J-W, Kwon C-T, Lee B-D, An G, Zhang Z, Li J, Li Z, Paek N-C. 2013. Natural variation in *OsPRR37* regulates heading date and contributes to rice cultivation at a wide range of latitudes. *Molecular Plant* **6**: 1877–1888.

Körner C. 2016. Plant adaptation to cold climates. *F1000Research* **5**: 2769.

Kreft H, Jetz W. 2007. Global patterns and determinants of vascular plant diversity. *Proceedings of the National Academy of Sciences of the United States of America* **104**: 5925–5930.

Laurie DA, Pratchett N, Bezant JH, Snape JW. 1995. RFLP mapping of five major genes and eight quantitative trait loci controlling flowering time in a winter × spring barley (*Hordeum vulgare* L.) cross. *Genome* **38**: 575–585.

Lee S-J, Kang K, Lim J-H, Paek N-C. 2022. Natural alleles of *CIRCADIAN CLOCK ASSOCIATED1* contribute to rice cultivation by fine-tuning flowering time. *Plant Physiology* **190**: 640–656.

Leng X, Müller H-G. 2005. Classification using functional data analysis for temporal gene expression data. *Bioinformatics* **22**: 68–76.

Li C, Distelfeld A, Comis A, Dubcovsky J. 2011. Wheat flowering repressor VRN2 and promoter CO2 compete for interactions with NUCLEAR FACTOR-Y complexes. *The Plant Journal* **67**: 763–773.

Li J, Grant GR, Hogenesch JB, Hughes ME. 2015. Considerations for RNA-seq analysis of circadian rhythms. *Methods in Enzymology* **551**: 349–367.

Li C, Lin H, Chen A, Lau M, Jernstedt J, Dubcovsky J. 2019. Wheat *VRN1*, *FUL2* and *FUL3* play critical and redundant roles in spikelet development and spike determinacy. *Development* **146**: dev175398.

Li C, Rudi H, Stockinger EJ, Cheng H, Cao M, Fox SE, Mockler TC, Westereng B, Fjellheim S, Rognli OA, *et al.* 2012. Comparative analyses reveal potential uses of *Brachypodium distachyon* as a model for cold stress responses in temperate grasses. *BMC Plant Biology* **12**: 65.

Li Q, Wang Y, Wang F, Guo Y, Duan X, Sun J, An H. 2016. Functional conservation and diversification of *APETALA1/ FRUITFULL* genes in *Brachypodium distachyon*. *Physiologia Plantarum* **157**: 507–518.

Li Y, Xu M. 2017. CCT family genes in cereal crops: A current overview. *The Crop Journal* **5**: 449–458.

Lin C. 2000. Photoreceptors and regulation of flowering time. *Plant Physiology* **123**: 39–50.

Lindberg CL, Hanslin HM, Schubert M, Marcussen T, Trevaskis B, Preston JC, Fjellheim S. 2020. Increased above-ground resource allocation is a likely precursor for independent evolutionary origins of annuality in the Pooideae grass subfamily. *New Phytologist* **228**: 318–329.

Linder HP, Antonelli A, Humphreys AM, Pirie MD, Wüest RO. 2013. What determines biogeographical ranges? Historical wanderings and ecological constraints in the danthonioid grasses. *Journal of Biogeography* **40**: 821–834.

Linder HP, Baeza M, Barker NP, Galley C, Humphreys AM, Lloyd KM, Orlovich DA, Pirie MD, Simon BK, Walsh N, *et al.* 2010. A generic classification of the Danthonioideae (Poaceae). *Annals of the Missouri Botanical Garden* **97**: 306–364.

Lindlöf A. 2010. Interplay between low-temperature pathways and light reduction. *Plant Signaling & Behavior* **5**: 820–825.

Litt A, Irish VF. 2003. Duplication and diversification in the *APETALA1/FRUITFULL* floral homeotic gene lineage: implications for the evolution of floral development. *Genetics* **165**: 821–833.

Liu X, Yang MCK. 2009. Identifying temporally differentially expressed genes through functional principal components analysis. *Biostatistics* **10**: 667–679.

Lynch M, Conery JS. 2000. The evolutionary fate and consequences of duplicate genes. *Science* **290**: 1151–1155.

MacKinnon KJ-M, Cole BJ, Yu C, Coomey JH, Hartwick NT, Remigereau M, Duffy T, Michael TP, Kay SA, Hazen SP. 2020. Changes in ambient temperature are the prevailing cue in determining *Brachypodium distachyon* diurnal gene regulation. *New Phytologist* **227**: 1709–1724.

Madrigal P, Krajewski P. 2015. Uncovering correlated variability in epigenomic datasets using the Karhunen–Loève transform. *BioData Mining* **8**: 20.

Maeda AE, Nakamichi N. 2022. Plant clock modifications for adapting flowering time to local environments. *Plant Physiology* **190**: 952–967.

Mathews S. 2010. Evolutionary studies illuminate the structural-functional model of plant phytochromes. *The Plant Cell* **22**: 4–16.

McKain MR, Tang H, McNeal JR, Ayyampalayam S, Davis JI, dePamphilis CW, Givnish TJ, Pires JC, Stevenson DW, Leebens-Mack JH. 2016. A phylogenomic assessment of ancient polyploidy and genome evolution across the Poales. *Genome Biology and Evolution* **8**: 1150–1164.

McKeown M, Schubert M, Marcussen T, Fjellheim S, Preston JC. 2016. Evidence for an early origin of vernalization responsiveness in temperate Pooideae grasses. *Plant Physiology* **172**: 416–426.

McKeown M, Schubert M, Preston JC, Fjellheim S. 2017. Evolution of the *miR5200–FLOWERING LOCUS T* flowering time regulon in the temperate grass subfamily Pooideae. *Molecular Phylogenetics and Evolution* **114**: 111–121.

McKinney HH. 1940. Vernalization and the growth-phase concept. *The Botanical Review* **6**: 25–47.

Mehta D, Krahmer J, Uhrig RG. 2021. Closing the protein gap in plant chronobiology. *The Plant Journal* **106**: 1509–1522.

Miao C, Xu Y, Liu S, Schnable PS, Schnable J. 2020. Increased power and accuracy of causal locus identification in time-series genome-wide association in sorghum. *Plant Physiology* **183**: 1898–1909.

Michael TP, Salomé PA, Yu HJ, Spencer TR, Sharp EL, McPeek MA, Alonso JM, Ecker JR, McClung CR. 2003. Enhanced fitness conferred by naturally occurring variation in the circadian clock. *Science* **302**: 1049–1053.

Millar AJ. 2004. Input signals to the plant circadian clock. *Journal of Experimental Botany* **55**: 277–283.

Moczek AP, Sultan S, Foster S, Ledón-Rettig C, Dworkin I, Nijhout HF, Abouheif E, Pfennig DW. 2011. The role of developmental plasticity in evolutionary innovation. *Proceedings of the Royal Society B: Biological Sciences* **278**: 2705 2713.

Monteagudo A, Igartua E, Contreras-Moreira B, Gracia MP, Ramos J, Karsai I, Casas AM. 2019. Fine-tuning of the flowering time control in winter barley: the importance of *HvOS2* and *HvVRN2* in non-inductive conditions. *BMC Plant Biology* **19**: 113.

Murfet IC. 1977. Environmental interaction and the genetics of flowering. *Annual Review of Plant Physiology* **28**: 253–278.

Nishida H, Ishihara D, Ishii M, Kaneko T, Kawahigashi H, Akashi Y, Saisho D, Tanaka K, Handa H, Takeda K, *et al.* 2013. *Phytochrome C* is a key factor controlling long-day flowering in barley. *Plant Physiology* **163**: 804–814.

Oliver SN, Deng W, Casao MC, Trevaskis B. 2013. Low temperatures induce rapid changes in chromatin state and transcript levels of the cereal *VERNALIZATION1* gene. *Journal of Experimental Botany* **64**: 2413–2422.

Oliver SN, Finnegan EJ, Dennis ES, Peacock WJ, Trevaskis B. 2009. Vernalization-induced flowering in cereals is associated with changes in histone methylation at the *VERNALIZATION1* gene. *Proceedings of the National Academy of Sciences of the United States of America* **106**: 8386–8391.

Oravec MW, Greenham K. 2022. The adaptive nature of the plant circadian clock in natural environments. *Plant Physiology* **190**: 968–980.

Pardo J, VanBuren R. 2021. Evolutionary innovations driving abiotic stress tolerance in C_4 grasses and cereals. *The Plant Cell* **33**: koab205-.

Pardo J, Wai CM, Chay H, Madden CF, Hilhorst HWM, Farrant JM, VanBuren R. 2020. Intertwined signatures of desiccation and drought tolerance in grasses. *Proceedings of the National Academy of Sciences of the United States of America* **117**: 10079–10088.

Pearce S, Kippes N, Chen A, Debernardi JM, Dubcovsky J. 2016. RNA-seq studies using wheat *PHYTOCHROME B* and *PHYTOCHROME C* mutants reveal shared and specific functions in the regulation of flowering and shade-avoidance pathways. *BMC Plant Biology* **16**: 141.

Petersen K, Didion T, Andersen CH, Nielsen KK. 2004. MADS-box genes from perennial ryegrass differentially expressed during transition from vegetative to reproductive growth. *Journal of Plant Physiology* **161**: 439–447.

Pham VN, Kathare PK, Huq E. 2017. Phytochromes and phytochrome interacting factors. *Plant Physiology* **176**: 1025–1038.

Pin PA, Nilsson O. 2012. The multifaceted roles of *FLOWERING LOCUS T* in plant development. *Plant, Cell & Environment* **35**: 1742–1755.

Pirie MD, Humphreys AM, Barker NP, Linder HP. 2009. Reticulation, data combination, and inferring evolutionary history: An example from Danthonioideae (Poaceae). *Systematic Biology* **58**: 612–628.

Pittendrigh CS. 1960. Circadian rhythms and the circadian organization of living systems. *Cold Spring Harbor Symposia on Quantitative Biology* **25**: 159–184.

Pittendrigh CS, Minis DH. 1964. The entrainment of circadian oscillations by light and their role as photoperiodic clocks. *The American Naturalist* **98**: 261–294.

Poethig RS. 1990. Phase change and the regulation of shoot morphogenesis in plants. *Science* **250**: 923–930.

Preston JC, Christensen A, Malcomber ST, Kellogg EA. 2009. MADS-box gene expression and implications for developmental origins of the grass spikelet. *American Journal of Botany* **96**: 1419–1429.

Preston JC, Fjellheim S. 2020. Understanding past, and predicting future, niche transitions based on grass flowering time variation. *Plant Physiology* **183**: 822–839.

Preston JC, Hileman LC, Cubas P. 2011. Reduce, reuse, and recycle: developmental evolution of trait diversification. *American Journal of Botany* **98**: 397–403.

Preston JC, Kellogg EA. 2006. Reconstructing the evolutionary history of paralogous *APETALA1/FRUITFULL*-like genes in grasses (Poaceae). *Genetics* **174**: 421–437.

Preston JC, Kellogg EA. 2007. Conservation and divergence of *APETALA1/FRUITFULL*-like gene function in grasses: evidence from gene expression analyses. *The Plant Journal* **52**: 69–81.

Preston JC, Kellogg EA. 2008. Discrete developmental roles for temperate cereal grass *VERNALIZATION1/FRUITFULL*-like genes in flowering competency and the transition to flowering. *Plant Physiology* **146**: 265–276.

Preston JC, Sandve SR. 2013. Adaptation to seasonality and the winter freeze. *Frontiers in Plant Science* **4**: 167.

Purvis ON. 1934. An analysis of the influence of temperature during germination on the subsequent development of certain winter cereals and its relation to the effect of length of day. *Annals of Botany* **48**: 919–955.

Quail PH. 2002. Phytochrome photosensory signalling networks. *Nature Reviews Molecular Cell Biology* **3**: 85–93.

Raissig MT, Woods DP. 2022. The wild grass *Brachypodium distachyon* as developmental model system. *Current Topics in Developmental Biology* **147**: 33–71.

Ramsay JO, Li X. 1998. Curve registration. *Journal of the Royal Statistical Society B: Statistical Methodology* **60**: 351–363.

Ramsay JO, Silverman BW. 2005. *Functional Data Analysis*. New York, NY, USA: Springer.

Ream TS, Woods DP, Amasino R. 2012. The molecular basis of vernalization in different plant groups. *Cold Spring Harbor Symposia on Quantitative Biology* **77**: 105–115.

Romaschenko K, Peterson PM, Soreng RJ, Garcia-Jacas N, Futorna O, Susanna A. 2012. Systematics and evolution of the needle grasses (Poaceae: Pooideae: Stipeae) based on analysis of multiple chloroplast loci, ITS, and lemma micromorphology. *Taxon* **61**: 18–44.

Sandve SR, Fjellheim S. 2010. Did gene family expansions during the Eocene–Oligocene boundary climate cooling play a role in Pooideae adaptation to cool climates? *Molecular Ecology* **19**: 2075–2088.

Sasani S, Hemming MN, Oliver SN, Greenup A, Tavakkol-Afshari R, Mahfoozi S, Poustini K, Sharifi H-R, Dennis ES, Peacock WJ, *et al.* 2009. The influence of vernalization and daylength on expression of flowering-time genes in the shoot apex and leaves of barley (*Hordeum vulgare*). *Journal of Experimental Botany* **60**: 2169–2178.

Sawa M, Kay SA, Imaizumi T. 2008. Photoperiodic flowering occurs under internal and external coincidence. *Plant Signaling & Behavior* **3**: 269 271.

Schubert M, Grønvold L, Sandve SR, Hvidsten TR, Fjellheim S. 2019a. Evolution of cold acclimation and its role in niche transition in the temperate grass subfamily Pooideae. *Plant Physiology* **180**: 404–419.

Schubert M, Humphreys AM, Lindberg CL, Preston JC, Fjellheim S. 2020. To *coldly* go where no grass has gone before: A multidisciplinary review of cold adaptation in Poaceae. *Annual Plant Reviews* **3**: 523–562.

Schubert M, Marcussen T, Meseguer AS, Fjellheim S. 2019b. The grass subfamily Pooideae: Cretaceous–Palaeocene origin and climate-driven Cenozoic diversification. *Global Ecology and Biogeography* **28**: 1168–1182.

Seaton DD, Graf A, Baerenfaller K, Stitt M, Millar AJ, Gruissem W. 2018. Photoperiodic control of the *Arabidopsis* proteome reveals a translational coincidence mechanism. *Molecular Systems Biology* **14**: e7962.

Shang HL. 2014. A survey of functional principal component analysis. *Advances in Statistical Analysis* **98**: 121–142.

Shantz HL. 1954. The place of grasslands in the earth's cover. *Ecology* **35**: 143–145.

Shaw LM, Turner AS, Laurie DA. 2012. The impact of photoperiod insensitive *Ppd-1a* mutations on the photoperiod pathway across the three genomes of hexaploid wheat (*Triticum aestivum*). *The Plant Journal* **71**: 71 84.

Somers DE. 1999. The physiology and molecular bases of the plant circadian clock. *Plant Physiology* **121**: 9–20.

Song JJ, Deng W, Lee H-J, Kwon D. 2008. Optimal classification for time-course gene expression data using functional data analysis. *Computational Biology and Chemistry* **32**: 426–432.

Song YH, Kubota A, Kwon MS, Covington MF, Lee N, Taagen ER, Cintrón DL, Hwang DY, Akiyama R, Hodge SK, *et al.* 2018. Molecular basis of flowering under natural long-day conditions in *Arabidopsis*. *Nature Plants* **66**: 441.

Song JJ, Lee H-J, Morris JS, Kang S. 2007. Clustering of time-course gene expression data using functional data analysis. *Computational Biology and Chemistry* **31**: 265–274.

Song YH, Shim JS, Kinmonth-Schultz HA, Imaizumi T. 2015. Photoperiodic flowering: Time measurement mechanisms in leaves. *Annual Review of Plant Biology* **66**: 441–464.

Soreng RJ, Peterson PM, Romaschenko K, Davidse G, Teisher JK, Clark LG, Barberá P, Gillespie LJ, Zuloaga FO. 2017. A worldwide phylogenetic classification of the Poaceae (Gramineae) II: An update and a comparison of two 2015 classifications. *Journal of Systematics and Evolution* **55**: 259–290.

Soreng RJ, Peterson PM, Romaschenko K, Davidse G, Zuloaga FO, Judziewicz EJ, Filgueiras TS, Davis JI, Morrone O. 2015. A worldwide phylogenetic classification of the Poaceae (Gramineae). *Journal of Systematics and Evolution* **53**: 117–137.

Soreng RJ, Peterson PM, Zuloaga FO, Romaschenko K, Clark LG, Teisher JK, Gillespie LJ, Barberá P, Welker CAD, Kellogg EA, *et al.* 2022. A worldwide phylogenetic classification of the Poaceae (Gramineae) III: An update. *Journal of Systematics and Evolution* **60**: 476–521.

Strömberg CAE. 2011. Evolution of grasses and grassland ecosystems. *Annual Review of Earth and Planetary Sciences* **39**: 517–544.

Trevaskis B, Hemming MN, Dennis ES, Peacock WJ. 2007. The molecular basis of vernalization-induced flowering in cereals. *Trends in Plant Science* **12**: 352–357.

Trevaskis B, Hemming MN, Peacock WJ, Dennis ES. 2006. *HvVRN2* responds to daylength, whereas *HvVRN1* is regulated by vernalization and developmental status. *Plant Physiology* **140**: 1397–1405.

Turck F, Fornara F, Coupland G. 2008. Regulation and identity of florigen: *FLOWERING LOCUS T* moves center stage. *Annual Review of Plant Biology* **59**: 573–594.

Turner A, Beales J, Faure S, Dunford RP, Laurie DA. 2005. The pseudo-response regulator Ppd-H1 provides adaptation to photoperiod in barley. *Science* **310**: 1031–1034.

Tzvelev NN. 1989. The system of grasses (Poaceae) and their evolution. *The Botanical Review* **55**: 141–203.

Veizer J, Godderis Y, François LM. 2000. Evidence for decoupling of atmospheric CO_2 and global climate during the Phanerozoic eon. *Nature* **408**: 698–701.

Vigeland MD, Spannagl M, Asp T, Paina C, Rudi H, Rognli OA, Fjellheim S, Sandve SR. 2013. Evidence for adaptive evolution of low-temperature stress response genes in a Pooideae grass ancestor. *New Phytologist* **199**: 1060–1068.

Visser V, Clayton WD, Simpson DA, Freckleton RP, Osborne CP. 2014. Mechanisms driving an unusual latitudinal diversity gradient for grasses. *Global Ecology and Biogeography* **23**: 61–75.

Visser V, Woodward FI, Freckleton RP, Osborne CP. 2012. Environmental factors determining the phylogenetic structure of C_4 grass communities. *Journal of Biogeography* **39**: 232–246.

Woods DP, Bednarek R, Bouché F, Gordon SP, Vogel JP, Garvin DF, Amasino R. 2017. Genetic architecture of flowering-time variation in *Brachypodium distachyon*. *Plant Physiology* **173**: 269 279.

Woods D, Dong Y, Bouché F, Bednarek R, Rowe M, Ream T, Amasino R. 2019. A florigen paralog is required for short-day vernalization in a pooid grass. *eLife* **8**: 27.

Woods DP, Li W, Sibout R, Shao M, Laudencia-Chingcuanco D, Vogel JP, Dubcovsky J, Amasino RM. 2023. PHYTOCHROME C regulation of photoperiodic flowering via *PHOTOPERIOD1* is mediated by *EARLY FLOWERING 3* in *Brachypodium distachyon*. *PLOS Genetics* **19**: e1010706.

Woods DP, McKeown M, Dong Y, Preston JC, Amasino R. 2016. Evolution of *VRN2/Ghd7*-like genes in vernalization-mediated repression of grass flowering. *Plant Physiology* **170**: 2124–2135.

Woods DP, Ream TS, Minevich G, Hobert O, Amasino R. 2014. PHYTOCHROME C is an essential light receptor for photoperiodic flowering in the temperate grass, *Brachypodium distachyon*. *Genetics* **198**: 397–408.

Wu G, Anafi RC, Hughes ME, Kornacker K, Hogenesch JB. 2016. MetaCycle: an integrated R package to evaluate periodicity in large scale data. *Bioinformatics* **32**: 3351–3353.

Wu S, Wu H. 2013. More powerful significant testing for time course gene expression data using functional principal component analysis approaches. *BMC Bioinformatics* **14**: 6.

Yakir E, Hilman D, Harir Y, Green RM. 2007. Regulation of output from the plant circadian clock. *The FEBS Journal* **274**: 335–345.

Yang J, Bertolini E, Braud M, Preciado J, Chepote A, Jiang H, Eveland AL. 2021. The SvFUL2 transcription factor is required for inflorescence determinacy and timely flowering in *Setaria viridis*. *Plant Physiology* **187**: 1202–1220.

Zachos J, Pagani M, Sloan L, Thomas E, Billups K. 2001. Trends, rhythms, and aberrations in global climate 65 Ma to present. *Science* **292**: 686–693.

Zeevaart JA. 2008. Leaf-produced floral signals. *Current Opinion in Plant Biology* **11**: 541–547.

Zhang L, Zhu X, Zhao Y, Guo J, Zhang T, Huang W, Huang J, Hu Y, Huang C-H, Ma H. 2022. Phylotranscriptomics resolves the phylogeny of Pooideae and uncovers factors for their adaptive evolution. *Molecular Biology and Evolution* **39**: msac026.

Zhao X, Guo Y, Kang L, Yin C, Bi A, Xu D, Zhang Z, Zhang J, Yang X, Xu J, *et al.* 2023. Population genomics unravels the Holocene history of bread wheat and its relatives. *Nature Plants* **9**: 403–419.

Zheng T, Sun J, Zhou S, Chen S, Lu J, Cui S, Tian Y, Zhang H, Cai M, Zhu S, *et al.* 2019. Post-transcriptional regulation of Ghd7 protein stability by phytochrome and OsGI in photoperiodic control of flowering in rice. *New Phytologist* **224**: 306–320.

Zhong J, Robbett M, Poire A, Preston JC. 2018. Successive evolutionary steps drove Pooideae grasses from tropical to temperate regions. *New Phytologist* **217**: 925–938.

Paper I

Independent recruitment of *FRUITFULL*-like transcription factors in the convergent origins of vernalization-responsive grass flowering

Paliocha M, Schubert M, Preston JC & Fjellheim S

Molecular Phylogenetics and Evolution, 2023, 179: 107678

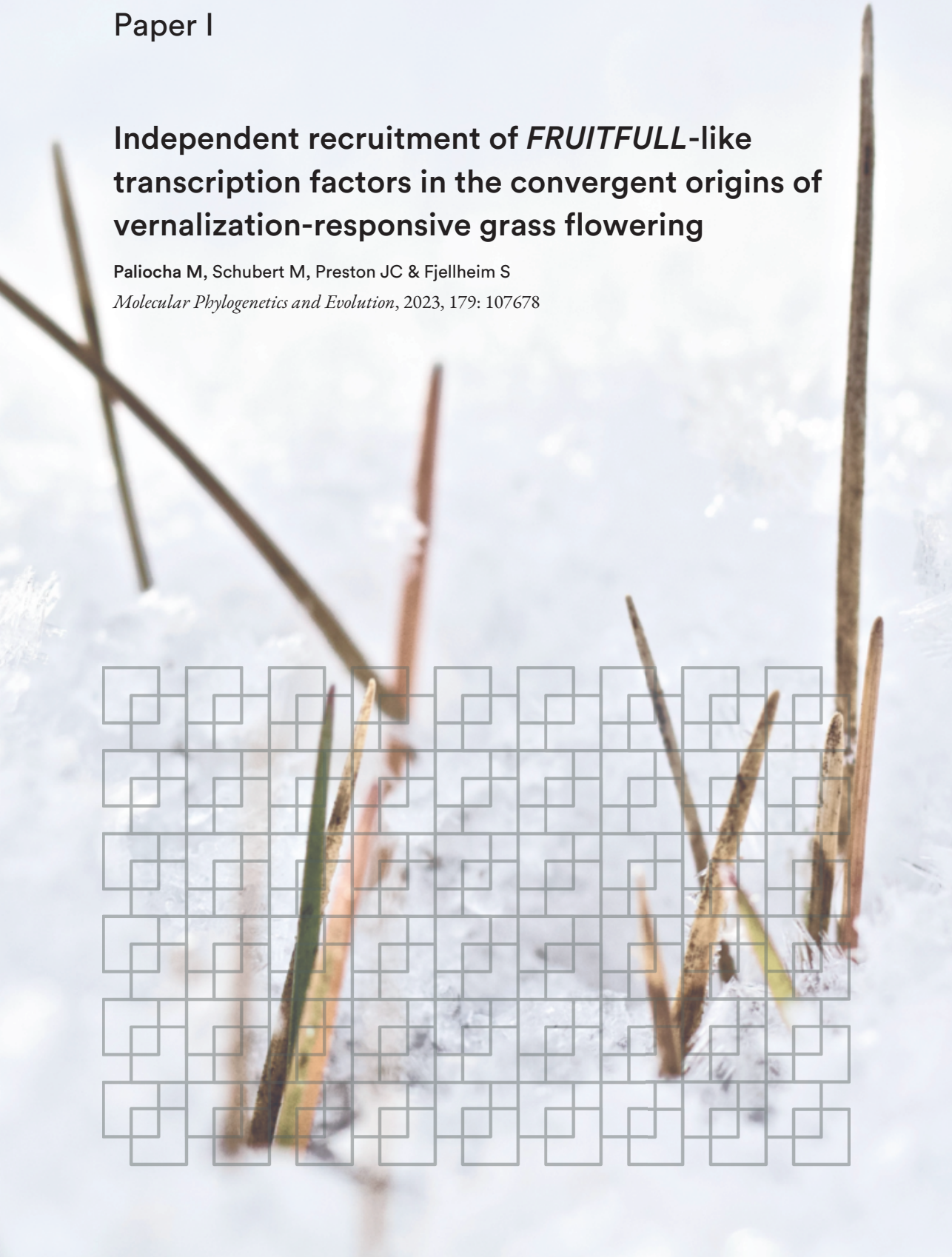

Molecular Phylogenetics and Evolution 179 (2023) 107678

Contents lists available at ScienceDirect

Molecular Phylogenetics and Evolution

journal homepage: www.elsevier.com/locate/ympev

Independent recruitment of *FRUITFULL*-like transcription factors in the convergent origins of vernalization-responsive grass flowering

Martin Paliocha [a], Marian Schubert [a], Jill Christine Preston [b], Siri Fjellheim [a,*]

[a] Department of Plant Sciences, Faculty of Biosciences, Norwegian University of Life Sciences, N-1432 Ås, Norway
[b] Department of Plant Biology, College of Agriculture and Life Sciences, The University of Vermont, Burlington, VT 05405, USA

ARTICLE INFO

Keywords:
Convergent evolution
Flowering time
Grass evolution
Parallel evolution
Vernalization
VRN1

ABSTRACT

Flowering in response to low temperatures (vernalization) has evolved multiple times independently across angiosperms as an adaptation to match reproductive development with the short growing season of temperate habitats. Despite the context of a generally conserved flowering time network, evidence suggests that the genes underlying vernalization responsiveness are distinct across major plant clades. Whether different or similar mechanisms underlie vernalization-induced flowering at narrower (e.g., family-level) phylogenetic scales is not well understood. To test the hypothesis that vernalization responsiveness has evolved convergently in temperate species of the grass family (Poaceae), we carried out flowering time experiments with and without vernalization in several representative species from different subfamilies. We then determined the likelihood that vernalization responsiveness evolved through parallel mechanisms by quantifying the response of Pooideae vernalization pathway *FRUITFULL* (*FUL*)-like genes to extended periods of cold. Our results demonstrate that vernalization-induced flowering has evolved multiple times independently in at least five grass subfamilies, and that different combinations of *FUL*-like genes have been recruited to this pathway on several occasions.

1. Introduction

Most plant species couple endogenous and exogenous cues to regulate growth and development (Bernier, 1988; Poethig, 1990), resulting in flower, fruit, and/or seed production when conditions are favorable, thus increasing reproductive output and fitness (Bäurle and Dean, 2006; Murfet, 1977). In temperate species, the ability to respond to inductive flowering cues (i.e., attain floral competency) can often be hastened by an extended period of non-freezing cold known as vernalization (Chouard, 1960; Gaβner, 1918). Once floral competency is achieved, long days trigger the subsequent transition to reproductive growth at the shoot apical meristem (SAM). This two-step induction of flowering, prompted by the interplay of vernalization and photoperiodic cues, is found in many species across angiosperms (Andrés and Coupland, 2012; Bouché et al., 2017; Preston and Fjellheim, 2020; Preston and Sandve, 2013; Ream et al., 2012; Xu and Chong, 2018).

The vernalization-mediated flowering response is particularly well-studied in agriculturally important temperate grasses. Many grass species are identified as vernalization responsive based on their flowering behavior, but almost all are members of the temperate subfamily Pooideae (Heide, 1994). According to the current model from vernalization responsive 'winter' wheat (*Triticum* spp.) and barley (*Hordeum vulgare*) (Pooideae), cold-induced floral competency is controlled by a genetic circuit involving the mutual regulation of three central genes: *VERNALIZATION 1–3* (*VRN1–3*) (Bouché et al., 2017; Dennis and Peacock, 2009; Greenup et al., 2009; Trevaskis et al., 2007). During autumnal growth of winter wheat and barley, transcription of the flowering pathway integrator gene *VRN3/FLOWERING LOCUS T (FT)*-like is repressed by the action of the long day induced CONSTANS-like protein VRN2, resulting in a block on flowering before the onset of winter (Ream et al., 2014; Szűcs et al., 2007; Yan et al., 2004). As plants start to experience cold, expression of the *FRUITFULL* (*FUL*)-like MADS-box gene *VRN1* (*FUL1*-clade in Preston and Kellogg, 2006) gradually increases, causing the eventual repression and de-repression of *VRN2* and *VRN3*, respectively (Danyluk et al., 2003; Gu et al., 1998; Hemming et al., 2008; Higgins et al., 2010; Oliver et al., 2009; Shimada et al., 2009; Trevaskis, 2010; Trevaskis et al., 2003; Woods et al., 2016; Yan et al., 2004, 2003). Production of VRN1 is elicited by cold-induced histone modifications at the *VRN1* locus, which links the perception of winter with the acquisition of flowering competency (Deng et al., 2015;

* Corresponding author at: Department of Plant Sciences, Faculty of Biosciences, Norwegian University of Life Sciences, P.O. BOX 5003, N-1432 Ås, Norway.
E-mail addresses: martin.paliocha@nmbu.no (M. Paliocha), marian.schubert@nmbu.no (M. Schubert), jill.preston@uvm.edu (J.C. Preston), siri.fjellheim@nmbu.no (S. Fjellheim).

https://doi.org/10.1016/j.ympev.2022.107678
Received 19 August 2022; Received in revised form 8 December 2022; Accepted 13 December 2022
Available online 16 December 2022

Distelfeld et al., 2009; Oliver et al., 2013, 2009). Furthermore, it is hypothesized that the florigen signal is enhanced by mutual positive feedback between the expression of *VRN1* and *VRN3*, whereby VRN1 carries out a secondary, deeply conserved function to promote flower development at the SAM (Ferrándiz et al., 2000; Gu et al., 1998; Preston and Kellogg, 2008; Tanaka et al., 2018).

In addition to *VRN1*, grasses have at least three other *FUL*-like genes (*FUL2, FUL3,* and *FUL4*, collectively referred to as *FUL*-like genes) derived from three duplication events (Wu et al., 2017; Zhang et al., 2022). One coinciding with the τ whole-genome duplication event in commelinids giving rise to the *FUL3/FUL4 and FUL1/FUL2* lineages (Jiao et al., 2014; Zhang et al., 2022), and the σ and ρ polyploidizations generating *FUL3* and *FUL4* in Poales and *VRN1* and *FUL2* in most of Poaceae, respectively (D'Hont et al., 2012; Graham et al., 2006; Litt and Irish, 2003; McKain et al., 2016; Paterson et al., 2004; Preston and Kellogg, 2006; Preston et al., 2009; Zhang et al., 2022). All three genes are expressed in the SAM during the floral transition (Danilevskaya et al., 2008; Kinjo et al., 2012; Preston and Kellogg, 2007), consistent with their likely ancestral function in floral meristem and organ identity specification (Litt, 2007). In wheat, *FUL*-like genes are redundantly involved in spikelet and inflorescence development, as well as flowering time and plant height (Li et al. 2019). While several angiosperm *FUL*-like genes are also expressed in leaves or bracts (Gu et al., 1998; Yang et al., 2021), a role for these genes in vernalization through their upregulation in leaves has only been described in Pooideae grasses (McKeown et al., 2016; Zhong et al. 2018). This is consistent with the inferred origin of vernalization responsiveness at the base of the subfamily (McKeown et al., 2016). However, the fact that *FUL2* transcripts also increase in response to cold in the Pooideae species *Lolium perenne* (Petersen et al., 2006, 2004), *Avena sativa* (Preston and Kellogg, 2007) *Triticum aestivum* (Chen and Dubcovsky, 2012), *Schedonorus pratensis* (Ergon et al., 2016, 2013), and *Brachypodium distachyon* (Li et al., 2016) either suggests the evolution of a common upstream regulator for these genes or a propensity of grass *FUL*-like genes to be independently co-opted into vernalization pathways.

Grasses are one of the largest plant families with 11,783 species organized into 12 subfamilies (Soreng et al., 2022). Most species are found in two large clades: the largely temperate/subtropicalBambusoideae–Oryzoideae–Pooideae (BOP) clade or the mainly tropical Panicoideae–Aristidoideae–Chlorioideae–Micrairoideae–Arundinoideae –Danthonioideae (PACMAD) clade. There are also three early-diverging subfamilies with a small number of species (Anomochlooideae, Pueloideae and Pharoideae; Saarela et al., 2015; Soreng et al., 2022; Hodkinson, 2018). Although most grasses have tropical to sub-tropical distributions (Schubert et al., 2019b; Visser et al., 2014), temperate grasses have evolved multiple times in both the major BOP and PACMAD clades (Grass Phylogeny Working Group II, 2012). Pooideae dominate the grass flora in temperate, continental, and Arctic regions (Hartley, 1973), and Danthonioideae constitute a southern temperate clade (Pirie et al., 2012; Peter Linder et al., 2013; Visser et al., 2014). Furthermore, several lineages from other subfamilies, most notably Chloridoideae and Arundinoideae have also diversified into cold climate environments (Schubert et al., 2020; Atkinson et al., 2016). Despite this, little is known about the impact of vernalization on flowering in temperate grass species outside Pooideae. Evans and Knox (1969) report that in some temperate, long day-responsive ecotypes of *Themeda triandra* (Panicoideae), flowering is hastened after vernalization treatment. Furthermore, evidence from a growth experiment carried out on several populations of *Rytidosperma caespitosa*, suggests that some Danthonioideae may also be able to accelerate flowering following exposure to long-term cold (Hodgkinson and Quinn, 1978).

To determine how widespread vernalization responsive flowering is across grasses, we carry out growth experiments on a phylogenetically diverse set of temperate PACMAD species and use these data to reconstruct the minimum number of origins of vernalization responsive flowering in grasses. We then investigate the genetic basis of these origins by examining the behavior of the paralogs *VRN1* and *FUL2* during prolonged cold. We find evidence for multiple origins of vernalization responsiveness across grasses and present data supporting evolution of this trait through the parallel recruitment of different *FUL* homologs.

2. Materials and methods

2.1. Plant material

Study species were selected to reflect the phylogenetic diversity and geographical distribution of temperate, perennial PACMAD grasses based on a previous study (Atkinson et al., 2016). Seeds for five species from a total of seven accessions (Table S1) were acquired from the United States Department of Agriculture (USDA) Germplasm Resources Information Network (GRIN). Imbibed seeds for four accessions were sown out in humid soil containing equal amounts of compost and peat with a small amount of river sand. To break seed dormancy and synchronize germination, seeds were stratified in the dark at 4 ℃ for 5 days, followed by 24 h at 25 ℃. Seedlings were pricked out and transferred to individual pots. For three *Danthonia decumbens* and two *Molinia caerulea* populations, wild full-grown plants were collected at four different locations in south-eastern and western Norway (Table S2).

To synchronize plants grown from seed and collected in nature, all individuals were pre-grown at 17 ℃ under long days (16 h light, 8 h darkness) for at least four weeks in a greenhouse at the Norwegian University of Life Sciences (NMBU). At least 30 plants per population/accession were grown per treatment. Artificial light was supplied in addition to natural light during the light period using Master HPI-T Plus 400 W/645 E40 1SL light bulbs (Philips). For every population, the SAM of the largest plant was dissected prior to vernalization treatment to ensure that meristems were in the vegetative state. At least 15 plants from every population were assigned to a vernalization (8 ℃) or control treatment (20 ℃), respectively and transferred to walk-in growth chambers for 56 days (8 weeks). A relatively high vernalization temperature within the temperature range for optimal vernalization (Preston and Fjellheim, 2022) was chosen based on preliminary experiments at lower (4–6 ℃) temperatures that resulted in high *T. triandra* mortality. Two chambers per condition were used to reduce chamber effects. In each chamber photoperiod was set to short days (8 h light, 16 h darkness) and the average light irradiance was 65 μmol m^{-2} s^{-1}. Subsequently, plants were transferred back to the greenhouse, wherein emergence of the first inflorescence (bolting or 'heading') was scored as days from germination to heading (*DTH*). During the entire experiment, plants were randomized and rotated every fourth day to minimize room effects.

To account for differential growth in the vernalized and control plants, corrected *DTH* (DTH_C) was calculated using temperature-adjusted days, rather than subtracting the entire duration of the temperature treatment from *DTH*. Assuming a linear relationship between growth and temperature (Baskerville and Emin, 1969), it was presumed that plants in the control treatment (17 ℃) accumulated 2.125 times more heat units than vernalized plants, given a growth baseline below 8 ℃. DTH_C for vernalized plants was thus calculated as:

$$DTH_C = DTH - \left[L \cdot \frac{(T_C - T_V)}{T_C}\right]$$

where L the length of the vernalization period (56 days), T_C the temperature for the control group (17 ℃), and T_V the vernalization temperature (8 ℃) (Baloch et al., 2003; Kirby et al., 1989; McKeown et al., 2016; Preston and Fjellheim 2022).

2.2. Sampling, RNA extraction, and cDNA synthesis

To test if *VRN1* and *FUL2* are induced by cold in species from the

PACMAD clade, we selected three species (*M. caerulea, D. decumbens*, and *B. gracilis*) for analysis of gene expression in leaves under vernalization. During the growth chamber experiments, leaf tissue from the longest leaf was collected for RNA extraction at zeitgeber time 3 (ZT3; i.e., 3 h after lights on) for three different time points: before the plants were moved to the growth chambers (day 0), and after six weeks (day 42) and eight weeks (day 56) of vernalization. A TissueLyser II bead mill and 3 mm tungsten carbide beads (QIAGEN) were used to disrupt deep frozen leaf tissue. Total RNA was isolated with RNeasy Plant Mini Kit (QIAGEN), following the manufacturer's instructions, including the additional centrifugation and elution step. Complementary DNA (cDNA) was synthesized using the iScript cDNA Synthesis Kit (Bio-Rad Laboratories) following the protocol provided by the manufacturer.

2.3. Target gene isolation

The target genes *M. caerulea VRN1* (*McVRN1*), *D. decumbens VRN1* (*DdVRN1*), *M. caerulea FUL2* (*McFUL2*), and *D. decumbens FUL2* (*DdFUL2*) were PCR-amplified from cDNA using primers designed by Preston and Kellogg (2006) and McKeown et al. (2016) as well as RT-qPCR primers created in this study (Table S4). Amplicons were purified with ExoSAP-IT (Affymetrix), sub-cloned using the pGEM-T Easy cloning vector system (Promega) and transformed into chemically competent *Escherichia coli* JM109 cells (Promega). All steps were performed following the manufacturer's protocol but using half the reaction volume for the ligation reaction with 1.5 μL PCR product. After plating and 24 h of incubation, successfully transformed colonies were picked from the growth medium. Sub-cloned PCR products were then amplified from the plasmid vector using M13 forward and reverse primers. Partial coding sequences were obtained by Sanger dideoxy sequencing performed at the University of Vermont (UVM) Integrative Genomics Resource using SP6 sequencing primers. Residual plasmid vector contamination was removed from putative *VRN1* and *FUL2* sequences using NCBI's UniVec database (NCBI Resource Coordinators, 2017) and blastn v2.7.1 (Altschul et al., 1990; Camacho et al., 2009; Zhang et al., 2000) with default search parameters prior to further analysis.

Target gene sequences for *T. triandra* were obtained by genome assembly of raw reads of seven genome-skimmed individuals (Dunning et al., 2017; Olofsson et al., 2016). Sequence data were downloaded from NCBI's Sequence Read Archive (Leinonen et al., 2011) and assembled using MaSuRCA v3.2.6 (Zimin et al., 2013) with *k*-mer length $k = 106$ estimated with KmerGenie v1.7051 (Chikhi and Medvedev, 2013), and SOAPdenovo2 r240 for scaffolding (Luo et al., 2012). Target genes were identified using megablast v2.7.1 (Camacho et al., 2009) with default search strategy and introns removed manually to obtain coding sequences. For *Bouteloua gracilis,* genes were identified by PCR amplification with primers designed for *T. triandra* and *D. decumbens* and confirmed by Sanger dideoxy sequencing and subsequent phylogenetic analysis.

2.4. Phylogenetic analysis

Target gene sequences were added to a representative selection of 54 *FUL* homologs from 32 monocot taxa (McKeown et al., 2016; Preston and Kellogg, 2006) and realigned using the R package DECIPHER v2.17.1 (Wright, 2016, 2015). *FUL3* sequences were retrieved from GenBank (Benson et al., 2012) and added to the multiple sequence alignment with MAFFT v7.505 L-INS-I using the –keeplength and –add options (Katoh and Standley, 2013). After manual inspection and adjustment of the alignment, the best nucleotide substitution model was determined based on AICc calculations by the modelTest function from the R package phangorn v2.5.5 (Darriba et al., 2012; Schliep, 2011). Gene trees were inferred using BEAST v1.10.4 (Suchard et al., 2018) and BEAGLE v3.1.2 (Ayres et al., 2012), assuming an uncorrelated, log-normal relaxed clock (Drummond et al., 2006), a general time-reversible substitution model including gamma distributed rate variations with four discrete categories, and invariable sites (GTR + Γ + I; Hasegawa et al., 1985; Tavaré, 1986; Yang, 1994), and a Yule two-parameter prior (Gernhard, 2008; Yule, 1925). Two independent BEAST analyses were run for 1.0×10^8 generations and sampled every 1,000th generation. Convergence of both runs combined was assessed using Tracer v1.7.1 (Rambaut et al., 2018) with 25 % of the trees discarded as burn-in. The maximum clade credibility tree was rescaled to reflect posterior node heights and visualized with ggtree v3.4.0 (Yu et al., 2017).

2.5. RT-qPCR

To quantify the relative abundance of *VRN1* and *FUL2* mRNA from the exemplar taxa *D. decumbens* 'SY', *M. caerulea* 'HV', *T. triandra* 'NSW', and *B. gracilis*, gene-specific RT-qPCR primers were designed using Primer3 v4.1.0 with default settings (Untergasser et al., 2012). Two housekeeping genes, *ELONGATION FACTOR 1α* (*EF1α*) and *UBIQUITIN 5* (*UBQ5*), served as references for the relative quantification and were amplified using primers designed by McKeown et al. (2016). Amplicon identity of target and reference genes was confirmed by Sanger dideoxy sequencing (Eurofins GATC and Azenta GENEWIZ). Primer efficiencies were determined using a 2-fold dilution series (Schmittgen and Livak, 2008), starting with a 1:10 cDNA dilution. Amplification efficiencies were between 0.90 and 1.10 for all primer pairs (Bustin et al., 2009; Pfaffl, 2001).

Transcript abundance was quantified with an Applied Biosystems 7500 Fast instrument (ThermoFisher Scientific; *M. caerulea*) or a CFX96 Touch Real-Time PCR Detection System (Bio-Rad Laboratories; *B. gracilis*, *D. decumbens*, and *T. triandra*), using Applied Biosystems SYBR Select Master Mix (ThermoFisher Scientific) with a total reaction volume of 10 μL per well. Quantification was carried out on five biological replicates (except *M. caerulea* week 8, vernalized, where $n = 4$ and *B. gracilis* week 6, where $n = 3$) and three technical replicates. Fluorescence data for each gene were pre-processed using the CPP function from the R package chipPCR v0.0.8–10 (Rödiger et al., 2015). Amplification curves were normalized between 0 and 1 and smoothed using a 3-point Savitzky–Golay filter (Savitzky and Golay, 1964). The slope of the overall background trend (baseline) was estimated by linear regression and subtracted from the fluorescence signals (Rödiger et al., 2015). Quantification cycles were determined by calculating the second derivative centre (geometric mean of the second derivative minimum and maximum) of the normalized, smoothed and baseline-corrected amplification curves (Tellinghuisen and Spiess, 2014). Mean expression of every gene at the first sampling point (week 0) was used as internal reference to calculate ΔC_q. Target gene expression was then normalized relative to the geometric mean of *EF1α* and *UBQ5* expression ($\Delta\Delta C_q$) (Vandesompele et al., 2002). All C_q values were corrected by the amplification efficiency of their corresponding RT-qPCR primers.

2.6. Statistical analyses

Computations and statistical analyses were carried out in R v4.0.2 (R Core Team, 2020). Flowering data was analyzed using Mann–Whitney *u*-tests (Mann and Whitney, 1947). Effects of temperature treatment, time and interaction between time and treatment on gene expression were analyzed using two-way ANOVAs using the lm function from R's stats package (R Core Team, 2020) omitting data from the reference time point (week 0). Post-hoc tests were carried out with multcomp v1.4–14 (Hothorn et al., 2008) using Tukey-type contrast matrices to construct appropriate general linear hypotheses between vernalized and non-vernalized material after 6 and 8 weeks, respectively.

3. Results

3.1. Identification of vernalization-responsive species

In total, 12 accessions from seven PACMAD species occurring in the temperate zone were surveyed in this study (Table S1-S2). Statistical analysis of differential flowering time was performed for populations that produced at least five flowering individuals per treatment until the termination of the experiment after 300 days (12 populations, see Fig. 1). In 11 of these 12 accessions, vernalized plants flowered significantly earlier ($P < 0.05$; Mann–Whitney *u*-test) than non-vernalized plants (Fig. 1). One population of *T. triandra* (Panicoideae) originating from Eastern Cape, South Africa (PI 206348; Table S2; 'ZA1′ in Fig. 1) was the only flowering accession that did not significantly respond to vernalization. The strongest response to vernalization was observed in *B. gracilis* (Chloridoideae) and one population of *M. caerulea* (Arundinoideae) collected as full-grown plants in Hvaler, south-eastern Norway ('HV' in Fig. 1).

3.2. Candidate gene identification

For two of the study species (*D. decumbens* and *M. caerulea*), partial coding sequences for *VRN1* and its paralog *FUL2* were obtained by bacterial plasmid sub-cloning. Subsequent Sanger sequencing from the vector yielded one 400 bp nucleotide sequence for *McVRN1* and *DdFUL2*. Primers designed for the RT-qPCR assay based on these sequences were used to amplify and isolate *M. caerulea FUL2* (*McFUL2*, using *DdFUL2* qPCR primers) and *D. decumbens VRN1* (*DdVRN1*, using *McVRN1* qPCR primers). This approach resulted in the amplification of shorter *McFUL2* and *DdVRN1* regions relative to *DdFUL2* and *McVRN1*. Thus, a 334 bp sequence of *DdVRN1* was isolated, in addition to a 115 bp amplicon of *McFUL2*. Partial coding sequences of *Themeda triandra VRN1* (*TtVRN1*) and *FUL2* (*TtFUL2*) recovered from genomic DNA were 785 bp and 714 bp long, respectively. Sequences from *Bouteloua gracilis* material generated with RT-qPCR primers from *D. decumbens* had lengths of 104 bp (*BgVRN1*) and 159 bp (*BgFUL2*), respectively.

Identity of newly generated *FUL*-like nucleotide sequences was confirmed by generating a gene tree using Bayesian inference. Putative *VRN1* and *FUL2* sequences were placed in two clades together with *VRN1* and *FUL2* orthologs from other PACMAD taxa, respectively (Fig. 2). The topology of the inferred gene tree is congruent with the results of Preston and Kellogg (2006), whose multiple sequence alignment served as the basis for the phylogenetic analysis. Consistent with previous findings (McKeown et al., 2016; Preston and Kellogg, 2006; Zhang et al., 2022), strong support for a gene duplication event at the base of the Poaceae giving rise to the paralogs *VRN1* and *FUL2* was found in the inferred gene tree. Within the *FUL2* clade, the division of the grass family into early-diverging and 'crown Poaceae' (BOP and PACMAD) is evident and well supported ($PP \geq 0.95$; Fig. 2). The division into lineages above subfamily-level received less support in the *VRN1* lineage ($PP = 0.73$; Fig. 2). Nevertheless, PACMAD taxa formed a distinct clade. Despite their relatively short length, the putative *VRN1* and *FUL2* sequences isolated from *D. decumbens*, *B. gracilis*, *M. caerulea*, and *T. triandra* were placed with other PACMAD taxa within the predicted clade (Fig. 2).

3.3. Gene expression in response to vernalization

Based on the hypothesis that *FUL*-like genes have been independently recruited for vernalization responsiveness in PACMAD grasses, we predicted that *VRN1* and/or *FUL2* transcription would increase significantly over time only in our cold-treated plants, manifesting in a significant time point by treatment interaction. Significant effects of temperature treatment on gene expression were detected for *DdVRN1* and *DdFUL2* ($P < 0.000$, ANOVA, Table S3), whereas sampling time had a significant effect on *McFUL2* ($P < 0.05$, ANOVA, Table S3). Post-hoc tests revealed significant differences in gene expression between vernalized and non-vernalized individuals for *DdVRN1* ($P < 0.005$), *DdFUL2* ($P < 0.000$) after six and eight weeks, respectively, and *McFUL2* after eight weeks ($P < 0.05$, Tukey's HSD test) with consistently higher expression levels in vernalized material. No treatment effects were found for *BgVRN1, BgFUL2, McVRN1, TtVRN1* or *TtFUL2* (Fig. 3, Table S3).

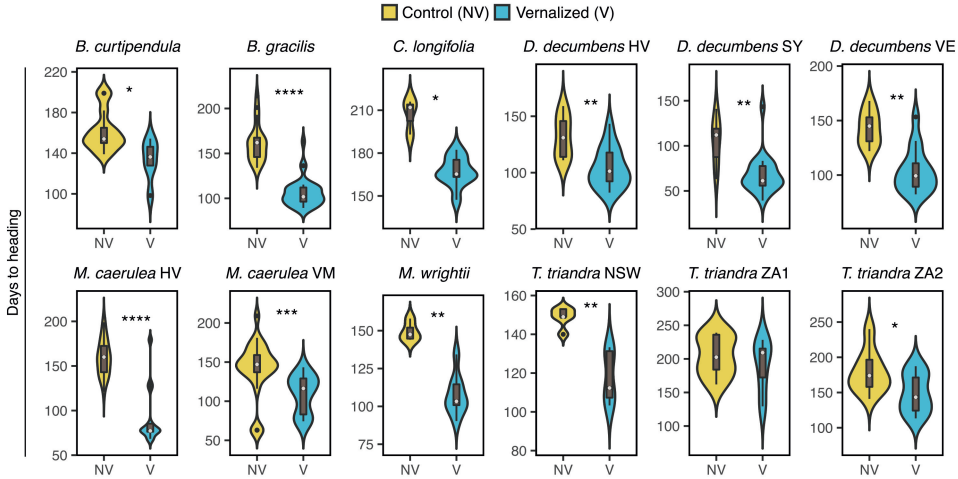

Fig. 1. Flowering behavior of 12 PACMAD accessions subjected to two different temperature treatments, measured in heat unit-adjusted days to heading (DTH_C). Colored areas represent density of the data and are scaled to resemble sample size, i.e., percentage of flowering plants. Grey rectangles indicate the interquartile range, lines 95 % confidence intervals, light dots the median, and dark dots outliers. The experiment was terminated after 300 days, and non-flowering individuals were omitted from the analysis. Significance codes: * $P < 0.05$, ** $P < 0.01$, *** $P < 0.001$, **** $P < 0.0001$ (Mann–Whitney *u*-test).

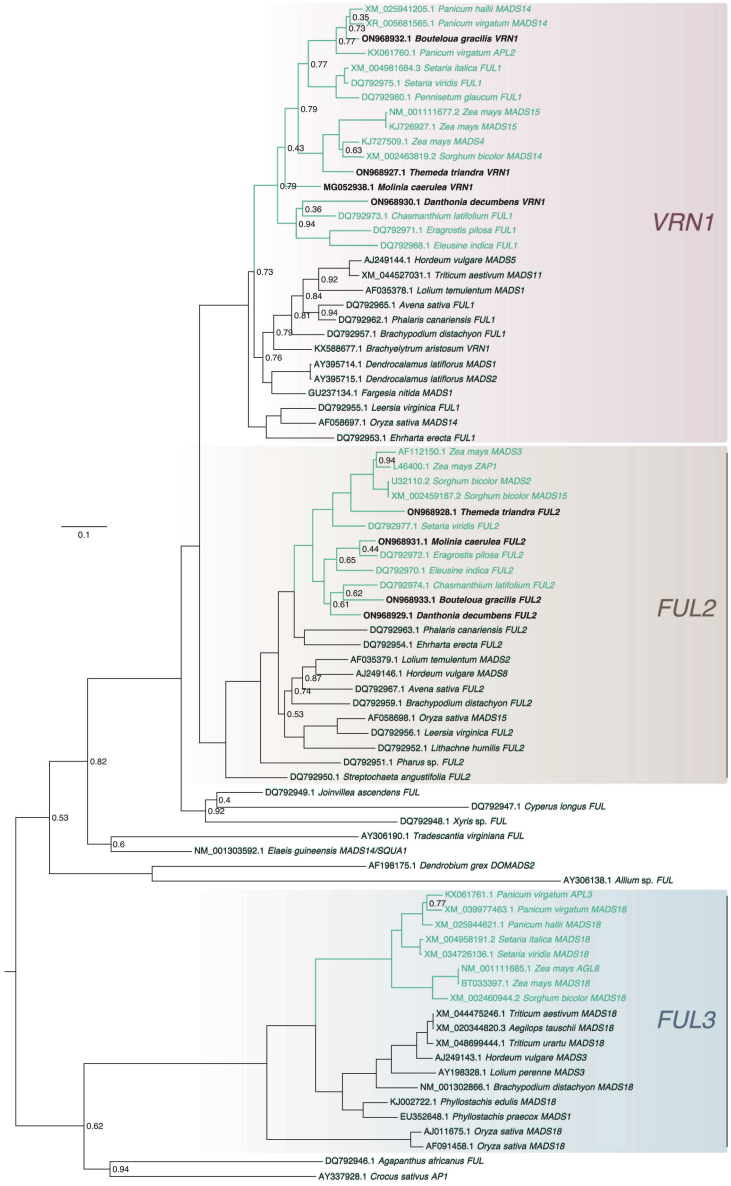

Fig. 2. Maximum clade credibility tree of *FUL*-like genes from 38 different monocot taxa inferred with BEAST. Branch lengths are scaled to represent relative nucleotide substitution rates. Sequences generated in this are highlighted in bold and other PACMAD taxa are highlighted in green. Numbers at nodes denote $PP < 0.95$ and identifiers are GenBank accession numbers. (For interpretation of the references to colour in this figure legend, the reader is referred to the web version of this article.)

4. Discussion

4.1. Vernalization responsiveness in PACMAD grasses

Significantly hastened flowering was observed in vernalized individuals of seven species from four different subfamilies (Panicoidae, Chloridoideae, Arundinoideae, and Danthonioideae), suggesting that vernalization-cued flowering may be a widespread phenomenon in temperate PACMAD grasses. Our results corroborate earlier findings on a few species (Evans and Knox, 1969; Hodgkinson and Quinn, 1978). Given that the majority of PACMAD taxa occur in tropical and subtropical climates, a vernalization response likely evolved independently in different temperate PACMAD lineages, concomitant with their transition to habitats that experience seasonal cold. Furthermore, recent estimates place the split between BOP and PACMAD grasses at ~ 81.42–80.2 million years ago (Ma) (Huang et al., 2022; Schubert et al., 2019b), pre-dating the seasonality increase in high latitudes during the Eocene–Oligocene boundary (Eldrett et al., 2009) that likely triggered

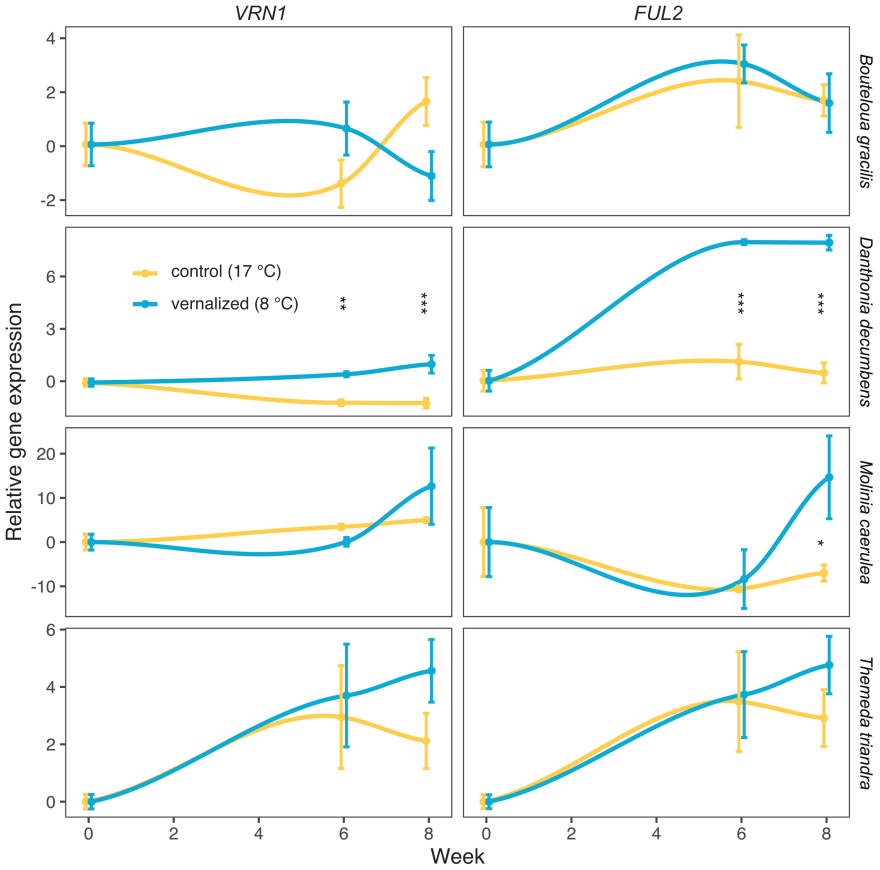

Fig. 3. Relative expression levels of *VRN1* and *FUL2* in the temperate PACMAD species *Bouteloua gracilis*, *Danthonia decumbens*, *Molinia caerulea*, and *Themeda triandra* with (blue lines) and without (yellow lines) vernalization. Significance codes: * $P < 0.05$, ** $P < 0.01$, *** $P < 0.001$ according to a Tukey's HSD test comparing treatments at specific timepoints. (For interpretation of the references to colour in this figure legend, the reader is referred to the web version of this article.)

the evolution of vernalization response in Pooideae (Fjellheim et al., 2014; McKeown et al., 2016; Preston and Sandve, 2013; Zhong et al., 2018). Rather than coinciding with a period of cooling, the BOP–PACMAD partition coincides with a period of global warming following the Cretaceous thermal maximum (Clarke and Jenkyns, 1999; Huber et al., 2002; Wilson et al., 2002), which makes the early evolution of vernalization response at the base of the PACMAD clade unlikely.

In addition to large variation in responses between species, we also found variation in vernalization responses between populations for *D. decumbens, M. caerula* and *T. triandra*, in line with previous findings for *T. triandra,* as well as several Pooideae species (Evans and Knox, 1969; Heide, 1994) (Fig. 1). Vernalization sensitivity has been shown to follow environmental clines in, for example, *Arabidopsis thaliana* (Lewandowska-Sabat et al., 2012; Mitchell-Olds and Schmitt, 2006; Riihimäki and Savolainen, 2004; Wollenberg and Amasino, 2012), *B. distachyon* (Schwartz et al., 2010; Tyler et al., 2016), and *Phleum pratense* (Fiil et al., 2011). In each case, populations originating from coastal environments, distinguished by milder winters, had stronger responses to vernalization than continental populations, suggesting that the need to time flowering adequately may be greater in environments with indistinct transitions between seasons. This is congruent with the flowering behavior observed in *M. caerulea*, where the coastal Hvaler population ('HV', Fig. 1) turned out to have a stronger vernalization response than cold-treated individuals originating from a slightly more continental habitat (Vestmarka/'VM', Fig. 1).

4.2. Genetic architecture of the PACMAD vernalization response

Our results suggest that the vernalization pathways of some PACMAD grasses involve genes homologous to the Pooideae vernalization genes *VRN1* and *FUL2*. In *M. caerulea*, vernalization seems to affect flowering through the up-regulation of a *FUL2*-like gene. Whereas *McFUL2* transcripts drastically increase following eight weeks of cold, leaf *McVRN1* transcription remains low regardless of temperature treatment. Although it is not possible to entirely discount that *McVRN1* is vernalization responsive in other tissues (specifically the SAM), our data support the independent recruitment of grass-specific *FUL*-like paralogs into a vernalization-mediated flowering pathway, possibly through differential neofunctionalization (Force et al., 1999; Hughes, 1994; He and Zhang, 2005). In *D. decumbens*, both *DdVRN1* and *DdFUL2*

are upregulated through vernalization, similar to the case in wheat (Chen and Dubcovsky, 2012; Li et al. 2019). Although our expression data indicate that *VRN1* and *FUL2* are involved in vernalization induced flowering in PACMAD grasses, we lack functional characterization to fully demonstrate this. Following this, our expression data preclude strong conclusions about functional redundancy in the vernalization pathway. However, VRN1 and FUL2 are known to be functionally redundant in other contexts, such as in promoting the floral transition (Yang et al., 2021). Functional redundancy among *FUL*-like genes might provide flexibility for fine-tuning flowering responses to specific environmental conditions. Although *T. triandra TtVRN1* and *TtFUL2* showed the expected trend of upregulation in response to cold, further sampling is warranted in the face of our non-significant results. In contrast, gene expression patterns of *BgVRN1* or *BgFUL2* do not support the recruitment of *VRN1/FUL2* paralogs into the vernalization pathway, begging the question as to whether other grass *FUL*-like genes (*FUL3* and *FUL4*) might be involved (cf. Li et al., 2019).

The propensity of *FUL*-like genes to be repeatedly co-opted into the vernalization pathway might stem from their ancestral function(s). In the case of *VRN1* and *FUL2*, their pre-duplication ancestor is inferred to have been involved in determining floral meristem identity (Gu et al., 1998; Litt and Irish, 2003; Preston and Kellogg, 2007; Theiβen et al., 1996). Comparative RNA *in situ* hybridization indicates that all *FUL*-like genes are strongly expressed in spikelet and floret meristems (Danilevskaya et al., 2008; Ergon et al., 2013; Gocal et al., 2001; Li et al., 2016; Preston and Kellogg, 2008, 2007; Yang et al., 2021), emphasizing their conserved, ancestral role in determining inflorescence meristem identity (Preston et al., 2009; Preston and Kellogg, 2007). In BOP grasses, *VRN1* is expressed in all floral whorls of the inflorescence meristem and postulated to specify overall meristem identity (Gocal et al., 2001; Kinjo et al., 2012; Moon et al., 1999; Preston and Kellogg, 2007), congruent with E-class transcription factors in the ABCDE model of floral development (Callens et al., 2018; Theiβen, 2001). On the other hand, *FUL2* is proposed to work with *VRN1* to exert a more specific function by regulating the differentiation of whorl-primordia into particular anatomical structures in numerous species (Ferrándiz et al., 2000; Gocal et al., 2001; Gu et al., 1998; Preston and Kellogg, 2008, 2007; Wu et al., 2017; Yang et al., 2021). These data support the hypothesis that the ancestral *FUL*-like gene was involved in mediating the transition to inflorescence development (Preston et al., 2009), and that the cold-induced up-regulation and subsequent co-option of *VRN1* into the Pooideae vernalization pathway is a derived trait (Li et al., 2016; McKeown et al., 2016; Preston et al., 2009; Preston and Kellogg, 2007).

Duplication and expansion of *FUL*-like genes at the base of the Poaceae has led to sub- and neofunctionalization among *FUL*-like paralogs, resulting in distinct expression patterns and developmental roles of *VRN1* and *FUL2* during inflorescence development (Preston et al., 2009; Preston and Kellogg, 2007). Up-regulation of *McFUL2* in *M. caerulea* and *DdFUL2/DdVRN1* in *D. decumbens* during vernalization might be another example of independent recruitment of closely related genes. In this case, we hypothesize that *FUL*-like gene recruitment has been a key mechanism underlying convergent origins of a complex physiological adaptation, like the parallel co-option of paralogous genes in convergent evolution of cold tolerance (Sandve and Fjellheim, 2010; Schubert et al., 2019a; Vigeland et al., 2013), C_4 photosynthesis (Christin et al., 2009), and floral zygomorphy (Hileman, 2014).

An interesting aspect of our study warranting further investigation is the timing of *VRN1/FUL2* recruitment into the PACMAD vernalization pathway. In Pooideae, the regulon perceiving, amplifying, and transmitting the vernalization signal is mostly conserved (although, see Woods et al., 2017), and is posited to have evolved after the origin of the subfamily (McKeown et al., 2016). This opens up the possibility that the recruitment of *VRN1/FUL2*-mediated vernalization in the different PACMAD subfamilies happened more recently in these clades as adaptations to increased temperature seasonality, and hence was temporally independent of the *VRN1/FUL2* co-option in Pooideae. Although *FUL*-like genes have often been recruited into the regulatory pathway conferring vernalization response, other genes might be involved in vernalization-responsive species where neither *VRN1* nor *FUL2* are cold responsive. This supports the hypothesis of multiple independent origins of vernalization response in PACMAD grasses harnessing different genetic mechanisms.

5. Concluding remarks

Taken together, our results provide a basis for the evolutionary and functional analysis of vernalization response and its underlying genetic machinery in PACMAD grasses. A vernalization response was detected in species from all four PACMAD subfamilies tested. We found evidence consistent with one or both *VRN1/FUL2* paralogs being involved in vernalization-mediated flowering of *M. caerulea* (Arundinoideae) and *D. decumbens* (Danthonioideae), and perhaps also *T. triandra* (Panicoideae). This suggests that *VRN1*, *FUL2*, and possibly other *FUL*-like genes like *FUL3* and *FUL4* (Chen and Dubcovsky, 2012; Li et al., 2019; Yang et al., 2021) are easily co-opted into adaptations to deal with increased temperature seasonality.

Declaration of Competing Interest

The authors declare that they have no known competing financial interests or personal relationships that could have appeared to influence the work reported in this paper.

Data availability

Newly generated VRN1 and FUL2 sequences are available on GenBank under accession numbers ON968927–ON968933 and MG052938.

Acknowledgements

We thank Øyvind Jørgensen and Lars Morten Opseth for excellent technical assistance during the vernalization experiment, Ane Charlotte Hjertaas for assisting with the RT-qPCR assays, and Camilla Lorange Lindberg, Mallikarjuna Rao Kovi, Maria Ahlin Moen, Erica Helen Leder, and Ursula Brandes for help during sampling of leaf material, and Luke T. Dunning for acquainting us with the genomic resources available for *Themeda triandra*.

Funding

This work was supported by grants to MP from Yara Norge AS, UMB's Research Foundation and the Norwegian branch of the Nordic Association of Agricultural Science (NJF Norway).

Appendix A. Supplementary data

Supplementary data to this article can be found online at https://doi.org/10.1016/j.ympev.2022.107678.

References

Altschul, S.F., Gish, W., Miller, W., Myers, E.W., Lipman, D.J., 1990. Basic local alignment search tool. J. Mol. Biol. 215, 403–410. https://doi.org/10.1006/jmbi.1990.9999.

Andrés, F., Coupland, G., 2012. The genetic basis of flowering responses to seasonal cues. Nat. Rev. Genet. 13, 627–639. https://doi.org/10.1038/nrg3291.

Atkinson, R.R.L., Mockford, E.J., Bennett, C., Christin, P.-A., Spriggs, E.L., Freckleton, R. P., Thompson, K., Rees, M., Osborne, C.P., 2016. C_4 photosynthesis boosts growth by altering physiology, allocation and size. Nat. Plants 2, 16038. https://doi.org/10.1038/nplants.2016.38.

Ayres, D.L., Darling, A., Zwickl, D.J., Beerli, P., Holder, M.T., Lewis, P.O., Huelsenbeck, J.P., Ronquist, F., Swofford, D.L., Cummings, M.P., Rambaut, A., Suchard, M.A., 2012. BEAGLE: An application programming interface and high-performance computing library for statistical phylogenetics. Syst. Biol. 61, 170–173. https://doi.org/10.1093/sysbio/syr100.

Baloch, D.M., Karow, R.S., Marx, E., Kling, J.G., Witt, M.D., 2003. Vernalization studies with Pacific Northwest wheat. Agron. J. 95, 1201–1208. https://doi.org/10.2134/agronj2003.1201.

Baskerville, G.L., Emin, P., 1969. Rapid estimation of heat accumulation from maximum and minimum temperatures. Ecology 50, 514–517. https://doi.org/10.2307/1933912.

Bäurle, I., Dean, C., 2006. The timing of developmental transitions in plants. Cell 125, 655–664. https://doi.org/10.1016/j.cell.2006.05.005.

Benson, D.A., Cavanaugh, M., Clark, K., Karsch-Mizrachi, I., Lipman, D.J., Ostell, J., Sayers, E.W., 2012. GenBank. Nucleic Acids Res. 41, D36–D42. https://doi.org/10.1093/nar/gks1195.

Bernier, G., 1988. The control of floral evocation and morphogenesis. Annu. Rev. Plant Physiol. 39, 175–219. https://doi.org/10.1146/annurev. pp. 39.060188.001135.

Bouché, F., Woods, D.P., Amasino, R., 2017. Winter memory throughout the plant kingdom: different paths to flowering. Plant Physiol. 173, 27–35. https://doi.org/10.1104/pp.16.01322.

Bustin, S.A., Benes, V., Garson, J.A., Hellemans, J., Huggett, J., Kubista, M., Mueller, R., Nolan, T., Pfaffl, M.W., Shipley, G.L., Vandesompele, J., Wittwer, C.T., 2009. The MIQE guidelines: minimum information for publication of quantitative real-time PCR experiments. Clin. Chem. 55, 611–622. https://doi.org/10.1373/clinchem.2008.112797.

Callens, C., Tucker, M.R., Zhang, D., Wilson, Z.A., 2018. Dissecting the role of MADS-box genes in monocot floral development and diversity. J. Exp. Bot. 69, 2435–2459. https://doi.org/10.1093/jxb/ery086.

Camacho, C., Coulouris, G., Avagyan, V., Ma, N., Papadopoulos, J., Bealer, K., Madden, T.L., 2009. BLAST+: architecture and applications. BMC Bioinform. 10, 421. https://doi.org/10.1186/1471-2105-10-421.

Chen, A., Dubcovsky, J., Trevaskis, B., 2012. Wheat TILLING mutants show that the vernalization gene *VRN1* down-regulates the flowering repressor *VRN2* in leaves but is not essential for flowering. PLOS Genet. 8 (12), e1003134.

Chikhi, R., Medvedev, P., 2013. Informed and automated *k*-mer size selection for genome assembly. Bioinformatics 30, 31–37. https://doi.org/10.1093/bioinformatics/btt310.

Chouard, P., 1960. Vernalization and its relations to dormancy. Annu. Rev. Plant Physiol. 11, 191–238. https://doi.org/10.1146/annurev. pp. 11.060160.001203.

Christin, P.-A., Samaritani, E., Petitpierre, B., Salamin, N., Besnard, G., 2009. Evolutionary insights on C4 photosynthetic subtypes in grasses from genomics and phylogenetics. Genome Biol. Evol. 1, 221–230. https://doi.org/10.1093/gbe/evp020.

Clarke, L.J., Jenkyns, H.C., 1999. New oxygen isotope evidence for long-term Cretaceous climatic change in the Southern Hemisphere. Geology 27, 699–702. https://doi.org/10.1130/0091-7613(1999)027<0699:noiefl>2.3.co;2.

D'Hont, A., Denoeud, F., Aury, J.-M., Baurens, F.-C., Carreel, F., Garsmeur, O., Noel, B., Bocs, S., Droc, G., Rouard, M., Da Silva, C., Jabbari, K., Cardi, C., Poulain, J., Souquet, M., Labadie, K., Jourda, C., Lengellé, J., Rodier-Goud, M., Alberti, A., Bernard, M., Correa, M., Ayyampalayam, S., Mckain, M.R., Leebens-Mack, J., Burgess, D., Freeling, M., Mbéguié-A-Mbéguié, D., Chabannes, M., Wicker, T., Panaud, O., Barbosa, J., Hribova, E., Heslop-Harrison, P., Habas, R., Rivallan, R., Francois, P., Poiron, C., Kilian, A., Burthia, D., Jenny, C., Bakry, F., Brown, S., Guignon, V., Kema, G., Dita, M., Waalwijk, C., Joseph, S., Dievart, A., Jaillon, O., Leclercq, J., Argout, X., Lyons, E., Almeida, A., Jeridi, M., Dolezel, J., Roux, N., Risterucci, A.-M., Weissenbach, J., Ruiz, M., Glaszmann, J.-C., Quétier, F., Yahiaoui, N., Wincker, P., 2012. The banana (*Musa acuminata*) genome and the evolution of monocotyledonous plants. Nature 488 (7410), 213–217.

Danilevskaya, O.N., Meng, X., Selinger, D.A., Deschamps, S., Hermon, P., Vansant, G., Gupta, R., Ananiev, E.V., Muszynski, M.G., 2008. Involvement of the MADS-box gene *ZMM4* in floral induction and inflorescence development in maize. Plant Physiol. 147, 2054–2069. https://doi.org/10.1104/pp.107.115261.

Danyluk, J., Kane, N.A., Breton, G., Limin, A.E., Fowler, D.B., Sarhan, F., 2003. TaVRT-1, a putative transcription factor associated with vegetative to reproductive transition in cereals. Plant Physiol. 132, 1849–1860. https://doi.org/10.1104/pp.103.023523.

Darriba, D., Taboada, G.L., Doallo, R., Posada, D., 2012. jModelTest 2: more models, new heuristics and parallel computing. Nat. Methods 9, 772. https://doi.org/10.1038/nmeth.2109.

Deng, W., Casao, M.C., Wang, P., Sato, K., Hayes, P.M., Finnegan, E.J., Trevaskis, B., 2015. Direct links between the vernalization response and other key traits of cereal crops. Nat. Commun. 6, 5882. https://doi.org/10.1038/ncomms6882.

Dennis, E.S., Peacock, W.J., 2009. Vernalization in cereals. J. Biol. 8, 57. https://doi.org/10.1186/jbiol156.

Distelfeld, A., Li, C., Dubcovsky, J., 2009. Regulation of flowering in temperate cereals. Curr. Opin. Plant Biol. 12, 178–184. https://doi.org/10.1016/j.pbi.2008.12.010.

Drummond, A.J., Ho, S.Y.W., Phillips, M.J., Rambaut, A., Penny, D., 2006. Relaxed phylogenetics and dating with confidence. PLOS Biol. 4 (5), e88.

Dunning, L.T., Liabot, A.-L., Olofsson, J.K., Smith, E.K., Vorontsova, M.S., Besnard, G., Simpson, K.J., Lundgren, M.R., Addicott, E., Gallagher, R.V., Chu, Y., Pennington, R. T., Christin, P.-A., Lehmann, C.E.R., 2017. The recent and rapid spread of *Themeda triandra*. Bot. Lett. 164, 327–337. https://doi.org/10.1080/23818107.2017.1391120.

Eldrett, J.S., Greenwood, D.R., Harding, I.C., Huber, M., 2009. Increased seasonality through the Eocene to Oligocene transition in northern high latitudes. Nature 459, 969–973. https://doi.org/10.1038/nature08069.

Ergon, Å., Hamland, H., Rognli, O.A., 2013. Differential expression of *VRN1* and other MADS-box genes in *Festuca pratensis* selections with different vernalization requirements. Biol. Plant. 57, 245–254. https://doi.org/10.1007/s10535-012-0283-z.

Ergon, Å., Melby, T.I., Höglind, M., Rognli, O.A., 2016. Vernalization requirement and the chromosomal *VRN1*-region can affect freezing tolerance and expression of cold-regulated genes in *Festuca pratensis*. Front. Plant Sci. 7, 207. https://doi.org/10.3389/fpls.2016.00207.

Evans, L.T., Knox, R.B., 1969. Environmental control of reproduction in *Themeda australis*. Aust. J. Bot. 17, 375–389. https://doi.org/10.1071/bt9690375.

Ferrándiz, C., Gu, Q., Martienssen, R., Yanofsky, M.F., 2000. Redundant regulation of meristem identity and plant architecture by *FRUITFULL*, *APETALA1* and *CAULIFLOWER*. Development 127, 725–734. https://doi.org/10.1242/dev.127.4.725.

Fiil, A., Jensen, L.B., Fjellheim, S., Lübberstedt, T., Andersen, J.R., 2011. Variation in the vernalization response of a geographically diverse collection of timothy genotypes. Crop Sci. 51, 2689–2697. https://doi.org/10.2135/cropsci2010.12.0677.

Fjellheim, S., Boden, S., Trevaskis, B., 2014. The role of seasonal flowering responses in adaptation of grasses to temperate climates. Front. Plant Sci. 5, 431. https://doi.org/10.3389/fpls.2014.00431.

Force, A., Lynch, M., Pickett, F.B., Amores, A., Yan, Y., Postlethwait, J., 1999. Preservation of duplicate genes by complementary, degenerative mutations. Genetics 151, 1531–1545. https://doi.org/10.1093/genetics/151.4.1531.

Gaßner, G., 1918. Beiträge zur physiologischen Charakteristik sommer- und winterannueller Gewächse, insbesondere der Getreidepflanzen. Z. Bot. 10, 417–480.

Gernhard, T., 2008. The conditioned reconstructed process. J. Theor. Biol. 253, 769–778. https://doi.org/10.1016/j.jtbi.2008.04.005.

Gocal, G.F.W., King, R.W., Blundell, C.A., Schwartz, O.M., Andersen, C.H., Weigel, D., 2001. Evolution of floral meristem identity genes. Analysis of *Lolium temulentum* genes related to *APETALA1* and *LEAFY* of *Arabidopsis*. Plant Physiol. 125, 1788–1801. https://doi.org/10.1104/pp.125.4.1788.

Graham, S.W., Zgurski, J.M., McPherson, M.A., Cherniawsky, D.M., Saarela, J.M., Horne, E.F.C., Smith, S.Y., Wong, W.A., O'Brien, H.E., Brown, V.L., Pires, J.C., Olmstead, R.G., Chase, M.W., Rai, H.S., 2006. Robust inference of monocot deep phylogeny using an expanded multigene plastid data set. Aliso 22, 3–21. https://doi.org/10.5642/aliso.20062201.02.

Grass Phylogeny Working Group II, 2012. New grass phylogeny resolves deep evolutionary relationships and discovers C_4 origins. New Phytol. 193, 304–312. https://doi.org/10.1111/j.1469-8137.2011.03972.x.

Greenup, A., Peacock, W.J., Dennis, E.S., Trevaskis, B., 2009. The molecular biology of seasonal flowering-responses in *Arabidopsis* and the cereals. Ann. Bot. 103, 1165–1172. https://doi.org/10.1093/aob/mcp063.

Gu, Q., Ferrándiz, C., Yanofsky, M.F., Martienssen, R., 1998. The *FRUITFULL* MADS-box gene mediates cell differentiation during *Arabidopsis* fruit development. Development 125, 1509–1517. https://doi.org/10.1242/dev.125.8.1509.

Hartley, W., 1973. Studies on the origin, evolution, and distribution of the Gramineae. V. The subfamily Festucoideae. Aust. J. Bot. 21, 201–234. https://doi.org/10.1071/bt9730201.

Hasegawa, M., Kishino, H., Yano, T., 1985. Dating of the human–ape splitting by a molecular clock of mitochondrial DNA. J. Mol. Evol. 22, 160–174. https://doi.org/10.1007/bf02101694.

He, X, Zhang, J, 2005. Rapid subfunctionalization accompanied by prolonged and substantial neofunctionalization in duplicate gene evolution. Genetics 169, 1157–1164. https://doi.org/10.1534/genetics.104.037051.

Heide, O.M., 1994. Control of flowering and reproduction in temperate grasses. New Phytol. 128, 347–362. https://doi.org/10.1111/j.1469-8137.1994.tb04019.x.

Hemming, M.N., Peacock, W.J., Dennis, E.S., Trevaskis, B., 2008. Low-temperature and daylength cues are integrated to regulate *FLOWERING LOCUS T* in barley. Plant Physiol. 147, 355–366. https://doi.org/10.1104/pp.108.116418.

Higgins, J.A., Bailey, P.C., Laurie, D.A., Hazen, S.P., 2010. Comparative genomics of flowering time pathways using *Brachypodium distachyon* as a model for the temperate grasses. PLOS One 5 (4), e10065.

Hileman, L.C., 2014. Trends in flower symmetry evolution revealed through phylogenetic and developmental genetic advances. Philos. Trans. R. Soc. B 369, 20130348. https://doi.org/10.1098/rstb.2013.0348.

Hodgkinson, K.C., Quinn, J.A., 1978. Environmental and genetic control of reproduction in *Danthonia caespitosa* populations. Aust. J. Bot. 26, 351–364. https://doi.org/10.1071/bt9780351.

Hodkinson, T.R., 2018. Evolution and taxonomy of the grasses (Poaceae): A model family for the study of species-rich groups. Annu. Plant Rev. Online 1, 255–294. https://doi.org/10.1002/9781119312994.apr0622.

Hothorn, T., Bretz, F., Westfall, P., 2008. Simultaneous inference in general parametric models. Biom. J. 50, 346–363. https://doi.org/10.1002/bimj.200810425.

Huang, W., Zhang, L., Columbus, J.T., Hu, Y., Zhao, Y., Tang, L., Guo, Z., Chen, W., McKain, M., Bartlett, M., Huang, C.-H., Li, D.-Z., Ge, S., Ma, H., 2022. A well-supported nuclear phylogeny of Poaceae and implications for the evolution of C_4 photosynthesis. Mol. Plant 15, 755–777. https://doi.org/10.1016/j.molp.2022.01.015.

Huber, B.T., Norris, R.D., MacLeod, K.G., 2002. Deep-sea paleotemperature record of extreme warmth during the Cretaceous. Geology 30, 123–126. https://doi.org/10.1130/0091-7613(2002)030<0123:dsproe>2.0.co;2.

Hughes, AL., 1994. The evolution of functionally novel proteins after gene duplication. Proceedings of the Royal Society B: Biological Sciences 256, 119–124. https://doi.org/10.1098/rspb.1994.0058.

Jiao, Y., Li, J., Tang, H., Paterson, A.H., 2014. Integrated syntenic and phylogenomic analyses reveal an ancient genome duplication in monocots. Plant Cell 26, 2792–2802. https://doi.org/10.1105/tpc.114.127597.

Katoh, K., Standley, D.M., 2013. MAFFT multiple sequence alignment software version 7: improvements in performance and usability. Mol. Biol. Evol. 30, 772–780. https://doi.org/10.1093/molbev/mst010.

Kinjo, H., Shitsukawa, N., Takumi, S., Murai, K., 2012. Diversification of three *APETALA1/FRUITFULL*-like genes in wheat. Mol. Genet. Genom. 287, 283–294. https://doi.org/10.1007/s00438-012-0679-7.
Kirby, E.J.M., Siddique, K.H.M., Perry, M.W., Kaesehagen, D., Stern, W.R., 1989. Variation in spikelet initiation and ear development of old and modern Australian wheat varieties. Field Crop. Res. 20, 113–128. https://doi.org/10.1016/0378-4290(89)90056-7.
Leinonen, R., Sugawara, H., Shumway, M., 2011. The sequence read archive. Nucleic Acids Res. 39 (Database), D19–D21.
Lewandowska-Sabat, A.M., Fjellheim, S., Rognli, O.A., 2012. The continental-oceanic climatic gradient impose clinal variation in vernalization response in *Arabidopsis thaliana*. Environ Exp Bot 78, 109–116. https://doi.org/10.1016/j.envexpbot.2011.12.033.
Li, C., Lin, H., Chen, A., Lau, M., Jernstedt, J., Dubcovsky, J., 2019. Wheat *VRN1*, *FUL2* and *FUL3* play critical and redundant roles in spikelet development and spike determinacy. Development 146, dev175398. https://doi.org/10.1242/dev.175398.
Li, Q., Wang, Y., Wang, F., Guo, Y., Duan, X., Sun, J., An, H., 2016. Functional conservation and diversification of *APETALA1/FRUITFULL* genes in *Brachypodium distachyon*. Physiol. Plantarum 157, 507–518. https://doi.org/10.1111/ppl.12427.
Litt, A., 2007. An evaluation of A-function: Evidence from the *APETALA1* and *APETALA2* gene lineages. Int. J. Plant Sci. 168, 73–91. https://doi.org/10.1086/509662.
Litt, A., Irish, V.F., 2003. Duplication and diversification in the *APETALA1/FRUITFULL* floral homeotic gene lineage: implications for the evolution of floral development. Genetics 165, 821–833. https://doi.org/10.1093/genetics/165.2.821.
Luo, R., Liu, B., Xie, Y., Li, Z., Huang, W., Yuan, J., He, G., Chen, Y., Pan, Q., Liu, Y., Tang, J., Wu, G., Zhang, H., Shi, Y., Liu, Y., Yu, C., Wang, B., Lu, Y., Han, C., Cheung, D.W., Yiu, S.-M., Peng, S., Xiaoqian, Z., Liu, G., Liao, X., Li, Y., Yang, H., Wang, J., Lam, T.-W., Wang, J., 2012. SOAPdenovo2: an empirically improved memory-efficient short-read de novo assembler. GigaScience 1, 18. https://doi.org/10.1186/2047-217x-1-18.
Mann, H.B., Whitney, D.R., 1947. On a test of whether one of two random variables is stochastically larger than the other. Ann. Math. Stat. 18, 50–60. https://doi.org/10.1214/aoms/1177730491.
McKain, M.R., Tang, H., McNeal, J.R., Ayyampalayam, S., Davis, J.I., dePamphilis, C.W., Givnish, T.J., Pires, J.C., Stevenson, D.W., Leebens-Mack, J.H., 2016. A phylogenomic assessment of ancient polyploidy and genome evolution across the Poales. Genome Biol. Evol. 8, 1150–1164. https://doi.org/10.1093/gbe/evw060.
McKeown, M., Schubert, M., Marcussen, T., Fjellheim, S., Preston, J.C., 2016. Evidence for an early origin of vernalization responsiveness in temperate Pooideae grasses. Plant Physiol. 172, 416–426. https://doi.org/10.1104/pp.16.01023.
Mitchell-Olds, T., Schmitt, J., 2006. Genetic mechanisms and evolutionary significance of natural variation in *Arabidopsis*. Nature 441, 947–952. https://doi.org/10.1038/nature04878.
Moon, Y.-H., Kang, H.-G., Jung, J.-Y., Jeon, J.-S., Sung, S.-K., An, G., 1999. Determination of the motif responsible for interaction between the rice APETALA1/AGAMOUS-LIKE9 family proteins using a yeast two-hybrid system. Plant Physiol. 120, 1193–1204. https://doi.org/10.1104/pp.120.4.1193.
Murfet, I.C., 1977. Environmental interaction and the genetics of flowering. Annu. Rev. Plant Physiol. 28, 253–278. https://doi.org/10.1146/annurev.pp.28.060177.001345.
NCBI Resource Coordinators, 2017. Database resources of the National Center for Biotechnology Information. Nucleic Acids Res. 45, D12–D17. http://doi.org/10.1093/nar/gkw1071.
Oliver, S.N., Finnegan, E.J., Dennis, E.S., Peacock, W.J., Trevaskis, B., 2009. Vernalization-induced flowering in cereals is associated with changes in histone methylation at the *VERNALIZATION1* gene. Proc. Natl. Acad. Sci. U.S.A. 106, 8386–8391. https://doi.org/10.1073/pnas.0903566106.
Oliver, S.N., Deng, W., Casao, M.C., Trevaskis, B., 2013. Low temperatures induce rapid changes in chromatin state and transcript levels of the cereal *VERNALIZATION1* gene. J. Exp. Bot. 64, 2413–2422. https://doi.org/10.1093/jxb/ert095.
Olofsson, J.K., Bianconi, M., Besnard, G., Dunning, L.T., Lundgren, M.R., Holota, H., Vorontsova, M.S., Hidalgo, O., Leitch, I.J., Nosil, P., Osborne, C.P., Christin, P.-A., 2016. Genome biogeography reveals the intraspecific spread of adaptive mutations for a complex trait. Mol. Ecol. 25, 6107–6123. https://doi.org/10.1111/mec.13914.
Paterson, A.H., Bowers, J.E., Chapman, B.A., 2004. Ancient polyploidization predating divergence of the cereals, and its consequences for comparative genomics. Proc. Natl. Acad. Sci. U.S.A. 101, 9903–9908. https://doi.org/10.1073/pnas.0307901101.
Peter Linder, H., Antonelli, A., Humphreys, A.M., Pirie, M.D., Wüest, R.O., Ladle, R., 2013. What determines biogeographical ranges? Historical wanderings and ecological constraints in the danthonioid grasses. J. Biogeogr. 40 (5), 821–834.
Petersen, K., Didion, T., Andersen, C.H., Nielsen, K.K., 2004. MADS-box genes from perennial ryegrass differentially expressed during transition from vegetative to reproductive growth. J Plant Physiol. 161, 439–447. https://doi.org/10.1078/0176-1617-01212.
Petersen, K., Kolmos, E., Folling, M., Salchert, K., Storgaard, M., Jensen, C.S., Didion, T., Nielsen, K.K., 2006. Two MADS-box genes from perennial ryegrass are regulated by vernalization and involved in the floral transition. Physiol. Plant. 126, 268–278. https://doi.org/10.1111/j.1399-3054.2006.00600.x.
Pfaffl, M.W., 2001. A new mathematical model for relative quantification in real-time RT-PCR. Nucleic Acids Res. 29, e45.
Pirie, M.D., Humphreys, A.M., Antonelli, A., Galley, C., Linder, H.P., 2012. Model uncertainty in ancestral area reconstruction: A parsimonious solution? Taxon 61, 652–664. https://doi.org/10.1002/tax.613013.
Poethig, R.S., 1990. Phase change and the regulation of shoot morphogenesis in plants. Science 250, 923–930. https://doi.org/10.1126/science.250.4983.923.
Preston, J.C., Fjellheim, S., 2020. Understanding past, and predicting future, niche transitions based on grass flowering time variation. Plant Physiol. 183, 822–839. https://doi.org/10.1104/pp.20.00100.
Preston, J.C., Fjellheim, S., 2022. Flowering time runs hot and cold: Evolution of temperature regulated flowering. Plant Physiol 190, 5–18. https://doi.org/10.1093/plphys/kiac111.
Preston, J.C., Kellogg, E.A., 2006. Reconstructing the evolutionary history of paralogous *APETALA1/FRUITFULL*-like genes in grasses (Poaceae). Genetics 174, 421–437. https://doi.org/10.1534/genetics.106.057125.
Preston, J.C., Kellogg, E.A., 2007. Conservation and divergence of *APETALA1/FRUITFULL*-like gene function in grasses: evidence from gene expression analyses. Plant J. 52, 69–81. https://doi.org/10.1111/j.1365-313x.2007.03209.x.
Preston, J.C., Kellogg, E.A., 2008. Discrete developmental roles for temperate cereal grass *VERNALIZATION1/FRUITFULL*-like genes in flowering competency and the transition to flowering. Plant Physiol. 146, 265–276. https://doi.org/10.1104/pp.107.109561.
Preston, J.C., Sandve, S.R., 2013. Adaptation to seasonality and the winter freeze. Front. Plant Sci. 4, 167. https://doi.org/10.3389/fpls.2013.00167.
Preston, J.C., Christensen, A., Malcomber, S.T., Kellogg, E.A., 2009. MADS-box gene expression and implications for developmental origins of the grass spikelet. Am. J. Bot. 96, 1419–1429. https://doi.org/10.3732/ajb.0900062.
R Core Team, 2020. R: A language and environment for statistical computing. R Foundation for Statistical Computing, Vienna, Austria. https://www.R-project.org/.
Rambaut, A., Drummond, A.J., Xie, D., Baele, G., Suchard, M.A., Susko, E., 2018. Posterior summarization in Bayesian phylogenetics using Tracer 1.7. Syst. Biol. 67 (5), 901–904.
Ream, T.S., Woods, D.P., Amasino, R., 2012. The molecular basis of vernalization in different plant groups. Cold Spring Harb. Symp. Quant. Biol. 77, 105–115. https://doi.org/10.1101/sqb.2013.77.014449.
Ream, T.S., Woods, D.P., Schwartz, C.J., Sanabria, C.P., Mahoy, J.A., Walters, E.M., Kaeppler, H.F., Amasino, R., 2014. Interaction of photoperiod and vernalization determines flowering time of *Brachypodium distachyon*. Plant Physiol. 164, 694–709. https://doi.org/10.1104/pp.113.232678.
Riihimäki, M., Savolainen, O., 2004. Environmental and genetic effects on flowering differences between northern and southern populations of *Arabidopsis lyrata* (Brassicaceae). Am. J. Bot. 91, 1036–1045. https://doi.org/10.3732/ajb.91.7.1036.
Rödiger, S., Burdukiewicz, M., Schierack, P., 2015. chipPCR: an R package to pre-process raw data of amplification curves. Bioinformatics 31, 2900–2902. https://doi.org/10.1093/bioinformatics/btv205.
Saarela, J.M., Wysocki, W.P., Barrett, C.F., Soreng, R.J., Davis, J.I., Clark, L.G., Kelchner, S.A., Pires, J.C., Edger, P.P., Mayfield, D.R., Duvall, M.R., 2015. Plastid phylogenomics of the cool-season grass subfamily: clarification of relationships among early-diverging tribes. AoB PLANTS 7, plv046.
Sandve, S.R., Fjellheim, S., 2010. Did gene family expansions during the Eocene-Oligocene boundary climate cooling play a role in Pooideae adaptation to cool climates? Mol. Ecol. 19, 2075–2088. https://doi.org/10.1111/j.1365-294x.2010.04629.x.
Savitzky, A., Golay, M.J.E., 1964. Smoothing and differentiation of data by simplified least squares procedures. Anal. Chem. 36, 1627–1639. https://doi.org/10.1021/ac60214a047.
Schliep, K.P., 2011. phangorn: phylogenetic analysis in R. Bioinformatics 27, 592–593. https://doi.org/10.1093/bioinformatics/btq706.
Schmittgen, T.D., Livak, K.J., 2008. Analyzing real-time PCR data by the comparative *CT* method. Nat. Protoc. 3, 1101–1108. https://doi.org/10.1038/nprot.2008.73.
Schubert, M., Grønvold, L., Sandve, S.R., Hvidsten, T.R., Fjellheim, S., 2019a. Evolution of cold acclimation and its role in niche transition in the temperate grass subfamily Pooideae. Plant Physiol. 180, 404–419. https://doi.org/10.1104/pp.18.01448.
Schubert, M., Marcussen, T., Meseguer, A.S., Fjellheim, S., 2019b. The grass subfamily Pooideae: Cretaceous-Palaeocene origin and climate-driven Cenozoic diversification. Glob. Ecol. Biogeogr. 28 https://doi.org/10.1111/geb.12923.
Schubert, M., Humphreys, A.M., Lindberg, C.L., Preston, J.C., Fjellheim, S., 2020. To *coldly* go where no grass has gone before: A multidisciplinary review of cold adaptation in Poaceae. Annu. Plant Rev. Online 3, 523–562. https://doi.org/10.1002/9781119312994.apr0739.
Schwartz, C.J., Doyle, M.R., Manzaneda, A.J., Rey, P.J., Mitchell-Olds, T., Amasino, R., 2010. Natural variation of flowering time and vernalization responsiveness in *Brachypodium distachyon*. BioEnergy Res 3, 38–46. https://doi.org/10.1007/s12155-009-9069-3.
Shimada, S., Ogawa, T., Kitagawa, S., Suzuki, T., Ikari, C., Shitsukawa, N., Abe, T., Kawahigashi, H., Kikuchi, R., Handa, H., Murai, K., 2009. A genetic network of flowering-time genes in wheat leaves, in which an *APETALA1/FRUITFULL*-like gene, *VRN1*, is upstream of *FLOWERING LOCUS T*. Plant J. 58, 668–681. https://doi.org/10.1111/j.1365-313x.2009.03806.x.
Soreng, R.J., Peterson, P.M., Zuloaga, F.O., Romaschenko, K., Clark, L.G., Teisher, J.K., Gillespie, L.J., Barberá, P., Welker, C.A.D., Kellogg, E.A., Li, D., Davidse, G., 2022. A worldwide phylogenetic classification of the Poaceae (Gramineae) III: An update. J. Syst. Evol. 60, 476–521. https://doi.org/10.1111/jse.12847.
Suchard, M.A., Lemey, P., Baele, G., Ayres, D.L., Drummond, A.J., Rambaut, A., 2018. Bayesian phylogenetic and phylodynamic data integration using BEAST 1.10. Virus Evol. 4, vey016. https://doi.org/10.1093/ve/vey016.
Szűcs, P., Skinner, J.S., Karsai, I., Cuesta-Marcos, A., Haggard, K.G., Corey, A.E., Chen, T.H.H., Hayes, P.M., 2007. Validation of the *VRN-H2/VRN-H1* epistatic model in barley reveals that intron length variation in *VRN-H1* may account for a continuum of vernalization sensitivity. Mol. Genet. Genom. 277, 249–261. https://doi.org/10.1007/s00438-006-0195-8.

Tanaka, C., Itoh, T., Iwasaki, Y., Mizuno, N., Nasuda, S., Murai, K., 2018. Direct interaction between VRN1 protein and the promoter region of the wheat *FT* gene. Genes Genet. Syst. 93, 25–29. https://doi.org/10.1266/ggs.17-00041.

Tavaré, S., 1986. Some probabilistic and statistical problems in the analysis of DNA sequences. Lect. Math. Life Sci. 17, 57–86.

Tellinghuisen, J., Spiess, A.-N., 2014. Comparing real-time quantitative polymerase chain reaction analysis methods for precision, linearity, and accuracy of estimating amplification efficiency. Anal. Biochem. 449, 76–82. https://doi.org/10.1016/j.ab.2013.12.020.

Theißen, G., 2001. Development of floral organ identity: stories from the MADS house. Curr. Opin. Plant Biol. 4, 75–85. https://doi.org/10.1016/s1369-5266(00)00139-4.

Theißen, G., Kim, J.T., Saedler, H., 1996. Classification and phylogeny of the MADS-box multigene family suggest defined roles of MADS-box gene subfamilies in the morphological evolution of eukaryotes. J. Mol. Evol. 43, 484–516. https://doi.org/10.1007/bf02337521.

Trevaskis, B., 2010. The central role of the *VERNALIZATION1* gene in the vernalization response of cereals. Funct. Plant Biol. 37, 479–487. https://doi.org/10.1071/fp10056.

Trevaskis, B., Bagnall, D.J., Ellis, M.H., Peacock, W.J., Dennis, E.S., 2003. MADS box genes control vernalization-induced flowering in cereals. Proc. Natl. Acad. Sci. U.S.A. 100, 13099–13104. https://doi.org/10.1073/pnas.1635053100.

Trevaskis, B., Hemming, M.N., Dennis, E.S., Peacock, W.J., 2007. The molecular basis of vernalization-induced flowering in cereals. Trends Plant Sci. 12, 352–357. https://doi.org/10.1016/j.tplants.2007.06.010.

Tyler, L., Lee, S.J., Young, N.D., DeIulio, G.A., Benavente, E., Reagon, M., Sysopha, J., Baldini, R.M., Troìa, A., Hazen, S.P., Caicedo, A.L., 2016. Population structure in the model grass *Brachypodium distachyon* is highly correlated with flowering differences across broad geographic areas. Plant Genome 9. https://doi.org/10.3835/plantgenome2015.08.0074.

Untergasser, A., Cutcutache, I., Koressaar, T., Ye, J., Faircloth, B.C., Remm, M., Rozen, S.G., 2012. Primer3—new capabilities and interfaces. Nucleic Acids Res. 40 (15).

Vandesompele, J., Preter, K.D., Pattyn, F., Poppe, B., Roy, N.V., Paepe, A.D., Speleman, F., 2002. Accurate normalization of real-time quantitative RT-PCR data by geometric averaging of multiple internal control genes. Genome Biol. 3 (research0034), 1. https://doi.org/10.1186/gb-2002-3-7-research0034.

Vigeland, M.D., Spannagl, M., Asp, T., Paina, C., Rudi, H., Rognli, O.A., Fjellheim, S., Sandve, S.R., 2013. Evidence for adaptive evolution of low-temperature stress response genes in a Pooideae grass ancestor. New Phytol. 199, 1060–1068. https://doi.org/10.1111/nph.12337.

Visser, V., Clayton, W.D., Simpson, D.A., Freckleton, R.P., Osborne, C.P., 2014. Mechanisms driving an unusual latitudinal diversity gradient for grasses. Glob. Ecol. Biogeogr. 23, 61–75. https://doi.org/10.1111/geb.12107.

Wilson, P.A., Norris, R.D., Cooper, M.J., 2002. Testing the Cretaceous greenhouse hypothesis using glassy foraminiferal calcite from the core of the Turonian tropics on Demerara Rise. Geology 30, 607–610. https://doi.org/10.1130/0091-7613(2002)030<0607:ttcghu>2.0.co;2.

Wollenberg, A.C., Amasino, R., 2012. Natural variation in the temperature range permissive for vernalization in accessions of *Arabidopsis thaliana*. Plant Cell Environ. 35, 2181–2191. https://doi.org/10.1111/j.1365-3040.2012.02548.x.

Woods, D.P., McKeown, M., Dong, Y., Preston, J.C., Amasino, R., 2016. Evolution of *VRN2/Ghd7*-like genes in vernalization-mediated repression of grass flowering. Plant Physiol. 170, 2124–2135. https://doi.org/10.1104/pp.15.01279.

Woods, D.P., Ream, T.S., Bouché, F., Lee, J., Thrower, N., Wilkerson, C., Amasino, R., 2017. Establishment of a vernalization requirement in *Brachypodium distachyon* requires *REPRESSOR OF VERNALIZATION1*. Proc. Natl. Acad. Sci. U.S.A. 114, 6623–6628. https://doi.org/10.1073/pnas.1700536114.

Wright, E.S., 2015. DECIPHER: harnessing local sequence context to improve protein multiple sequence alignment. BMC Bioinform. 16, 322. https://doi.org/10.1186/s12859-015-0749-z.

Wright, E.S., 2016. Using DECIPHER v2.0 to analyze big biological sequence data in R. R J. 8, 352–359. https://doi.org/10.32614/RJ-2016-025.

Wu, F., Shi, X., Lin, X., Liu, Y., Chong, K., Theißen, G., Meng, Z., 2017. The ABCs of flower development: mutational analysis of *AP1/FUL*-like genes in rice provides evidence for a homeotic (A)-function in grasses. Plant J. 89, 310–324. https://doi.org/10.1111/tpj.13386.

Xu, S., Chong, K., 2018. Remembering winter through vernalisation. Remembering winter through vernalisation. Nat Plants 4 (12), 997–1009.

Yan, L., Loukoianov, A., Tranquilli, G., Helguera, M., Fahima, T., Dubcovsky, J., 2003. Positional cloning of the wheat vernalization gene *VRN1*. Proc. Natl. Acad. Sci. U.S.A. 100, 6263–6268. https://doi.org/10.1073/pnas.0937399100.

Yan, L., Loukoianov, A., Blechl, A., Tranquilli, G., Ramakrishna, W., SanMiguel, P., Bennetzen, J.L., Echenique, V., Dubcovsky, J., 2004. The wheat *VRN2* gene is a flowering repressor down-regulated by vernalization. Science 303, 1640–1644. https://doi.org/10.1126/science.1094305.

Yang, Z., 1994. Maximum likelihood phylogenetic estimation from DNA sequences with variable rates over sites: Approximate methods. J. Mol. Evol. 39, 306–314. https://doi.org/10.1007/bf00160154.

Yang, J., Bertolini, E., Braud, M., Preciado, J., Chepote, A., Jiang, H., Eveland, A.L., 2021. The SvFUL2 transcription factor is required for inflorescence determinacy and timely flowering in *Setaria viridis*. Plant Physiol. 187, 1202–1220. https://doi.org/10.1093/plphys/kiab169.

Yu, G., Smith, D.K., Zhu, H., Guan, Y., Lam, T.-T.-Y., McInerny, G., 2017. ggtree: an R package for visualization and annotation of phylogenetic trees with their covariates and other associated data. Methods. Ecol. Evol. 8, 28–36. https://doi.org/10.1111/2041-210x.12628.

Yule, G.U., 1925. A mathematical theory of evolution, based on the conclusions of Dr. J. C. Willis, F.R.S. Philos. Trans. R. Soc. B 213, 21–87. https://doi.org/10.1098/rstb.1925.0002.

Zhang, Z., Schwartz, S., Wagner, L., Miller, W., 2000. A greedy algorithm for aligning DNA sequences. J. Comput. Biol. 7, 203–214. https://doi.org/10.1089/10665270050081478.

Zhang, L., Zhu, X., Zhao, Y., Guo, J., Zhang, T., Huang, W., Huang, J., Hu, Y., Huang, C.-H., Ma, H., 2022. Phylotranscriptomics resolves the phylogeny of Pooideae and uncovers factors for their adaptive evolution. Mol. Biol. Evol. 39, msac026. https://doi.org/10.1093/molbev/msac026.

Zhong, J., Robbett, M., Poire, A., Preston, J.C., 2018. Successive evolutionary steps drove Pooideae grasses from tropical to temperate regions. New Phytol. 217, 925–938. https://doi.org/10.1111/nph.14868.

Zimin, A.V., Marçais, G., Puiu, D., Roberts, M., Salzberg, S.L., Yorke, J.A., 2013. The MaSuRCA genome assembler. Bioinformatics 29, 2669–2677. https://doi.org/10.1093/bioinformatics/btt476.

Tables

Supplementary Table S1: Overview over the seven accessions retrieved from the United States Department of Agriculture (USDA) Germplasm Resource Information Network (GRIN).

***Species* (Abbreviation)**	***Subfamily***	***GRIN ID***	***Country***	***Location***
Bouteloua curtipendula	Chloridoideae	PI 476980	USA	South Dakota
Bouteloua gracilis	Chloridoideae	PI 591814	USA	South Dakota
Calamovilfa longifolia	Chloridoideae	W6 50718	USA	Nebraska
Muhlenbergia wrightii	Chloridoideae	PI 674964	USA	Colorado
Themeda triandra (NSW)	Panicoideae	PI 281968	Australia	New South Wales
Themeda triandra (ZA1)	Panicoideae	PI 206348	South Africa	Eastern Cape
*Themeda triandra (*ZA2*)*	Panicoideae	PI 365061	South Africa	Limpopo

Supplementary Table S2: Sampling locations for *Danthonia decumbens* and *Molinia caerulea*.

***Species* (Abbreviation)**	***Subfamily***	***Latitude***	***Longitude***	***Country***	***Location***
Danthonia decumbens (HV)	Danthonioideae	59.08259	11.03726	Norway	Kirkøy, Hvaler
Danthonia decumbens (SY)	Danthonioideae	59.90340	10.29282	Norway	Altanåsen, Sylling
Danthonia decumbens (VE)	Danthonioideae	61.49140	5.39683	Norway	Vevring kyrkje, Vevring
Molinia caerulea (HV)	Arundinoideae	59.08860	11.03807	Norway	Kirkøy, Hvaler
Molinia caerulea (VM)	Arundinoideae	59.94413	11.99221	Norway	Jerpset,Vestmarka

Supplementary Table S3: Test statistics and post-hoc contrasts for linear models calculating the effects of temperature treatment and sampling time point on relative gene expression of *VRN1* and *FUL2* in the temperate PACMAD species *Bouteloua gracilis*, *Danthonia decumbens*, *Molinia caerulea*, and *Themeda triandra*.

	B. gracilis		*D. decumbens*		*M. caerulea*		*T. triandra*	
VRN1	*F*-value	*P*-value	*F*-value	*P*-value	*F*-value	*P*-value	*F*-value	*P*-value
ANOVA	2.525	0.1069	**13.61**	**0.0001**	1.852	0.1842	0.5095	0.6813
Treatment	1.0332	0.32946	**39.0900**	**0.0000**	0.1619	0.69346	1.1931	0.2909
Timepoint	0.4382	0.52050	0.8156	0.3799	3.3314	0.08938	0.0001	0.9922
Timepoint × Treatment	**6.1040**	**0.02946**	0.9232	0.3509	2.0625	0.17293	0.3355	0.5705
Post-hoc (Tukey's HSD)	*t*-value	*P*-value	*t*-value	*P*-value	*t*-value	*P*-value	*t*-value	*P*-value
Week 6: vernalized vs. control			**3.742**	**0.003527**				
Week 8: vernalized vs. control			**5.100**	**0.000213**				
FUL2	*F*-value	*P*-value	*F*-value	*P*-value	*F*-value	*P*-value	*F*-value	*P*-value
ANOVA	0.3945	0.7593	**45.73**	**0.0000**	**4.081**	**0.02818**	0.3293	0.8042
Treatment	0.0291	0.8674	**136.6377**	**0.0000**	3.7352	0.07377	0.6052	0.4480
Timepoint	1.0365	0.3287	0.3051	0.5884	**5.5452**	**0.03365**	0.0285	0.8681
Timepoint × Treatment	0.1180	0.7371	0.2528	0.6219	2.9623	0.10724	0.3544	0.5600
Post-hoc (Tukey's HSD)	*t*-value	*P*-value	*t*-value	*P*-value	*t*-value	*P*-value	*t*-value	*P*-value
Week 6: vernalized vs. control			**7.910**	**0.0000**	0.293	0.9471		
Week 8: vernalized vs. control			**8.621**	**0.0000**	**2.571**	**0.0431**		

Supplementary Table S4: RT-qPCR primers used for gene expression analysis.

Name	Sequence (5'-3')	Direction	Gene	Reference
McVRN1_29F	GTCGCGCTCATCATCTTCTC	forward	*McVRN1*	
McVRN1_190R	TCTATATTCGTGGCGCCAGT	reverse	*McVRN1*	
TtFUL1-127A_F	GTCGCGCTCATCATCTTCTC	forward	*TtVRN1*	
TtFUL1-190A_R	CCATGCATGAATCGGTGGAG	reverse	*TtVRN1*	
FUL1-14F	GTGCAGCTGAAGCGGATC	forward	*DdVRN1, BgVRN1*	
FUL1-121R	TCGCAGAGCACGGAGATC	reverse	*DdVRN1, BgVRN1*	
FUL2-123F	GGTCGCCGTCATCGTCTT	forward	*DdFUL2, BgFUL2*	
FUL2-281R	TCATGGCACCAATTTCCCTC	reverse	*DdFUL2, BgFUL2*	
McFUL2_F212	ATTCGTGGCACCAATTTCCC	forward	*McFUL2*	
McFUL2_R363	CGTCATCGTCTTCTCCCCAA	reverse	*McFUL2*	
TtFUL2-474A_F	CAGGCACAGACAAGCTCATC	forward	*TtFUL2*	
TtFUL2-526A_R	TGCTGATCCTGCCTCATCAT	reverse	*TtFUL2*	
GrassUBQ5F	CGCCGACTACAACATCCAG	forward	*UBQ5*, all species	McKeown *et al.* (2016)
GrassUBQ5R	TCACCTTCTTGTGCTTGTGC	reverse	*UBQ5*, all species	McKeown *et al.* (2016)
EF1α_594F	GTGACAACATGATTGAGAGG	forward	*EF1α*, all species	McKeown *et al.* (2016)
EF1α_1064R	AGGTGTGGCAGTCCAGCACTG	reverse	*EF1α*, all species	McKeown *et al.* (2016)

Paper II

Major niche transitions in Pooideae correlate with variation in photoperiodic flowering and evolution of CCT domain genes

Fjellheim S, Young DA, **Paliocha M**, Johnsen SS, Schubert M & Preston JC

Journal of Experimental Botany, 2022, 73 (12): 4079–4093

Journal of Experimental Botany, Vol. 73, No. 12 pp. 4079–4093, 2022
https://doi.org/10.1093/jxb/erac149 Advance Access Publication 8 April 2022
This paper is available online free of all access charges (see https://academic.oup.com/jxb/pages/openaccess for further details)

RESEARCH PAPER

Major niche transitions in Pooideae correlate with variation in photoperiodic flowering and evolution of CCT domain genes

Siri Fjellheim[1,*], Darshan A. Young[2], Martin Paliocha[1], Sylvia Sagen Johnsen[1], Marian Schubert[1] and Jill C. Preston[3]

[1] Department of Plant Sciences, Faculty of Biosciences, Norwegian University of Life Sciences, 1432 Ås, Norway
[2] Department of Animal and Aquacultural Sciences, Faculty of Biosciences, Norwegian University of Life Sciences, 1432 Ås, Norway
[3] Department of Plant Biology, The University of Vermont, Burlington, VT 05405, USA

* Correspondence: siri.fjellheim@nmbu.no

Received 10 December 2021; Editorial decision 29 March 2022; Accepted 7 April 2022

Editor: Rainer Melzer, University College Dublin, Ireland

Abstract

The external cues that trigger timely flowering vary greatly across tropical and temperate plant taxa, the latter relying on predictable seasonal fluctuations in temperature and photoperiod. In the grass family (Poaceae) for example, species of the subfamily Pooideae have become specialists of the northern temperate hemisphere, generating the hypothesis that their progenitor evolved a flowering response to long days from a short-day or day-neutral ancestor. Sampling across the Pooideae, we found support for this hypothesis, and identified several secondary shifts to day-neutral flowering and one to short-day flowering in a tropical highland clade. To explain the proximate mechanisms for the secondary transition back to short-day-regulated flowering, we investigated the expression of CCT domain genes, some of which are known to repress flowering in cereal grasses under specific photoperiods. We found a shift in *CONSTANS 1* and *CONSTANS 9* expression that coincides with the derived short-day photoperiodism of our exemplar species *Nassella pubiflora*. This sets up the testable hypothesis that *trans*- or *cis*-regulatory elements of these CCT domain genes were the targets of selection for major niche shifts in Pooideae grasses.

Keywords: CCT domain genes, *CONSTANS*-like genes, flowering, grasses, photoperiod, Pooideae, *VRN2*.

Introduction

The ability of plants to coordinate flowering with favorable environmental conditions results in optimization of reproductive fitness through increased seed set and survival (Greenup *et al.*, 2009). The exact timing of flowering is determined by several different external (e.g. photoperiod and temperature) and internal (e.g. age and hormone) signals that are integrated at the shoot apical meristem (SAM) throughout the lifetime of the plant. In the non-equatorial tropics, shortening photoperiods signal that the rainy season or monsoon is coming to an end, resulting in flowering of short-day grasses (Poaceae) such as rice (*Oryza sativa*) and maize (*Zea mays*) at the end of the greening period, prior to the extreme heat of summer (Naranjo *et al.*, 2014; Mascheretti *et al.*, 2015; Preston and Fjellheim, 2020).

In contrast, lengthening photoperiods during the impending warm season of temperate regions trigger flowering in long-day plants such as the grasses wheat (*Triticum aestivum*) and barley (*Hordeum vulgare*), circumventing the negative effects of winter freezing (Nishida *et al.*, 2013; Chen *et al.*, 2014). Photoperiodicity in flowering is thus a good predictor of current plant distributions (Zhang *et al.*, 2015; Preston and Fjellheim, 2020), but the evolutionary genetic basis of switches between long- and short-day responses is not well understood.

Similar to angiosperms as a whole (Hochuli and Feist-Burkhardt, 2013; Mannion *et al.*, 2014), the grass family evolved when the terrestrial Earth was largely tropical (Burke *et al.*, 2016; Gallaher *et al.*, 2019; Schubert *et al.*, 2019a), suggesting that the ancestor would either have flowered under short days or been daylength neutral (Preston and Fjellheim, 2020). Indeed, of the ~12 000 extant grass species (Soreng *et al.*, 2015), the majority remain in the tropics, with only a couple of major subfamilies—Danthonioideae and Pooideae—dominating southern and northern temperate regions, respectively (Edwards and Smith, 2010; Visser *et al.*, 2014; Schubert *et al.*, 2020). Evidence suggests that the ability of an early Pooideae ancestor to respond to inductive photoperiods was contingent upon receiving a prolonged period of winter cold (vernalization) (McKeown *et al.*, 2016), although data also suggest later modifications to this ancestral vernalization pathway (Woods *et al.*, 2016). It is further hypothesized that the last common ancestor of Pooideae evolved from a daylength-neutral/short- to a long-day plant, the mechanisms underlying which are unknown (Preston and Fjellheim, 2020).

Comparative analyses across both long- and short-day angiosperms have revealed remarkable conservation in the photoperiod flowering pathway, suggesting that flowering in response to different daylengths evolved through fine-tuning of a shared ancestral pathway (Andrés and Coupland, 2012; Matsubara *et al.*, 2014). Central in this pathway is the florigen FLOWERING LOCUS T (FT). FT and related proteins act as universal signals to integrate flowering pathways and promote reproduction. Crucial for perception of photoperiod are various light receptors, one of which is *PHYTOCHROME C* (*PHYC*). *PHYC* is a weak floral repressor in short days in rice (Takano *et al.*, 2005), whereas it promotes flowering under long days in barley and *Brachypodium distachyon* (Nishida *et al.*, 2013; Woods *et al.*, 2014). Another gene family that has been implicated in fine-tuning flowering is the CCT [CO, CO-LIKE, and TIMING OF CAB EXPRESSION 1 (Robson *et al.*, 2001)] domain gene family of transcription factors, with nine members in long-day barley (Pooideae) and 16 members in short-day rice (Oryzoideae) (Griffiths *et al.*, 2003; Song *et al.*, 2015). Examples of CCT domain-containing genes implicated in intraspecific variation in flowering responses are barley *PHOTOPERIOD 1* (*PPD1*) and its ortholog *PSEUDORESPONSEREGULATOR 37* (*PRR37*) in rice, barley *CO1* and *CO2* and their ortholog *HEADING DATE 1* (*Hd1*) in rice, *CO9*, and barley *VERNALIZATION 2* (*VRN2*) and ortholog *Grain number, plant height, and heading date 7* (*Ghd7* or *OsI*) in rice (Komiya *et al.*, 2008; Xue *et al.*, 2008; Stracke *et al.*, 2009; Takahashi *et al.*, 2009; Lu *et al.*, 2012; Koo *et al.*, 2013; Wei *et al.*, 2014; Zhang *et al.*, 2015; McKeown *et al.*, 2016; Zheng *et al.*, 2016; Zhang *et al.*, 2017; Shaw *et al.*, 2020).

Like its *CO* ortholog in *Arabidopsis thaliana* (Brassicaceae), *CO1* in barley and wheat is up-regulated in the afternoon by the *PHYTOCHROME A* and *B* (*PHYA/B*)-mediated circadian clock under both long- and short-day conditions (Campoli *et al.*, 2012; Mulki and von Korff, 2016). In *A. thaliana*, photoperiod regulation through *CO* occurs at the protein level in the presence of light-induced stabilizing proteins, resulting in the up-regulation of *FT* to induce flowering only under long days (Yanovsky and Kay, 2002; Valverde *et al.*, 2004; Hayama *et al.*, 2017). Although it has not been confirmed that similar light-induced protein stabilization exists for CO1, genetic evidence from barley and wheat cultivars with non-functional *PPD1* alleles has shown that this protein also promotes flowering under long-day conditions, concomitant with peak expression in the light (Campoli *et al.*, 2012; Mulki and von Korff, 2016; Shaw *et al.*, 2020). On the other hand, in the presence of functional *PPD1* and *VRN2* alleles, at least wheat *CO1* is converted to a mild floral repressor under long days to prevent precocious pre-winter flowering, probably as a result of protein–protein interactions between PPD1, CO1, CO2, and possibly VRN2 (Shaw *et al.*, 2020).

In rice, the CO1 ortholog Hd1 is also assumed to be regulated by light- and dark-dependent proteins, and also forms an Hd1/CO1–PRR37/PPD1–Ghd7/VRN2 protein complex under long days to repress flowering via repression of *Early heading date 1* (*Ehd1*) and hence *FT/Hd3a* (Griffiths *et al.*, 2003; Xue *et al.*, 2008; Zhang *et al.*, 2015; Fujino *et al.*, 2019). Together with the fact that rice *Hd1* and wheat *CO2* promote and repress flowering under short days, respectively, these data support a role for changing *CO*-like protein interactions in transitions between short-day, day-neutral, and long-day flowering photoperiodism (Kitagawa *et al.*, 2012; Song *et al.*, 2015; Mulki and von Korff, 2016).

In addition to positively and negatively regulating *FT* (also named *VRN3*; Yan *et al.*, 2006) in barley and wheat, CO1 and CO2 are involved in a regulatory feedback loop with VRN2 (Mulki and von Korff, 2016). *VRN2* is a monocot-specific repressor of flowering that is negatively regulated by vernalization in the large 'core' Pooideae clade, comprising species such as wheat, ryegrasses (*Lolium* sp.), and oats (*Avena* sp.). However, *VRN2* is not down-regulated in response to cold in other 'non-core' Pooideae clades, including vernalization-responsive *B. distachyon* (Woods *et al.*, 2016). Under long days of the early autumn, winter barley *VRN2* is strongly up-regulated in leaves by the action of CO1, CO2, and PPD1 (Distelfeld *et al.*, 2009). Overexpression of *CO1* and *CO2* in spring barley results in up-regulation of *VRN2*, leading to delayed flowering in both long and short days (Mulki and von Korff, 2016). In turn, VRN2 negatively regulates *CO1/2* and *PPD1*, thereby

dampening its own expression (Mulki and von Korff, 2016). As winter approaches, low-temperature-induced expression of the flowering promoter *VERNALIZATION 1* (*VRN1*; Oliver *et al.*, 2009) results in the gradual repression of *VRN2*, and a concomitant increase in *FT*, partly mediated by CO1/2 and PPD1 (Song *et al.*, 2015; Mulki and von Korff, 2016).

CO9 is a grass-specific paralog of *VRN2/Ghd7* (Woods *et al.*, 2016), and overexpression in rice suggests that it acts as a floral repressor (Kikuchi *et al.*, 2012). Based on expression and functional analyses, this occurs under both short and long days, where transcript abundance peaks early after dawn (Kikuchi *et al.*, 2012). Since barley *VRN2* is expressed at its highest level towards the end of the light period (Trevaskis *et al.*, 2006), and rice *Ghd7* is expressed at high levels throughout the light period (Xue *et al.*, 2008), these data suggest evolution of *VRN2/CO9* genes in terms of both photoperiodic and circadian regulation following both duplication and speciation events.

Here, we reconstruct the evolution of photoperiodic flowering in Pooideae to test the hypothesis that flowering in response to long days evolved early in the subfamily and hence facilitated a range shift into northern temperate regions. We show that ancestral Pooideae was probably long day responsive, and that a secondary transition back to tropical climates was coincident with a shift back to short-day flowering. To determine if this derived short-day responsiveness can be explained by changes in the (co-)expression of CCT domain genes, we assess relative transcript levels for long- and short-day light–dark cycles across time in exemplar long- and short-day flowering species.

Materials and methods

Plant growth and experimental conditions

Forty-seven Pooideae species (13 core and 34 non-core) and the outgroup *Ehrharta calycina* from subfamily Oryzoideae (Supplementary Table S1) were selected to represent phylogenetic and geographic diversity across Pooideae. The plants were grown under different treatment conditions to score for long-day, short-day, or day-neutral flowering. Fifteen plants were grown per treatment. All seeds were stratified in moist soil (Gartnerjord, Tjerbo Torvfabrikk AS, Rakkestad, Norway) in complete darkness for 6 d, first under 4 °C for 5 d, followed by 1 d at room temperature. Seeds were then transferred to an open greenhouse in long days (16 h light:8 h dark) at 17 °C and grown for 4 weeks before the plants were randomized and assigned to one of four treatments: 17 °C short days (8 h light:16 h dark), 17 °C long days, 4 °C short days, or 4 °C long days for 12 weeks. We included vernalization in two of the treatments to see the effect of photoperiod even in vernalization-responsive species. All short- and long-day-grown plants were then maintained in short or long days, respectively, at 17 °C until flowering (calculated as days to heading) or termination of the experiment at 200 d. The experiment was repeated following the same conditions, except for reduction of the vernalization period to 8 weeks, switching the upper temperature to 20 °C, and termination of the experiment at 120 d. Light intensity under vernalization was 50 ± 5 μmol m^{-2} s^{-1}, and for all other conditions it was 150 ± 10 μmol m^{-2} s^{-1}. Light used in the experiment was produced by HQI lightning systems (LU400/XO/T/40 Philips Osram, General Electric, Hungary) giving a red/far-red ratio of 1.8 ± 0.2. Plants were watered and fertilized (water containing 4% Yara Kristalon Indigo and 3% YaraTera Calcium Nitrate, Yara Norway AS), adjusted to an electron conductivity of 1.5 as needed, and moved to a new position twice a week within the chamber.

To investigate more closely molecular responses to different photoperiods, two non-core Pooideae species in tribe Stipeae, long-day *Oloptum miliaceum* (USDA GRIN PI207772) and short-day *Nassella pubiflora* (USDA GRIN PI478575), and the long-day flowering Meliceae species *Melica ciliata* (Millennium Seed Bank 31675) were chosen for a follow up-experiment based on results from the first growth experiment. *Ehrharta calycina* (USDA GRIN PI284803 and PI578674) from the subfamily Oryzoideae was included as an outgroup. None of these species had an absolute vernalization requirement. Growth experiments were performed in two Conviron CMP6010 (Conviron, Winnipeg, Canada) growth chambers. Approximately 160 seeds of each of *M. ciliata*, *N. pubiflora,* and *O. miliaceum*, and 88 seeds of *E. calycina* were sown on moist filter paper and stratified under darkness for 4 d at 4 °C followed by 1 d at room temperature. Seeds were then planted in Metro-Mix 380, grown under long days at 20 °C for 4 weeks, and randomly assigned either to a long-day 20 °C or short-day 20 °C treatment until flowering, death, or termination of the experiment. For each plant, days to heading, number of leaves on the main stem at flowering, and tillers at flowering were recorded. The top fully expanded leaf of at least three plants without repeated measures were sampled at 2, 16, and 30 d after the initial 4 weeks growth under long days at 2, 8, 14, and 20 h post-dawn (ZT).

DNA extraction and sequencing

Genomic DNA was extracted from leaf material using the DNeasy Plant MiniKit (Qiagen, Valencia, CA, USA), following the manufacturer's protocol. We obtained sequences for three DNA plastid regions *matK*, *ndhF*, and *rbcL*, using custom Pooideae-specific primers (Schubert *et al.*, 2019a; Supplementary Table S2). PCR was performed on a Tetrad 2 Thermal Cycler (Bio-Rad, Hercules, CA, USA) and a Mastercycler ep Gradient Thermal Cycler (Eppendorf, Hamburg, Germany) using JumpStart REDTaq ReadyMix (Sigma-Aldrich, St. Louis, MO, USA) and standard conditions with 58 °C annealing and 2 min extension. PCR products were Sanger-sequenced in both directions using the same primers as for PCR. Chromatograms and sequences were inspected in BioEdit (Hall, 1999), and automatic alignments generated with manual adjustments (Supplementary Datasets S1–S3).

Ancestral state reconstruction of flowering responses

Phylogenetic trees were generated for the concatenated *matK*, *ndhF*, and *rbcL* chloroplast dataset in MrBayes on XSEDE (Miller *et al.*, 2010) implemented through the CIPRES Science Gateway v.3.3. The dataset was partitioned by gene, rooted with sequences from maize (*Zea mays* ssp. *mays*), and run twice for 10 million generations sampling every 1000 generations, with four chains, 25% burn-in, and other default parameters. The consensus tree was visualized in FigTree v1.4.3 (http://tree.bio.ed.ac.uk/software/figtree/) and edited in Adobe Illustrator CS6. To account for uncertainty in topology prior to ancestral state reconstruction, 200 rooted trees with branch lengths were collated from the two independent runs as input for BayesTraits v2 (Pagel *et al.*, 2004; Pagel and Meade, 2006). BayesTraits was run using the Multistate function, and a one-rate/symmetrical model was chosen based on results of stepping-stone estimation comparing symmetrical and asymmetrical state transition models. Markov chain Monte Carlo (MCMC) analyses were run with 10 million generations, sampling every 1000th generation, with a burn-in of 25%. Trait states for all internal nodes in the Bayesian consensus tree were inferred by calculating the means of posterior probability distributions for each node.

Scanning electron microscopy

To document if differences in time of transition reflect the flowering phenotype, we chose a representative subset of our focal species to investigate this at the level of SAM development under different photoperiods. We documented the developmental stage of *O. miliaceum*, *N. pubiflora*, and *E. calycina* SAMs across time points and treatments by dissecting meristems and subjecting them to SEM. At 2, 16, 27, and 41 d after onset of treatment, three SAMs from each species were fixed in formalin acetic acid (FAA) (50% ethanol, 5% glacial acetic acid, 10% of 37% formaldehyde) solution for 8–12 h. Following this, meristems were progressively transferred in five steps from 50% to 100% ethanol before critical point drying. Meristems were mounted on stubs, sputter coated with argon, and photographed using a JEOL 6060 SEM with an accelerating voltage of 25 kV.

RNA extraction, cDNA synthesis, and quantitative PCR

Leaves of *M. ciliata*, *O. miliaceum*, *N. pubiflora*, and *E. calycina* were flash-frozen in liquid nitrogen, stored at –80 °C, and later macerated for RNA extraction using TriReagent (Ambion, Thermo Fisher Scientific, Waltham, MA, USA) followed by removal of DNA by DNase treatment with the TURBO DNA-free kit (Ambion). cDNA was then synthesized from 500 ng of RNA using the iScript cDNA synthesis kit (Bio-Rad, Hercules, CA, USA). All procedures followed the manufacturer's instructions.

A *CO9* ortholog from *E. calycina* and *VRN2* orthologs from *N. pubiflora* and *O. miliaceum* were amplified in a standard PCR with cDNA pooled across time points and treatments for each species using previously published (Woods *et al.*, 2016), as well as newly designed, primers (see Supplementary Table S2). Amplicons were ligated into pGEM-T (Promega, Madison, WI, USA), plasmids used to transform competent DH5α *Escherichia. coli* cells, and ~10 clones were sequenced per amplicon by the Advanced Genomes Technology Core at The University of Vermont. *VRN2* from *M. ciliata* has previously been published (Woods *et al.*, 2016). To identify orthologs of *CO9* from *O. miliaceum*, *N. pubiflora*, and *M. ciliata*, as well as orthologs of *PPD1*, *CO1*, and *PHYC* from all Pooideae species, we generated transcriptomes for each species from leaves sampled in both conditions throughout a 24 h cycle. Briefly, leaves were flash-frozen in liquid nitrogen, and total RNA was extracted from homogenized tissue using the RNeasy Plant Mini Kit (Qiagen) including purification using the Invitrogen TURBO DNA-free kit (Thermo Fisher Scientific). Sequencing libraries with an insert size of 350 bp were constructed with the TruSeq Stranded mRNA Library Prep kit (Illumina, San Diego, CA, USA). Library preparation and paired-end sequencing was carried out by the Norwegian Sequencing Centre (NSC) at the University of Oslo on an Illumina HiSeq 4000 System (Illumina) with 150 bp reads. Read trimming and quality assessment of the transcriptomes followed Schubert *et al.* (2019b). The target sequences were identified through a BLAST search against the transcriptomes from the respective species using verified sequences from *H. vulgare* as queries (Supplementary Datasets S4–S7).

Nucleotide sequences of *PHYC*, *PPD1*, *CO1/CO2/Hd1*, *VRN2/Ghd7*, or *CO9* were identified in model grass species through BLAST searches using verified sequences from *H. vulgare* as queries (see Supplementary Datasets S4–S7). To verify orthology, new sequences from our focal species were aligned with sequences of model species using MAFFT (Katoh and Standley, 2013) followed by manual adjustments, and maximum likelihood phylogenetic analysis using PHYML through NGPhylogeny.fr using default parameters and 500 bootstrap replicates (Dereeper *et al.*, 2008; Lemoine *et al.*, 2019).

For each target gene and focal species, we designed primers for quantitative reverse transcription–PCR (RT–qPCR) (Supplementary Table S2). Primers for *VRN3* and the housekeeping genes *UBIQUITIN 5* (*UBQ5*) and *ELONGATION FACTOR 1α* (*EF1α*) were either previously published (Ream *et al.*, 2014) or designed based on conserved regions in alignments of *Lolium perenne*, wheat, and *Oryza brachyantha* or rice, whereas *VRN2* primers were constructed based on previously published alignments (McKeown *et al.*, 2016). All new primers were designed using Primer3 (Rozen and Skaletsky, 2000), and the amplification efficiency of each primer pair was determined using a dilution series as previously described (Scoville *et al.*, 2011). To quantify relative gene expression, target gene critical threshold c(T) values were normalized against the geometric mean of the two housekeeping genes after correction for primer efficiency with three technical and at least three biological replicates.

Western blot

An alignment was made of translated transcript sequences of *CO9* and *VRN2* from *N. pubiflora*, *O. miliaceum*, and *M. ciliata* as well as a selection of other grass species (Supplementary Dataset S8). Polyclonal antibodies were constructed for *N. pubiflora* and *O. miliaceum* (antigenic peptide sequence RRGMRCGVADLNRGC) and *M. ciliata* (a mix of the antigenic peptide sequences AGRRCGVAADLNLRC and VDQQEPAVIGGGGAC) to avoid cross-reactivity with VRN2. Leaf tissue was sampled from three biological replicates of each species subjected to long or short days at ZT2, 8, 14, and 20 one week after start of treatment, as previously described. Approximately 100 mg of tissue was ground in liquid nitrogen using a mortar and pestle, before adding 200 µl of DTE extraction buffer [3 mM DTT, 20 mM sucrose, 3 mM Na_2CO_3, 0.5% SDS, 1 mM EDTA, and 1:100 v/v of protease inhibitor cocktail (Sigma)]. Each sample was mixed briefly by vortexing, sonicated for 2.5 min (5 s on, 5 s off for a total of 5 min), and centrifuged at 12 000 *g* for 20 min at 4 °C. The supernatant was then transferred to a fresh tube and centrifuged for another 15 min. A 50 µl aliquot of the supernatant was precipitated using 500 µl of 10% trichloroacetic acid (TCA), and centrifuged at maximum speed (20 000 *g*) for 10 min at 4 °C. The liquid was removed, and the pellet left to air-dry before being dissolved in 0.1% NaOH. The concentration of protein extract was measured using a Qubit protein assay kit after adding 1:1 volume of 2× Laemmli sample buffer containing 5% β-mercaptoethanol. Three technical replicates of protein extract were incubated at 75 °C for 10 min, put briefly on ice, and centrifuged at 12 000 *g* for 1 min at 4 °C.

A 25 µg aliquot of protein was applied to a 12% Mini-PROTEAN® TGX Stain-Free™ Precast Gel, using 3 µl of Precision Plus Protein Unstained Standard as a marker. The gel was run at 200 V for 40-45 min in 1× Tris/Glycine/SDS buffer (Bio-Rad), UV-activated for 1 min using GelDoc Stain Free gel application, and the proteins blotted onto a 0.2 µm polyvinylidene difluoride (PVDF) membrane using the Trans-Blot Turbo Mini 0.2 µm PVDF Transfer Packs (Bio-Rad) and Trans-Blot® Turbo™ Transfer System (Bio-Rad). The Turbo program was set at 25 V and 2.5 mA for 3 min, and the membrane was analyzed using GelDoc Stain Free Blot application for loading control and normalization as per the manufacturer's instructions. After being left to air-dry, the membrane was activated for 3 min with methanol and blocked in 2% dry milk solution in 1× TBS-T (500 mM NaCl, 20 mM Tris–HCl pH 7.5) for 1 h at room temperature. After washing twice for 10 min in TBS-T, the membrane was incubated with primary antibody diluted in blocking solution at 4 °C overnight. Dilutions were 0.25 µg ml^{-1} for *N. pubiflora* and 0.5 µg ml^{-1} for *O. miliaceum*. Following this, membranes were washed for 6 × 10 min in TBS-T followed by incubation for 1 h at room temperature with a 1:1000 dilution of mouse anti-rabbit horseradish peroxidase (HRP)-conjugated secondary antibody (SC-2357 Santa Cruz Biotechnology, Dallas, TX, USA). Subsequently, the membrane was washed 6 × 10 min in TBS-T and the signal was developed using Clarity™ Western ECL Substrate (Bio-Rad). After visualizing the signal using the GelDoc Chemi application, quantitation and analysis were performed using the Image Lab 6 software.

Statistical analyses

To capture both qualitative and quantitative variation in flowering behavior across species, we calculated both the proportion of individuals flowering per treatment and absolute dates to heading per treatment. In cases where flowering consistently occurred in the absence of vernalization, we used non-vernalized long- and short-day-treated plants to calculate the photoperiod response. However, when plants had an absolute requirement for vernalization to flower, we used vernalized long- and short-day-treated plants to calculate the photoperiod response. We classified species as long day responsive if the proportion of individuals flowering was significantly more ($P<0.05$ as determined by a χ^2 test), and/or days to heading was significantly less ($P<0.05$ determined by a two-tailed *t*-test) in long as compared with short days, and vice versa for short-day-responsive species.

For the relative gene expression data, two-way ANOVAs were performed with expression of *PHYC*, *PPD1*, *CO1*, *VRN2*, and *CO9* as dependent variables, and treatment and ZT time as independent variables. We removed the effect of sampling day (samples were taken at days 2, 16, and 30 after onset of treatment) by centering and standardizing expression data for all days using the 'scale' and 'center' functions in R. This was repeated for all genes and species, except for *VRN3* that is expected to increase in expression only after receiving several upstream inductive signals; in this case, expression was analyzed over the three sampling days separately. Analyses were done using both raw and transformed data, and analyses where the residuals best fitted a normal distribution were chosen for further interpretation. To investigate the effect of photoperiod on expression at specific time points, we performed post-hoc contrasts for all species, genes, and time points. All ANOVAs and post-hoc tests were carried out in R (RCoreTeam, 2016) using the stats and emmeans (Lenth, 2021) packages.

Each western blot was run with one complete set of samples from both treatments from one species, with three technical replicates. Three biological replicates were run per species. One of the replicates of *M. ciliata* produced smeared bands and we were unable to quantify protein abundance. As values cannot be compared directly across different blots, we removed the effect of blotting gels by centering and standardizing the protein expression data per blot using the 'scale' and 'center' functions in R, before averaging over technical replicates, and the biological replicates for each time points in each treatment. Graphs of mRNA and protein abundance were plotted in R (RCoreTeam, 2016), using packages ggplot2 (Wickham, 2016), tidyverse (Wickham *et al.*, 2019), ggalt (Rudis *et al.*, 2017), and patchwork (Pedersen, 2019). We visually inspected the resulting graphs to find the diurnal expression pattern.

Results

Long-day flowering evolved early in Pooideae

Of the 47 Pooideae species tested for flowering responses to different photoperiods, we characterized 21 as long day responsive, five as short day responsive, and five as day neutral. For the remaining species, five (*Diarrhena obovata*, *Duthiea brachypodium*, *Hesperostipa spartea*, *Nassella neesiana*, and *Schizachne purpurascens*) failed to give a statistically clear response due to too few individuals flowering, and 11 species were completely non-flowering (*Ampelodesmos mauretanicus*, *Brachypodium pinnatum*, *Brachypodium sylvaticum*, *Diarrhena americana*, *Helictrotrichon hookeri*, *Helictotrichon pubescens*, *Lygeum spartum*, *Phaenosperma globosa*, *Stipa barbata*, *Stipa lagascae*, and *Stipa pennata*; Fig. 1). Twenty-two species flowered in adequate numbers without vernalization, five of which were identified as short day responsive, either because they flowered significantly faster (*N. pubiflora* and *Nassella brachyphylla*, *t*-test, $P<0.05$) or because significantly more individuals flowered (*Nassella cernua*, *Nassella lepida*, and *Nassella pulchra*, χ^2 test, $P<0.05$) in short than in long days. The five species identified as day neutral either showed no significant difference in flowering time between photoperiodic treatments (*Glyceria striata*, *Macrochloa tenacissima*, *Bromus inermis*, and *Boissera squarrosa*, *t*-test, $P>0.05$) or produced conflicting results between different treatments in flowering time and frequency (*Nardus stricta*). Twelve species were identified as long day responsive in the absence of vernalization due to them flowering faster (*Glyceria occidentalis*, *Achnatherum bromoides*, *Piptochaetium avenaceum*, and *Achnella caduca*, *t*-test, $P<0.05$), or with significantly more individuals flowering (*Brachypodium distachyon*, *Melica altissima*, *Melica californica*, *M. ciliata*, *Melica transsilvanica*, *O. miliaceum*, *Elymus caninus*, and *Elymus hystrix*, χ^2 test, $P<0.05$) in long versus short days.

Nine species (*Melica nutans*, *Festuca pratensis*, *Poa alpina*, *Dactylis glomerata*, *Anthoxanthum odoratum*, *Lolium perenne*, *Piptatherum aequiglume*, *Hordeum bulbosum*, and *Hordeum vulgare*) flowered in adequate numbers only after vernalization. Of these, only *M. nutans* flowered in response to both photoperiods and was scored as long day responsive because flowering was faster in long compared with short days (*t*-test, $P<0.05$). All other Pooideae species were evaluated as long day responsive as significantly more individuals flowered in long than in short days (χ^2 test, $P<0.05$). As predicted, the outgroup species *E. calycina* (Oryzoideae) was classified as short day responsive as it flowered significantly more in short versus long days without vernalization ($P<0.05$).

To reconstruct the ancestral history of Pooideae photoperiodic flowering, we added several GenBank accessions to our new chloroplast dataset, resulting in alignment lengths of 1582 bp for *matK*, 1348 bp for *ndhF*, and 1104 bp for *rbcL*. Bayesian ancestral state reconstruction based on this concatenated dataset and flowering behaviors supported an early origin of long-day-induced flowering at or around the base of Pooideae (Fig. 2). In addition, at least four transitions to day-neutral flowering were inferred to occur in as many tribes across the tree, and one origin of short-day flowering was inferred near the base of *Nassella* (tribe Stipeae). We here ignore previous reports on day-neutral flowering in artificially selected crop cultivars (Dubcovsky *et al.*, 2006; Beales *et al.*, 2007; Faure *et al.*, 2012; Campoli *et al.*, 2013; Nishida *et al.*, 2013; Turner *et al.*, 2013; Pankin *et al.*, 2014), as we focus on reconstructing the natural evolution of photoperiodic flowering. No transitions from short- to long-day photoperiodic flowering were inferred in Pooideae. The position of long-day *Achnella caduca* within the short-day *Nassella* tribe should be qualified by it being a hybrid between *Nassella viridula* and *Achnatherum hymenoides*. These data support the hypothesis that loss of long-day flowering (i.e. day neutrality) is easier than to gain than short-day flowering, or that there has been stronger selection pressure for the former.

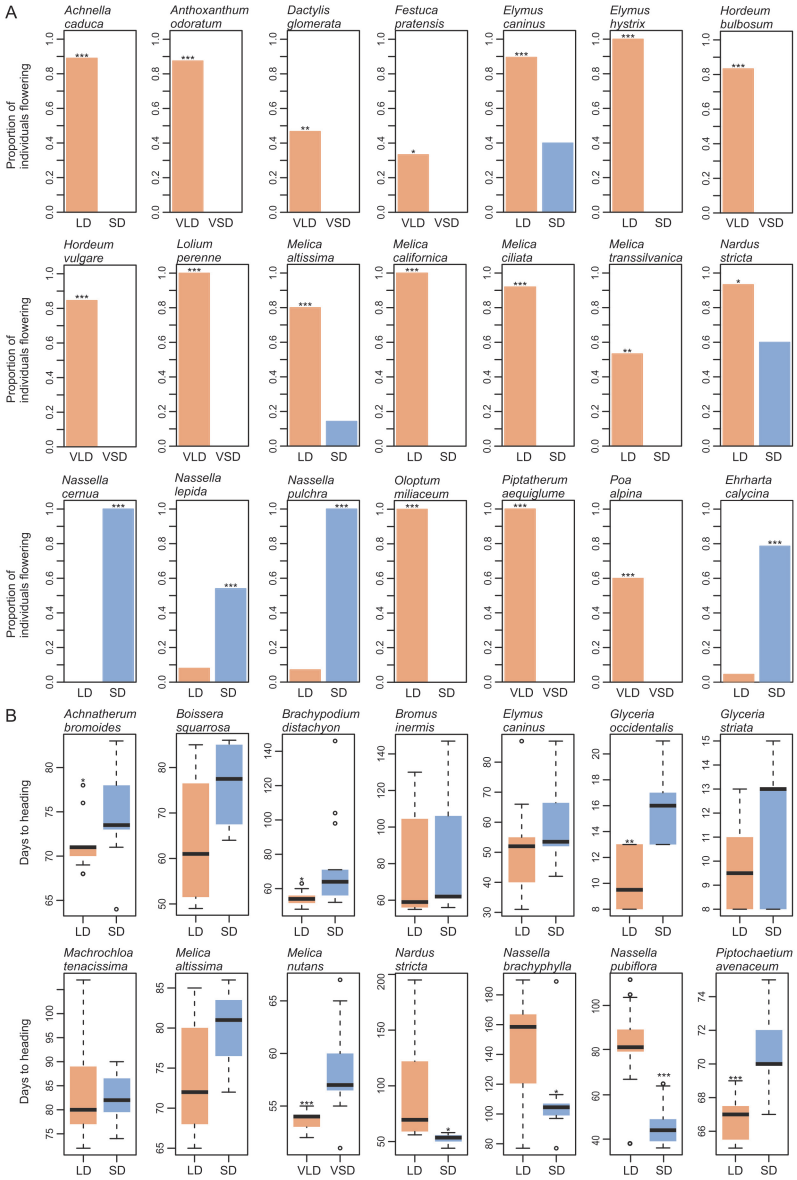

Fig. 1. Flowering behavior for 31 of the 47 tested Pooideae species as well as *Ehrharta calycina* of the Oryzoideae. Comparisons were made between either long- or short-day treated plants (LD/SD) or between vernalized plants followed by long- or short-day treatments (VLD/VSD). (A) Barplots of proportion of individuals flowering under different photoperiods. (B) Boxplots of days to heading under different photoperiods. Three species are included in both (A) and (B) as they flowered in both compared treatments, but in inadequate numbers for *t*-tests (*Melica altissima*) or results were conflicting between comparisons of proportion of plants flowering and heading dates (*Elymus caninus* and *Nardus stricta*). *Nassella pulchra* and *Nassella lepida* flowered with only one individual in one of the treatments, and plots for heading date are not shown. The remaining 18 species failed to flower consistently enough to score. **P*>0.05, ***P*>0.005, ****P*>0.001. Red color indicates long-day treatment and blue color indicates short-day treatment.

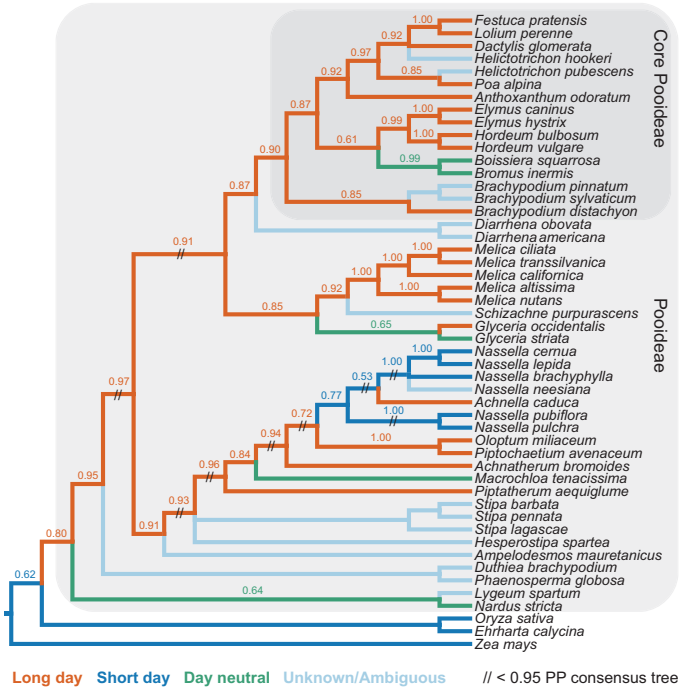

Fig. 2. Consensus Bayesian Pooideae tree showing Bayesian state reconstruction for photoperiodicity in flowering. Colored internal branches refer to best-supported [>0.50 posterior probability (PP), shown as numbers above branches] inferred character states: long day (red), short day (dark blue), and day neutral (green). Extant species with light blue branches did not flower, and the internal branches were inferred as ambiguous (PP=0.33 long day, 0.33 short day, and 0.33 day neutral). Tip branches are colored based on results of experiments (see Fig. 1). The topology is supported by >0.95 PP except branches bearing a double backslash. Outgroups are *Zea mays* (Panicoideae), and *Ehrharta calycina* and *Oryza sativa* (Oryzoideae).

FT/VRN3 *mRNA is a consistent marker of flowering*

To complement our ancestral reconstruction with gene expression analyses, we conducted a second flowering time experiment under different photoperiods in exemplar species: outgroup *E. calycina*, long-day Pooideae *M. ciliata* and *O. miliaceum*, and short-day Pooideae *N. pubiflora*. Unexpectedly, *E. calycina* plants failed to flower under either long or short days in our follow-up experiment. The lack of adult vegetative or inflorescence meristems at day 27 in both photoperiods suggests that these plants failed to become competent to flower (Supplementary Fig. S1). This result was consistent with no detectable *FT/VRN3* expression.

For *M. ciliata* and *O. miliaceum*, ANOVA verified the prediction that *FT/VRN3* expression would be higher in long as compared with short days ($P<0.001$ and $P<0.001$, respectively, Fig. 3), consistent with clear spikelet meristems being visible by day 41 under long but not short days in *O. miliaceum* (Supplementary Fig. S1; data for *M. ciliata* not collected). In contrast, and in line with the observation of well-developed inflorescences at day 41 in short but not long days (Supplementary Fig. S1), *N. pubiflora* showed significantly higher *FT/VRN3* in short days ($P<0.001$) (Fig. 3).

Pooideae PHYC *and* PPD1 *expression is generally conserved*

After phylogenetically confirming orthology with other single-copy *PHYC*- and *PPD1*-like grass genes, we determined transcript levels for our focal Pooideae taxa, first to determine any differences between naturally occurring long- and short-day Pooideae, and second to provide context for expression of other CCT genes whose protein products potentially interact with PPD1. For *PHYC*, ANOVA showed no significant effect of photoperiod on expression for long-day *O. miliaceum* and *M. ciliata* or short-day *N. pubiflora* (Fig. 4). In contrast, photoperiod had a significant effect on expression levels of *PPD1* for both *O. miliaceum* and *M. ciliata* ($P<0.001$ for both, Fig. 4). Post-hoc tests showed significantly higher expression in long as compared with short days at ZT2, ZT8, and ZT14 in *O.*

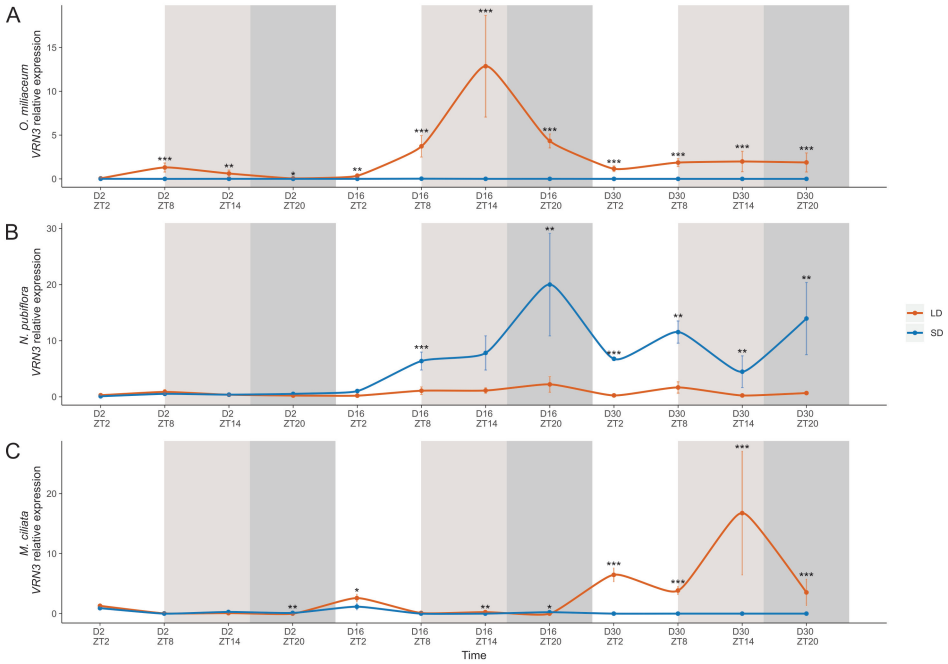

Fig. 3. Relative expression of *VRN3* in long- or short-1 day treated plants of (A) *Oloptum miliaceum*, (B) *Nassella pubiflora*, and (C) *Melica ciliata*. Sampling time points are given as Zeitgeber time (ZT) indicating hours after dawn per sampling day. Error bars indicate standard error. White background represents time points that are in the light period in both treatments, light gray background represents time points that are in the dark in the short-day treatment and in the light in the long-day treatment, whereas dark gray background represents time points that are in the dark in both treatments. ***P<0.001, **P<0.01, *P<0.05.

miliaceum (P<0.005, P<0.001, and P<0.05, respectively) and ZT8 and ZT14 in *M. ciliata* (P<0.005 and P<0.001, respectively). ANOVA showed no significant effect of photoperiod on *PPD1* expression in *N. pubiflora* (Fig. 4); however, the post-hoc test showed that expression was higher in long days at ZT14 (P<0.05). For all species, expression peaked in the dark in both photoperiods.

Evolution of CO1 *and* CO9 *expression is consistent with derived short-day flowering in Stipeae*

Previous authors have suggested that *CO1* and *CO2* were derived from a segmental duplication event at the base of grasses (Higgins *et al.*, 2010). Since both Pooideae copies have been implicated as flowering promoters in the absence of a functional PPD1, or flowering repressors in the presence of PPD1, and *CO1* is expressed more highly than *CO2* at least in wheat, we chose *CO1* for further analysis (Shaw *et al.*, 2020). No effect of photoperiod on *CO1* expression was identified in long-day *O. miliaceum* and *M. ciliata*. However, ANOVA showed a significantly higher expression of *CO1* in long versus short days in *N. pubiflora* (P<0.001), and post-hoc tests identified significant differences identified at ZT8, 14, and 20 (P=0.05, P<0.05, and P<0.001, respectively). For all species, expression was at its lowest at ZT2 for both photoperiods and increased throughout the day.

It was previously reported that barley *CO9* is more highly expressed under short versus long days, and peaks in expression during the light (Kikuchi *et al.*, 2012). No data are currently available for the model species rice or *B. distachyon*. To determine if photoperiod regulation of *CO9* is conserved across the BOP clade, and if changes in regulation are associated with the secondary shift to short-day Pooideae flowering, *CO9* expression was profiled in all focal species (Fig. 4). ANOVA and post-hoc tests showed that *CO9* expression in the short-day outgroup *E. calycina* and long-day *M. ciliata* was similar in abundance across photoperiods, with the peak of expression coinciding with the light period under both conditions (Fig. 4). This pattern for *M. ciliata* CO9 appeared to be confirmed at the protein level based on results of the western blot (Fig. 5; but see the Discussion for potential caveats) (*E. calycina* not tested). ANOVA did not identify a significant

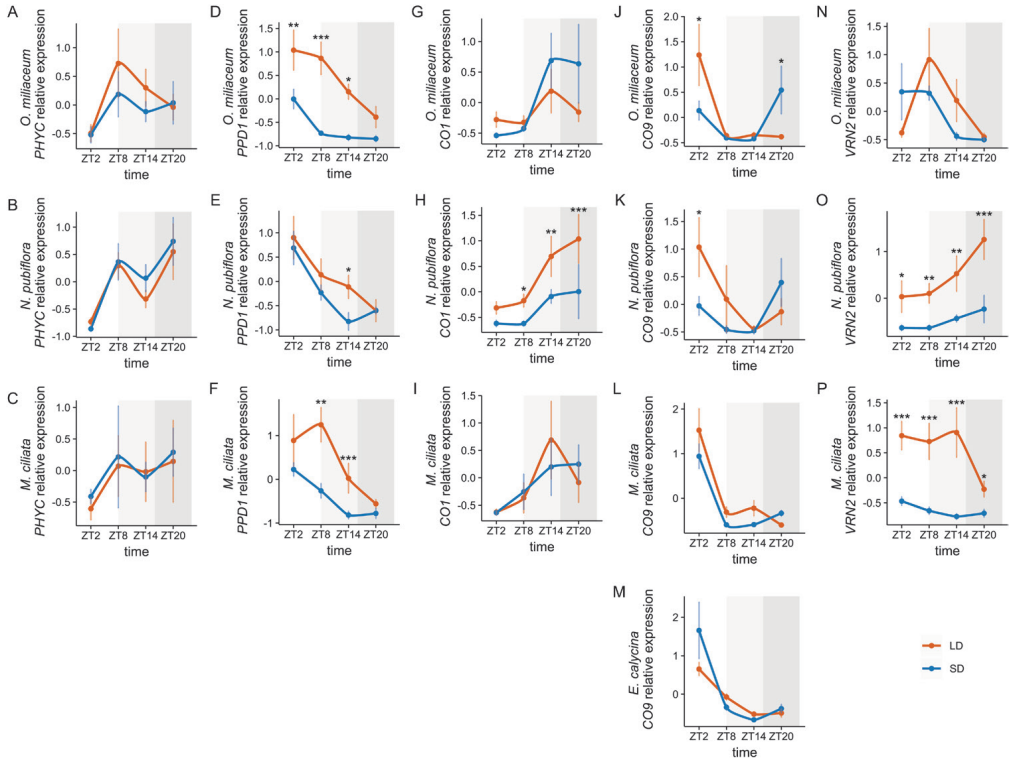

Fig. 4. Relative expression of *PHYC*, *PPD1*, *CO1*, *CO9*, and *VRN2* in long- and short-day-treated plants of (A, D, G, J, N) *Oloptum miliaceum*, (B, E, H, K, O) *Nassella pubiflora*, and (C, F, I, L, P) *Melica ciliata.* (M) Relative expression of *CO9* in *Ehrharta calycina*. Sampling time points are given as Zeitgeber time (ZT) indicating hours after dawn. Error bars indicate the SE. A white background represents time points that are in the light period in both treatments, a light gray background represents time points that are in the dark in the short-day treatment and in the light in the long-day treatment, whereas a dark gray background represents time points that are in the dark in both treatments. ***$P<0.001$, **$P<0.01$, *$P<0.05$.

effect of photoperiods on expression for *O. miliaceum* and *N. pubiflora CO9*. However, in both species, variation in periodicity resulted in a peak of expression in the light for long days and dark for short days for mRNA (Fig. 4), with a significant difference of expression between long and short days at ZT2 ($P=0.01$, Fig. 4). Furthermore, whereas the peak of mRNA expression was in the light for long days and the dark for short days (Fig. 4), CO9 protein peaked in abundance during the light of both photoperiods and species (Fig. 5), potentially suggesting transcriptional instability or protein degradation in the dark.

VRN2 *expression has evolved in both long- and short-day Stipeae*

VRN2/Ghd7 is positively regulated by long days in rice and barley (Trevaskis *et al.*, 2006; Xue *et al.*, 2008). To determine if this long-day response is generally conserved, or has evolved in short-day Pooideae taxa, we assessed *VRN2* expression in *M. ciliata*, *O. miliaceum*, and *N. pubiflora* (Fig. 4). Unfortunately, we were unable to amplify the rice *Ghd7* ortholog from *E. calycina*, suggesting either low expression in leaf tissues under our experimental conditions or high levels of sequence divergence relative to rice. ANOVA showed a significant effect of photoperiod on expression of *VRN2/Ghd7* in *M. ciliata* ($P<0.0001$) and expression was higher in long as compared with short days at all time points ($P<0.01$, $P<0.01$, $P<0.001$, and $P<0.05$, respectively, Fig. 4), peaking in the light in both photoperiods (Fig. 4). Contrary to prediction, *O. miliaceum* showed no significant difference in *VRN2/Ghd7* transcript levels between photoperiods (Fig. 4), and expression during the light period in both long and short days. Finally, despite its relatively close relationship to *O. miliaceum*, and its short-day responsiveness, *N. pubiflora VRN2/Ghd7* was expressed at a significantly higher

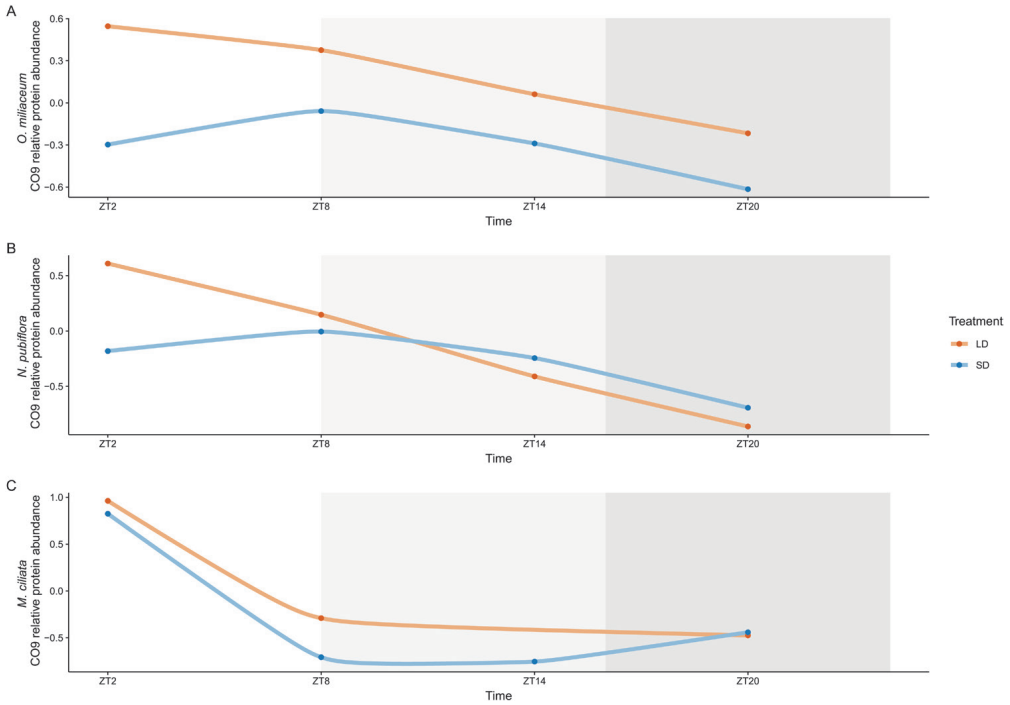

Fig. 5. Relative abundance of CO9 protein in long- or short-day-treated plants of (A). *Oloptum miliaceum*, (B) *Nassella pubiflora*, and (C) *Melica ciliata*. Sampling time points are given as Zeitgeber time (ZT) indicating hours after dawn. A white background represents time points that are in the light period in both treatments, a light gray background represents time points that are in the dark in the short-day treatment and in the light in the long-day treatment, whereas a dark gray background represents time points that are in the dark in both treatments.

level under long compared with short days ($P<0.0001$) at all time points ($P<0.05$, $P<0.01$, $P<0.01$ and $P<0.001$, respectively, Fig. 4). Interestingly, expression peaked during the dark for both photoperiods (Fig. 4). Beyond expression patterns within species averaged across days, interspecific comparisons of *VRN2* demonstrated relatively weak expression for *M. ciliata* and *O. miliaceum* under both photoperiods, with much stronger expression observed for *N. pubiflora VRN2* under long days by treatment day 16 (Supplementary Fig. S2). Assuming that VRN2 is a conserved repressor of flowering, these data are consistent with stronger long-day suppression of flowering in a short-day versus long-day species.

Discussion

Variation in photoperiodic flowering correlates with major niche transitions in the BOP clade

Pooideae is the most dominant grass subfamily of the northern temperate, continental, and Arctic regions (Hartley, 1973). We hypothesized that one of the keys to this success was the use of lengthening days in the spring and summer as a cue to flower rapidly at the appropriate time within limited growing seasons. In line with predictions of this hypothesis, ancestral state reconstruction of photoperiodic flowering responses supports both the dominance of long-day-induced flowering in Pooideae, and its evolution relatively early in the subfamily, after it diverged from Bambusoideae (bamboos). An obvious caveat to our study is the lack of exhaustive sampling across Pooideae, at both the inter- and intraspecific level. However, we believe our attempt to capture accessions spanning geographic variation within the subfamily makes our findings robust to any sampling deficits.

An early origin of vernalization-mediated flowering was previously reconstructed for Pooideae (McKeown *et al.*, 2016), which together with our data (Fig. 2) suggests that the dual photoperiod–temperature induction of flowering long known from winter Pooideae cereals (Heide, 1994) was a key step toward colonizing newly expanding temperate climates. Recent dating of the grasses (Burke *et al.*, 2016; Gallaher *et al.*, 2019; Schubert *et al.*, 2019a) places the origin of Pooideae at the transition

between the Cretaceous and Paleocene, 60–70 million years ago (Mya), at a time when mean temperatures were relatively high (Zachos *et al.*, 2001) and seasonality in temperature relatively low (Archibald *et al.*, 2013). Biogeographic studies suggest a Eurasian origin for Pooideae (Bouchenak-Khelladi *et al.*, 2010), and a recent reconstruction of the ancestral niche of Pooideae suggests that its ancestor experienced frost (Schubert *et al.*, 2019a), consistent with a cold micro-habitat origin, possibly in montane Eurasia. Together, these results imply that Pooideae was already to some degree adapted to the cool, seasonal northern climates that developed after the Eocene–Oligocene (E–O) boundary 34 Mya (Strömberg, 2011), and that the early origins of vernalization responsiveness and long-day flowering played crucial roles in the shift of Pooideae from tropical to temperate regions.

Equally as interesting was the evolution of short-day-responsive species within the Stipeae tribe that correlates with a shift back to the tropics (Fig. 2). Specifically, *Nassella pubiflora*, *N. neesiana*, and *N. brachyphylla* are all native to the South American Andes, although *N. neesiana* has been introduced to other parts of the world (www.gbif.org). On the other hand, *N. cernua*, *N. lepida*, and *N. pulchra* are endemic to California. Faster flowering under the short- versus long-day conditions of our experiment seems counter-intuitive to the fact that *N. pulchra* naturally flowers in June and July. However, we previously found that this species also has a strong vernalization response (McKeown *et al.*, 2016). We thus suggest that vernalization responsiveness has adapted *N. cernua*, *N. lepida*, and *N. pulchra* to the northern warm temperate growth cycle by blocking flowering in the shortening days of warm autumns. Whereas long days alone would delay flowering, the coincidence of lengthening days after a winter cold spell allows some physiological release, resulting in eventual flowering in the summer.

In addition to flowering, many traits, such as abscission, dormancy, cold acclimation, senescence, growth, and metabolism, are under the control of photoperiod (Salisbury, 1981). Molecular crosstalk between the networks controlling these traits has the potential to constrain their evolution through antagonistic or adaptive pleiotropy. In our experiment, most species flowered under both long and short days, although it was usually faster or biased in one condition (Fig. 1). This is consistent with data found for other grass species (Preston and Fjellheim, 2020), and suggests that Pooideae have the molecular machinery to flower under both photoperiods. Given this interpretation, other internal or external constraints must be invoked to account for the strong partitioning in geographic space between the Pooideae and other grass subfamilies (Visser *et al.*, 2014). One possible explanation is that competition prohibits the expansion of species with maladapted flowering phenotypes into areas already occupied by species with more favorable flowering responses (Sherry *et al.*, 2007). If long-day-responsive flowering evolved early in Pooideae species inhabiting a cold Eurasian montane micro-niche, it could have given the Pooideae a competitive advantage and been an important facilitator for the group's rapid expansion into the emerging and expanding temperate biomes that followed the E–O split.

Conservation of flowering time gene expression across Pooideae

The ability of many grasses to flower under both long and short days, but still be faster flowering under certain photoperiods, underscores the complexity of the flowering time gene network (Shaw *et al.*, 2020; this study). In this regard, understanding what aspects of flowering control are conserved provides important context to determine how the pathways might have changed. In the case of the evolutionary transition to short-day flowering in Stipeae, we noted that expression of *PHYC* and *PPD1* in our exemplar short-day flowering species *N. pubiflora* broadly matched the pattern found for long-day species (Fig. 4).

PHYC conveys photoperiod sensitivity to plants, with wild-type alleles promoting flowering in long-day barley, but repressing flowering in short-day rice (Takano *et al.*, 2005; Nishida *et al.*, 2013). These opposing roles are mediated through epistatic interactions with other flowering time genes, as exemplified by the fact that expression of barley *HvPHYC* actually delays flowering in a rice *phyA/phyC* background (Nishida *et al.*, 2013). In our focal species, *M. ciliata*, *O. miliaceum*, and *N. pubiflora*, *PHYC* mRNA levels were similar under both long and short days, and, as in the case of barley, generally peaked after dusk (Nishida *et al.*, 2013).

PPD1 is a downstream target of PHYC whose exact function is again affected by epistatic interactions with other flowering time genes (Zhang *et al.*, 2019; Shaw *et al.*, 2020). In wheat and barley, *PPD1* is expressed under both long and short days during the light period, but only accelerates flowering under long days or in response to a flash of light during long nights (i.e. short days) (Nishida *et al.*, 2013; Pearce *et al.*, 2017). Although the *PPD1* ortholog *PRR37* delays flowering under long days in its native rice (Zhang *et al.*, 2019), like *PHYC* its expression in long-day plants accelerates flowering, suggesting conservation of protein function (but see the effect of mutant alleles on day-length sensitivity) (Koo *et al.*, 2013; Shaw *et al.*, 2020). *PPD1* transcript abundance in *O. miliaceum*, *N. pubiflora*, and *M. ciliata* peaked in the light in both treatments (Fig. 4), as in wheat and barley (Shaw *et al.*, 2020; Gauley and Boden, 2021), and was higher under long versus short days. Given the roles of *PHYC* and *PPD1* in photoperiodicity, it is not surprising that their expression patterns are conserved across long- and short-day grasses. On the other hand, it would be interesting to assess perturbations in their expression patterns that might explain loss of long-day photoperiodism in non-core Pooideae, such as high latitude *Nardus stricta* and the widespread Eurasian–North American *Glyceria striata*.

Evolution of VRN3 *and CCT family gene expression in both short- and long-day flowering Pooideae*

As expected based on similar work across a range of angiosperms (Andrés and Coupland, 2012), *FT/VRN3* expression

tracked the flowering behavior of our focal Pooideae grasses (Fig. 3). Among others, CCT domain-containing genes are known direct regulators of *FT/VRN3* and often function in a photoperiod-dependent manner (Shen *et al.*, 2020). These attributes make them good candidates to explain evolutionary transitions between long-day, short-day, and day-neutral flowering in Pooideae through the differential regulation of *FT/VRN3*.

In the absence of a functional *VRN2/Ghd7* allele, or when *VRN2/Ghd7* transcripts are low, both *CO1* and *PPD1* have been shown to promote the expression of *FT/VRN3* in grasses, leading to the acceleration of flowering (Campoli *et al.*, 2012; Yang *et al.*, 2014; Mulki and von Korff, 2016; Zhang *et al.*, 2017). For long-day *M. ciliata* and *O. miliaceum*, *CO1* was expressed in a similar manner to rice and sorghum in that its expression level was no different in long versus short days (Fig. 4). However, *PPD1* was more highly expressed in long as compared with short days, whereas *VRN2* expression was low under both photoperiods (Fig. 4). Assuming conservation of the model from wheat, barley, and rice, the lack of strong *VRN2* transcription suggests that CO1–PPD1 will work as part of a floral activator complex under long-day conditions, consistent with long-day-regulated flowering in both *M. ciliata* and *O. miliaceum*.

In contrast to *M. ciliata* and *O. miliaceum*, *CO1* and *VRN2* transcripts were both high specifically under long days in the derived short-day flowering species *N. pubiflora* (Fig. 4; Supplementary Fig. S2). In wheat, barley, and rice, high levels of functional VRN2/Ghd7 form a repressor complex with Hd1/CO1 and PRR37/PPD1 (Yang *et al.*, 2014; Mulki and von Korff, 2016; Fujino *et al.*, 2019). Thus, again assuming functional conservation of the CO1–PPD1–VRN2 complex, these data provide at least a partial mechanism for the evolution of short-day flowering in Stipeae, whereby the VRN2–PPD1–CO1 repressor complex is strengthened specifically under long days.

In addition to the CCT domain-containing genes *CO1*, *VRN2*, and *PPD1*, *CO9* has been implicated as a repressor of flowering under both long and short days in barley, but no data are available for rice or sorghum (Kikuchi *et al.*, 2012). Expression data from the short-day rice relative *Ehrharta calycina* and long-day *M. ciliata* revealed a conserved pattern of expression, with no difference between long and short days, and transcript levels peaking in the light under both photoperiods (Fig. 4). In contrast, *CO9* expression peaked in the morning under long days and in the dark under short days for *O. miliaceum* and *N. pubiflora*, revealing a shift in the diurnal rhythm within Stipeae (Fig. 4). Since light is required to stabilize at least *A. thaliana* CO protein (Hayama *et al.*, 2017), we compared mRNA with protein accumulation in all three non-core Pooideae species and found that the short-day dark peak for *O. miliaceum* and *N. pubiflora* CO9 appeared to deteriorate at the protein level. As a result, CO9 protein was higher under long versus short days, representing a second avenue by which the loss of short-day flowering repression could have evolved in *N. pubiflora* (Fig. 5).

A potential caveat to the protein data relates to the fact that the western blot band for the CO9 antibody was ~8 kDa larger than predicted based on the amino acid sequences derived from transcriptomes of the target species (Supplementary Fig. S3). This result might be interpreted as non-specific binding to off-target proteins. However, given that the results were consistent using two independent antibodies that were designed to avoid cross-targeting to other CO-like proteins, and were generally in line with the mRNA expression profiles, we feel this unlikely. Rather, we posit that the larger size indicates ubiquitination of the target CO9 proteins, which is a common mechanism of regulating flowering time proteins (Piñeiro and Jarillo, 2013). In particular, light–dark regulation of *A. thaliana* CO involves its ubiquitination (Liu *et al.*, 2008).

Assuming correct interpretation of the protein data, less clear is the effect of high long-day CO9 protein expression in *O. miliaceum* that flowers more rapidly under long days (Fig. 5). One possible explanation is that short-day flowering evolved early in Stipeae, with the unique gain of short-day-specific *VRN2* expression in *O. miliaceum* resulting in a novel block to flowering under short photoperiods. One argument against this is the fact that *VRN2* levels are relatively low in *O. miliaceum*. Investigation into further Stipeae species and the use of functional approaches will be required to test these alternative hypotheses.

Conclusions

Daylength is used as a cue to promote or repress the reproductive transition in most plants, and the photoperiod pathway largely shares a common evolutionary basis (Andrés and Coupland, 2012). We have shown that a switch from short- to long-day induction of flowering was probably a major evolutionary innovation allowing Pooideae grasses to establish and diversify within temperate climates. However, whereas transitions to daylength-neutral flowering are common and phylogenetically widespread, reversions to short-day flowering appear relatively difficult and/or uncommon. We suggest that changes in the diurnal and long-term regulation of *CCT* domain genes by photoperiod have been important drivers of ecologically important niche shifts. Together, these data highlight both the complexity and flexibility of flowering time evolution in plants and provide novel hypotheses that can be tested through further sampling and functional analyses.

Supplementary data

The following supplementary data are available at *JXB* online.

Table S1. Materials used in the study.

Table S2. Primer sequences used in the study.

Dataset S1. *ndhF* alignment.

Dataset S 2. *matK* alignment.
Dataset S 3. *rbcL* alignment.
Dataset S4. *CO9/VRN2* alignment.
Dataset S5. *PPD1* alignment.
Dataset S6. *CO1* alignment.
Dataset S7. *PHYC* alignment.
Dataset S8. CO9/VRN2 alignment.
Fig. S1. Effect of photoperiod on Pooideae meristem development.
Fig. S2. Relative expression of *VRN2*.
Fig. S3. Western blots of CO9.

Acknowledgements

We are grateful to Øyvind Jørgensen for help with the growth experiments, Ane Charlotte Hjertaas for help with RT–qPCR, and Thomas Marcussen for assistance with growth experiments, sequencing, and making the alignment.

Author contributions

JCP and SP: conceptualization; SF, SSJ, DAY, and JCP: conducting the experiments; JCP, DAY, and SF: data analysis; JCP, DAY, and SF: interpretion of the data with input from MP, SSJ, and MS; JCP and SF—writing, with input from all authors.

Conflict of interest

The authors declare no conflicts of interest.

Funding

This work was funded by grants from United States Department of Agriculture (USDA)-HATCH (VT-H02712 to JCP) and The Research Council of Norway (231009 to SF).

Data availability

All data are available in the supplementary data. Sequences for constructing the phylogeny are available in GenBank under accession numbers OK020205–OK020264.

References

Andrés F, Coupland G. 2012. The genetic basis of flowering responses to seasonal cues. Nature Reviews. Genetics **13**, 627–639.

Archibald SB, Greenwood DR, Mathewes RW. 2013. Seasonality, montane beta diversity, and Eocene insects: testing Janzen's dispersal hypothesis in an equable world. Palaeogeography, Palaeoclimatology, Palaeoecology **371**, 1–8.

Beales J, Turner A, Griffiths S, Snape JW, Laurie DA. 2007. A pseudo-response regulator is misexpressed in the photoperiod insensitive *Ppd-D1a* mutant of wheat (*Triticum aestivum* L.). Theoretical and Applied Genetics **115**, 721–733.

Bouchenak-Khelladi Y, Verboom AG, Savolainen V, Hodkinson TR. 2010. Biogeography of the grasses (Poaceae): a phylogenetic approach to reveal evolutionary history in geographical space and geological time. Botanical Journal of the Linnean Society **162**, 543–557.

Burke SV, Lin C-S, Wysocki WP, Clark LG, Duvall MR. 2016. Phylogenomics and plastome evolution of tropical forest grasses (*Leptaspis*, *Streptochaeta*: Poaceae). Frontiers in Plant Science **7**, 1993.

Campoli C, Drosse B, Searle I, Coupland G, von Korff M. 2012. Functional characterisation of *HvCO1*, the barley (*Hordeum vulgare*) flowering time ortholog of *CONSTANS*. The Plant Journal **69**, 868–880.

Campoli C, Pankin A, Drosse B, Casao CM, Davis SJ, von Korff M. 2013. HvLUX1 is a candidate gene underlying the *early maturity 10* locus in barley: phylogeny, diversity, and interactions with the circadian clock and photoperiodic pathways. New Phytologist **199**, 1045–1059.

Chen A, Li C, Hu W, Lau MY, Lin H, Rockwell NC, Martin SS, Jernstedt JA, Lagarias JC, Dubcovsky J. 2014. *PHYTOCHROME C* plays a major role in the acceleration of wheat flowering under long-day photoperiod. Proceedings of the National Academy of Sciences, USA **111**, 10037–10044.

Dereeper A, Guignon V, Blanc G, *et al*. 2008. Phylogeny.fr: robust phylogenetic analysis for the non-specialist. Nucleic Acids Research **36**, W465–W469.

Distelfeld A, Li C, Dubcovsky J. 2009. Regulation of flowering in temperate cereals. Current Opinion in Plant Biology **12**, 178–184.

Dubcovsky J, Loukoianov A, Fu D, Valarik M, Sanchez A, Yan L. 2006. Effect of photoperiod on the regulation of wheat vernalization genes VRN1 and VRN2. Plant Molecular Biology **60**, 469–480.

Edwards EJ, Smith SA. 2010. Phylogenetic analyses reveal the shady history of C_4 grasses. Proceedings of the National Academy of Sciences, USA **107**, 2532–2537.

Faure S, Turner AS, Gruszka D, Christodoulou V, Davis SJ, von Korff M, Laurie DA. 2012. Mutation at the circadian clock gene *EARLY MATURITY 8* adapts domesticated barley (*Hordeum vulgare*) to short growing seasons. Proceedings of the National Academy of Sciences, USA **109**, 8328–8333.

Fujino K, Yamanouchi U, Nonoue Y, Obara M, Yano M. 2019. Switching genetic effects of the flowering time gene *Hd1* in LD conditions by *Ghd7* and *OsPRR37* in rice. Breeding Science **69**, 127–132.

Gallaher TJ, Adams DC, Attigala L, Burke SV, Craine JM, Duvall MR, Klahs PC, Sherratt E, Wysocki WP, Clark LG. 2019. Leaf shape and size track habitat transitions across forest–grassland boundaries in the grass family (Poaceae). Evolution **73**, 927–946.

Gauley A, Boden SA. 2021. Stepwise increases in *FT1* expression regulate seasonal progression of flowering in wheat (*Triticum aestivum*). New Phytologist **229**, 1163–1176.

Greenup A, Peacock WJ, Dennis ES, Trevaskis B. 2009. The molecular biology of seasonal flowering-responses in Arabidopsis and the cereals. Annals of Botany **103**, 1165–1172.

Griffiths S, Dunford RP, Coupland G, Laurie DA. 2003. The evolution of *CONSTANS*-like gene families in barley, rice, and Arabidopsis. Plant Physiology **131**, 1855–1867.

Hall TA. 1999. BioEdit: a user-friendly biological sequence alignment editor and analysis program for Windows 95/98/NT. Nucleic Acids Symposium Series **41**, 95–98.

Hartley W. 1973. Studies on origin, evolution, and distribution of Gramineae. 5. The subfamily Festucoideae. Australian Journal of Botany **21**, 201–234.

Hayama R, Sarid-Krebs L, Richter R, Fernández V, Jang S, Coupland G. 2017. PSEUDO RESPONSE REGULATORs stabilize CONSTANS protein to promote flowering in response to day length. The EMBO Journal **36**, 904–918.

Heide OM. 1994. Control of flowering and reproduction in temperate grasses. New Phytologist **128**, 347–362.

Higgins JA, Bailey PC, Laurie DA. 2010. Comparative genomics of flowering time pathways using *Brachypodium distachyon* as a model for the temperate grasses. PLoS One **5**, e10065.

Hochuli P, Feist-Burkhardt S. 2013. Angiosperm-like pollen and Afropollis from the Middle Triassic (Anisian) of the Germanic Basin (Northern Switzerland). Frontiers in Plant Science **4**, 344.

Katoh K, Standley DM. 2013. MAFFT: multiple sequence alignment software version 7: improvements in performance and usability. Molecular Biology and Evolution **30**, 772–780.

Kikuchi R, Kawahigashi H, Oshima M, Ando T, Handa H. 2012. The differential expression of *HvCO9*, a member of the *CONSTANS*-like gene family, contributes to the control of flowering under short-day conditions in barley. Journal of Experimental Botany **63**, 773–784.

Kitagawa S, Shimada S, Murai K. 2012. Effect of *Ppd-1* on the expression of flowering-time genes in vegetative and reproductive growth stages of wheat. Genes & Genetic Systems **87**, 161–168.

Komiya R, Ikegami A, Tamaki S, Yokoi S, Shimamoto K. 2008. *Hd3a* and *RFT1* are essential for flowering in rice. Development **135**, 767–774.

Koo BH, Yoo SC, Park JW, Kwon CT, Lee BD, An G, Zhang Z, Li J, Li Z, Paek NC. 2013. Natural variation in *OsPRR37* regulates heading date and contributes to rice cultivation at a wide range of latitudes. Molecular Plant **6**, 1877–1888.

Lemoine F, Correia D, Lefort V, Doppelt-Azeroual O, Mareuil F, Cohen-Boulakia S, Gascuel O. 2019. NGPhylogeny.fr: new generation phylogenetic services for non-specialists. Nucleic Acids Research **47**, W260–W265.

Lenth R. 2021. emmeans: estimated marginal means, aka least-squares means. R package version 1.6.2-1. https://github.com/rvlenth/emmeans

Liu L-J, Zhang Y-C, Li Q-H, Sang Y, Mao J, Lian H-L, Wang L, Yang H-Q. 2008. COP1-mediated ubiquitination of CONSTANS is implicated in cryptochrome regulation of flowering in Arabidopsis. The Plant Cell **20**, 292–306.

Lu L, Yan W, Xue W, Shao D, Xing Y. 2012. Evolution and association analysis of *Ghd7* in rice. PLoS One **7**, e34021.

Mannion PD, Upchurch P, Benson RBJ, Goswami A. 2014. The latitudinal biodiversity gradient through deep time. Trends in Ecology & Evolution **29**, 42–50.

Mascheretti I, Turner K, Brivio RS, Hand A, Colasanti J, Rossi V. 2015. Florigen-encoding genes of day-neutral and photoperiod-sensitive maize are regulated by different chromatin modifications at the floral transition. Plant Physiology **168**, 1351–1363.

Matsubara K, Hori K, Ogiso-Tanaka E, Yano M. 2014. Cloning of quantitative trait genes from rice reveals conservation and divergence of photoperiod flowering pathways in Arabidopsis and rice. Frontiers in Plant Science **5**, 193.

McKeown M, Schubert M, Marcussen T, Fjellheim S, Preston JC. 2016. Evidence for an early origin of vernalization responsiveness in temperate Pooideae grasses. Plant Physiology **172**, 416–426.

Miller MA, Pfeiffer W, Schwartz T. 2010. Creating the CIPRES Science Gateway for inference of large phylogenetic trees. In: 2010 Gateway Computing Environments Workshop 1–8.

Mulki MA, von Korff M. 2016. *CONSTANS* controls floral repression by up-regulating *VERNALIZATION2* (*VRN-H2*) in barley. Plant Physiology **170**, 325–337.

Naranjo L, Talón M, Domingo C. 2014. Diversity of floral regulatory genes of *japonica* rice cultivated at northern latitudes. BMC Genomics **15**, 101.

Nishida H, Ishihara D, Ishii M, *et al*. 2013. *Phytochrome c* is a key factor controlling long-day flowering in barley. Plant Physiology **163**, 804–814.

Oliver SN, Finnegan EJ, Dennis ES, Peacock WJ, Trevaskis B. 2009. Vernalization-induced flowering in cereals is associated with changes in histone methylation at the *VERNALIZATION1* gene. Proceedings of the National Academy of Sciences, USA **106**, 8386–8391.

Pagel M, Meade A. 2006. Bayesian analysis of correlated evolution of discrete characters by reversible-jump Markov chain Monte Carlo. The American Naturalist **167**, 808–825.

Pagel M, Meade A, Barker D. 2004. Bayesian estimation of ancestral character states on phylogenies. Systematic Biology **53**, 673–684.

Pankin A, Campoli C, Dong X, *et al*. 2014. Mapping-by-sequencing identifies *HvPHYTOCHROME C* as a candidate gene for the *early maturity 5* locus modulating the circadian clock and photoperiodic flowering in barley. Genetics **198**, 383–396.

Pearce S, Shaw LM, Lin H, Cotter JD, Li C, Dubcovsky J. 2017. Night-break experiments shed light on the photoperiod1-mediated flowering. Plant Physiology **174**, 1139–1150.

Pedersen TL. 2019. patchwork: the composer of plots. https://CRAN.R-project.org/package=patchwork

Piñeiro M, Jarillo JA. 2013. Ubiquitination in the control of photoperiodic flowering. Plant Science **198**, 98–109.

Preston JC, Fjellheim S. 2020. Understanding past, and predicting future, niche transitions based on grass flowering time variation. Plant Physiology **183**, 822–839.

RCoreTeam. 2016. R: a language and environment for statistical computing. Vienna, Austria: R Foundation for Statistical Computing. https://www.r-project.org/

Ream TS, Woods DP, Schwartz CJ, Sanabria CP, Mahoy JA, Walters EM, Kaeppler HF, Amasino RM. 2014. Interaction of photoperiod and vernalization determines flowering time of *Brachypodium distachyon*. Plant Physiology **164**, 694–709.

Robson F, Costa MM, Hepworth SR, Vizir I, Piñeiro M, Reeves PH, Putterill J, Coupland G. 2001. Functional importance of conserved domains in the flowering-time gene CONSTANS demonstrated by analysis of mutant alleles and transgenic plants. The Plant Journal **28**, 619–631.

Rozen S, Skaletsky H. 2000. Primer3 on the WWW for general users and for biologist programmers. Methods in Molecular Biology **132**, 365–386.

Rudis B, Bolker B, Schulz J. 2017. ggalt: extra coordinate systems, geoms', statistical transformations, scales and fonts for 'ggplot2'. https://CRAN.R-project.org/package=ggalt

Salisbury F. 1981. Responses to photoperiod. In: Lange OL Nobel P, Osmond CB, Ziegler H, eds. Physiological plant ecology I: encyclopedia of plant physiology, Vol. **12**. Berlin: Springer, 135–167.

Schubert M, Grønvold L, Sandve SR, Hvidsten TR, Fjellheim S. 2019b. Evolution of cold acclimation and its role in niche transition in the temperate grass subfamily Pooideae. Plant Physiology **180**, 404–419.

Schubert M, Humphreys AM, Lindberg CL, Preston JC, Fjellheim S. 2020. To coldly go where no grass has gone before: a multidisciplinary review of cold adaptation in Poaceae. Annual Plant Reviews Online **3**, 523–562.

Schubert M, Marcussen T, Meseguer AS, Fjellheim S. 2019a. The grass subfamily Pooideae: Cretaceous–Palaeocene origin and climate-driven Cenozoic diversification. Global Ecology and Biogeography **28**, 1168–1182.

Scoville AG, Barnett LL, Bodbyl-Roels S, Kelly JK, Hileman LC. 2011. Differential regulation of a MYB transcription factor is correlated with transgenerational epigenetic inheritance of trichome density in *Mimulus guttatus*. New Phytologist **191**, 251–263.

Shaw LM, Li C, Woods DP, Alvarez MA, Lin H, Lau MY, Chen A, Dubcovsky J. 2020. Epistatic interactions between PHOTOPERIOD1, CONSTANS1 and CONSTANS2 modulate the photoperiodic response in wheat. PLoS Genetics **16**, e1008812.

Shen C, Liu H, Guan Z, Yan J, Zheng T, Yan W, Wu C, Zhang Q, Yin P, Xing Y. 2020. Structural insight into DNA recognition by CCT/NF–YB/YC complexes in plant photoperiodic flowering. The Plant Cell **32**, 3469–3484.

Sherry RA, Zhou X, Gu S, Arnone JA, Schimel DS, Verburg PS, Wallace LL, Luo Y. 2007. Divergence of reproductive phenology under climate warming. Proceedings of the National Academy of Sciences, USA **104**, 198–202.

Song YH, Shim JS, Kinmonth-Schultz HA, Imaizumi T. 2015. Photoperiodic flowering: time measurement mechanisms in leaves. Annual Reviews in Plant Biology **66**, 441–464.

Soreng RJ, Peterson PM, Romaschenko K, Davidse G, Zuloaga FO, Judziewicz EJ, Filgueiras TS, Davis JI, Morrone O. 2015. A

worldwide phylogenetic classification of the Poaceae (Gramineae). Journal of Systematics and Evolution **53**, 117–137.

Stracke S, Haseneyer G, Veyrieras J-B, Geiger HH, Sauer S, Graner A, Piepho H-P. 2009. Association mapping reveals gene action and interactions in the determination of flowering time in barley. Theoretical and Applied Genetics **118**, 259–273.

Strömberg CAE. 2011. Evolution of grasses and grassland ecosystems. Annual Review of Earth and Planetary Sciences **39**, 517–544.

Takahashi Y, Teshima KM, Yokoi S, Innan H, Shimamoto K. 2009. Variations in Hd1 proteins, Hd3a promoters, and Ehd1 expression levels contribute to diversity of flowering time in cultivated rice. Proceedings of the National Academy of Sciences, USA **106**, 4555–4560.

Takano M, Inagaki N, Xie X, *et al*. 2005. Distinct and cooperative functions of phytochromes A, B, and C in the control of deetiolation and flowering in rice. The Plant Cell **17**, 3311–3325.

Trevaskis B, Hemming MN, Peacock WJ, Dennis ES. 2006. *HvVRN2* responds to daylength, whereas *HvVRN1* is regulated by vernalization and developmental status. Plant Physiology **140**, 1397–1405.

Turner AS, Faure S, Zhang Y, Laurie DA. 2013. The effect of day-neutral mutations in barley and wheat on the interaction between photoperiod and vernalization. Theoretical and Applied Genetics **126**, 2267–2277.

Valverde F, Mouradov A, Soppe W, Ravenscroft D, Samach A, Coupland G. 2004. Photoreceptor regulation of CONSTANS protein in photoperiodic flowering. Science **303**, 1003–1006.

Visser V, Clayton WD, Simpson DA, Freckleton RP, Osborne CP. 2014. Mechanisms driving an unusual latitudinal diversity gradient for grasses. Global Ecology and Biogeography **23**, 61–75.

Wei X, Qiao W, Yuan N, Chen Y, Wang R, Cao L, Zhang W, Yang Q, Zeng H. 2014. Domestication and association analysis of *Hd*1 in Chinese mini-core collections of rice. Genetic Resources and Crop Evolution **61**, 121–142.

Wickham H. 2016. ggplot2: elegant graphics for data analysis. https://ggplot2.tidyverse.org

Wickham H, Averick M, Bryan J, *et al*. 2019. Welcome to the Tidyverse. Journal of Open Source Software **4**, 1686.

Woods D, Mckeown M, Dong Y, Preston JC, Amasino RM. 2016. Evolution of *VRN2/GhD7*-like genes in vernalization-mediated repression of grass flowering. Plant Physiology **170**, 2124–2135.

Woods DP, Ream TS, Minevich G, Hobert O, Amasino RM. 2014. PHYTOCHROME C is an essential light receptor for photoperiodic flowering in the temperate grass, *Brachypodium distachyon*. Genetics **198**, 397–408.

Xue WY, Xing YZ, Weng XY, *et al*. 2008. Natural variation in *Ghd7* is an important regulator of heading date and yield potential in rice. Nature Genetics **40**, 761–767.

Yan L, Fu D, Li C, Blechl A, Tranquilli G, Bonafede M, Sanchez A, Valarik M, Yasuda S, Dubcovsky J. 2006. The wheat and barley vernalization gene *VRN3* is an orthologue of *FT*. Proceedings of the National Academy of Sciences, USA **103**, 19581–19586.

Yang S, Weers BD, Morishige DT, Mullet JE. 2014. CONSTANS is a photoperiod regulated activator of flowering in sorghum. BMC Plant Biology **14**, 148.

Yanovsky MJ, Kay SA. 2002. Molecular basis of seasonal time measurement in Arabidopsis. Nature **419**, 308–312.

Zachos J, Pagani M, Sloan L, Thomas E, Billups K. 2001. Trends, rhythms, and aberrations in global climate 65 Ma to present. Science **292**, 686–693.

Zhang B, Liu H, Qi F, Zhang Z, Li Q, Han Z, Xing Y. 2019. Genetic interactions among *Ghd7*, *Ghd8*, *OsPRR37* and *Hd1* contribute to large variation in heading date in rice. Rice **12**, 48.

Zhang J, Zhou X, Yan W, *et al*. 2015. Combinations of the *Ghd7*, *Ghd8* and *Hd1* genes largely define the ecogeographical adaptation and yield potential of cultivated rice. New Phytologist **208**, 1056–1066.

Zhang Z, Hu W, Shen G, Liu H, Hu Y, Zhou X, Liu T, Xing Y. 2017. Alternative functions of Hd1 in repressing or promoting heading are determined by Ghd7 status under long-day conditions. Scientific Reports **7**, 5388.

Zheng X-M, Feng L, Wang J, Qiao W, Zhang L, Cheng Y, Yang Q. 2016. Nonfunctional alleles of long-day suppressor genes independently regulate flowering time. Journal of Integrative Plant Biology **58**, 540–548.

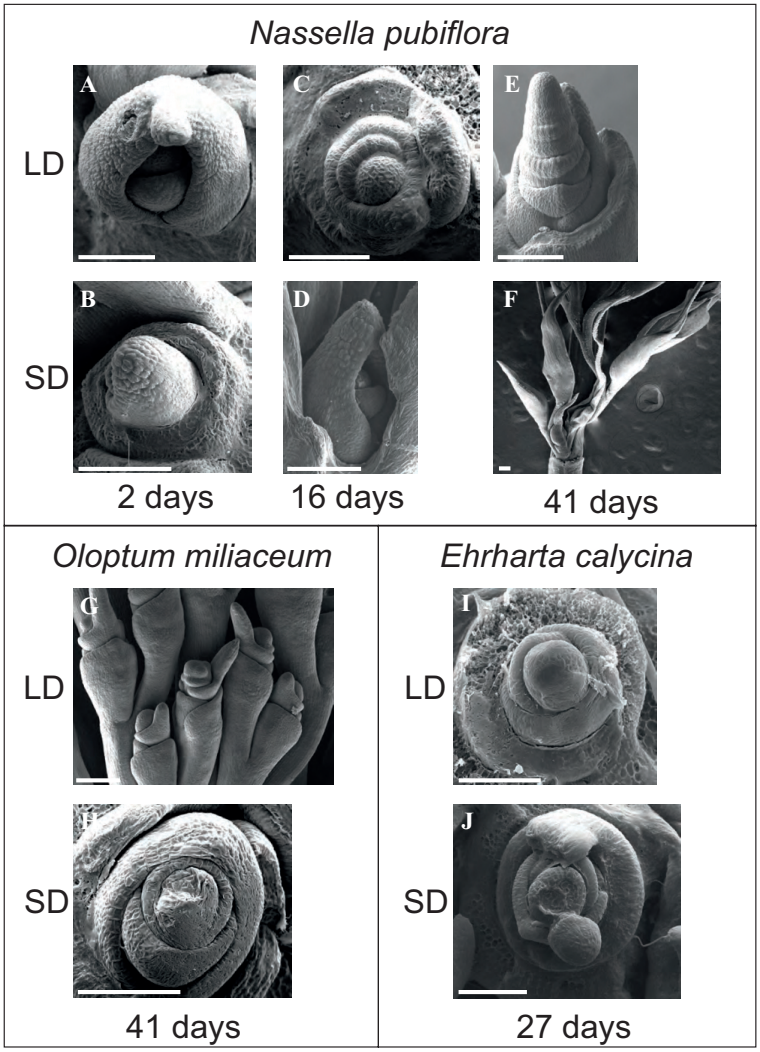

Supplementary figure S1. Effect of photoperiod on Pooideae flowering. A. *Nassella pubiflora* shoot apical meristem (SAM) with 2 long-days. B. *N. pubiflora* SAM with 2 short-days. C. *N. pubiflora* SAM with 16 long-days. D. *N. pubiflora* SAM with 16 short-days. E. *N. pubiflora* SAM with 41 long-days. F. *N. pubiflora* inflorescence with 41 short-days. G. *Oloptum miliaceum* inflorescence with 41 long-days. H. *O. miliaceum* SAM with 41 short-days. I. *Ehrharta calycina* SAM with 27 long-days. J. *E. calycina* SAM with 27 short-days. Scale bar is 100 µm.

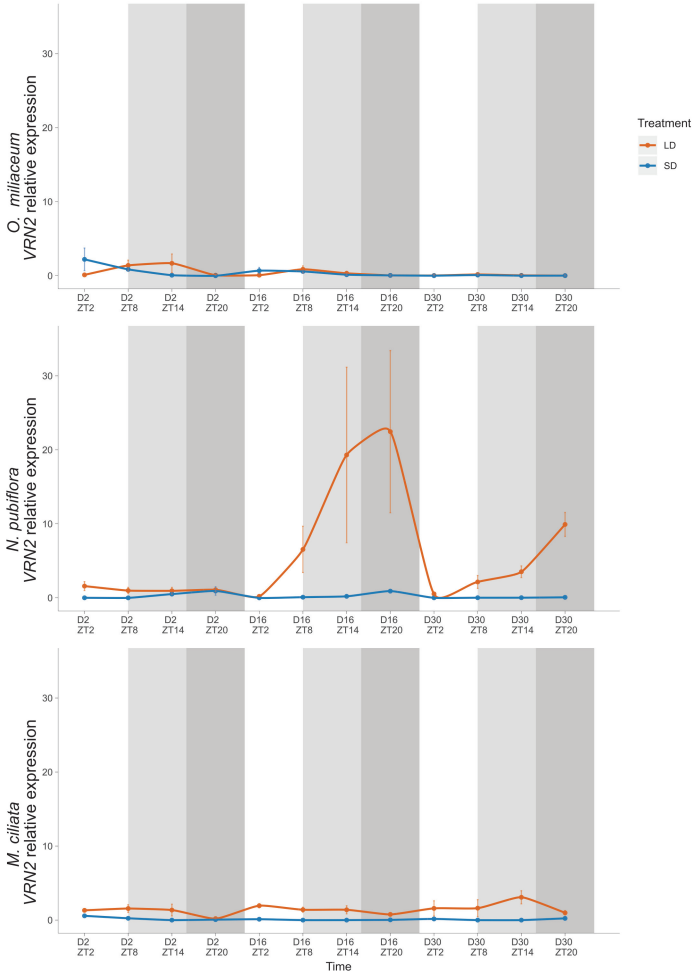

Supplementary figure 2. Relative expression of VRN2 in long- or short-day treated plants of A. Oloptum miliaceum, B. Nassella pubiflora and C. Melica ciliata. Sampling time points are given as zeitgeber time (ZT) indicating hours after dawn per sampling day. Error bars indicate standard error. White background represents time points that are in the light period in both treatments, light gray background represents time points that are in the dark in the short-day treatment and in the light in the long-day treatment, whereas dark gray background represents time points that are in the dark in both treatments

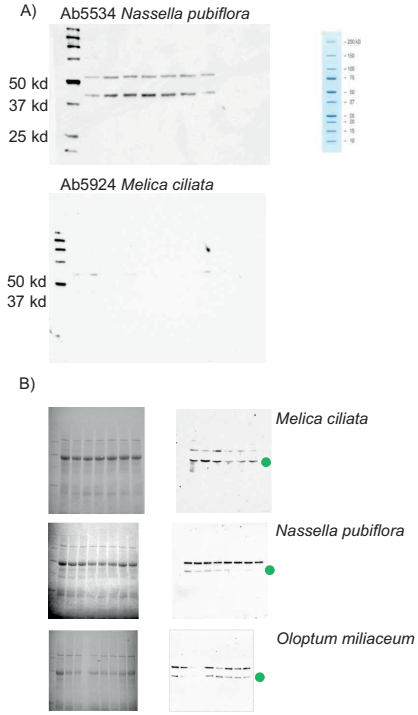

Supplementary figure 3. Western blots of CO9 proteins. A) Size of bands in relation to a ladder for the two antibodies. Staining of the Precision Plus Protein Unstained Standard (Bio - Rad) using StrepTactin-HRP Conjugate was left out in the final blots as the ladder then dominated the blot during exposure B) Exemplary blots for *Melica ciliata, Nassella pubiflora* and *Oloptum miliaceum,* stain free blots to the left and the CO9 blots to the right. Green dots represent the target bands.

Supplemental table 1. Material used in the study.

Species	Seed bank	Accession number	Location
Achnatherum bromoides	GRIN	PI253581	Israel
Achnella caduca	GRIN	PI578861	USA
Anthoxanthum odoratum	NORDGEN	NGB16571	Finland
Ampelodesmos mauretanicus	B&T World Seeds	BTWS 62975	Unknown
Boissiera squarrosa	GRIN	PI314138	Uzbekistan
Brachypodium distachyon	GRIN	PI253334	Morocco
Brachypodium pinnatum	GRIN	PI325216	Russia
Brachypodium sylvaticum		Unknown	Unknown
Bromus inermis	NORDGEN	NGB5420	Norway
Dactylis glomerata	NORDGEN	NGB7723	Norway
Diarrhena obovata	B&T World Seeds	BTWS 516238	Unknown
Diarrhena americana	B&T World Seeds	BTWS 405986	Unknown
Duthiea brachypodium	GRIN	W6 23553, 23539, 23613	China
Elymus caninus	Collected by Thomas Marcussen	TM-Langebåt 2015	Norway
Ehrharta calycina	GRIN	PI284803	Australia
Ehrharta calycina	GRIN	PI578674	USA
Elymus hystrix	MSB	235174	Unknown
Festuca pratensis	NORDGEN	NGB2910	Norway
Glyceria occidentalis	GRIN	Ames31334	USA
Glyceria striata	GRIN	PI387926	Canada
Helictotrichon hookeri	MSB	336026	Canada
Helictotrichon pubescens	MSB	65160	UK
Hesperostipa spartea	GRIN	PI372565	Canada
Hordeum bulbosum	GRIN	PI639320	Tadjikistan
Hordeum vulgare		Cultivar Sonja	
Lolium perenne	NORDGEN	NGB14263	Sweden
Lygeum spartum	MSB	105167	Unknown
Macrochloa tenacissima	GRIN	PI239234	Tunisia
Melica altissima	GRIN	W625184	Kazakhstan
Melica californica	GRIN	W647499	USA
Melica ciliata	GRIN	PI494705	Romania

Melica nutans	GRIN	PI442519	Belgium
Melica transsilvanica	GRIN	PI619447	China
Nardus stricta	Collected by Siri Fjellheim	SF-Røros 2014	Norway
Nassella brachyphylla	GRIN	PI478588	Peru
Nassella cernua	GRIN	W645567	USA
Nassella lepida	GRIN	W645113	USA
Nassella neesiana	GRIN	PI237818	Spain
Nassella pubiflora	GRIN	PI478575	Peru
Nassella pulchra	GRIN	NSL439946	USA
Piptatherum aequiglume	GRIN	PI271588	India
Oloptum miliaceum	GRIN	PI207772	Israel
Piptochaetium avenaceum	GRIN	PI266189	Jordan
Phaenosperma globosum	B&T World Seeds	BTWS 448347	Unknown
Poa alpina	NORDGEN	NGB1197	Sweden
Schizachne purpurascens	MSB	428103	USA
Stipa barbata	GRIN	PI384952	Iran
Stipa lagascae	GRIN	PI252059	Jordan
Stipa pennata	GRIN	PI314395	Russia

Supplemental table 2. Primer sequences used in this study.

Gene	Primer	Sequence	Species	Reference
Chloroplast marker				
ndhF	ndhF_Po_1F	CCGATGCTATGGARGGACCC	Pooideae in Fig. 2	(Schubert *et al.*, 2019)
	ndhF_Po_652F	TTTTTCCCCATAARGATATTGAA	Pooideae in Fig. 2	(Schubert et al., 2019)
matK	matK_Po_1F	TGTTCTGACCATATTGCACTATG	Pooideae in Fig. 2	(Schubert et al., 2019)
	matK_Po_1526	ACGCTCACTGTGTGATCCAC	Pooideae in Fig. 2	(Schubert et al., 2019)
rbcL	rbcL_Po_1F	ACCACAAACAGAAACTAAAGC	Pooideae in Fig. 2	(Schubert et al., 2019)
	rbcL_Po_590R	CATAAATGGTTGTGAGTTTACG	Pooideae in Fig. 2	(Schubert et al., 2019)
Cloning				
VRN2/CO9	CO-like_994f	GAGAAGCARATCCGSTAYGMGTC	NP, OM, EC	(Woods *et al.*, 2016)
	CO-like_1175r	CGGAACCAYCCGAGGTSRAG	NP, OM, EC	
qPCR				
Ef1α	LolEf1αF	CCTTGCTTGAGGCTCTTGAC	OM, NP, MC	(Woods *et al.*, 2016)
	LolEf1αR	GTTCCAATGCCACCAATCTT	OM, NP, MC	(Woods *et al.*, 2016)
UBQ5	GrassUBQ5F	CGCCGACTACAACATCCAG	NP, OM, EC, MC	(Woods *et al.*, 2016)
	GrassUBQ5R	TCACCTTCTTGTGCTTGTGC	NP, EC, MC	(Woods *et al.*, 2016)
	UBQ5_poace_R1	CAGTAGTGGCGGTCGAAGTG	OM	
Elf4α	Elf4α_poaceae_F2	CGCAAGGTGGACTGGCTCAC	EC	
	Elf4α_poaceae_R2	GAACTCCCTCATGATGATGT	EC	
VRN3	NassPub_VRN3_1012_f	GCAGGAGGTGGTATGCTACG	NP	(McKeown *et al.*, 2016)
	NassPub_VRN3_1304_r	CCCTGGTGTTGAAGTTCTGG	NP	(McKeown *et al.*, 2016)
	OM_VRN3_seq_354F	GGAGGTGATGTGCTACGAGA	OM	
	OM_VRN3_seq_480R	CCTGGTGTTGAAGTTCTGGC	OM	
	cMelica_VRN3_401_f	TGGTCACTGATATCCCTGGAA	MC	
	cMelica_VRN3_612_r	AACAGCACGAACACGAAGC	MC	
	EC_FT_31F	AGCGACCCCAATCTTAGAGAG	EC	
	EC_FT_158R	GTTGAAGTTCTGGCGCCAC	EC	

VRN2	NassPub_qVRN2_f	GGTACGAGTCCAGGAAAGCA	NP	(Woods *et al.*, 2016)
	NassPub_qVRN2_alt.r	GAGGTCGAGTCTGCTTGGATGT	NP	(Woods *et al.*, 2016)
	OM_VRN2a.F3	AGGAAAACTTACGCCGAGATG	OM	
	OM_VRN2a.R3	ACGTCTTGAGCTACCTTGGC	OM	
	MelCil.VRN2.F2	GGAGCCAATTATGGTCATCG	MC	
	MelCil.VRN2.R1	CATGTACCTCGTCACCTTCG	MC	
CO9	NP_CO9_497F	GGAGAGAAATACCGTTCACCG	NP	
	NP_CO9_715R	ACCGGATCTGCTTCTCGTAC	NP	
	OM_CO9_8F	TCTGCGGGAGAGAAACGTTA	OM	
	OM_CO9_241R	ACCGGATCTGCTTCTCGTAC	OM	
	MelCil.CO9.300q.F	CTCGAGCATGTGAAGGGTTG	MC	
	MelCil.CO9.501q.R	AGATGACGGAGAGGTTGCAA	MC	
	EC_CO9_qpcr_188F	GCGTACATAGGCCAAGCATT	EC	
	EC_CO9_qpcr_296R	CTGCTAGTCATCGATCACATACA	EC	
PPD1	OM ppd1 68 F	ACTCGCCATCTCTTCTCCCT	OM	
	OM ppd1 230 R	TTCTTGTGGAGGAAGCGGTC	OM	
	NP ppd1 1601 F	CTGCTCCGATGAAACAGGGT	NP	
	NP ppd1 1790 R	TCACCCATCTTCTTGCCCAC	NP	
	MC PPD1 1212F	GCCGCATGATAACAGCTTGG	MC	
	MC PPD1 1392R	CGCTGACGTGTGTGCATTAG	MC	
CO1	CO1_NPUB_468_F	CAGTGAGAGCAACAACAGCA	NP	
	CO1_NPUB_650_R	ACACACTCGTTCCCTTCCTT	NP	
	CO1_OMIL_414_F	AAAGGAGGTGGAGTCTTGGC	OM	
	CO1_OMIL_645_R	CTCGCTCCCTTCCTTCTCTC	OM	
	MelCil.CO1.FP1	CGTATCAGCAGCAACCAAGAGC	MC	
	MelCil.CO1.RP1	CGCTCAACATTACAGCCTGC	MC	
PHYC	OM PHYC 3867 F	TGGGAGAGCCTAGCTGATGT	OM	
	OM PHYC 3950 R	TCCTGCTCCCCAAACATCAC	OM	
	NP PHYC 592 F	CAGCCTATCAGCCTCTGTGG	NP	
	NP PHYC 720 R	CCCGTCCTCCTCATCCTCAT	NP	
	MelCil.PHYC.FP	CCACTTCGACTACTCCTCGTCG	MC	
	MelCil.PHYC.RP	GCATGTTCTGGAGGTAGGCAGAG	MC	

McKeown M, Schubert M, Marcussen T, Fjellheim S, Preston JC. 2016. Evidence for an Early Origin of Vernalization Responsiveness in Temperate Pooideae Grasses. Plant Physiology **172**, 416-426.
Schubert M, Marcussen T, Meseguer AS, Fjellheim S. 2019. The grass subfamily Pooideae: Cretaceous–Palaeocene origin and climate-driven Cenozoic diversification. Global Ecology and Biogeography **28**, 1168-1182.
Woods D, Mckeown M, Dong Y, Preston JC, Amasino RM. 2016. Evolution of *VRN2/GhD7*-like genes in vernalization-mediated repression of grass flowering. Plant Physiology **170**, 2124–2135.

Paper III

Modulation of diurnal gene regulation under contrasting photoperiods in the early-diverging Pooideae grass *Melica ciliata*

Paliocha M, Schubert M, Aunbakk NB, Hvidsten TR, Preston JC , Frøslie KF & Fjellheim S

Manuscript, 2023

Modulation of diurnal gene regulation under contrasting photoperiods in the early-diverging Pooideae grass *Melica ciliata*

Martin Paliocha[1], Marian Schubert[1], Nikolai Bøgseth Aunbakk[2], Torgeir R. Hvidsten[2], Jill Christine Preston[3], Kathrine Frey Frøslie[2], Siri Fjellheim[1,*]

ORCID-ID: 0000-0001-6717-1021 (M.P.), 0000-0001-7579-3832 (M.S.), 0000-0001-6097-2539 (T.R.H.), 0000-0002-9211-5061 (J.C.P), 0000-0003-4771-5495 (K.F.F), 0000-0003-1282-2733 (S.F.)

[1] Department of Plant Sciences, Faculty of Biosciences, Norwegian University of Life Sciences, N-1432 Ås, Norway

[2] Faculty of Chemistry, Biotechnology, and Food Science, Norwegian University of Life Sciences, N-1432 Ås, Norway

[3] Department of Plant Biology, College of Agriculture and Life Sciences, The University of Vermont, Burlington, VT 05405, United States of America

* Author for correspondence:

Professor Siri Fjellheim
Norwegian University of Life Sciences
P.O. Box 5003 NMBU
N-1432 Ås
Norway
e-mail: siri.fjellheim@nmbu.no

Abstract

Photoperiod is an integral cue for the coordinated growth and development of plants. In combination with the circadian clock, plants utilise this signal to maximise fitness through the synchronisation of biological processes with favourable conditions. Although photoperiodic processes are well-studied in plants, genome-wide responses to photoperiod in wild crop relatives are scarce. Here, we explore the diurnal transcriptome of *Melica ciliata*, a perennial, temperate grass under contrasting photoperiods simulating long (LD) and short days (SD). We use functional data analysis (FDA) to explore the diurnal transcriptomic landscape of *M. ciliata* and demonstrate the applicability of this statistical framework for the biological analysis of time-course expression data generated from *de novo* transcriptome sequencing data. Aided by functional principal components analysis (FPCA), we were able to detect and classify gene expression in *M. ciliata* according to diurnal rhythmicity and photoperiodic responsiveness. This approach revealed novel associations between circadian clock and photoreceptor genes and central metabolic and developmental processes, emphasising the significant impact of photoperiod on global expression dynamics in temperate grasses.

Introduction

Light is the energy source and the dominant signalling input for photoautotrophic organisms. Availability and quality of light varies not only within a single day but also substantially throughout the course of a year in non-equatorial habitats. Surviving, growing, and developing under fluctuating light conditions is imperative for the reproductive and evolutionary success of plants (Green *et al.* 2002, Michael *et al.* 2003, Dodd *et al.* 2005). Consequently, metabolism, growth and developmental transitions are tightly coordinated with diurnal and seasonal changes in daylight conditions. A wide range of processes such as photosynthesis, growth rates, whole plant architecture and direction of growth, carbon supply during night, various developmental processes such as flowering, abiotic stress responses, plant defence, and hybrid vigour are under photoperiodic control (Müller *et al.* 2014, Bendix *et al.* 2015, Flis *et al.* 2016). These light-mediated processes have captivated plant biologists for centuries (Quetelet 1842, Gaßner 1918, Garner and Allard 1920, 1923, 1931).

Plants synchronise their seasonal and diurnal behaviour with the environment using an endogenous time-keeping mechanism known as the circadian clock, a regulatory machine with relatively simple architecture and complex developmental functions. The circadian clock is driven by oscillations generated by a set of transcriptional regulators and feedback loops that initiate physiological responses, with one part depending on light quality, quantity and photoperiod, and another part oscillating independently of environmental signals (Greenham and McClung 2015). Oscillatory gene expression in plants is commonly divided into two classes: circadian and diurnal. Circadian genes have a period close to 24 hours and are regulated autonomously, yielding predictable, rhythmic patterns of expression. They maintain oscillating expression even under the absence of environmental cues, the constant breaks between which are referred to as the free-running period. Circadian oscillations are adjusted by exogenous signals following coherent rhythms, such as periodical changes in photoperiod, irradiance, and temperature (Wijnen and Young 2006), but also by metabolites such as sugars and various hormones (Webb *et al.* 2019). These signals coordinate internal rhythms of the clock to external rhythms of environmentally important conditions. Diurnal fluctuations in gene expression, on the other hand, synchronise with the day–night cycle and are commonly entrained by photoperiod (Andrés and Coupland 2012, Laosuntisuk *et al.* 2023).

The genetic mechanisms underlying circadian and diurnal rhythms that trigger flowering and other developmental transitions have largely been elucidated in model systems like

Arabidopsis thaliana. The light signal itself is perceived by PHYTOCHROME (PHY) photoreceptors, acting through CRYPTOCHROMEs (CRYs), PHYTOCHROME INTERACTING PROTEINs (PIFs) and ZEITLUPE (ZTL) to provide input to the oscillatory system (Somers *et al.* 1998, 2004, Martínez-García *et al.* 2000, Hsu and Harmer 2014). The circadian clock consists of a morning and an evening complex that form feedback loops to ensure oscillation of the clock. At the centre of the clock are the genes *CIRCADIAN CLOCK ASSOCIATED 1* (*CCA1*), *LATE ELONGATED HYPOCOTYL* (*LHY*) and *TIMING OF CAB EXPRESSION 1* (*TOC1*), which form interlocking feedback loops with *PSEUDO-RESPONSE REGULATOR* (*PRR*) *9*, *PRR7* and *PRR5* during the morning and *GIGANTEA* (*GI*), *EARLY FLOWERING (ELF) 3*, *ELF4* and *LUX ARRYTHMO* (*LUX*) in the evening (Schaffer *et al.* 1998, Wang and Tobin 1998, Fowler *et al.* 1999, McWatters *et al.* 2000, Alabadí *et al.* 2001, Nakamichi *et al.* 2010, 2012, Helfer *et al.* 2011, Nusinow *et al.* 2011, Gendron *et al.* 2012, Herrero *et al.* 2012, Huang *et al.* 2012, Pokhilko *et al.* 2012). These circadian clock genes are largely conserved between monocots and dicots and regulate daily rhythms through oscillations of transcription factors influencing a wide range of biochemical and developmental processes (McClung 2010, Greenham and McClung 2015).

Although individual genes of the molecular clock are well-characterised, studies that capture global transcriptome-level responses to photoperiodic changes are scarce, especially in non-model organisms. As climates change, constant photoperiods will be linked to novel environmental conditions, potentially providing a mismatch between environmental cues and the responses they have invoked to evolve. As such, we need to improve knowledge on how plants respond to these changes by unravelling how they perceive and respond to a shifting environment on a molecular genetic level.

Diurnal or seasonal shifts in physiology and development are critical determinants of organismal fitness. In plants, processes such as photosynthesis and respiration are largely negatively correlated during the day and night, whereas the transition from vegetative to reproductive growth occurs over the course of a year for many temperate taxa (Venkat and Muneer 2022). Work on *A. thaliana* has elucidated a plethora of molecular connections between the circadian clock and the photoperiod pathway that regulate the seasonal transition to flowering (Johansson and Staiger 2014, Gendron and Staiger 2023). Many elements of this time-of-day-dependent sensitivity appear to be conserved across angiosperms, but variation in LD versus SD responses suggests at least some level of evolutionary divergence (Brambilla *et*

al. 2017). The genetic basis of daily fluctuations in growth, metabolism, and stress responses is less well understood, although this too is an active area of research (Seo and Mas 2015, Dakhiya *et al.* 2017, Markham and Greenham 2021).

In this study, we take a novel approach to elucidate how light in general, and contrasting photoperiods in particular, affect gene expression in *Melica ciliata* (hairy melic, silky-spike melic, or eyelash pearl grass; Meliceae), a perennial Pooideae grass adapted to seasonal temperate climates. Due to its placement in an early-diverging lineage within Pooideae, *M. ciliata* is a useful study taxon in comparative evolutionary analyses involving other agronomically important grass species, such as wheat (*Triticum aestivum*), barley (*Hordeum vulgare*), oat (*Avena sativa*), ryegrasses (*Lolium* spp.), fescues (*Festuca* spp.), and the model species *Brachypodium distachyon* (Soreng *et al.* 2022).

A common issue arising during the analysis of time-dependent expression data is that of temporal resolution. Many analytical tools have been developed to study oscillatory gene expression (Hughes *et al.* 2017). However, the underlying computation often demands dense sampling over several periods, and a large number of biological replicates to successfully estimate oscillation parameters such as phase and amplitude of gene expression with sufficient confidence and statistical power (Wu *et al.* 2016, Hughes *et al.* 2017, Sun *et al.* 2020). An elegant method of dealing with temporal data is considering data as a set of continuous functions rather than a compilation of point measurements or estimates with complex variance structure. Functional data analysis (FDA) provides a statistical framework to analyse such data over a continuum. This is particularly relevant for commonly collected biological samples used to investigate temporal features of developmental processes that are controlled by the coincidence of external stimuli at specific time points, such as photoperiodism in plants. Although FDA approaches have proven successful for the classification of periodic gene expression patterns in a few single-gene and microarray studies (Barra 2004, Leng and Müller 2005, Song *et al.* 2007, 2008), they have been largely overlooked for the analysis of whole transcriptomes. Here, we use functional principal components analysis (FPCA) to identify and characterise genes expressed in rhythmic and arhythmic patterns to quantify how many genes follow differential diurnal expression patterns under short-day (SD) versus long-day (LD) light regimes. We then explore the biological processes that each category of genes is associated with to gain insight into the overall photobiology of this long-day flowering species.

Methodology

Growth experiment

Melica ciliata seeds were originally collected on September 19, 1984, approximately 8 km outside the city of Mangalia, Romania where daytime fluctuates from 8:50 hrs (hibernal solstice) to 15:25 hrs (estival solstice). The seeds were retrieved from the US National Plant Germplasm System (NPGS) maintained by the Agricultural Research Service (ARS) of the United States Department of Agriculture (USDA) via the Global Germplasm Resources Information Network (GRIN-Global) under the accession number PI 494705. *M. ciliata* has previously been identified as an obligate long-day plant that is not flowering in photoperiods shorter than 8 h (Fjellheim *et al.* 2022).

Approximately 200 seeds were sown out in moist soil (Gartnerjord, Tjerbo AS, Norway) and stratified under complete darkness at 4 °C for five days, followed by one day at room temperature in trays wrapped in light-impermeable plastic foil. Following stratification, seeds were germinated in a greenhouse in LDs (16 h light : 8 h dark) at 17 °C. Seedlings were individually transplanted into 7-cm pots containing gardening soil. Four weeks after germination, plants were randomly assigned to growth chambers with either LD photoperiod (16 light : 8 h dark) or SD photoperiod (8 h light : 16 h dark). The photoperiods were aligned in the middle of the light period (Fig. 1A) and temperature maintained at 17 °C. In both treatments, temperature was maintained at 17 °C and relative humidity kept at 50–55%. Light conditions were generated with ConstantColor CMH Tubular Clear high-intensity ceramic metal halide discharge lamps (CMH400/TT/UVC/U/830/E40, GE Lighting Kft., Hungary) supplied with clear AGL B22 60 W bulbs (NARVA Lichtquellen GmbH + Co. KG, Germany) to adjust incandescence. The average irradiance was 185 µmol m^{-2} s^{-1} at plant level with an average red/far-red (R/FR) ratio of 2.1–2.3. Plants were moved to a new position twice-weekly to minimise room effects in the greenhouse and the growth chambers and fertilised with water containing 4% YaraTera Kristalon Indigo and 3% YaraTera Calcinit (Yara Norge AS, Norway). Seven days after transferring plants to the growth chambers, samples were taken every 4th hour throughout the 8th day of the treatment at 03:00, 07:00, 11:00, 15:00, 19:00, and 23:00 h (Fig. 1A). At each time point, tissue from the longest, fully emerged leaf was sampled from four individual plants, immediately flash-frozen in liquid nitrogen, and stored in 2 ml DNA LoBind tubes (Eppendorf AG, Germany) at -80 °C until RNA isolation. In the dark period, samples were taken under dim green light to minimise interference with light-induced

gene expression. Plants were kept in the growth chamber after sampling, and the experiment was terminated after all individuals in LD started heading. For each photoperiod, a total of 24 measurements was available per transcript: four biological replicates per time point at six evenly spaced sampling time points.

RNA purification and sequencing

Frozen leaf tissue was disrupted in a ball mill (QIAGEN TissueLyser) using 2 mm tungsten carbide beads (QIAGEN) under a constant supply of liquid nitrogen. Total RNA was extracted from homogenised tissue using the RNeasy Plant Mini Kit (QIAGEN), following the manufacturer's protocol. The extracts were further purified using Invitrogen TURBO DNA-free Kit (ThermoFisher Scientific) to remove residual DNA. Purity, concentration, and integrity of the isolated RNA was evaluated using an Invitrogen Qubit fluorometer (ThermoFisher Scientific), a NanoDrop 8000 Spectrophotometer (ThermoFisher Scientific), and a 2100 Bioanalyzer (Agilent). Sequencing libraries with an average insert size of 350 bp were constructed with the TruSeq Stranded mRNA Library Prep kit (Illumina) for every individual sample. Library preparation and paired-end sequencing was carried out by the Norwegian Sequencing Centre (NSC) at the University of Oslo on an Illumina HiSeq 4000 system with 150-bp reads.

Transcriptome Assembly

Adapters were removed from the raw reads using trimmomatic v0.39 (Bolger *et al.* 2014), also removing the leading and trailing low-quality bases with a phred-score $Q < 20$. Reads were scanned with a 5-bp sliding-window, a lower cut-off at $Q = 20$, and minimum read length was set to 40 bp. Read quality was evaluated with FastQC v0.11.9 (Andrews 2010). A *de novo* transcriptome was assembled using Trinity v2.8.4 (Grabherr *et al.* 2011) with default parameters and considering strand-specificity. Transcriptome completeness was assessed by Benchmarking of Universal Single-Copy Orthologues (BUSCO) (Simão *et al.* 2015, Waterhouse *et al.* 2017) using the Embryophyta database in OrthoDB v10 (Kriventseva *et al.* 2019).

Contaminant transcripts were identified with blastn v2.10.1 (Altschul *et al.* 1990, Camacho *et al.* 2009), and Corset v1.07 (Davidson and Oshlack 2014) by querying individual Trinity contigs against NCBI's 'nt' database (NCBI Resource Coordinators 2017). Full taxonomic information was assigned to the blast hits with the R package taxonomizr v0.6.0 (Sherrill-Mix

2019). In case of ambiguity below the taxonomic rank 'class', information was reduced to one entry by retaining the taxonomy for the hit with the lowest *E*-value. Contigs were regarded contaminants if phylum did not match 'Streptophyta' and superkingdom was other than 'Eukaryota', or unassigned.

Fragments of ribosomal, plastid, and mitochondrial transcripts were further removed to reduce their influence on relative read count estimates. We obtained complete chloroplast genomes for *B. distachyon* (GenBank: LT558588.1) and *Phaenosperma globosa* (GenBank: KM974745.1), complete mitochondrial genomes for *H. vulgare spontaneum* (AP017300.1) and rice (*Oryza sativa*) (GenBank: JF281153.1), and ribosomal sequences for various non-plant species (MH047190.1, MH047190.1, AB250414.1, KT445934.2, JQ997495.1) from NCBI GenBank (Benson *et al.* 2013) and added them as baits to the *de novo* transcriptomes. For each individual sequencing library, paired-end reads were aligned to *de novo* transcriptomes with Bowtie v2.4.1 (Langmead and Salzberg 2012), allowing reads to be mapped to multiple contigs during the inference of read counts. The resulting SAM files were sorted and converted to BAM files using SAMtools v1.11 (Li *et al.* 2009).

Gene-level counts were obtained by combining reads mapping to multiple transcripts with Corset v1.07 (Davidson and Oshlack 2014), a method that merges *de novo* transcripts with high sequence similarity and shared expression patterns into transcript clusters. First, we ran Corset with a high -D parameter which prevents transcripts from being assigned to different clusters. Secondly, we ran Corset with default values for the -D option to only allow clustering of transcripts that share a significant number of reads. We then removed all transcripts from the second Corset run that clustered with previously added chloroplast, mitochondrial and ribosome baits. Silent transcript clusters were discarded, and only clusters with a raw count > 1 in at least five samples, or all four replicates of the same timepoint, were retained.

Reference proteome processing, functional annotation, and orthologue inference

We used annotated genomes and coding sequences (CDSs) for barley *(H. vulgare*, IBSC_v2), *Aegilops tauschii strangulata* (Aet_v4.0), *T. urartu* (ASM34745v1), *B. distachyon* (Brachypodium_distachyon_v3.0), Japonica rice (*Oryza sativa japonica*, IRGSP-1.0), and Indica rice (*O. sativa indica*, ASM465v1) from Ensembl Plants (Howe *et al.* 2020, Yates *et al.* 2020) for orthologue inference and annotation. CDSs were aligned to chromosome-level genome sequences with GMAP v2019-06-10 (Wu and Watanabe 2005) and redundant

225 transcripts were combined with the merging function from GffRead v0.11.6 (Pertea and Pertea
226 2020), discarding any transcripts lacking start- or stop-codons. Processed transcriptomes were
227 then translated to reference proteomes using GffRead.

228 The resulting non-redundant proteomes of barley, *B. distachyon*, and rice were used as
229 references for functional annotation of *de novo* transcripts using blastx implemented in
230 DIAMOND v0.9.22 (Buchfink *et al.* 2015). Using the BLAST trace-back operation (BTOP)
231 string, we identified and removed frameshifts introduced to the *de novo*-transcripts during the
232 transcriptome assembly with Trinity (Leder *et al.* 2021). Finally, amino acid sequences were
233 obtained with exonerate v2.2.0 (Slater and Birney 2005) and used to infer orthologues with
234 OrthoFinder v2.5.4 (Emms and Kelly 2015, 2019) and IQ-TREE v2.2.0.3 (Minh *et al.* 2020).

235 **Normalisation of read counts and gene expression profiling**

236 After removing lowly expressed transcripts with a read count below 10 in at least 75% of
237 samples from each time point and photoperiod treatment, we calculated normalisation factors
238 for the quantification of gene expression with the trimmed mean of M values (TMM) method
239 using the calcNormFactors function implemented in edgeR v3.36.0 (Robinson *et al.* 2010).
240 Normalisation-factor scaled counts per million reads mapped (CPM) were calculated with the
241 function cpm.DGEList from edgeR and $\log_2$-transformed with a default prior count of 2.

242 **Fitting transcript expression curves and expression difference curves**

243 For each photoperiod treatment (LD and SD), 24 $\log_2$(CPM)-measurements for each of the
244 62,727 transcripts were used to estimate the underlying curve (Fig. 1B). Each quadruplicate
245 was replaced by its mean (Fig. 1B), and these sets of six means per transcript and treatment
246 were used as the raw data for the original transcript expression curves. Standardised data (*z*-
247 scores) were calculated by subtracting the mean and dividing by the standard deviation of each
248 transcript-treatment combination. We also calculated the differences in transcript expression
249 between LD and SD treatment (i.e., differences in raw data) by subtracting the six means from
250 the SD treatment from the six LD treatment means.

251 Continuous curves were fitted to each set of six raw data points (Fig. 1B), resulting in 62,727
252 pairs of continuous transcript expression curves for each photoperiod (Fig. 2A). Throughout
253 the paper, these will be denoted *raw expression curves*. Similarly, 62,727 pairs of s*tandardised*
254 *expression curves* were fitted to the standardised data. Finally, 62,727 transcript *expression*

255 *difference curves* were fitted to the difference data. All curves were estimated using a 7-term
256 Fourier series expansion assuming a 24-h period and smoothed with a roughness penalty of λ
257 = 2.5. The value of the smoothing parameter was set according to a generalized cross-validation
258 criterion. Individually fitted curves formed the basis for the subsequent FPCAs. Data
259 processing and statistical analyses were carried out in R v4.2.2 (R Core Team 2022) using the
260 R package fda v6.0.5 (Ramsay *et al.* 2022) for curve fitting and FPCA.

261 **Analysing temporal variation by FPCA**

262 FDA denotes statistical techniques specifically developed for analysing curve data (Ramsay
263 and Silverman 2002, 2005). In FDA, a set of discrete temporal observations is transformed into
264 a single, continuous curve. Statistical analyses are then performed on a sample of continuous
265 functions, rather than on the original data points. Curve fitting is therefore a mandatory,
266 preparatory step of FDA. In a sample of curves, the mean curve is used descriptively, usually
267 in combination with results from an FPCA. The FPCA is used to identify and describe the
268 temporal variation in the data and allowing the characterisation and interpretation of diurnal
269 changes in transcript levels over time. Similar to traditional PCA, FPCA seeks to decompose
270 the variation in a data set and express it by a combination of principal components (PCs), which
271 are common for the sample and can be interpreted biologically, and corresponding individual
272 PC scores. In FPCA, these components are curves (functional PCs, FPCs), and the variation of
273 interest is temporal. The FPCA also assigns FPC scores to each individual curve. These FPC
274 scores quantify how the trajectory of the individual curve corresponds to the general features
275 of the corresponding FPC curve. This is commonly visualised by showing how an individual
276 trajectory deviates from the mean curve if its FPC scores are high or low. An individual curve
277 with all FPC scores equal to 0 equals the mean curve.

278 We characterised the circadian transcriptome of *M. ciliata* with five FPCAs. First, we
279 considered expression curves from LD and SD separately and conducted FPCAs on each set
280 of 62,727 curves ($FPCA_{LD}$ and $FPCA_{SD}$, respectively). Second, to compare expression between
281 both photoperiods, we pooled the expression curves from both treatments and conducted
282 FPCAs on all 2 × 62,727 curves. Separate FPCAs were done for the raw ($FPCA_{Raw}$) and
283 standardised curves ($FPCA_{Z}$). Third, we conducted an FPCA of the difference curves (LD -
284 SD, raw data, $FPCA_{D}$).

285 **Defining groups of expression profiles based on differing diurnal rhythms and expression**
286 **levels**

287 To explore the impact of photoperiods on the rhythm and expression level of transcript pairs
288 from contrasting treatments, we used the output of the combined FPCA analysis to divide the
289 transcripts into pre-defined groups (Hoffman *et al.* 2010). Because differences in expression
290 level and rhythm are gradual, cut-off values are needed when defining differences or
291 similarities in FPCA scores. Since FPCA scores follow a standard normal distribution, the
292 distance between a score to the mean (0) is proportional to the correlation between the original
293 curve and the corresponding eigenfunction. Distances can thus be used as a proxy for how
294 much expression deviates from the mode of variation captured by the respective FPC. We
295 tested different combinations of cut-offs for the criteria from a range of 0.50–1.50 standard
296 deviations from the mean, which is a conservative approach to defining a transcript as rhythmic
297 or not. More specifically, expression levels of transcript pairs were defined as similar if the
298 difference in FPCA scores between LD and SD transcripts fell within ±0.75 standard deviations
299 from the mean of the differences between FPCA scores. By contrast, they were defined as
300 different if they fell outside 1 standard deviation. Low FPCA scores were defined as values
301 that fell within ±0.75 standard deviations around the mean FPCA score, and extreme values
302 were those that fell outside 1 standard deviation. Finally, to detect transcripts that have similar
303 rhythms in both treatments, we used the variance in the curvature of the difference curves as a
304 criterion. We defined transcripts as having a similar rhythmic expression pattern if the variance
305 of the curvature was among the lowest 5% in the data set. Transcript pairs were assigned to
306 group 1–5 based on a combination of these criteria, as shown in Tab. 1: 1) similar expression
307 levels in LD and SD and no rhythmic pattern, 2) different expression levels in LD and SD and
308 no rhythmic pattern, 3) similar expression levels in LD and SD and similar rhythm, 4) different
309 expression levels in LD and SD and similar rhythm, and 5) different rhythm in LD and SD.

310 **Heat maps and clustering**

311 Hierarchical clustering was performed on transcripts considered different in both rhythm and
312 level (group 5). First, we calculated pairwise Pearson correlation coefficients (PCCs) between
313 the standardised LD and SD gene expression profiles. Thereafter, we performed hierarchical
314 clustering on the distance correlation (1 - PCC) matrix using Ward's method (Ward 1963,
315 Murtagh and Legendre 2014). The dendrogram was pruned to retain minimum 1000 transcripts

316 per cluster using dynamicTreeCut v1.63-1 (Langfelder *et al.* 2007), and the results visualised
317 with ComplexHeatmap v2.13.1 (Gu *et al.* 2016).

318 **Functional enrichment analyses**

319 We performed enrichment analyses for gene ontology (GO) terms (Gene Ontology Consortium
320 2004) on the gene sets identified by the FPCAs and within the clusters in group 5. Plant-specific
321 GO slim annotations for the reference species were downloaded from Ensembl Plants (Howe
322 *et al.* 2021) using biomaRt v2.52.0 (Durinck *et al.* 2005), and assigned to orthogroups
323 containing orthologues from at least one reference and *M. ciliata*. Enrichment tests for
324 biological process (BP) annotations with at least 25 annotated genes per term were performed
325 with the R package topGO v2.48.0 (Alexa *et al.* 2006) using Fisher's exact test ($P < 0.05$), and
326 the weight01 algorithm with all annotated transcripts as background.

327 **Candidate gene expression profiling**

328 Expression profiles for putative circadian clock and photoreceptor genes (Higgins *et al.* 2010,
329 Ream *et al.* 2014, Woods *et al.* 2017, MacKinnon *et al.* 2020, Fjellheim *et al.* 2022) were
330 visualised individually. To highlight photoperiodic variation in terms of gene expression level
331 and rhythm, we reported both raw as well as *standardised* expression curves. Candidate genes
332 were identified through the closest *B. distachyon,* or barley orthologue as inferred by
333 OrthoFinder. FPCA scores for transcripts originating from these candidate loci are also
334 highlighted in Fig. 6.

335 Results

336 **Summary of transcriptome and annotation**

337 A total of 48 samples were obtained during the growth experiment, yielding 47 RNA-seq
338 libraries (library preparation failed for one biological replicate in 16h:LD) with a total of
339 4,648,195,586 reads assembled into 568,337 Trinity contigs producing 150,509 Corset clusters
340 ('transcripts'). Following normalization and pre-processing, 62,727 transcripts were retained
341 and used for orthologue inference. A total of 25,931 orthogroups containing *M. ciliata* and a
342 minimum of one reference species was recovered in this analysis. In terms of completeness,
343 the assembled *de novo* transcriptome has 1.2% missing and 8.4% fragmented, and 90%
344 complete BUSCOs (29.4% single-copy, 61% duplicated).

FPCA of smoothed expression curves

FPCA of separate LD and SD expression curves

The main temporal characteristics in the expression curves are markedly different between plants grown under LD and SD. The curve characteristic accounting for the largest part of the temporal variation in the LD data ($FPC1_{LD}$, Fig. 2A) is a marked expression incline or decline at 15 h paired with moderate changes during the rest of the day. This accounts for about half of the variation in LDs. The most dominant characteristic in the SD expression curves, in contrast, consists of a steep incline or decline around 4 h. This latter pattern is followed by an equally sharp change in the opposite direction around 15 h ($FPC1_{SD}$, 51.7%; Fig. 2B), with less variation between the curves obtaining extreme FPCA scores compared to that observed for LDs (Fig. 2A–B, lower panel). The second most important curve characteristic consists of late morning peaks/troughs between 3–11 h in LDs ($FPC2_{LD}$, 18.3%) and 4–12 h in SDs ($FPC2_{SD}$, 26.3%) with sign changes occurring around 15 h and 16 h, respectively. Oscillations beyond these patterns account for 29.5% in LDs and 19.8% in SDs (FPC3 + FPC4), demonstrating that gene expression in SDs is dominated by fewer and more pronounced peaks than under LD conditions.

FPCA of all expression curves

Considered together, transcript expression curves displayed large variation, both in the general level of transcript expression, and in diurnal behaviour. FPCA of the raw expression curves (Fig. 3A) show that the most dominant temporal variation in these curves is differences in the overall expression level (Fig. 3A, $FPC1_{Raw}$). This characteristic explains 94.1% of the total variation in the original raw curves. Due to dominance of overall expression level, temporal fluctuations are to a very little extent captured by $FPC1_{Raw}$. Diurnal variation is captured by $FPC2–4_{Raw}$, but the amount of variance explained by these components is small.

In the *standardised* curves (Fig. 3B), fluctuations in temporal variation are accentuated. The first four FPCs account for 97% of the temporal variation (47.4%, 23.4%, 14.9% and 11.36%, respectively) (Fig. 3B). $FPC1_Z$ explains approximately half of the temporal variance in the combined data set (47.4%, Fig. 3B). This component identifies expression profiles that peak/trough in the early morning at 4 h and a peak/trough in the other direction around 15 h. The overall pattern captured by $FPC2_Z$ (23.4%, Fig. 3B) is similar in shape, but with a wider first peak/trough at 6–11 h and a phase shift towards the evening/night, culminating in a pronounced peak/trough in the opposite direction at 22h. Minor perturbances in gene

377 expression are described by $FPC3_Z$ (14.9%) and $FPC4_Z$ (11.6%), capturing variance beyond
378 the main patterns identified by $FPC1–2_Z$.

379 *FPCA of difference curves*

380 To identify transcripts differentially expressed between LDs and SDs, we computed difference
381 curves (LD - SD, raw curves) and conducted an FPCA on those in order to complement the
382 separate and combined FPCAs of individual curves. The most prominent temporal feature in
383 $FPC1_D$ are differences attributed to the previously identified peaks/troughs occurring at 15 h
384 as well as towards midnight (46%, Fig. 3C). The latter midnight peak/trough constitutes the
385 main characteristic in $FPC2_D$ (32.4%, Fig. 3C), whereas $FPC3_D$ (11.4%) and $FPC4_D$ (5.9%)
386 accounts for differences occurring during the early morning, coinciding with the transition from
387 light to dark in the respective treatments (LDs in $FPC3_D$ and SDs in $FPC4_D$).

388 **Classification of transcripts into groups**

389 In total, 37,807 (60.2%) transcripts were assigned to at least one of five pre-defined groups
390 based on their FPCA scores from the combined FPCAs (Fig. 3). Out of the transcripts that were
391 defined arhythmic/non-oscillatory, 356 have a similar expression level in LDs and SDs (Fig.
392 4A, group 1), whereas 26 transcripts are expressed at different levels in LDs and SDs (Fig. 4B,
393 group 2). Transcripts with diurnal expression profiles were similarly divided into being
394 expressed at similar (Fig. 4C, group 3) or different (Fig. 4D, group 4) levels in LDs and SDs.
395 A total of 102 transcripts with diurnal oscillations and similar absolute levels of expression
396 were identified, whereas 62 transcripts with similar diurnal expression curves, but different
397 levels, were identified between LDs and SDs. The majority of classified transcripts (37,261)
398 fell into a category containing profiles with different levels and/or different diurnal expression
399 patterns between the two photoperiods (Fig. 4G–H, group 5) and were therefore divided into
400 smaller sets using hierarchical clustering (see next section).

401 **Clustering and GO enrichment**

402 The largest of our pre-defined categories consisted of transcripts with different diurnal rhythms
403 under opposite photoperiods (Group 5, Fig. 4, Tab. 1). To identify transcripts that were
404 similarly affected by photoperiod we clustered them based on their rhythms and examined the
405 clusters for enrichment of specific biological processes. The most prevalent characteristic of
406 LD gene expression were marked expression peaks and troughs centred around 15 h.
407 Corresponding SD profiles in these clusters were often shifted in phase with expression peaks

occurring both earlier (cluster 9, Fig. 5) or later (clusters 2–3, Fig. 5) in SD than in LD. Furthermore, a large number of genes displayed widening and narrowing of expression profiles under contrasting photoperiods, as seen in clusters 5 and 8 (Fig. 5). Changes in gene expression frequently coincided with light–dark/dark–light transitions in LD, whereas directional changes in SD expression occurred during light or dark phases in most clusters.

We detected significant enrichment of 28 plant GO slim terms in the different clusters. Enrichments for biological processes 'response to biotic stimulus', 'response to external stimulus', and 'response to stress' were, each occurring in six clusters. In total 11 GO slim terms were distinct to only one cluster, such as 'reproductive structure development' (cluster 9, Fig. 5) and 'reproduction' (cluster 5, Fig. 5). The term 'circadian rhythm' had in total two occurrences in clusters harbouring orthologs of many of our pre-defined candidate genes (cluster 1 and 9, Fig. 5) and co-occurred with terms related to development such as 'cell differentiation' and 'reproductive structure development'. Notably, these genes reached peak expression during dawn (cluster 1 SD, Fig. 5) and dusk (cluster 9 LD, Fig.5), indicating a potential role of morning and evening protein complexes in SD and LD gene expression in *M. ciliata*. Circadian marker gene expression was associated with metabolic as well as developmental processes, suggesting the involvement of multiple transcriptional systems controlling basic functions influenced by photoperiod. The term 'photosynthesis' was enriched in only a single cluster featuring increasing gene expression during the light period in both LD and SD (cluster 9, Fig. 5), with peak gene expression towards the end of the day in LD and peaks centred around noon in SD. Interestingly, the term 'growth' was significantly enriched in only a single cluster characterised by peak gene expression during dark in both LD and SD (cluster 11) and early morning in LD, indicating that biomass production in *M. ciliata* predominately occurs during night and early day, irrespective of photoperiod.

Proof of concept for gene discovery

We identified a set of known clock and photoperiod pathway genes from the literature and examined their expression to assess FPCA's ability to identify genes involved in diurnally-regulated processes. Most of these transcripts had extremely high or low $FPC1_Z$ and $FPC2_Z$ scores (cf. Fig. 3B), as indicated by their positions toward the periphery of the first FPC_Z plot (Fig. 6A). A few of these genes also had extreme $FPC3_Z$ and $FPC4_Z$ values, such as *CONSTANS 9* (*CO9)*, *CO1*, *CO2*, and *NIGHT LIGHT-INDUCIBLE AND CLOCK-REGULATED GENE 2*

439 (*LNK2*), consistent with their peaking in expression throughout the day specifically under LD
440 conditions (Fig. 6B).

441 The majority of clock and photoperiod pathway genes followed different diurnal fluctuations
442 under LDs versus SDs. This is evident from the fact that transcripts obtain different relative
443 scores across all four main FPC_Z axes (Fig. 6), as well as from the expression profiles of a
444 subset of clock and photoreceptor genes that show common phase-shift patterns (e.g.,
445 *PRR1*/*TOC1*) (Fig. 7). In general, the clock genes and photoreceptors were expressed at the
446 same level in both photoperiods, although differences in diurnal rhythms between photoperiods
447 give time-specific differences in expression levels between LDs and SDs. The exception is the
448 flowering pathway integrator gene *FLOWERING LOCUS T 1* (*FT1)*, which was barely
449 expressed in SDs, and highly expressed in LDs. Some genes had very similar absolute
450 expression levels under both, LDs and SDs, including *ELF3*, *LWD*, *CRY2*, *PHOT2*, *PHYA*,
451 *PHYB*, *PHYC* and *LUX*, with their rhythmicity only being evident from standardised expression
452 profiles. Another set of genes, such as *CCA1*, *GI*, *LNK1*, *TOC1*, *PRR37*, *PRR73*, *PRR95*, *CRY2*,
453 *PHOT2*, *PHYC,* and *RVE86*, was expressed at similar levels and with similar diurnal rhythms,
454 but with a slight phase shift between photoperiods. Interestingly, the latter genes all shifted in
455 the same direction, with a delayed expression peak in LDs. Some genes also showed large
456 differences in rhythmicity in the two photoperiods (e.g., *CO9*, *CO1*, *CO2*, *LNK2*, *REV2*, *CRY1*,
457 *PHOT1, RVE68,* and *ZTL*), with more than one peak through the day in at least one of the
458 treatments.

459 Discussion

460 Functional data analysis provides a useful framework for temporal gene expression 461 analysis

462 The ability to detect time-dependent changes in transcription is critical for the study of
463 rhythmic gene regulation. Functional data analysis provides a powerful framework for the
464 exploration of temporal regulatory relations in transcriptomes. By treating expression profiles
465 as continuous functions over time rather than a set of point estimates, FDA overcomes many
466 limitations of more conventional approaches that can obstruct the exploration of time-
467 dependent relationships. Obtaining good time-series gene expression data that reveal transient
468 changes is challenging when resources are limited and requires careful balance between sample
469 size and temporal resolution. A common outcome of this trade-off is data too complex to be

470 analysed with conventional approaches that detect differentially expressed genes between
471 predefined contrasts (Conesa *et al.* 2016, McDermaid *et al.* 2018, Raghavan *et al.* 2022). On
472 the other hand, the time-series may be too sparse to be explored with methods commonly
473 applied assess rhythmicity in gene expression analyses (e.g., Wu *et al.* 2016). We believe that
474 the analytical methods applied in this study offer a more nuanced understanding of longitudinal
475 gene expression data in non-model organisms and blaze way for the comprehensive analysis
476 of time-dependent processes across different species. The methodological framework outlined
477 in this study identifies genes involved in diurnal and photoperiodic mechanisms, deepening our
478 understanding of plant physiology, and illuminating evolutionary origins of adaptations to
479 different day lengths.

480 **Photoperiod has an almost universal impact on both the level and rhythmicity of gene**
481 **expression**

482 The most prominent signal from our analysis is that the expression profiles of *M. ciliata* genes
483 under contrasting photoperiods can be characterised by just a few basic expression patterns
484 (Fig. 2A–B). Irrespective of photoperiod, there is a peak/through at 15:00 h, explaining most
485 of the variation in SDs ($FPC1_{SD}$) and a little less in LDs ($FPC2_{LD}$), and another peak/through
486 in the morning ($FPC1_{LD}$; $FPC2_{SD}$). There are also photoperiod-dependent peaks/throughs that
487 have a major impact on gene expression during the dark period (Fig. 2A–B), with SDs inducing
488 more pronounced expression peaks/throughs during the dark period than LDs (Fig. 2A–B).
489 These data suggest that dawn and dusk are major elicitors of gene activation in *M. ciliata*. This
490 closely parallels findings in other grasses like maize (Khan *et al.* 2010), *B. distachyon*
491 (MacKinnon *et al.* 2020), sugarcane (*Saccharum* sp.) (Hotta *et al.* 2013), and barley (Müller *et*
492 *al.* 2020) that identified dawn and dusk as influential regulatory signals (Deng *et al.* 2015,
493 Greenham and McClung 2015).

494 Another compelling pattern when comparing the expression responses in SD versus LD is that
495 94.1% of the total variance in the *M. ciliata* transcriptome is explained by differences in overall
496 gene expression level irrespective of rhythmicity (Fig. 3A, $FPC1_{Raw}$). The amount of mRNA
497 produced can be significantly influenced by the quantity of light, resulting in differential
498 transcript abundance (Tobin and Silverthorne 1985). It is thus plausible that the observed
499 variation captured by $FPC1_{Raw}$ can be attributed to differential transcriptional activity due to
500 contrasting light amounts.

501 To identify genes responding to changes in photoperiod, we developed a pipeline to sort the
502 genes into five *a priori* groups based on a set of FPC analyses, covering all possible
503 combinations of phase and expression level variation (Table 1, Fig. 4). Ninety-nine percent of
504 transcripts fall into group 5, which is characterised by different diurnal oscillations between
505 LDs and SDs. In terms of variation in phase, the high ratio of photoperiod-dependent (group 5,
506 Fig. 4E–H, 5) to photoperiod-independent (group 3 and 4, Fig. 4C–D) *M. ciliata* transcripts is
507 in line with previous studies showing that many of the pathways influenced by the circadian
508 clock are linked to exogenous signals, with few rhythms being upheld entirely independent of
509 photoperiod (Huang *et al.* 2017, MacKinnon *et al.* 2020). For instance, null mutations in the
510 central rice clock gene *OsGI* did not measurably impair key facets of primary metabolism and
511 yield, such as photosynthesis and the rate of carbon assimilation under field conditions with
512 strong environmental cues (Izawa *et al.* 2011). However, the majority of genes underwent
513 phase shifts in the *OsGI* mutant, demonstrating that photoperiodic gene expression is the result
514 of crosstalk between hub genes of the circadian clock and external cues that set the state of
515 photoperiod-dependent oscillations (Izawa *et al.* 2011). Global gene expression thus seems
516 coordinated by the perception of exogenous signals and is fine-tuned through phase shifts of
517 central circadian clock genes that generate oscillations but are themselves subject to
518 adjustments by environmental cues.

519 Merely 164 of the 37,807 transcripts classified as rhythmic had similar expression patterns
520 under both, LDs and SDs (0.43%; Fig. 4C–D). Since our experimental design only involved
521 changes in photoperiod, it appears that these genes are not entrained by light cues and therefore
522 likely a part of the *M. ciliata* circadian clock or directly influenced by it. Previous studies in
523 other grass taxa have generally found higher percentages of expressed genes following
524 circadian clock oscillations, with reports ranging from 1.6% in *Setaria viridis* (Huang *et al.*
525 2017) to 3.6% in *B. distachyon* (MacKinnon *et al.* 2020) and 33% in sugarcane (Hotta *et al.*
526 2013), and most estimates falling between 6-15% (MacKinnon *et al.* 2020). The disparity
527 between studies probably reflects a combination of true biological variation across study
528 species, as well as variation in environmental parameters and analytical approaches like
529 sequencing technology and choice of statistical methods.

530 In our analyses, groups were identified by a combination of temporal patterns in the raw,
531 standardised, and difference curves. Standardised curves played a major role in identifying the
532 largest group (different rhythm in SD and LD, group 5, Fig. 4G–H). When standardising the

533 data, even small temporal fluctuations will be exaggerated, and transcripts with low read counts
534 may express the same temporal pattern as more abundant transcripts. Measurement errors in
535 lowly expressed transcripts may therefore cause artifacts in curve patterns, artificially inflating
536 rhythmic differences between treatments. Hence, the estimated proportion of transcripts
537 without rhythmic expression might be somewhat underestimated.

538 **Circadian clock genes show differential entrainment in LDs and SDs**

539 Specific analysis of several well-characterised genes controlled by the circadian clock (Fig. 6,
540 7), such as the morning-loop genes *CCA1, REV2, REV86, REV89* and *ZTL* and the evening
541 complex genes *PRR1*/*TOC1* and *PCL1/LUX*, indicate that the overall dynamic of the *M. ciliata*
542 circadian clock is congruent with what has been resolved in other species (Higgins *et al.* 2010,
543 Hong *et al.* 2010, Koda *et al.* 2017, Weng *et al.* 2019, MacKinnon *et al.* 2020, Müller *et al.*
544 2020, Rees *et al.* 2022). In *A. thaliana*, rice, and *M. ciliata*, the single daily expression peak of
545 the morning loop genes (*CCA1, REV2, REV68, REV86* and *ZTL)* occurs just after dawn in LDs
546 and before dawn in SDs, suggesting slightly different entrainment of the 24-hour cycle
547 depending on photoperiod (Alabadí *et al.* 2002, Lee *et al.* 2022). By contrast, *A. thaliana*, rice,
548 and *M. ciliata PRR1*/*TOC1*, at least the former of which peaks every 23–24 h under constant
549 photoperiods, are upregulated at dusk under both LDs and SDs (Murakami *et al.* 2007, Nagel
550 *et al.* 2015). A central component of the evening complex, *ELF3*, shows highly contrasting
551 expression profiles under LDs and SDs. Its expression in LDs follows expression of the evening
552 complex, whereas its expression peaks in the dark period just before dawn in SDs. In barley,
553 *ELF3* induces transcriptional oscillations (Deng *et al.* 2015), and plants with non-functional
554 *ELF3* show disrupted circadian rhythms and flower early irrespective of photoperiod (Faure *et*
555 *al.* 2012, Zakhrabekova *et al.* 2012). However, in wheat (*T. aestivum* and *T. monococcum*), the
556 evening complex gene *ELF3* seems to reach peak expression towards the end of the dark period
557 (Alvarez *et al.* 2016, 2023, Wittern *et al.* 2023), indicating some diversity in the architecture
558 of mechanisms perceiving light–dark transition. Our results indicate that *ELF3* is a central
559 component in modulating photoperiodic responses of the circadian clock, in particular
560 mediating photoperiodic induction of flowering in *M. ciliata*.

561 A well-known pattern of circadian rhythm genes is the delay in phase in response to
562 lengthening day (Leung *et al.* 2022). This largely holds true also for the set of pre-defined
563 photoperiod and circadian genes in our work (Fig. 7). This likely reflects plants tracking the
564 end of the photoperiod to take advantage of photosynthetic input to maximize metabolic

processes, corroborating findings from barley, maize, *Arabidopsis*, and *Ipomoea nil* (Hayama *et al.* 2007, 2018, Jończyk *et al.* 2011, Deng *et al.* 2015, Seluzicki *et al.* 2017).

A noteworthy pattern is the lack of circadian clock and photoreceptor genes among transcripts with high scores in $FPC2_Z$. This suggests that only a limited number of *M. ciliata* clock components and photoreceptors are expressed in the middle of the dark period. This aligns with observations made in *Arabidopsis* and crop species where several flowering genes, such as *GIGANTEA* (*GI*), *FLAVIN-BINDING, KELCH REPEAT, F-BOX 1* (*FKF1*), *ZEITLUPE* (*ZTL*), *LOV KELCH PROTEIN 2* (*LKP2*) and *FLOWERING BHLH 1–4* (*FBH1–4*), reach peak activity during light (Brambilla and Fornara 2017). An exception are *CO1* and *CO2* that are expressed in the afternoon under both light and dark conditions. In *A. thaliana*, *CO* expression is confined to the afternoon due to the repressive action of CYCLING DOF FACTORs (CDFs) and inductive photoreceptors. However, the night peak that requires additional activators is currently unexplained (Brambilla and Fornara 2017). Further dark-expressed genes are likely associated with processes such as defence, stress, and respiration (e.g., cluster 2, 3, 8, 12; Fig. 5).

Expression profiles of the circadian clock and photoreceptor candidate genes (Fig. 7) provide proof-of-concept for the use of our FPCA approach to identify photoperiod-responsive genes. Most of these genes follow one of the four main expression patterns. Their scores as described by the principal component curves of the FPCAs (Fig. 3) fit well with their diurnal expression patterns (Fig. 7), indicating that our approach is suitable for gene discovery and comparative analyses.

Linking transcriptional behaviour to temporally variable biological processes

The by far largest of our pre-defined group was the one containing transcripts with different diurnal rhythms in contrasting photoperiods (Group 5, Fig. 4, Table 1). A variety of clusters with differential gene expression profiles were identified, suggesting that many different photoperiod sensing systems or transcriptional networks control gene expression. We find that various terms reflecting metabolism are enriched across most differential gene expression profiles, suggesting that different photoperiodic sensing systems/pathways control basic functions. Several differential expression patterns are found across the circadian clock genes and photoreceptors (Fig. 7) and they are co-expressed with genes enriched for different functions such a carbohydrate metabolic process, transport, reproduction and DNA metabolic

processes (*CO1/2, PHOT1, RVE86, CCA1, REV2* and *RVE68*), response to chemical, circadian rhythm, lipid metabolic process, response to endogenous stimulus, multicellular organism development, secondary metabolic process, cell differentiation (*CO9, LNK1, LNK 2* and *CRY2*) and response to endogenous stimulus, circadian rhythm, photosynthesis, response to abiotic stimulus, reproductive structure development (*GI, PRR37, PRR73* and *PRR95*). This suggests that different mechanisms connect the photoperiod with the circadian clock, similar to what has been found in *Arabidopsis thaliana* for flowering and metabolism (Liu *et al.* 2021, Leung *et al.* 2022). Reproduction is enriched in a group which also contain central flowering genes like *CO1/2, PHOT1, RVE86, CCA1, REV2* and *RVE68*. Interestingly, also carbohydrate metabolism and transport is enriched in this cluster, which has a strong peak in the morning in LD whereas their expression is in the dark in SD. It is known that sugar signaling through transport to the SAM is involved in flowering in *Arabidopsis thaliana* and likely also in other species (Turnbull 2011). The co-regulated genes in this cluster may thus be essential for the LD-flowering induction in *M. ciliata*.

Numerous genes influenced by changing photoperiod were associated with sensory processes involved in anticipation and transmission of biotic stimuli and abiotic stress, indicating complex relationships with multiple photoperiod-sensing systems in *M. ciliata*. This aligns with findings from *Arabidopsis* where light-induced transcriptional rewiring is prompted by numerous photoreceptors transferring light signals into circadian and photoperiod pathways (Ma *et al.* 2001). Substantial co-regulation of response processes with core circadian clock genes signifies the importance of photoperiodic entrainment of adaptive traits. In fact, many stress-responsive genes are under circadian regulation to limit energy-demanding responses to times when stress is most severe and most beneficial to survival (Yakir *et al.* 2007, Markham and Greenham 2021). Exploring the linkages between circadian stress responses and their entrainment by photoperiod in *M. ciliata* provides an exciting opportunity for further investigation. This is particularly relevant given the greater abundance and diversity of circadian clock-regulated stress-responses in undomesticated species than cultivated crops (Markham and Greenham 2021), and their cross-talk of stress signals with reproductive development and flowering (Riboni *et al.* 2014, Takeno 2016).

Conclusions

Our results show great flexibility of the circadian clock in controlling different biological processes in a temperate, perennial grass. Such flexibility is likely a central part of adaptation

to environments that vary across time (e.g., seasons) and space (e.g., latitude), like flowering, bud burst, seed set and senescence. Photoperiod and temperature are major signals plants rely on to time phenological events and are thus the two major regulators of rhythmicity in gene expression. With ongoing climate change, the flexibility of the clock will dictate how well plants can respond to novel combinations of temperature and photoperiod. As of today, we know little about the variation in photoperiodic responses of diurnal rhythms within and across species and more comparative studies are needed. The approach used here can easily be extended to evaluate photoperiodic gene expression and the evolution of day-length responses across species.

Author Contributions

S.F. and J.C.P. conceived and designed the study; M.P. carried out the growth experiment, laboratory work, and implemented all formal analyses; M.S. conceived the annotation pipeline, contributed to sequence and statistical analyses; K.F.F. assisted with FDA with contributions from N.B.A. and T.R.H.; S.F., K.F.F., and M.P. wrote the paper with contributions from all authors.

Funding

Work carried out in this study was part of Martin Paliocha's PhD project funded by the Faculty of Biosciences (BIOVIT) at the Norwegian University of Life Sciences (NMBU). Sequencing and the growth experiment were funded by the Norwegian Research Council (grant number 231009 to Siri Fjellheim).

Acknowledgements

We thank Øyvind Jørgensen, Ane Charlotte Hjertaas, and Camilla Lorange Lindberg for excellent plant care during the growth experiment, and Erica Helen Leder provision of scripts and conceptualising the annotation pipeline together with Marian Schubert.

References

655 Alabadí, D., Oyama, T., Yanovsky, M.J., Harmon, F.G., Más, P., and Kay, S.A., 2001.
656 Reciprocal regulation between TOC1 and LHY/CCA1 within the Arabidopsis circadian
657 clock. *Science*, 293 (5531), 880–883.

658 Alabadí, D., Yanovsky, M.J., Más, P., Harmer, S.L., and Kay, S.A., 2002. Critical role for
659 CCA1 and LHY in maintaining circadian rhythmicity in Arabidopsis. *Current Biology*, 12
660 (9), 757–761.

661 Alexa, A., Rahnenführer, J., and Lengauer, T., 2006. Improved scoring of functional groups
662 from gene expression data by decorrelating GO graph structure. *Bioinformatics*, 22 (13),
663 1600–1607.

664 Altschul, S.F., Gish, W., Miller, W., Myers, E.W., and Lipman, D.J., 1990. Basic local
665 alignment search tool. *Journal of Molecular Biology*, 215 (3), 403–410.

666 Alvarez, M.A., Li, C., Lin, H., Joe, A., Padilla, M., Woods, D.P., and Dubcovsky, J., 2023.
667 EARLY FLOWERING 3 interactions with PHYTOCHROME B and PHOTOPERIOD1
668 are critical for the photoperiodic regulation of wheat heading time. *PLOS Genetics*, 19 (5),
669 e1010655.

670 Alvarez, M.A., Tranquilli, G., Lewis, S., Kippes, N., and Dubcovsky, J., 2016. Genetic and
671 physical mapping of the earliness per se locus Eps-Am1 in Triticum monococcum
672 identifies EARLY FLOWERING 3 (ELF3) as a candidate gene. *Functional & Integrative*
673 *Genomics*, 16 (4), 365–382.

674 Andrés, F. and Coupland, G., 2012. The genetic basis of flowering responses to seasonal
675 cues. *Nature Reviews Genetics*, 13 (9), 627–639.

676 Andrews, S., 2010. *A quality control tool for high throughput sequence data*.

677 Barra, V., 2004. Analysis of gene expression data using functional principal components.
678 *Computer Methods and Programs in Biomedicine*, 75 (1), 1–9.

679 Bendix, C., Marshall, C.M., and Harmon, F.G., 2015. Circadian clock genes universally
680 control key agricultural traits. *Molecular Plant*, 8 (8), 1135–1152.

681 Benson, D.A., Cavanaugh, M., Clark, K., Karsch-Mizrachi, I., Lipman, D.J., Ostell, J., and
682 Sayers, E.W., 2013. GenBank. *Nucleic Acids Research*, 41 (D1), D36–D42.

683 Bolger, A.M., Lohse, M., and Usadel, B., 2014. Trimmomatic: a flexible trimmer for Illumina
684 sequence data. *Bioinformatics*, 30 (15), 2114–2120.

685 Brambilla, V. and Fornara, F., 2017. Y flowering? Regulation and activity of CONSTANS
686 and CCT-domain proteins in Arabidopsis and crop species. *Biochimica et Biophysica*
687 *Acta*, 1860 (5), 655–660.

688 Brambilla, V., Gomez-Ariza, J., Cerise, M., and Fornara, F., 2017. The importance of being
689 on time: Regulatory networks controlling photoperiodic flowering in cereals. *Frontiers in*
690 *Plant Science*, 8, 665.

691 Buchfink, B., Xie, C., and Huson, D.H., 2015. Fast and sensitive protein alignment using
692 DIAMOND. *Nature Methods*, 12 (1), 59–60.

693 Camacho, C., Coulouris, G., Avagyan, V., Ma, N., Papadopoulos, J., Bealer, K., and Madden,
694 T.L., 2009. BLAST+: architecture and applications. *BMC Bioinformatics*, 10 (1), 421.

695 Conesa, A., Madrigal, P., Tarazona, S., Gomez-Cabrero, D., Cervera, A., McPherson, A.,
696 Szcześniak, M.W., Gaffney, D.J., Elo, L.L., Zhang, X., and Mortazavi, A., 2016. A survey
697 of best practices for RNA-seq data analysis. *Genome Biology*, 17 (1), 13.

698 Dakhiya, Y., Hussien, D., Fridman, E., Kiflawi, M., and Green, R., 2017. Correlations
699 between circadian rhythms and growth in challenging environments. *Plant Physiology*,
700 173 (3), 1724–1734.

701 Davidson, N.M. and Oshlack, A., 2014. Corset: enabling differential gene expression analysis
702 for de novo assembled transcriptomes. *Genome Biology*, 15 (7), 410.

703 Deng, W., Clausen, J., Boden, S., Oliver, S.N., Casao, M.C., Ford, B., Anderssen, R.S., and
704 Trevaskis, B., 2015. Dawn and dusk set states of the circadian oscillator in sprouting
705 barley (Hordeum vulgare) seedlings. *PLOS One*, 10 (6), e0129781.

706 Dodd, A.N., Salathia, N., Hall, A., Kévei, E., Tóth, R., Nagy, F., Hibberd, J.M., Millar, A.J.,
707 and Webb, A.A.R., 2005. Plant circadian clocks increase photosynthesis, growth, survival,
708 and competitive advantage. *Science*, 309 (5734), 630–633.

709 Durinck, S., Moreau, Y., Kasprzyk, A., Davis, S., Moor, B.D., Brazma, A., and Huber, W.,
710 2005. BioMart and Bioconductor: a powerful link between biological databases and
711 microarray data analysis. *Bioinformatics*, 21 (16), 3439–3440.

712 Emms, D.M. and Kelly, S., 2015. OrthoFinder: solving fundamental biases in whole genome
713 comparisons dramatically improves orthogroup inference accuracy. *Genome Biology*, 16
714 (1), 157.

715 Emms, D.M. and Kelly, S., 2019. OrthoFinder: phylogenetic orthology inference for
716 comparative genomics. *Genome Biology*, 20 (1), 238.

717 Faure, S., Turner, A.S., Gruszka, D., Christodoulou, V., Davis, S.J., von Korff, M., and
718 Laurie, D.A., 2012. Mutation at the circadian clock gene EARLY MATURITY 8 adapts
719 domesticated barley (Hordeum vulgare) to short growing seasons. *Proceedings of the*
720 *National Academy of Sciences of the United States of America*, 109 (21), 8328–8333.

721 Fjellheim, S., Young, D.A., Paliocha, M., Johnsen, S.S., Schubert, M., and Preston, J.C.,
722 2022. Major niche transitions in Pooideae correlate with variation in photoperiodic
723 flowering and evolution of CCT domain genes. *Journal of Experimental Botany*, 73 (12),
724 4079–4093.

725 Flis, A., Sulpice, R., Seaton, D.D., Ivakov, A.A., Liput, M., Abel, C., Millar, A.J., and Stitt,
726 M., 2016. Photoperiod-dependent changes in the phase of core clock transcripts and global
727 transcriptional outputs at dawn and dusk in Arabidopsis. *Plant, Cell & Environment*, 39
728 (9), 1955–1981.

Fowler, S., Lee, K., Onouchi, H., Samach, A., Richardson, K., Morris, B., Coupland, G., and Putterill, J., 1999. GIGANTEA: a circadian clock-controlled gene that regulates photoperiodic flowering in Arabidopsis and encodes a protein with several possible membrane-spanning domains. *The EMBO Journal*, 18 (17), 4679–4688.

Garner, W.W. and Allard, H.A., 1920. Effect of the relative length of day and night and other factors of the environment on growth and reproduction in plants. *Journal of Agricultural Research*, 18 (11), 553–606.

Garner, W.W. and Allard, H.A., 1923. Further studies in photoperiodism, the response of the plant to relative length of day and night. *Journal of Agricultural Research*, 23 (11), 871–920.

Garner, W.W. and Allard, H.A., 1931. Effect of abnormally long and short alternations of light and darkness on growth and development of plants. *Journal of Agricultural Research*, 42 (10), 629–651.

Gaßner, G., 1918. Beiträge zur physiologischen Charakteristik sommer- und winterannueller Gewächse, insbesondere der Getreidepflanzen. *Zeitschrift für Botanik*, 10, 417–480.

Gendron, J.M., Pruneda-Paz, J.L., Doherty, C.J., Gross, A.M., Kang, S.E., and Kay, S.A., 2012. Arabidopsis circadian clock protein, TOC1, is a DNA-binding transcription factor. *Proceedings of the National Academy of Sciences of the United States of America*, 109 (8), 3167–3172.

Gendron, J.M. and Staiger, D., 2023. New horizons in plant photoperiodism. *Annual Review of Plant Biology*, 74, 481–509.

Gene Ontology Consortium, 2004. The Gene Ontology (GO) database and informatics resource. *Nucleic Acids Research*, 32 (S1), D258–D261.

Grabherr, M.G., Haas, B.J., Yassour, M., Levin, J.Z., Thompson, D.A., Amit, I., Adiconis, X., Fan, L., Raychowdhury, R., Zeng, Q., Chen, Z., Mauceli, E., Hacohen, N., Gnirke, A., Rhind, N., di Palma, F., Birren, B.W., Nusbaum, C., Lindblad-Toh, K., Friedman, N., and Regev, A., 2011. Full-length transcriptome assembly from RNA-seq data without a reference genome. *Nature Biotechnology*, 29 (7), 644–652.

Green, R.M., Tingay, S., Wang, Z.-Y., and Tobin, E.M., 2002. Circadian rhythms confer a higher level of fitness to Arabidopsis plants. *Plant Physiology*, 129 (2), 576–584.

Greenham, K. and McClung, C.R., 2015. Integrating circadian dynamics with physiological processes in plants. *Nature Reviews Genetics*, 16 (10), 598–610.

Gu, Z., Eils, R., and Schlesner, M., 2016. Complex heatmaps reveal patterns and correlations in multidimensional genomic data. *Bioinformatics*, 32 (18), 2847–2849.

Hayama, R., Agashe, B., Luley, E., King, R., and Coupland, G., 2007. A circadian rhythm set by dusk determines the expression of FT homologs and the short-day photoperiodic flowering response in Pharbitis. *The Plant Cell*, 19 (10), 2988–3000.

Hayama, R., Mizoguchi, T., and Coupland, G., 2018. Differential effects of light-to-dark transitions on phase setting in circadian expression among clock-controlled genes in Pharbitis nil. *Plant Signaling & Behavior*, 13 (6), 1–7.

Helfer, A., Nusinow, D.A., Chow, B.Y., Gehrke, A.R., Bulyk, M.L., and Kay, S.A., 2011. LUX ARRHYTHMO encodes a nighttime repressor of circadian gene expression in the Arabidopsis core clock. *Current Biology*, 21 (2), 126–133.

Herrero, E., Kolmos, E., Bujdoso, N., Yuan, Y., Wang, M., Berns, M.C., Uhlworm, H., Coupland, G., Saini, R., Jaskolski, M., Webb, A., Gonçalves, J., and Davis, S.J., 2012. EARLY FLOWERING4 recruitment of EARLY FLOWERING3 in the nucleus sustains the Arabidopsis circadian clock. *The Plant Cell*, 24 (2), 428–443.

Higgins, J.A., Bailey, P.C., and Laurie, D.A., 2010. Comparative genomics of flowering time pathways using Brachypodium distachyon as a model for the temperate grasses. *PLOS One*, 5 (4), e10065.

Hoffman, D.E., Jonsson, P., Bylesjö, M., Trygg, J., Antti, H., Eriksson, M.E., and Moritz, T., 2010. Changes in diurnal patterns within the Populus transcriptome and metabolome in response to photoperiod variation. *Plant, Cell & Environment*, 33 (8), 1298–1313.

Hong, S.-Y., Lee, S., Seo, P.J., Yang, M.-S., and Park, C.-M., 2010. Identification and molecular characterization of a Brachypodium distachyon GIGANTEA gene: functional conservation in monocot and dicot plants. *Plant Molecular Biology*, 72 (4–5), 485–497.

Hotta, C.T., Nishiyama, M.Y., and Souza, G.M., 2013. Circadian rhythms of sense and antisense transcription in sugarcane, a highly polyploid crop. *PLOS ONE*, 8 (8), e71847.

Howe, K.L., Achuthan, P., Allen, J., Allen, J., Alvarez-Jarreta, J., Amode, M.R., Armean, I.M., Azov, A.G., Bennett, R., Bhai, J., Billis, K., Boddu, S., Charkhchi, M., Cummins, C., Da Rin Fioretto, L., Davidson, C., Dodiya, K., El Houdaigui, B., Fatima, R., Gall, A., Garcia Giron, C., Grego, T., Guijarro-Clarke, C., Haggerty, L., Hemrom, A., Hourlier, T., Izuogu, O.G., Juettemann, T., Kaikala, V., Kay, M., Lavidas, I., Le, T., Lemos, D., Gonzalez Martinez, J., Marugán, J.C., Maurel, T., McMahon, A.C., Mohanan, S., Moore, B., Muffato, M., Oheh, D.N., Paraschas, D., Parker, A., Parton, A., Prosovetskaia, I., Sakthivel, M.P., Salam, A.I.A., Schmitt, B.M., Schuilenburg, H., Sheppard, D., Steed, E., Szpak, M., Szuba, M., Taylor, K., Thormann, A., Threadgold, G., Walts, B., Winterbottom, A., Chakiachvili, M., Chaubal, A., De Silva, N., Flint, B., Frankish, A., Hunt, S.E., IIsley, G.R., Langridge, N., Loveland, J.E., Martin, F.J., Mudge, J.M., Morales, J., Perry, E., Ruffier, M., Tate, J., Thybert, D., Trevanion, S.J., Cunningham, F., Yates, A.D., Zerbino, D.R., and Flicek, P., 2021. Ensembl 2021. *Nucleic Acids Research*, 49 (D1), D884–D891.

Howe, K.L., Contreras-Moreira, B., Silva, N.D., Maslen, G., Akanni, W., Allen, J., Alvarez-Jarreta, J., Barba, M., Bolser, D.M., Cambell, L., Carbajo, M., Chakiachvili, M., Christensen, M., Cummins, C., Cuzick, A., Davis, P., Fexova, S., Gall, A., George, N., Gil, L., Gupta, P., Hammond-Kosack, K.E., Haskell, E., Hunt, S.E., Jaiswal, P., Janacek, S.H., Kersey, P.J., Langridge, N., Maheswari, U., Maurel, T., McDowall, M.D., Moore, B., Muffato, M., Naamati, G., Naithani, S., Olson, A., Papatheodorou, I., Patricio, M., Paulini, M., Pedro, H., Perry, E., Preece, J., Rosello, M., Russell, M., Sitnik, V., Staines,

808 D.M., Stein, J., Tello-Ruiz, M.K., Trevanion, S.J., Urban, M., Wei, S., Ware, D.,
809 Williams, G., Yates, A.D., and Flicek, P., 2020. Ensembl Genomes 2020—enabling non-
810 vertebrate genomic research. *Nucleic Acids Research*, 48 (D1), D689–D695.

811 Hsu, P.Y. and Harmer, S.L., 2014. Wheels within wheels: the plant circadian system. *Trends*
812 *in Plant Science*, 19 (4), 240–249.

813 Huang, H., Gehan, M.A., Huss, S.E., Alvarez, S., Lizarraga, C., Gruebbling, E.L., Gierer, J.,
814 Naldrett, M.J., Bindbeutel, R.K., Evans, B.S., Mockler, T.C., and Nusinow, D.A., 2017.
815 Cross-species complementation reveals conserved functions for EARLY FLOWERING 3
816 between monocots and dicots. *Plant Direct*, 1 (4), e00018.

817 Huang, W., Pérez-García, P., Pokhilko, A., Millar, A.J., Antoshechkin, I., Riechmann, J.L.,
818 and Mas, P., 2012. Mapping the core of the Arabidopsis circadian clock defines the
819 network structure of the oscillator. *Science*, 336 (6077), 75–79.

820 Hughes, M.E., Abruzzi, K.C., Allada, R., Anafi, R., Arpat, A.B., Asher, G., Baldi, P., Bekker,
821 C. de, Bell-Pedersen, D., Blau, J., Brown, S., Ceriani, M.F., Chen, Z., Chiu, J.C., Cox, J.,
822 Crowell, A.M., DeBruyne, J.P., Dijk, D.-J., DiTacchio, L., Doyle, F.J., Duffield, G.E.,
823 Dunlap, J.C., Eckel-Mahan, K., Esser, K.A., FitzGerald, G.A., Forger, D.B., Francey, L.J.,
824 Fu, Y.-H., Gachon, F., Gatfield, D., Goede, P. de, Golden, S.S., Green, C., Harer, J.,
825 Harmer, S., Haspel, J., Hastings, M.H., Herzel, H., Herzog, E.D., Hoffmann, C., Hong, C.,
826 Hughey, J.J., Hurley, J.M., Iglesia, H.O. de la, Johnson, C., Kay, S.A., Koike, N.,
827 Kornacker, K., Kramer, A., Lamia, K., Leise, T., Lewis, S.A., Li, J., Li, X., Liu, A.C.,
828 Loros, J.J., Martino, T.A., Menet, J.S., Merrow, M., Millar, A.J., Mockler, T., Naef, F.,
829 Nagoshi, E., Nitabach, M.N., Olmedo, M., Nusinow, D.A., Ptáček, L.J., Rand, D., Reddy,
830 A.B., Robles, M.S., Roenneberg, T., Rosbash, M., Ruben, M.D., Rund, S.S.C., Sancar, A.,
831 Sassone-Corsi, P., Sehgal, A., Sherrill-Mix, S., Skene, D.J., Storch, K.-F., Takahashi, J.S.,
832 Ueda, H.R., Wang, H., Weitz, C., Westermark, P.O., Wijnen, H., Xu, Y., Wu, G., Yoo, S.-
833 H., Young, M., Zhang, E.E., Zielinski, T., and Hogenesch, J.B., 2017. Guidelines for
834 genome-scale analysis of biological rhythms. *Journal of Biological Rhythms*, 32 (5), 380–
835 393.

836 Izawa, T., Mihara, M., Suzuki, Y., Gupta, M., Itoh, H., Nagano, A.J., Motoyama, R., Sawada,
837 Y., Yano, M., Hirai, M.Y., Makino, A., and Nagamura, Y., 2011. Os-GIGANTEA confers
838 robust diurnal rhythms on the global transcriptome of rice in the field. *The Plant Cell*, 23
839 (5), 1741–1755.

840 Johansson, M. and Staiger, D., 2014. Time to flower: interplay between photoperiod and the
841 circadian clock. *Journal of Experimental Botany*, 66 (3), 719–730.

842 Jończyk, M., Sobkowiak, A., Siedlecki, P., Biecek, P., Trzcinska-Danielewicz, J., Tiuryn, J.,
843 Fronk, J., and Sowiński, P., 2011. Rhythmic diel pattern of gene expression in juvenile
844 maize leaf. *PLOS ONE*, 6 (8), e23628.

845 Khan, S., Rowe, S.C., and Harmon, F.G., 2010. Coordination of the maize transcriptome by a
846 conserved circadian clock. *BMC Plant Biology*, 10 (1), 126.

847 Koda, S., Onda, Y., Matsui, H., Takahagi, K., Uehara-Yamaguchi, Y., Shimizu, M., Inoue,
848 K., Yoshida, T., Sakurai, T., Honda, H., Eguchi, S., Nishii, R., and Mochida, K., 2017.

849 Diurnal transcriptome and gene network represented through sparse modeling in
850 Brachypodium distachyon. *Frontiers in Plant Science*, 8, 2055.

851 Kriventseva, E.V., Kuznetsov, D., Tegenfeldt, F., Manni, M., Dias, R., Simão, F.A., and
852 Zdobnov, E.M., 2019. OrthoDB v10: sampling the diversity of animal, plant, fungal,
853 protist, bacterial and viral genomes for evolutionary and functional annotations of
854 orthologs. *Nucleic Acids Research*, 47 (D1), D807–D811.

855 Langfelder, P., Zhang, B., and Horvath, S., 2007. Defining clusters from a hierarchical cluster
856 tree: the Dynamic Tree Cut package for R. *Bioinformatics*, 24 (5), 719–720.

857 Langmead, B. and Salzberg, S.L., 2012. Fast gapped-read alignment with Bowtie 2. *Nature*
858 *Methods*, 9 (4), 357–359.

859 Laosuntisuk, K., Elorriaga, E., and Doherty, C.J., 2023. The game of timing: Circadian
860 rhythms intersect with changing environments. *Annual Review of Plant Biology*, 74 (1),
861 511–538.

862 Leder, E.H., André, C., Alan, L.M., Töpel, M., Blomberg, A., Havenhand, J.N., Lindström,
863 K., Volckaert, F.A.M., Kvarnemo, C., Johannesson, K., and Svensson, O., 2021. Post-
864 glacial establishment of locally adapted fish populations over a steep salinity gradient.
865 *Journal of Evolutionary Biology*, 34 (1), 138–156.

866 Lee, S.-J., Kang, K., Lim, J.-H., and Paek, N.-C., 2022. Natural alleles of CIRCADIAN
867 CLOCK ASSOCIATED1 contribute to rice cultivation by fine-tuning flowering time.
868 *Plant Physiology*, 190 (1), 640–656.

869 Leng, X. and Müller, H.-G., 2005. Classification using functional data analysis for temporal
870 gene expression data. *Bioinformatics*, 22 (1), 68–76.

871 Leung, C.C., Tarté, D.A., Oliver, L.S., and Gendron, J.M., 2022. Diverse photoperiodic gene
872 expression patterns are likely mediated by distinct transcriptional systems in Arabidopsis.
873 *bioRxiv*, 2022.10.05.510993.

874 Li, H., Handsaker, B., Wysoker, A., Fennell, T., Ruan, J., Homer, N., Marth, G., Abecasis,
875 G., Durbin, R., and 1000 Genome Project Data Processing Subgroup, 2009. The Sequence
876 Alignment/Map format and SAMtools. *Bioinformatics*, 25 (16), 2078–2079.

877 Liu, W., Feke, A., Leung, C.C., Tarté, D.A., Yuan, W., Vanderwall, M., Sager, G., Wu, X.,
878 Schear, A., Clark, D.A., Thines, B.C., and Gendron, J.M., 2021. A metabolic daylength
879 measurement system mediates winter photoperiodism in plants. *Developmental Cell*, 56
880 (17), 2501-2515.e5.

881 Ma, L., Li, J., Qu, L., Hager, J., Chen, Z., Zhao, H., and Deng, X.W., 2001. Light control of
882 Arabidopsis development entails coordinated regulation of genome expression and cellular
883 pathways. *The Plant Cell*, 13 (12), 2589–2607.

884 MacKinnon, K.J.-M., Cole, B.J., Yu, C., Coomey, J.H., Hartwick, N.T., Remigereau, M.,
885 Duffy, T., Michael, T.P., Kay, S.A., and Hazen, S.P., 2020. Changes in ambient

temperature are the prevailing cue in determining Brachypodium distachyon diurnal gene regulation. *New Phytologist*, 227 (6), 1709–1724.

Markham, K.K. and Greenham, K., 2021. Abiotic stress through time. *New Phytologist*, 231 (1), 40–46.

Martínez-García, J.F., Huq, E., and Quail, P.H., 2000. Direct targeting of light signals to a promoter element-bound transcription factor. *Science*, 288 (5467), 859–863.

McClung, C.R., 2010. A modern circadian clock in the common angiosperm ancestor of monocots and eudicots. *BMC Biology*, 8 (1), 55–55.

McDermaid, A., Monier, B., Zhao, J., Liu, B., and Ma, Q., 2018. Interpretation of differential gene expression results of RNA-seq data: review and integration. *Briefings in Bioinformatics*, 20 (6), 2044–2054.

McWatters, H.G., Bastow, R.M., Hall, A., and Millar, A.J., 2000. The ELF3 zeitnehmer regulates light signalling to the circadian clock. *Nature*, 408 (6813), 716–720.

Michael, T.P., Salomé, P.A., Yu, H.J., Spencer, T.R., Sharp, E.L., McPeek, M.A., Alonso, J.M., Ecker, J.R., and McClung, C.R., 2003. Enhanced fitness conferred by naturally occurring variation in the circadian clock. *Science*, 302 (5647), 1049–1053.

Minh, B.Q., Schmidt, H.A., Chernomor, O., Schrempf, D., Woodhams, M.D., von Haeseler, A., and Lanfear, R., 2020. IQ-TREE 2: New models and efficient methods for phylogenetic inference in the genomic era. *Molecular Biology and Evolution*, 37 (5), 1530–1534.

Müller, L.M., Mombaerts, L., Pankin, A., Davis, S.J., Webb, A.A.R., Goncalves, J., and Korff, M. von, 2020. Differential effects of day/night cues and the circadian clock on the barley transcriptome. *Plant Physiology*, 183 (2), 765–779.

Müller, L.M., von Korff, M., and Davis, S.J., 2014. Connections between circadian clocks and carbon metabolism reveal species-specific effects on growth control. *Journal of Experimental Botany*, 65 (11), 2915–2923.

Murakami, M., Tago, Y., Yamashino, T., and Mizuno, T., 2007. Characterization of the rice circadian clock-associated pseudo-response regulators in Arabidopsis thaliana. *Bioscience, Biotechnology, and Biochemistry*, 71 (4), 1107–1110.

Murtagh, F. and Legendre, P., 2014. Ward's hierarchical agglomerative clustering method: Which algorithms implement Ward's criterion? *Journal of Classification*, 31 (3), 274–295.

Nagel, D.H., Doherty, C.J., Pruneda-Paz, J.L., Schmitz, R.J., Ecker, J.R., and Kay, S.A., 2015. Genome-wide identification of CCA1 targets uncovers an expanded clock network in Arabidopsis. *Proceedings of the National Academy of Sciences of the United States of America*, 112 (34), E4802–E4810.

Nakamichi, N., Kiba, T., Henriques, R., Mizuno, T., Chua, N.-H., and Sakakibara, H., 2010. PSEUDO-RESPONSE REGULATORS 9, 7, and 5 are transcriptional repressors in the Arabidopsis circadian clock. *The Plant Cell*, 22 (3), 594–605.

Nakamichi, N., Kiba, T., Kamioka, M., Suzuki, T., Yamashino, T., Higashiyama, T., Sakakibara, H., and Mizuno, T., 2012. Transcriptional repressor PRR5 directly regulates clock-output pathways. *Proceedings of the National Academy of Sciences of the United States of America*, 109 (42), 17123–17128.

NCBI Resource Coordinators, 2017. Database resources of the National Center for Biotechnology Information. *Nucleic Acids Research*, 45 (D1), D12–D17.

Nusinow, D.A., Helfer, A., Hamilton, E.E., King, J.J., Imaizumi, T., Schultz, T.F., Farré, E.M., and Kay, S.A., 2011. The ELF4–ELF3–LUX complex links the circadian clock to diurnal control of hypocotyl growth. *Nature*, 475 (7356), 398–402.

Pertea, G. and Pertea, M., 2020. GFF Utilities: GffRead and GffCompare. *F1000Research*, 9, 304.

Pokhilko, A., Fernández, A.P., Edwards, K.D., Southern, M.M., Halliday, K.J., and Millar, A.J., 2012. The clock gene circuit in Arabidopsis includes a repressilator with additional feedback loops. *Molecular Systems Biology*, 8 (1), 574–574.

Quetelet, A., 1842. Instructions pour l'observation des phénomènes périodiques. *Bulletins de l'Académie Royale des Sciences, des lettres et des beaux-arts de Belgique*, 9 (1), 65–95.

R Core Team, 2022. *R: A language and environment for statistical computing*.

Raghavan, V., Kraft, L., Mesny, F., and Rigerte, L., 2022. A simple guide to de novo transcriptome assembly and annotation. *Briefings in Bioinformatics*, 23 (2), bbab563.

Ramsay, J.O., Graves, S., and Hooker, G., 2022. *fda: Functional Data Analysis*.

Ramsay, J.O. and Silverman, B.W., 2002. *Applied Functional Data Analysis: Methods and Case Studies*. 1st ed. New York, NY, USA: Springer.

Ramsay, J.O. and Silverman, B.W., 2005. *Functional Data Analysis*. 2nd ed. New York, NY, USA: Springer.

Ream, T.S., Woods, D.P., Schwartz, C.J., Sanabria, C.P., Mahoy, J.A., Walters, E.M., Kaeppler, H.F., and Amasino, R., 2014. Interaction of photoperiod and vernalization determines flowering time of Brachypodium distachyon. *Plant Physiology*, 164 (2), 694–709.

Rees, H., Rusholme-Pilcher, R., Bailey, P., Colmer, J., White, B., Reynolds, C., Ward, S.J., Coombes, B., Graham, C.A., Dantas, L.L. de B., Dodd, A.N., and Hall, A., 2022. Circadian regulation of the transcriptome in a complex polyploid crop. *PLOS Biology*, 20 (10), e3001802.

Riboni, M., Test, A.R., Galbiati, M., Tonelli, C., and Conti, L., 2014. Environmental stress and flowering time. *Plant Signaling & Behavior*, 9 (7), e29036.

Robinson, M.D., McCarthy, D.J., and Smyth, G.K., 2010. edgeR: a Bioconductor package for differential expression analysis of digital gene expression data. *Bioinformatics*, 26 (1), 139–140.

Schaffer, R., Ramsay, N., Samach, A., Corden, S., Putterill, J., Carré, I.A., and Coupland, G., 1998. The late elongated hypocotyl mutation of Arabidopsis disrupts circadian rhythms and the photoperiodic control of flowering. *Cell*, 93 (7), 1219–1229.

Seluzicki, A., Burko, Y., and Chory, J., 2017. Dancing in the dark: darkness as a signal in plants. *Plant, Cell & Environment*, 40 (11).

Seo, P.J. and Mas, P., 2015. STRESSing the role of the plant circadian clock. *Trends in Plant Science*, 20 (4), 230–237.

Sherrill-Mix, S., 2019. *taxonomizr: Functions to work with NCBI accessions and taxonomy*.

Simão, F.A., Waterhouse, R.M., Ioannidis, P., Kriventseva, E.V., and Zdobnov, E.M., 2015. BUSCO: assessing genome assembly and annotation completeness with single-copy orthologs. *Bioinformatics*, 31 (19), 3210–3212.

Slater, G.S.C. and Birney, E., 2005. Automated generation of heuristics for biological sequence comparison. *BMC Bioinformatics*, 6 (1), 31.

Somers, D.E., Devlin, P.F., and Kay, S.A., 1998. Phytochromes and cryptochromes in the entrainment of the Arabidopsis circadian clock. *Science*, 282 (5393), 1488–1490.

Somers, D.E., Kim, W.-Y., and Geng, R., 2004. The F-box protein ZEITLUPE confers dosage-dependent control on the circadian clock, photomorphogenesis, and flowering time. *The Plant Cell*, 16 (3), 769–782.

Song, J.J., Deng, W., Lee, H.-J., and Kwon, D., 2008. Optimal classification for time-course gene expression data using functional data analysis. *Computational Biology and Chemistry*, 32 (6), 426–432.

Song, J.J., Lee, H.-J., Morris, J.S., and Kang, S., 2007. Clustering of time-course gene expression data using functional data analysis. *Computational Biology and Chemistry*, 31 (4), 265–274.

Soreng, R.J., Peterson, P.M., Zuloaga, F.O., Romaschenko, K., Clark, L.G., Teisher, J.K., Gillespie, L.J., Barberá, P., Welker, C.A.D., Kellogg, E.A., Li, D., and Davidse, G., 2022. A worldwide phylogenetic classification of the Poaceae (Gramineae) III: An update. *Journal of Systematics and Evolution*, 60 (3), 476–521.

Sun, L., Ma, J., Turck, C.W., Xu, P., and Wang, G.-Z., 2020. Genome-wide circadian regulation: A unique system for computational biology. *Computational and Structural Biotechnology Journal*, 18, 1914–1924.

992 Takeno, K., 2016. Stress-induced flowering: the third category of flowering response.
993 *Journal of Experimental Botany*, 67 (17), 4925–4934.

994 Tobin, E.M. and Silverthorne, J., 1985. Light regulation of gene expression in higher plants.
995 *Annual Review of Plant Physiology*, 36 (1), 569–593.

996 Turnbull, C., 2011. Long-distance regulation of flowering time. *Journal of Experimental*
997 *Botany*, 62 (13), 4399–4413.

998 Venkat, A. and Muneer, S., 2022. Role of circadian rhythms in major plant metabolic and
999 signaling pathways. *Frontiers in Plant Science*, 13, 836244.

1000 Wang, Z.-Y. and Tobin, E.M., 1998. Constitutive expression of the CIRCADIAN CLOCK
1001 ASSOCIATED 1 (CCA1) gene disrupts circadian rhythms and suppresses its own
1002 expression. *Cell*, 93 (7), 1207–1217.

1003 Ward, J.H., 1963. Hierarchical grouping to optimize an objective function. *Journal of the*
1004 *American Statistical Association*, 58 (301), 236–244.

1005 Waterhouse, R.M., Seppey, M., Simão, F.A., Manni, M., Ioannidis, P., Klioutchnikov, G.,
1006 Kriventseva, E.V., and Zdobnov, E.M., 2017. BUSCO applications from quality
1007 assessments to gene prediction and phylogenomics. *Molecular Biology and Evolution*, 35
1008 (3), 543–548.

1009 Webb, A.A.R., Seki, M., Satake, A., and Caldana, C., 2019. Continuous dynamic adjustment
1010 of the plant circadian oscillator. *Nature Communications*, 10 (1), 550.

1011 Weng, X., Lovell, J.T., Schwartz, S.L., Cheng, C., Haque, T., Zhang, L., Razzaque, S., and
1012 Juenger, T.E., 2019. Complex interactions between day length and diurnal patterns of gene
1013 expression drive photoperiodic responses in a perennial C4 grass. *Plant, Cell &*
1014 *Environment*, 42 (7), 2165–2182.

1015 Wijnen, H. and Young, M.W., 2006. Interplay of circadian clocks and metabolic rhythms.
1016 *Annual Review of Genetics*, 40 (1), 409–448.

1017 Wittern, L., Steed, G., Taylor, L.J., Ramirez, D.C., Pingarron-Cardenas, G., Gardner, K.,
1018 Greenland, A., Hannah, M.A., and Webb, A.A.R., 2023. Wheat EARLY FLOWERING 3
1019 affects heading date without disrupting circadian oscillations. *Plant Physiology*, 191 (2),
1020 1383–403.

1021 Woods, D.P., Bednarek, R., Bouché, F., Gordon, S.P., Vogel, J.P., Garvin, D.F., and
1022 Amasino, R., 2017. Genetic architecture of flowering-time variation in Brachypodium
1023 distachyon. *Plant Physiology*, 173 (1), 269 279.

1024 Wu, G., Anafi, R.C., Hughes, M.E., Kornacker, K., and Hogenesch, J.B., 2016. MetaCycle:
1025 an integrated R package to evaluate periodicity in large scale data. *Bioinformatics*, 32
1026 (21), 3351–3353.

1027 Wu, T.D. and Watanabe, C.K., 2005. GMAP: a genomic mapping and alignment program for
1028 mRNA and EST sequences. *Bioinformatics*, 21 (9), 1859–1875.

Yakir, E., Hilman, D., Harir, Y., and Green, R.M., 2007. Regulation of output from the plant circadian clock. *The FEBS Journal*, 274 (2), 335–345.

Yates, A.D., Achuthan, P., Akanni, W., Allen, J., Allen, J., Alvarez-Jarreta, J., Amode, M.R., Armean, I.M., Azov, A.G., Bennett, R., Bhai, J., Billis, K., Boddu, S., Marugán, J.C., Cummins, C., Davidson, C., Dodiya, K., Fatima, R., Gall, A., Giron, C.G., Gil, L., Grego, T., Haggerty, L., Haskell, E., Hourlier, T., Izuogu, O.G., Janacek, S.H., Juettemann, T., Kay, M., Lavidas, I., Le, T., Lemos, D., Martinez, J.G., Maurel, T., McDowall, M., McMahon, A., Mohanan, S., Moore, B., Nuhn, M., Oheh, D.N., Parker, A., Parton, A., Patricio, M., Sakthivel, M.P., Abdul Salam, A.I., Schmitt, B.M., Schuilenburg, H., Sheppard, D., Sycheva, M., Szuba, M., Taylor, K., Thormann, A., Threadgold, G., Vullo, A., Walts, B., Winterbottom, A., Zadissa, A., Chakiachvili, M., Flint, B., Frankish, A., Hunt, S.E., IIsley, G., Kostadima, M., Langridge, N., Loveland, J.E., Martin, F.J., Morales, J., Mudge, J.M., Muffato, M., Perry, E., Ruffier, M., Trevanion, S.J., Cunningham, F., Howe, K.L., Zerbino, D.R., and Flicek, P., 2020. Ensembl 2020. *Nucleic Acids Research*, 48 (D1), D682–D688.

Zakhrabekova, S., Gough, S.P., Braumann, I., Müller, A.H., Lundqvist, J., Ahmann, K., Dockter, C., Matyszczak, I., Kurowska, M., Druka, A., Waugh, R., Graner, A., Stein, N., Steuernagel, B., Lundqvist, U., and Hansson, M., 2012. Induced mutations in circadian clock regulator Mat-a facilitated short-season adaptation and range extension in cultivated barley. *Proceedings of the National Academy of Sciences of the United States of America*, 109 (11), 4326–4331.

Figure and Table Texts

Figure 1: Overview of the data collection and curve fitting process. **A)** Plants were subjected to contrasting photoperiods imitating long day (16 h light : 8 h dark) and short day (8 h light : 16 h dark). Samples were taken every 4th hour (dotted lines) after one week of acclimation in the growth chamber, starting at 4:00 h. **B)** Two upper panels: Yellow and brown dots are single transcript expression measurements in log2(CPM); quadruplets at each time point in LD and SD, respectively. These were replaced by their respective means (dashes in the left plot). The six means were used to fit a smoothed curve (central plot). The variation in curve trajectories is exemplified by transcript expression curves of 14 randomly chosen transcripts (right plot). Lower panel: The left plot shows the differences between transcript expression means from short day and long day treatment, for the measurements in the plots above. The middle plot shows the resulting smoothed difference curve, and the left plot shows variation in difference curve trajectories, for 14 different transcripts. The background colour of the plot indicates light period (white) or darkness (grey).

Figure 2: Results from functional principal component analyses (FPCA) of standardised transcript expression curves from LD **(A)** and SD **(B)** treatments, respectively. The top rows show the temporal variation identified by the principal component curves (i.e., how the shape of an individual curve differs from the mean curve if a multiple of the FPC curve is added to (++) or subtracted from (--) the mean curve, where the multiple corresponds to 1 SD of the corresponding FPC scores) and the bottom rows contain individual curves with extreme scores of one of the FPCs from LD (yellow lines), and SD (brown lines).

Figure 3: Results from FPCA of fitted transcript expression curves from both long and short-day treatments for **A)** raw data **B)** standardised data, and **C)** differences in transcript measurements (LD_{Raw} - SD_{Raw}). The top row shows the temporal variation identified by the principal component curves (i.e., how the shape of an individual curve differs from the mean curve if a multiple of the FPC curve is added to (++) or subtracted from (--) the mean curve, where the multiple corresponds to 1 SD of the corresponding FPC scores) and the bottom row contain individual curves with extreme scores of one of the FPCs. Yellow and brown lines are transcript curves from long day and short day-treatment, respectively. The background colour of the plot indicates light period (white) or darkness (grey), with light grey indicating darkness in one of the treatments, and darker grey indicating darkness in both treatments.

Figure 4: Transcript expression curves classified to the pre-specified groups (see Tab. 1). **A–D)** show curves classified to group 1–4, respectively. **E–H)** show curves classified to group 5. Since the transcripts in group 5 span a diverse set of trajectories and differences, these curves were sorted according to their $FPCA_D$ scores, and displayed in separate columns, according to the lower and upper tails of the $FPC1–4_D$ scores. The upper plots show the raw expression curves, the second and third plots show centred curves and standardised curves, respectively. The lower plots show the corresponding difference curves (of the raw expression curves). Yellow and brown lines are raw expression curves from long day (LD) and short day (SD) treatment, respectively, and these are plotted in pairs. Green lines are differences in transcript

expression between LD and SD. The background colour of the plot indicates light period (white) or darkness (grey), with light grey indicating darkness in one of the treatments, and darker grey indicating darkness in both treatments.

Figure 5. Hierarchical clustering of transcripts with differing SD and LD expression patterns as identified by the FPCA analyses ('Group 5'). The dendrogram is pruned to a minimum cluster size of 1,000 transcript pairs. Light and dark period indicated by the bars at the bottom. Significant GO enrichments for all transcripts in a given cluster are shown to the right ($P < 0.05$, Fisher's exact test, biological process annotation). Expression values are standardised. Placement of *Brachypodium distachyon* (*Bd*) photoreceptors and circadian clock orthologues is indicated with arrows.

Figure 6. Score plots of $FPCA_Z$. **A)** $FPC1_Z$ and **B)** FPC2z Grey lines indicate 1 standard deviation. FPCA scores of *Brachypodium distachyon* (*Bd*) orthologues involved in circadian clock activity and photoperiodic flowering are highlighted. Transcripts represented more than once represent multiple isoforms or paralogues.

Figure 7. Expression profiles of known **A)** circadian clock and **B)** photoreceptor genes. The top row shows fitted raw curves and the bottom row shows standardised curves.

Table 1. Overview of pre-specified groups and corresponding criteria for the identification these. The specifications of the terms *similar*, *different*, *low,* and *extreme*, in relation to levels, FPCA scores, rhythm and variance, are described thoroughly in the main text.

Figure 1

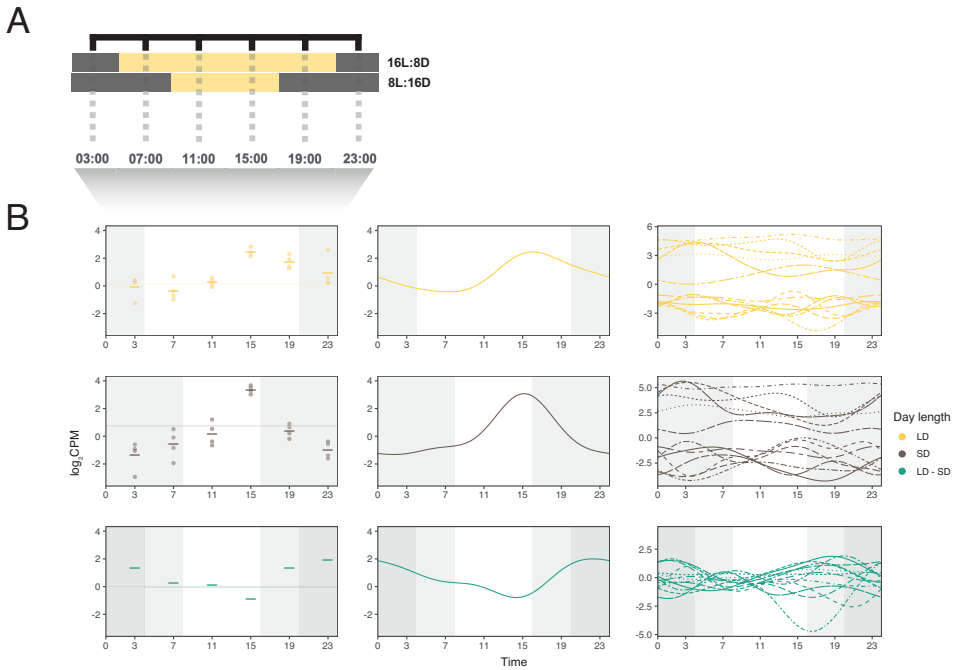
A
16L:8D
8L:16D
03:00
07:00
11:00
15:00
19:00
23:00
B
log2CPM
Time
Day length
LD
SD
LD - SD

Figure 2

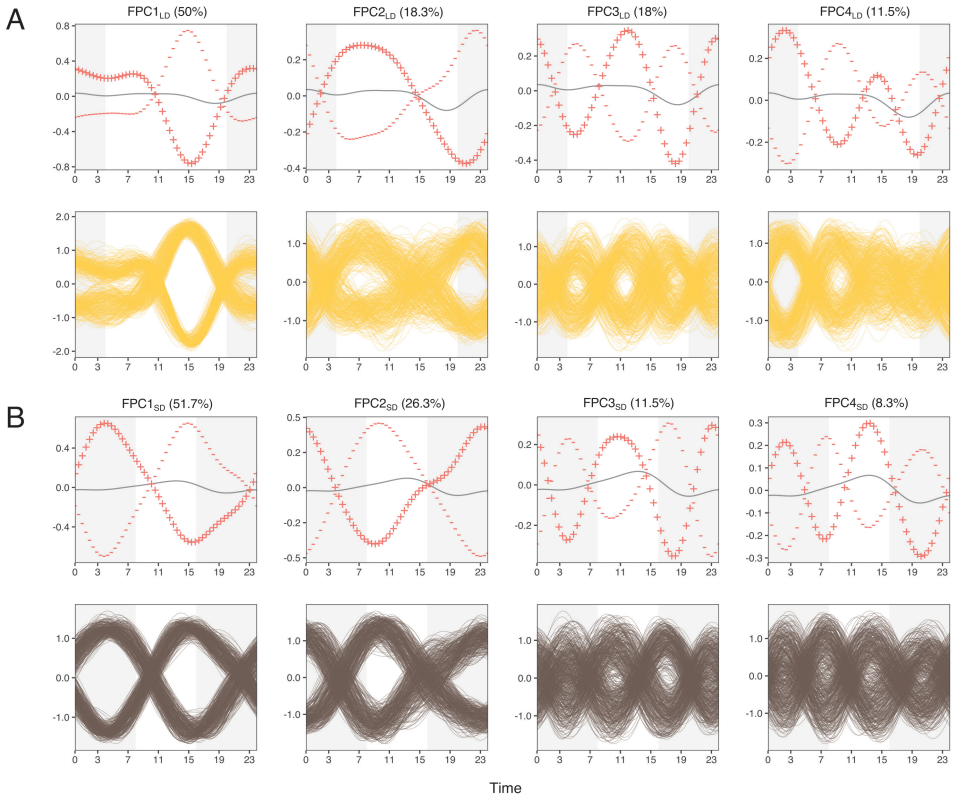
A
FPC1LD (50%)
FPC2LD (18.3%)
FPC3LD (18%)
FPC4LD (11.5%)
B
FPC1SD (51.7%)
FPC2SD (26.3%)
FPC3SD (11.5%)
FPC4SD (8.3%)
Time

1117 Figure 3

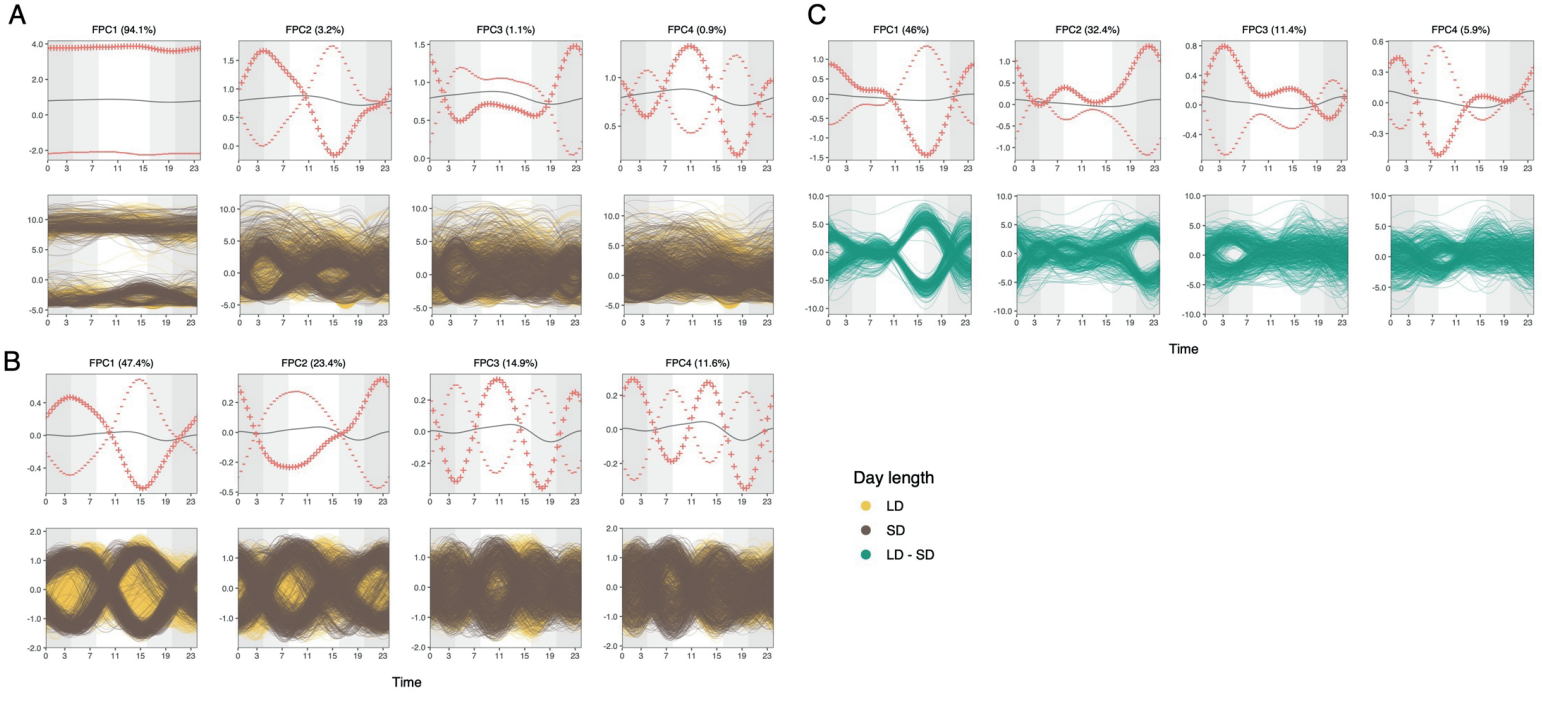

Figure 4

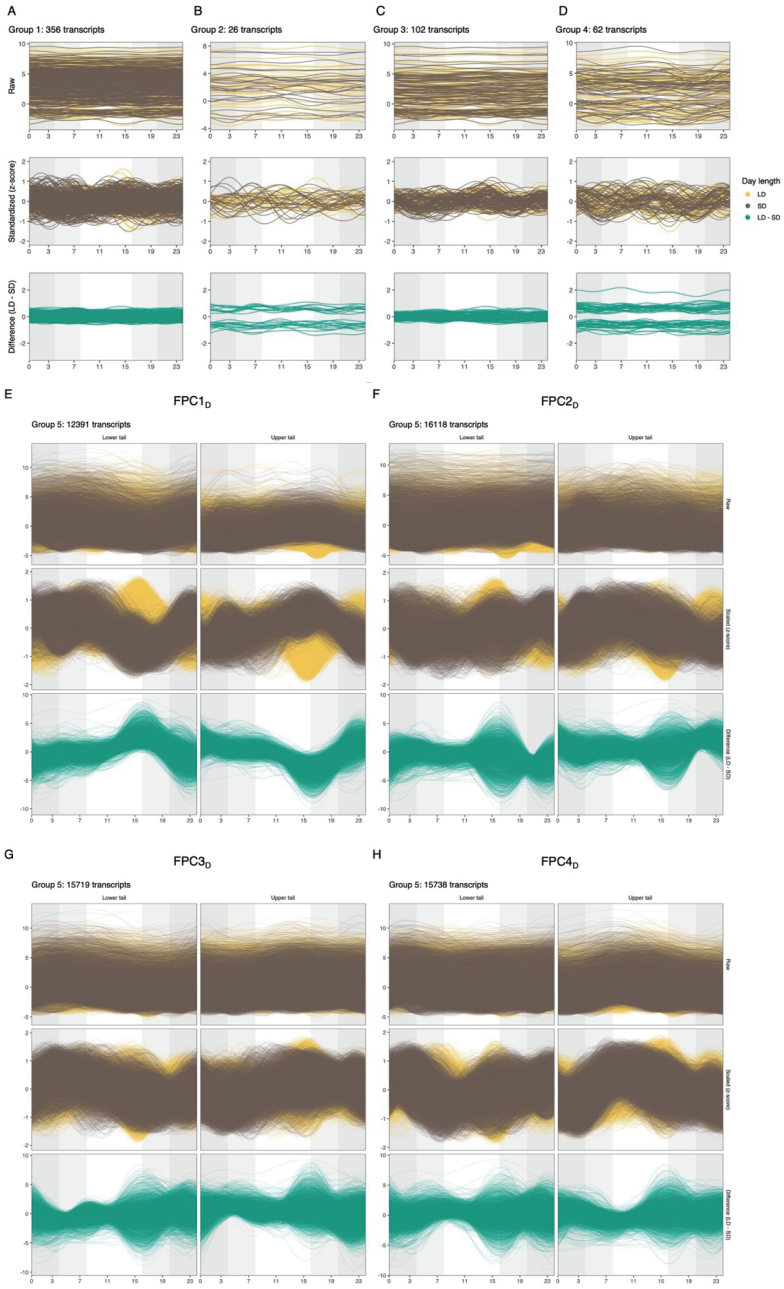
A
Group 1: 356 transcripts
B
Group 2: 26 transcripts
C
Group 3: 102 transcripts
D
Group 4: 62 transcripts
Raw
Standardized (z-score)
Difference (LD - SD)
Day length
LD
SD
LD - SD
E
FPC1D
Group 5: 12391 transcripts
F
FPC2D
Group 5: 16118 transcripts
G
FPC3D
Group 5: 15719 transcripts
H
FPC4D
Group 5: 15738 transcripts
Lower tail
Upper tail

1121 Figure 5

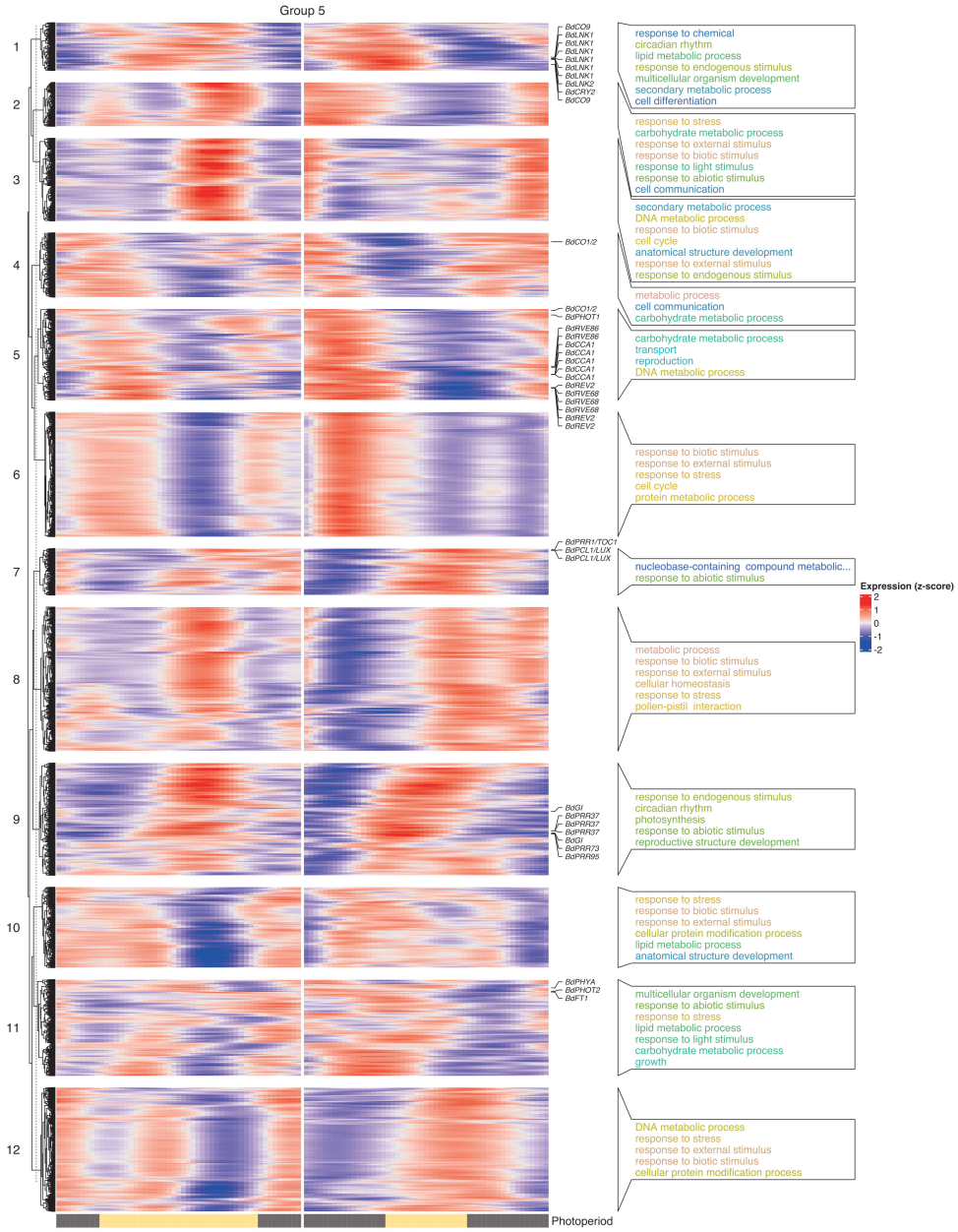

1122

Figure 6

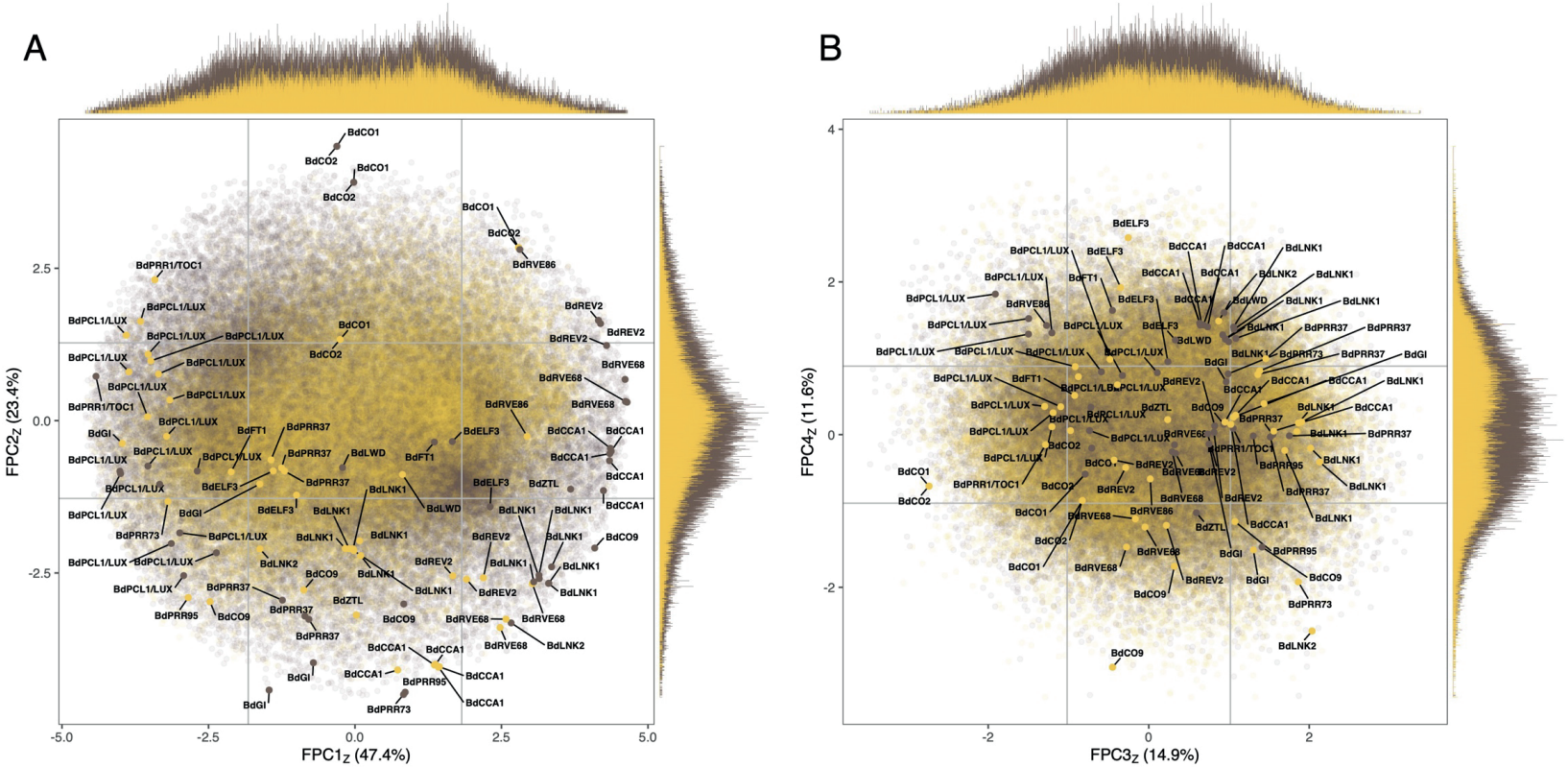
A
B
FPC2Z (23.4%)
FPC1Z (47.4%)
FPC4Z (11.6%)
FPC3Z (14.9%)
BdCO1
BdCO2
BdPRR1/TOC1
BdPCL1/LUX
BdREV2
BdRVE68
BdRVE86
BdGI
BdFT1
BdPRR37
BdELF3
BdLWD
BdCCA1
BdZTL
BdLNK1
BdLNK2
BdCO9
BdPRR73
BdPRR95

Figure 7

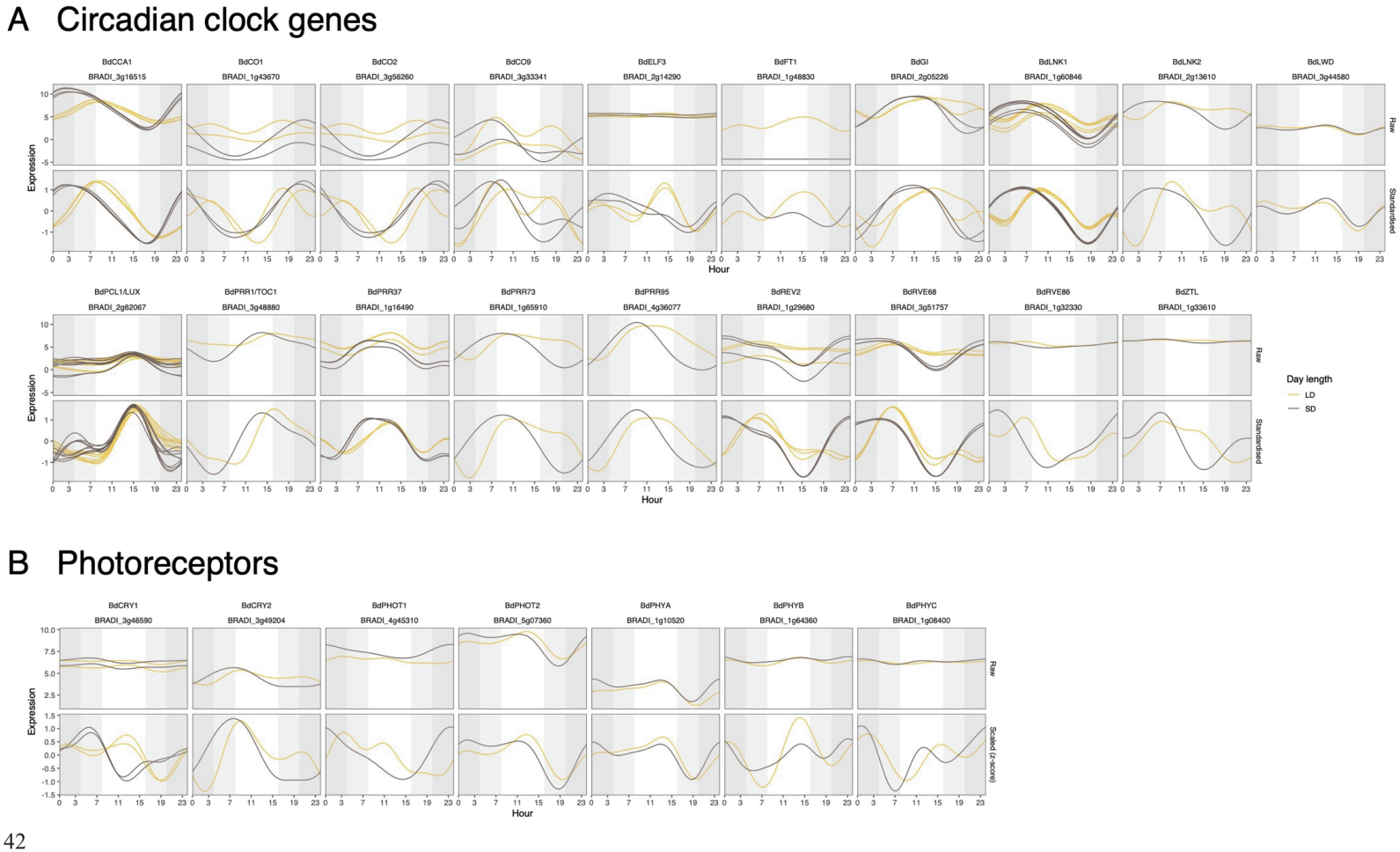
A Circadian clock genes
BdCCA1
BRADI_3g16515
BdCO1
BRADI_1g43670
BdCO2
BRADI_3g56260
BdCO9
BRADI_3g33341
BdELF3
BRADI_2g14290
BdFT1
BRADI_1g48830
BdGI
BRADI_2g05226
BdLNK1
BRADI_1g60846
BdLNK2
BRADI_2g13610
BdLWD
BRADI_3g44580
BdPCL1/LUX
BRADI_2g62067
BdPRR1/TOC1
BRADI_3g48880
BdPRR37
BRADI_1g16490
BdPRR73
BRADI_1g65910
BdPRR95
BRADI_4g36077
BdREV2
BRADI_1g29680
BdRVE68
BRADI_3g51757
BdRVE86
BRADI_1g32330
BdZTL
BRADI_1g33610
Expression
Hour
Raw
Standardised
Day length
LD
SD
B Photoreceptors
BdCRY1
BRADI_3g46590
BdCRY2
BRADI_3g49204
BdPHOT1
BRADI_4g45310
BdPHOT2
BRADI_5g07360
BdPHYA
BRADI_1g10520
BdPHYB
BRADI_1g64360
BdPHYC
BRADI_1g08400
Expression
Hour
Raw
Scaled (z-score)

1127 Table 1

1128

1129

Pre-specified groups of biological interest		Expected trajectories		Criteria based on functional principal component analysis of individually fitted transcript curves (raw or standardised curves), or difference curves (LDRaw - SD_{Raw})		
		Individual curves	Difference curves (LDRaw - SD_{Raw})	$FPCA_{Raw}$	$FPCA_Z$	$FPCA_D$
Group 1	*Similar level, no rhythm*	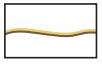		Similar $FPC1_{Raw}$ scores for LD and SD	Low $FPC1\text{-}4_Z$ scores for LD and SD	Low variance (curvature) in difference curve (lowest 5%)
Group 2	*Different level, no rhythm*	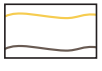	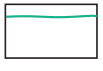	Different $FPC1_{Raw}$ scores for LD and SD	Low $FPC1\text{-}4_Z$ scores for LD and SD	
Group 3	*Similar level, similar rhythm*	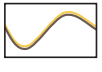		Similar $FPC1_{Raw}$ scores for LD and SD	Similar $FPC1\text{-}4_Z$ scores for LD and SD ***and*** Extreme FPC_Z scores for at least one component	
Group 4	*Different level, similar rhythm*	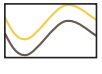	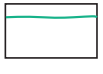	Different $FPC1_{Raw}$ scores for LD and SD	Similar $FPC1\text{-}4_Z$ scores for LD and SD ***and*** Extreme FPC_Z scores for at least one component	
Group 5	*Different rhythm (or lack thereof)*	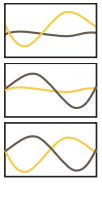	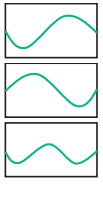	*Less relevant*	Extreme FPC_Z scores for LD and/or SD for at least one component	

Paper IV

Comparative transcriptomics of photoperiod-mediated flowering in temperate grasses

Paliocha M, Schubert M, Frøslie KF, Preston JC, Hvidsten TR & Fjellheim S

Manuscript, 2023

Comparative transcriptomics of daylength-mediated flowering in temperate grasses

Martin Paliocha[1], Marian Schubert[1], Kathrine Frey Frøslie[2], Jill Christine Preston[3], Torgeir R. Hvidsten[2], Siri Fjellheim[1,*]

ORCID-ID: 0000-0001-6717-1021 (M.P.), 0000-0001-7579-3832 (M.S.), 0000-0001-6097-2539 (T.R.H.), 0000-0003-4771-5495 (K.F.F), 0000-0002-9211-5061 (J.C.P), 0000-0003-1282-2733 (S.F.)

[1] Department of Plant Sciences, Faculty of Biosciences, Norwegian University of Life Sciences, N-1432 Ås, Norway

[2] Faculty of Chemistry, Biotechnology, and Food Science, Norwegian University of Life Sciences, N-1432 Ås, Norway

[3] Department of Plant Biology, College of Agriculture and Life Sciences, The University of Vermont, Burlington, VT 05405, United States of America

[*] Author for correspondence:

Professor Siri Fjellheim
Norwegian University of Life Sciences
P.O. Box 5003 NMBU
N-1432 Ås
Norway
e-mail: siri.fjellheim@nmbu.no

Abstract

Flowering time, a crucial adaptive trait influenced by various forces such as photoperiod, plays a pivotal role in the evolutionary trajectory of temperate grasses (Pooideae). Certain species in the ancestrally long-day (LD) responsive Pooideae tribe Stipeae have transitioned back to short-day (SD) responsive flowering in a clade that is now found in neotropical montane habitats. Considering the evolutionary significance of flowering time in habitat transition, our objective is to identify key differences within diurnal organisation of gene expression that may explain the evolution of opposite photoperiodic flowering strategies between closely related Pooideae species. Here, we take advantage of comparative transcriptomics and functional data analysis to investigate the temporal organisation of global gene expression in two closely related LD and SD plants, *Oloptum miliaceum* and *Nassella pubiflora* (Poaceae: Pooideae, tribe Stipeae). We identified candidate genes involved in the evolution of divergent photoperiodic flowering responses that possibly facilitate the transition from LD- to SD-flowering in Pooideae. Further, our findings indicate that the diurnal transcriptome undergoes substantial rewiring in response to daylength changes in both species. However, the differential expression between them was confined to a limited subset of annotated orthologous genes. Divergent gene expression between LD- and SD-flowering Stipeae was notably pronounced under SDs and involved floral integrators, light-signalling genes, and target genes of the circadian clock associated with flowering.

Introduction

Adequately timed flowering is crucial to ensure reproduction when environmental conditions are most favourable. In seasonally variable habitats, flowering is limited by periodical changes of the environment that are unfavourable to reproduction and survival. Under such conditions, daylength is the most reliable environmental cue. Many plants have therefore adopted flowering strategies that make use of photoperiod to pre-empt optimal conditions of flowering (Garner and Allard 1920, Murfet 1977, Bäurle and Dean 2006). In temperate habitats where growth and reproduction are confined to a relatively short growing season, increasing daylengths in spring trigger or significantly hasten flowering in long-day (LD) plants, such as *Arabidopsis thaliana* and barley (*Hordeum vulgare*). Conversely, flowering in tropical and sub-tropical plants is often accelerated when daylength falls below a certain threshold to ensure reproduction between the rainy and dry season, like in the short-day (SD) plants rice (*Oryza sativa*) and maize (*Zea mays*) (Colasanti and Coneva 2009). In the grass

family (Poaceae), radiations into temperate habitats are closely tied to the acquisition of adaptive traits to seasonal fluctuations of the environment like cold acclimation and frost tolerance (Humphreys and Linder 2013, Vigeland *et al.* 2013, Zhong *et al.* 2018, Schubert, Grønvold, *et al.* 2019), timely flowering triggered by prolonged periods of cold (vernalisation) (McKeown *et al.* 2016, Woods *et al.* 2016, Paliocha, Schubert, Preston, *et al.* 2023), and photoperiod (Fjellheim *et al.* 2022). Pooideae are the most dominant grass lineage in temperate zones (Hartley 1973, Schubert *et al.* 2020), and the prevailing understanding of their evolutionary trajectory suggests sequential gain of these key traits from an ancestral species likely exhibiting SD-flowering or day-neutrality (Preston and Fjellheim 2020). There is considerable support for a relatively early acquisition of temperate adaptations in Pooideae that predate or coincide with major diversification events during the Eocene–Oligocene cooling period and expansion of temperate habitats (Schubert, Marcussen, *et al.* 2019, Preston and Fjellheim 2020). Ancestral Pooideae swiftly adapted to these emerging niches at higher latitudes, as evidenced by the gain of LD-flowering which is inferred to have happened at the base of the subfamily (Preston and Fjellheim 2020, Fjellheim *et al.* 2022). However, a lineage in the early-diverging tribe Stipeae seems to have transitioned back from warm temperate to tropical montane habitats accompanied by the reversion to the ancestral SD-flowering strategy (Fjellheim *et al.* 2022). This is exemplified by the genus *Nassella* (needlegrasses) which is particularly diverse in South American highlands (Cialdella *et al.* 2014, Soreng *et al.* 2022), and inferred to primarily consist of SD-flowering species evolved from a LD-responsive ancestor (Fjellheim *et al.* 2022). This peculiar, lineage-specific reversal of photoperiodic flowering behaviour can partly be attributed to differential shifts in diurnal regulation of genes involved in the daylength-mediated flowering (Fjellheim *et al.* 2022).

The photoperiodic flowering pathway is tightly linked to endogenous cues produced by the circadian clock. Plants discern between LDs and SDs depending on whether light cues coincide with internal cycles generated by circadian oscillators, thereby periodically altering their sensitivity to periods of darkness and light (Johansson and Staiger 2014). The circadian clock is a complex regulatory network comprised of interlocking morning, central, and evening loops that peak during different times of the day and sustain rhythmic oscillations through mutual feed-back (Calixto *et al.* 2015, Creux and Harmer 2019). In *Arabidopsis*, the morning loop is comprised of CIRCADIAN CLOCK ASSOCIATED 1 (CCA1), LATE ELONGATED HYPOCOTYL (LHY) which repress *PSEUDO-RESPONSE REGULATOR*s (*PRR*s) such as *PRR9*, *PRR7*, and *PRR5*. These, in turn, are themselves repressors of *CCA1* and *LHY*, thus forming the morning feedback loop. Mutual repression between CCA1/LHY, TIMING OF

CAB EXPRESSION 1 (TOC1), and GIGANTEA (GI) forms the central loop. TOC1 represses the transcription of *GI* and components of the third feedback circuit peaking at dusk, the evening complex (EC), like *LUX ARRHYTMO* (*LUX* or *PHYTOCLOCK 1* (*PCL1*)), *EARLY FLOWERING 3* (ELF3), and *ELF4* (Covington *et al.* 2001, Helfer *et al.* 2011, Nusinow *et al.* 2011, Huang and Nusinow 2016). In synergy with external cues like temperature and photoperiod, the rhythms established by the circadian clock orchestrate the expression of a myriad of genes involved in an extensive array of developmental and metabolic processes (Hotta *et al.* 2007, Covington *et al.* 2008, Dalchau *et al.* 2010). Light signals are perceived by a system of photoreceptors like PHYTOCHROMEs and CRYPTOCHROMEs at the beginning of the photoperiodic flowering cascade (Lin 2000, Sanchez *et al.* 2020). These act as floral promotors or repressors in different species, depending on the configuration of the downstream signalling pathways they network with (Sanchez *et al.* 2020). Signalling components such as PHYTOCHROME INTERACTING PROTEINs (PIFs), and ZEITLUPE (ZTL) eventually convey daylength information into the oscillatory system, forming the basis of light entrainment and developmental responses to photoperiod. Due to its central role the core clock mechanism is remarkably conserved between LD and SD plants, implying that evolution of daylength-mediated flowering occurs through precise adjustments within a shared, ancestral pathway (Amasino and Michaels 2010, Andrés and Coupland 2012).

The main flowering signal produced by the *Arabidopsis* circadian clock is *CONSTANS* (*CO*) which is transcribed in a stable oscillatory pattern culminating during the second half of the day. CO is a floral activator fostering the expression of the *Arabidopsis* florigen *FLOWERING LOCUS T* (*FT*). As translation of *CO* mRNA is regulated by enzymatic complexes degraded in dark (Valverde *et al.* 2004), *FT* transcription is promoted only when late afternoon light and *CO* transcription coincide as it is the case under lengthening photoperiods. Diversity in the output layer of the photoperiodic flowering pathway is associated with plasticity of photoperiodic flowering responses in temperate grasses. Variation of grass orthologs of *AtCO* and their interactions with other members of the CCT (CO, CO-like, and TOC1; Strayer *et al.* 2000) domain gene family and PRRs have been identified as primary drivers of photoperiod responses in LD, SD, and day-neutral species (Mizuno and Nakamichi 2005, Brambilla and Fornara 2017, Liu *et al.* 2020). Central CCT domain genes fine-tuning flowering time include *PHOTOPERIOD 1* (*PPD1*) known as *PRR37* in rice, barley *CO1* and *CO2* and their orthologue in rice *HEADING DATE 1* (*HD1*), the paralogues *CO9* and *VERNALIZATION 2* (*VRN2*) and their rice orthologue *GRAIN NUMBER, PLANT HEIGHT, AND HEADING DATE 7 (GHD7)* (Trevaskis *et al.* 2006, Takahashi *et al.* 2009, Higgins *et al.*

2010, Kikuchi *et al.* 2011, Lu *et al.* 2012, Koo *et al.* 2013, Woods *et al.* 2016, Zheng *et al.* 2016, Zhang *et al.* 2017, Shaw *et al.* 2020). A key difference between LD- and SD-flowering grasses is how these genes interact with each other on the protein level (Preston and Fjellheim 2020). In the core-Pooideae cereal wheat (*Triticum aestivum*), VRN2 acts as a floral repressor by inhibiting the expression of *VRN3*/*FT1* through its interaction with NUCLEAR FACTOR-Y (NF-Y) protein complexes (Li *et al.* 2011). However, CO2 competes with VRN2 in this binding, thereby counteracting its repressive function (Li *et al.* 2011). This antagonistic interaction between VRN2 and CO2 introduces flexibility to the regulation of flowering in wheat depending on the relative abundance of their protein products (Li *et al.* 2011). Conversely, in rice, this relationship is reversed, as the VRN2 orthologue GHD7 alters the role of the functional rice CO-orthologue HD1a from a floral promotor to an indirect repressor of the rice *VRN3*/*FT1*-ortholog *HD3a* under LDs, thus delaying the flowering process under non-inductive daylengths (Okada *et al.* 2017, Herath 2019). Diversification of CCT domain genes is an important factor of flowering time in grasses and has been crucial for the domestication of major crops like barley, sorghum (*Sorghum bicolor*), and wheat (Cockram *et al.* 2012), and it is thus reasonable to posit that their role in enabling niche transitions in grasses is of equal importance on larger evolutionary scales.

Similar to the competitive binding of CCT domain genes is the formation of florigen activator complexes (FACs) and florigen repressor complexes (FRCs) at the shoot apex encompassing phosphatidylethanolamine-binding proteins (PEBPs) from the *FT/TFL1*-like gene family, known as *VERNALIZATION 3* (*VRN3*) or *FT1* in temperate grasses (Yan *et al.* 2006) and *HEADING DATE 3a* (*HD3a*) in rice. Analogously to phloem-mobile hormones, *FT/TFL1*-like genes are expressed in leaves, transported through the vascular system to the shoot apex where they deliver potent flowering signals (Conti and Bradley 2007, Jaeger and Wigge 2007, Zeevaart 2008). In the shoot apical meristem (SAM), FT1 forms a FAC with 14-3-3 and FD-like proteins (Li and Dubcovsky 2008, Lv *et al.* 2014), which ultimately alters the developmental faith of the meristem from vegetative to reproductive. Despite high sequence similarity, TFL1 antagonises the function of FT1 and represses floral meristem formation (Hanzawa *et al.* 2005, Danilevskaya *et al.* 2010, Hanano and Goto 2011). In rice, for instance, TFL1-like competes with the FT1 orthologue HD3a during the polymerisation of the florigen compound which leads to the assembly of FRCs mitigating the floral transition (Kaneko-Suzuki *et al.* 2018). Formation of such repressive transcription factor complexes involving VRN3/FT1-antagonising TFL1 proteins is a common mode of flowering regulation across Poaceae (Jensen *et al.* 2001, 2004, Ahn *et al.* 2006, Olsen *et al.* 2006, Kikuchi *et al.* 2009, Danilevskaya *et al.*

2010, Li *et al.* 2015, Brambilla *et al.* 2017, Bi *et al.* 2019, Giaume *et al.* 2023, Linhares-Neto *et al.* 2023). Noteworthy, *FT*/*TFL1*-like genes have significantly proliferated in monocots and have undergone a particularly dramatic expansion in grasses where at least 12 distinct *FT*-like lineages are reported (Chardon and Damerval 2005, Bennett and Dixon 2021). Although fundamentally conserved, grass *FT*/*TFL1*-like genes are strongly divergent relative to eudicot *FT*/*TFL1* orthologues, reflecting their versatility in the initiation and modulation of floral transition. Diversity and expansion of *FT*/*TFL1*-paralogues in grasses suggests strong evolutionary selection pressure towards diverse flowering responses through neofunctionalisation of these central developmental regulators (Bennett and Dixon 2021, Jin *et al.* 2021) that may form many different flowering promoting or repressing compounds depending on the current environmental context (Lv *et al.* 2014, Liu *et al.* 2020).

As such, there are several possible layers in which photoperiodic flowering can be fine-tuned to promote flowering under the most suitable conditions. This fine-tuning is often achieved through the precise coordination and coinciding diurnal expression of various components within the floral network. It can involve regulatory novelties in the photosensory system, adjustments to the circadian clock, or variations in clock output genes or floral integrators that act as either floral promotors or inhibitors (Sanchez *et al.* 2011, 2020). This intricate interplay allows for the dynamic modulation of flowering responses and ensures flowering adaptation to specific photoperiodic environments, thus facilitating the spread of temperate grass lineages into novel habitats (Preston and Fjellheim 2020). To delve deeper into this line of investigation, we examine whether diurnal expression shifts also occur at the whole-transcriptome level in two selected Stipeae species with opposing photoperiodic flowering strategies, namely *Oloptum miliaceum* and its SD-flowering relative *Nassella pubiflora* (Fjellheim *et al.* 2022). Our objective is to determine if shifts in diurnal gene regulation in response to photoperiod are a universal mode of adaptive flowering evolution in temperate grasses. Moreover, we aim to identify regulatory divergence of diurnally expressed genes involved in light-signalling, the circadian clock, and flower development to provide a more comprehensive understanding of the molecular basis of reversible flowering strategies associated with habitat transitions in Pooideae.

Materials and Methods

Plant Material

Seeds for the experiment were retrieved from the US National Plant Germplasm System (NPGS) via the Global Germplasm Resources Information Network (GRIN-Global). *Nassella*

pubiflora (Desvaux 1853) seeds (GRIN accession number PI 478575) were gathered in September 1981 in Puno, Peru on a field trial plot maintained by the Universidad Nacional del Altiplano de Puno at an altitude of 3835 m.a.s.l., with daytime fluctuating from 10:15–12:14 hrs (austral hibernal–austral estival solstice). *N. pubiflora* is a perennial, montane grass species with a native range from Ecuador to north-western Argentina (Barkworth and Torres 2001). *N. pubiflora* is a facultative SD plant (Fjellheim *et al.* 2022). Seeds of *Oloptum miliaceum* (Hamasha *et al.* 2012) (GRIN accession number PI 207772) collected at the Newe Ya'ar Research Centre, Agricultural Research Organization, Northern District, Israel in April 1953, which has an approximate annual daytime range from 9:56–14:15 hrs (boreal hibernal–boreal estival solstice). *O. miliaceum* (2n = 24, Romaschenko *et al.* 2012) is a subtropical grass with perennial life-history natively occurring in Macronesia, the Mediterranean, and middle East to Iran. *O. miliaceum* is a facultative LD plant (Fjellheim *et al.* 2022). Both study species belong to the early-diverging Pooideae tribe Stipeae that split from the remaining Pooideae ~59.6–48.99 mya, and started diversifying during the late Eocene, ~38.6–33.37 mya (Schubert, Marcussen, *et al.* 2019, Gallaher *et al.* 2022, Soreng *et al.* 2022). Both species are unresponsive to vernalisation (McKeown *et al.* 2016).

Growth Experiment and Sampling

Seeds were stratified in plastic foil-wrapped trays filled with moist soil under darkness at 4 °C for five days followed by one day at room temperature. Seed trays were then transferred to a greenhouse and germinated under LDs (16 h light : 8 h dark) at 17 °C. Individual seedlings were transferred to 7 × 7 × 7 cm pots filled with gardening soil (Gartnerjord, Tjerbo AS, Norway). After germination and four weeks of pre-growth, we randomly assigned plants to growth chambers with photoperiods simulating either LD (16 h light : 8 h dark) or SD (8 h light : 16 h dark). Both treatments were symmetrically aligned around noon. Light conditions were generated with ConstantColor CMH Tubular Clear high-intensity metal halide discharge lamps (CMH400/TT/UVC/U/830/E40, GE Lighting Kft., Hungary), providing an average photosynthetic photon flux density of 185 μmol × m^{-2} × s^{-1} at plant level. Red/far-red ratios were adjusted with incandescent light bulbs (AGL B22 60 W clear, NARVA Lichtquellen GmbH + Co. KG, Germany) to an average of 2.1–2.3 at plant height. To minimise room effects, we used two growth chambers per treatment, and moved plants to new positions twice a week. Plants were fertilised twice-weekly with water containing 4% YaraTera Kristalon Indigo and 3% YaraTera Calcinit (Yara Norge AS, Norway). Relative humidity and temperature in the growth chambers were kept constant and maintained at 50–55% and 17 °C, respectively.

Tissue of the longest, fully emerged leaf was harvested seven days after transfer to the growth chambers. We sampled four individual plants per species and treatment, starting at 03:00 h every 4th hour until 23:00 h, in total six time points per treatment. During the dark period, sampling was carried out under dim green light to minimise interference by photosynthetically active radiation. Leaf tissue was cut into 2 ml LoBind tubes (Eppendorf AG, Germany) and immediately flash-frozen in liquid nitrogen and stored at -80 °C until RNA purification. Plants were kept in growth chambers until the emergence of inflorescences (heading). Heading was registered daily until all plants had started to produce inflorescences, whereupon the growth experiment was terminated. Days to heading (DTH) were calculated from the germination date of the individual plants.

RNA Isolation, Library Preparation, and Sequencing

Frozen leaves were disrupted with 2 mm tungsten carbide beads in a TissueLyser ball mill (QIAGEN) under the constant supply of liquid nitrogen. Total RNA was isolated from frozen, finely ground tissue using the RNeasy Plant Mini Kit (QIAGEN), following the manufacturer's protocol. Residual DNA was removed with the Invitrogen TURBO DNA-free kit (ThermoFisher Scientific). Integrity, purity, and concentration of the RNA extracts was evaluated with an Invitrogen Qubit fluorometer (ThermoFisher Scientific), a NanoDrop 8000 spectrophotometer (ThermoFisher Scientific), and a 2100 Bioanalyzer (Agilent). Paired-end sequencing libraries with an average insert size of 350 bp were constructed with the TruSeq Stranded mRNA Library Prep kit (Illumina) for every individual sample. Library preparation and paired-end sequencing was carried out by the Norwegian Sequencing Centre (NSC) at the University of Oslo on an Illumina HiSeq 4000 system with 150-bp reads.

Transcriptome Assembly

Sequencing adapters and low-quality bases were removed with trimmomatic v0.39 (Bolger *et al.* 2014) using a 5-bp sliding-window. The lower phred-score cut-off was set to $Q = 20$, and the minimum read-length to 40 bp after evaluating the read quality with FastQC v0.11.9 (Andrews 2010). *De novo* transcriptomes were assembled with Trinity v2.8.4 (Grabherr *et al.* 2011, Haas *et al.* 2013) with default parameters. Benchmarking of Universal Single-Copy Orthologs (BUSCO) was carried out to evaluate the completeness and quality of the resulting transcriptome assemblies (Simão *et al.* 2015, Waterhouse *et al.* 2017) with OrthoDB v10 at Embryophyta level as reference (Kriventseva *et al.* 2019).

Phylogenetic placement of individual Trinity contigs was determined to remove putative contaminant sequences using blastn v2.10.1 (Altschul *et al.* 1990, Camacho *et al.* 2009) and NCBI's 'nt' database (NCBI Resource Coordinators 2017). Taxonomic information of the BLAST results was obtained with taxonomizr v0.6.0 (Sherrill-Mix 2019) for the hit with the lowest *E*-value. Contigs were removed from the assembly when phylum was other than 'Streptophyta' and superkingdom was other than 'Eukaryota', or unassigned. Furthermore, we removed fragments of ribosomal, mitochondrial and plastid transcripts by adding baits to the transcriptomes. We added chloroplast genomes of *B. distachyon* and *Phaenosperma globosa* (GenBank IDs: LT558588.1, KM974745.1), complete mitochondrial genomes of *H. vulgare spontaneum* and *O. sativa* (AP017300.1, JF281153.1) as well as ribosomal sequences from various non-plant species (MH047190.1, MH047190.1, AB250414.1, KT445934.2, JQ997495.1) to the transcriptomes. These sequences were downloaded from NCBI GenBank (Benson *et al.* 2013). All reads mapping uniquely to these baits were removed prior to read normalisation to reduce the influence of contaminant, plastid, organelle, and ribosomal RNA on the estimation of relative read counts.

Ortholog Inference

Orthologs were inferred with OrthoFinder v2.5.4 and IQ-TREE v2.2.0.3 (Emms and Kelly 2015, 2019, Minh *et al.* 2020). We used publicly available coding sequences and annotated genomes from *Hordeum vulgare* (IBSC_v2), *Aegilops tauschii* subsp. *strangulata* (Aet_v4.0), *Triticum urartu* (ASM34745v1), *Brachypodium distachyon* (Brachypodium_distachyon_v3.0), *Oryza sativa* var. *japonica* (IRGSP-1.0), and *O. sativa* var. *indica* (ASM465v1) to anchor orthologs from our study species. After sourcing the references from Ensembl Plants (Howe *et al.* 2020, Yates *et al.* 2020), we aligned the coding sequences to chromosome-level genome sequences with GMAP v2019-06-10 (Wu and Watanabe 2005). Redundant transcripts were merged and translated to amino acid sequences with GffRead v0.11.6 (Pertea and Pertea 2020). Transcripts without start- or stop-codons were discarded.

The resulting non-redundant proteomes of *H. vulgare*, *B. distachyon*, and *O. sativa* were used as references for functional annotation of *de novo*-transcripts with DIAMOND v0.9.22 (Buchfink *et al.* 2015). We also added the *de novo* transcriptome of the non-core Pooideae species *Melica ciliata* to increase phylogenetic resolution (Paliocha, Schubert, Hvidsten, *et al.* 2023). Frameshifts introduced to the *de novo*-transcripts during the transcriptome assembly with Trinity were identified using the strand information from the BLAST trace-back operation (BTOP) string (cf. Leder *et al.* 2021). Finally, amino acid sequences for *O. miliaceum*, *N.*

pubiflora, and *M. ciliata* were obtained with exonerate v2.2.0 (Slater and Birney 2005) and used for ortholog detection in OrthoFinder.

Generation of Expression Data

RNA-sequencing reads were aligned to the processed and cleaned *de novo* transcriptomes using Bowtie v2.4.1 (Langmead and Salzberg 2012), allowing for multimapping. Output files were processed, sorted, and compressed with SAMtools v1.11 (Li *et al.* 2009). Gene-level counts were obtained with Corset v1.07 (Davidson and Oshlack 2014), which combines reads mapping to multiple Trinity contigs based on sequence similarity and expression patterns into so-called 'clusters'. Initially, Corset was executed with a high -D parameter to enforce unambiguous mapping and target putative contaminant reads mapping exclusively to bait sequences. Subsequently, another run of Corset was performed with default -D values, allowing clustering of contigs sharing a significant number. We excluded reads mapping to chloroplast, mitochondrial, and ribosome baits during the first run and removed bait sequences alongside silent transcript clusters prior to downstream analysis.

Normalisation and Estimation of Expression Profiles

Read counts were normalised with the trimmed mean of M (TMM) method implemented in edgeR v3.36.0 (Robinson *et al.* 2010) after removal of transcripts with <100 counts per time point or <250 counts in total. Two faulty libraries in *N. pubiflora* were removed from the analysis at LD19 and SD19, resulting in $n = 2$ remaining samples for timepoint SD19 due to the loss of one sample during tissue disruption. Size of the remaining two *N. pubiflora* SD19 libraries varied considerably, ranging from 4,327,911 (sample N05) to 37,326,514 reads (sample N33). A much higher frequency of zero counts in sample N05 compared to the remaining replicate library led to the introduction of a prominent expression trough in *N. pubiflora* SD profiles at 19:00 h. To retain some level of variability and statistical power for comprehensive analysis in SD19, we decided to retain the N05 sample in the data set. Consequently, we excluded transcripts with zero counts in at least one biological replicate for each sampling time point from further analysis to avoid ambiguity between lowly expressed transcripts and technical artifacts. Normalisation factors were calculated after the removal of lowly expressed genes for each species × treatment × timepoint combination and normalised, $\log_2$-transformed counts per million reads ($\log_2$CPM) were calculated with edgeR. The expression at each time point was summarised by computing the mean. We then transformed the profile of each individual transcript to *z*-scores to enable interspecific comparison. This

transformation involved subtracting the mean expression of a transcript in a treatment and dividing by the treatment-wise standard deviation.

Assembly Thinning

To minimise redundancy of the transcriptomes, we merged transcripts in multi-copy orthologs by expression similarity. We computed pairwise Pearson correlation coefficients (ρ) of the smoothed expression profiles between orthologs with ≥2 transcripts per species. Orthologs with exactly two transcripts were summarised into a single mean profile per species and treatment if $\rho > 0.70$. For multi-copy orthologues with more than two transcripts, we performed hierarchical clustering of the expression profiles using Ward's clustering criterion and correlation distance ($1 - \rho$) as a measure (Ward 1963, Murtagh and Legendre 2014). The resulting dendrograms were cut at a height corresponding to $\rho = 0.70$, and expression profiles within the same group merged by calculating their mean. Thinning reduced the total number of available profiles in the LD and SD transcriptomes of *O. miliaceum* and *N. ciliata* from 75,357 to 53,000.

Functional Principal Component Analysis

Continuous expression curves were interpolated, smoothed, and evaluated at a 51-point grid spanning 24 h with a roughness penalty of $\lambda = 2.5$ determined with generalised cross-validation and manual inspection. Principal component weight functions were approximated through a 7-term Fourier series expansion assuming a 24-h period to emphasise diurnal oscillations. All statistical analyses were carried out in R v4.2.2 (R Core Team 2022), using the R package fda v6.0.5 (Ramsay *et al.* 2009, 2022) for curve approximation and functional data analyses. Functional principal components (FPCs) were estimated after a centring procedure involving the subtraction of the mean function from each individual gene expression curve to warrant normally distributed FPC scores with mean zero and unit variance.

Identification of Differential Diurnal Expression

The smoothed circadian expression profiles were treated as a sample of random functions and evaluated with functional principal components analysis (FPCA) to assess variation of temporal expression in response to photoperiod and identify genes with differential diurnal rhythms. Initially, we considered the LD and SD transcriptomes separately to characterise the most dominant modes of variance in diurnal gene expression in each species to investigate if the circadian transcriptomes of *N. pubiflora* and *O. miliaceum* could be decomposed in a similar manner. Next, we combined the LD and SD transcriptomes of our study species and ran joint FPCAs with the goal of identifying genes with different diurnal expression across species

348 within each treatment. All FPCAs incorporated a centring procedure to ensure that the FPC
349 scores adhered to standard normal distributions. Hence, FPC scores provided a consistent and
350 comparable measure of temporal variation that we used as indicative measure for circadian
351 rhythmicity across species. We opted to incorporate the FPCs that accounted for up to 95% of
352 the total variance (FPC1–4 in LD and SD).

353 To efficiently combine the features captured by the first four FPCs, we computed the
354 Mahalanobis (1936) distance (D^2) derived from the scores distributions of FPC1–4 and used it
355 as a proxy measure for circadian rhythmicity (Supplementary Fig. S1). D^2 is essentially the
356 squared sum of FPC scores and can be approximated by a χ^2-distribution with four degrees of
357 freedom (corresponding to the number of FPCs used as input; cf. Leemis 1986) and provides a
358 statistically robust measure for the distance from the centre of a multivariate PC score
359 distribution (Brereton 2015). In the context of FPCA, centrality of a FPC score can be
360 understood as the deviance of the corresponding expression curve from the mean expression
361 curve along the main direction of change identified by the respective FPC. To detect rhythmic
362 transcripts, we focused on the upper 10% of the D^2-distribution. Orthologous transcripts falling
363 within this top decile for both species were deemed to display significant circadian variation.
364 To pinpoint transcripts with different rhythmic profiles that have diverged between species
365 within the same photoperiod, we computed pairwise differences between FPC1–4 scores of all
366 transcripts from the same orthogroup. We applied the same procedure as above on the standard
367 normal distribution of the FPC score differences (*Nassella* - *Oloptum*) to detect differential
368 time-dependency between orthologous LD and SD transcripts in *O. miliaceum* and *N. pubiflora*.
369 Intersecting the resulting lists of rhythmic and different transcripts yielded orthologous gene
370 pairs with differential circadian expression. These were used in subsequent analyses to detect
371 candidate genes linked to photoperiodic flowering.

372 **Circadian marker genes**

373 We used a pre-defined set of circadian marker genes to demonstrate the efficacy of our
374 analytical approach and provide an instructive example of diurnal expression dynamics of
375 central developmental pathways in closely related LD and SD species. This gene set comprised
376 photoreceptors, circadian clock genes from the morning- and evening-loop as well as
377 transcription factors involved in photoperiodic flowering characterised in different model and
378 crop species.

379 **Candidate gene identification**

380 Orthologs with differential circadian gene expression between *N. pubiflora* and *O. miliaceum*
381 were classified by hierarchical clustering using Ward's method (Ward 1963, Murtagh and
382 Legendre 2014) with the distance correlation matrix (1 - ρ) of LD and SD profiles as input.
383 Hierarchical cluster dendrograms were cut with dynamicTreeCut v1.63-1 (Langfelder *et al.*
384 2007). The resulting clusters were tested for enrichment of biological processes using slimmed,
385 plant-specific gene ontology (GO) terms (Gene Ontology Consortium 2004). GO slim
386 annotations for the reference species were downloaded Ensembl Plants using biomaRt v2.52.0
387 (Durinck *et al.* 2005, Howe *et al.* 2021). Enrichment tests were carried out using the weighted
388 Fisher's exact test implemented in topGO v2.48.0 using all expressed genes annotated in the *de*
389 *novo* transcriptomes as background (Fisher 1922, Alexa *et al.* 2006). The cut-off for false
390 discovery rate (FDR) corrected *P* values was set to 0.05. Heatmaps were generated with
391 complexHeatmap v2.13.1 (Gu *et al.* 2016).

392 Results

393 **Presence of opposite flowering strategies in Stipeae**

394 Comparative analysis of flowering time (DTH) confirmed the presence of differential
395 photoperiodic flowering responses in our study species (Fig. 1). While the commencement of
396 reproductive growth was not obligatory restricted to a specific photoperiod in neither *O.*
397 *miliaceum* nor *N. pubiflora*, we detected significant differences in the timing of inflorescence
398 emergence. Individuals of *O. miliaceum* exposed to LD flowered on average significantly
399 earlier compared to plants under SD conditions, with DTH 57.6 ± 0.66 (mean ± SE) in LD, and
400 82.4 ± 2.21 in SD. Instead, flowering in *N. pubiflora* was promoted by SDs with DTH ranging
401 from 80.0 ± 0.64 in SD to 92.8 ± 0.97 in LD. Opposite photoperiodic flowering responses in
402 *Nassella* and *Oloptum* align with previous results on flowering time (Fjellheim *et al.* 2022),
403 validating the presence of distinct adaptive strategies for optimal reproduction in response to
404 different daylengths in the early-diverging Pooideae tribe Stipeae.

405 **Differential effects of long and short days gene regulation**

406 Whole-transcriptome FPCA captured the most essential temporal features of global gene
407 expression in *N. pubiflora* and *O. miliaceum*. Across both species and photoperiods, four FPCs
408 captured >95% of the cumulative variance in the data. The first two components revealed
409 distinct expression peaks and troughs under contrasting photoperiods, while FPC3 and FPC4
410 captured less deterministic diurnal perturbations throughout the day. Notably, features

411 identified in SD showed greater similarity between species compared to LD, which displayed
412 more species-specific patterns.

413 In *Nassella* plants exposed to SD, FPC1 captured patterns of peak and trough expression
414 during dawn and dusk interspersed by sign changes near 11:00 h, accounting for 41.3% of the
415 cumulative variance in the LD data (Fig. 2A). This pattern was complemented by FPC2
416 (36.5%), which identified expression peaks and troughs centred around 11:00 h and mid-night
417 (Fig. 2A). Less conspicuous perturbations of *N. pubiflora* LD expression were covered by FPC3
418 (16.6%) and FPC4 (10.2%). Similar dynamics were apparent under SDs (Fig. 2B), with slightly
419 more evenly distributed explained variance between the first two components. FPC1 (39.5%)
420 contrasted curves with expression peaks and troughs centred around noon and the late dark
421 period located at 03:00 h. The second FPC explained (36.5%) of the SD variance in *Nassella*
422 and contrasted transcripts with peaks/troughs aligned with dusk and dawn (Fig. 2B), indicating
423 the importance of dark/light transitions for diurnal gene regulation. Minor deviances from the
424 SD mean expression were explained by FPC3 (12.9%) and FPC4 (8.8%) and contributed
425 slightly less to the total temporal variation than the corresponding components in LD (Fig. 2B).

426 In *Oloptum*, the first two FPCs in LD identified through and peak expression centred
427 around 15:00 h (FPC1, 36.9%) and 07:00 h (FPC2, 38.2%), respectively (Fig. 3A). Both
428 components also accounted for peak/troughs during the dark period. FPC1 identifies symmetric
429 profiles with more evenly spaced light and dark extremes than FPC2, with less pronounced
430 changes in the former from 15:00 h to 03:00 h. The remaining two FPCs in *O. miliaceum* LD
431 accounted for 11.8% and 8.6% of the summative temporal variance and identified minor
432 perturbations during dawn and dusk (FPC3) and the dark phase (FPC4). Short-day expression
433 in *O. miliaceum* was distinguished by prominent expression peaks troughs during the late dark
434 phase (07:00 h), followed by sign changes centred around noon and expression culminating
435 into wider and more attenuated peaks and troughs from the onset of the dark period (FPC1, Fig.
436 3B). Oscillations identified by FPC1 accounted for almost half of the total variance in *O.*
437 *miliaceum* SD expression curves (46.7%). The second FPC (35.4%) contrasted SD profiles with
438 more symmetric expression with peaks and troughs centred around 11:00 h and 03:00 h, and
439 sign changes coinciding with dark–light transition. Variance captured by FPC3 (8.8%) and
440 FPC4 (7.1%) was caused by minor fluctuations (Fig. 3B).

441 **Global and circadian clock gene expression in *Nassella* and *Oloptum***

442 Combined *N. pubiflora* and *O. miliaceum* FPCAs identified comparable modes of temporal
443 variation in the LD and SD data, as evidenced by the consistent loadings and contributions of

444 FPC1–4 across both treatments (Fig. 4B, D). The first two FPCs accounted for most of the
445 cumulative variance, jointly explaining 73.5% (LD) and 77.4% (SD). Transcripts with
446 peak/trough expression around 07:00 h and 15:00 h, and directional changes at 11:00 h were
447 contrasted by FPC1 under both photoperiods. Conversely, FPC2 seized variation introduced
448 through peaks/troughs during the light (~11:00 h) and dark period (~02:00 h). The last two
449 components (FPC3–4) identified minor diurnal oscillations in both photoperiods.

450 Genes exhibiting oscillating expression profiles that align with the primary features
451 delineated by the FPC functions were characterised by high or low scores on one of the initial
452 four FPCs. As such, orthologs of circadian marker genes mostly accumulated in the tails of the
453 LD and SD scores distributions (Fig. 4A, C), resulting in high D^2 values (Supplementary Fig.
454 S). Expression profiles of these genes further validated the suitability of our approach for
455 detecting diurnal oscillations (Fig. 5A). We observed stable diurnal gene expression in
456 numerous orthologous circadian clock components such as *CO1*/*2*, *GI*, *TOC1*/*PRR1*, and
457 *PRR73* (Fig. 5B) under both photoperiods, indicative of high degree of conservation between
458 the photoperiodic entrainment of circadian clock genes in *Nassella* and *Oloptum*. Noteworthy
459 exceptions were the morning-loop genes *CCA1* and *RVE68*, and the evening complex
460 constituents *ELF3* and *PCL1*/*LUX* with mismatched expression between species under LD and
461 SD. Although diurnal variation in *OmCCA1* and *LUX* expression was almost identical in both
462 treatments, expression of *OmLUX* and *OmCCA1* were shifted in phase, with a noticeable ~2–3
463 h lag relative to *Nassella* (Fig. 5B). The CCT domain transcription factor *PPD1* pointed out as
464 instrumental to the evolution of variable flowering strategies in Stipeae (Fjellheim *et al.* 2022)
465 reached peak expression at 7:00 and 17:00 under both photoperiods (Fig. 5C).

466 When the diurnal expression profiles of rhythmically expressed genes varied between
467 species, orthologous gene pairs accumulated scores at opposing ends of the FPC score
468 distributions (Fig. 5A). Such regulatory divergence was most noticeable between orthologues
469 known to confer light signals such as *CRY1*, *PHOT1*, *PHYC*, and *ZTL* with markedly altered
470 profiles across species (Fig. 5B). Diurnal expression of *PHOT1*, for instance, exhibited a phase
471 shift between *Oloptum* and *Nassella* under LD, whereas up- and down-regulations occurred at
472 similar time points in SD, although with mismatched trough expression during the late dark
473 phase (Fig. 5B). In the case PHYC, we noticed a trough in *Nassella* LD around 19 h under LD
474 that was absent in *OmPHYC*. Comparably, *NpPHYB* had a trough in the early SD dark phase
475 that lacked in *OmPHYB* (Fig. 5B).

476 **Light-signalling and flowering genes are most divergently expressed**

To isolate interspecific shifts in LD and SD gene expression, we estimated the main modes of diurnal variance using FPCA in the combined LD and SD transcriptomes of *N. pubiflora* and *O. miliaceum*. Information captured by the FPCs allowed us to isolate the most divergently expressed genes between species. While altered photoperiod caused considerable rewiring of the circadian transcriptome in both species, differential interspecific expression shifts were limited to only a small subset of the annotated orthologues.

Under LD, expression of diurnally expressed genes seemed to be more coordinated in *Nassella*, with peak and trough expression preferentially tethered to dark/light transitions (Fig. 6A). In contrast, *O. miliaceum* displayed less coordinated regulation under LDs with most of the diurnal variation caused by minor perturbations (Fig. 6A). Clustering and enrichment analyses of LD-divergent genes revealed association with metabolic and response processes (Fig. 6A).

Diurnal oscillations under SDs, however, appeared to play a more substantial role in differential regulation of developmental processes that could potentially underlie the observed variations in flowering phenotypes between the two species (Fig. 6B). Furthermore, the expression patterns in SD displayed more prominent peaks and troughs, suggesting a higher degree of coordination in gene expression in both species (Fig. 6B). Divergent timing of these expression peaks and troughs, however, suggest that differential phasing may the predominant mode of gene expression evolution under SD conditions. We found in total eight orthologous genes associated with 'flowering development', nine orthologues associated with 'response to light stimulus' as well as one circadian clock gene (*ELF3*) among the orthologues expressed genes in SD (Fig. 6C; Tab. 2). Remarkably, ELF3 was the only core circadian clock gene defined *a priori* that emerged as a potential candidate through our analysis. Transcription profiles of candidate genes with putative effects on photoperiodic flowering evolution are more thoroughly discussed in the next section.

Table 1: Number of *Nassella pubiflora* and *Oloptum miliaceum* orthologues (transcripts) deemed to be rhythmically expressed, have sufficiently diverged expression patterns between species, and both, diurnally expressed (rhythmic) and divergent between species. Orthologues with divergent diurnal control visualised in Fig. 6.

Photoperiod	Species	Rhythmic	Divergent	Both
LD	*Nassella pubiflora*	1,079 (1,099)	670 (694)	300
	Oloptum miliaceum	1,072 (1,090)		
SD	*Nassella pubiflora*	975 (993)	590 (630)	257
	Oloptum miliaceum	1,031 (1,049)		

507 # Discussion

508 The transition of Pooideae grasses from tropical to northern temperate climates (Gallaher *et al.*
509 2019, Schubert, Marcussen, *et al.* 2019) likely required the evolution of multiple traits, some
510 of which influence the timing of phenological events such as flowering (Preston and Fjellheim
511 2020). It was previously demonstrated that vernalisation-based flowering competency and LD
512 flowering induction evolved early in the evolutionary history of Pooideae, consistent with these
513 being key traits underlying the tropical to temperate niche transition (Heide 1994, McKeown *et*
514 *al.* 2016, Woods *et al.* 2016, Fjellheim *et al.* 2022). Since then, vernalisation responsiveness
515 and LD-flowering have been lost repeatedly following both natural and artificial selection
516 (Trevaskis *et al.* 2007, King and Heide 2009, Fjellheim *et al.* 2014). In the case of flowering
517 induction by LDs, most losses have involved the evolution of day-neutral flowering, with a
518 single inferred reversion back to SD-flowering in or before the origin of low latitude-tropical
519 montane *Nassella* (Fjellheim *et al.* 2022). Comparative analyses between SD-flowering *N.*
520 *pubiflora* and its close LD-flowering relative, *O. miliaceum* indicate that the LD- to SD-
521 flowering reversal occurred via modifications in the diurnal expression cycle of genes in the
522 CCT domain family (Fjellheim *et al.* 2022). To find other candidate genes involved in this trait
523 shift, we compared diurnal gene expression cycles across the two species and discuss the results
524 here.

525 **Stipeae are a promising system for the study of photoperiodic flowering strategies**

526 Despite having diverged ~20–25 Mya (Schubert, Marcussen, *et al.* 2019, Gallaher *et al.* 2022),
527 diurnal gene regulation is remarkably conserved between SD-flowering *N. pubiflora* and LD-
528 flowering *O. miliaceum*. Most genes exhibited the same fundamental pattern of diurnal
529 oscillations in both species. Under both LD and SDs, peak/trough expression was centred
530 around the middle of the dark and light periods and transitions between light and dark. These
531 predominant patterns explained the same variance in gene expression across *Nassella* and
532 *Oloptum*, indicating comparable contribution of these major diurnal oscillations to circadian
533 gene expression under LDs and SDs (Fig. 3–4). Across the plant kingdom, comparative diurnal
534 transcriptome analyses have revealed conserved, overarching expression dynamics, even
535 among photosynthetic eukaryotes exhibiting diverse morphology, life-cycles, and
536 photoperiodic adaptations (Ferrari *et al.* 2019). This parallels observations in our focal Stipeae
537 species, where most of the diurnal gene expression was conserved, with only 300 and 257
538 divergently expressed transcripts identified under LD and SD, respectively.

539 Interspecific differences manifested through unique lengths or timings of peak and
540 trough expression that are likely caused by differential responses to changes in photoperiod
541 (Fig. 6A, C). In fact, divergent selection by contrasting diurnally-varying environments is
542 known to generate diversity in the onset and offset of biological processes across terrestrial
543 plants (Filichkin *et al.* 2011, de los Reyes *et al.* 2017, Serrano-Bueno *et al.* 2017). For example,
544 temporal partitioning of metabolism and growth is greatly influenced by photocycles
545 (Covington *et al.* 2008, Michael *et al.* 2008), with even closely related species exhibiting time-
546 rewiring of fundamental mechanisms like photosynthesis (Jiang *et al.* 2023). This pattern is
547 also evident in *N. pubiflora* and *O. miliaceum*, indicating that Stipeae grasses provide an ideal
548 study system for investigating the evolutionary adaptations to photoperiods due to their
549 remarkable conservation of diurnal gene expression and response to contrasting daylengths,
550 with the few differences linked to crucial adaptive processes.

551 Regulatory divergence of basic processes is evident from the prevalence of GO terms
552 related to metabolism (LD, Fig. 6A) and development (SD, Fig. 6B) among the most
553 divergently expressed genes in our study. This is illustrated by severe differential regulation of
554 the photosynthesis genes *LIGHT-HARVESTING COMPLEX* (*LHC*) *A4* and *LHCB7* (Wang *et*
555 *al.* 1997, Harmer *et al.* 2000) between *Nassella* and *Oloptum* under SDs and LDs, and
556 transcriptional divergence of genes related to metabolic processes in LDs (Fig. 6A).
557 Furthermore, we observed greater divergence between the transcriptional profiles of genes
558 involved in developmental processes related to flowering in the SD-divergent compared to the
559 LD-divergent gene set (Fig. 6B). This suggests an asymmetry in the transcriptional remodelling
560 of floral regulatory networks, with more pervasive changes under SDs. Given that *N. pubiflora*
561 and *O. miliaceum* have comparable life-history strategies (perennial) and growth habits
562 (tussock-forming), divergent expression under SDs indicates that these regulatory alterations
563 might be a consequence of adaptation to SDs from an ancestral LD-flowering state in an
564 ancestor of *N. pubiflora*. This aligns with the proposed evolutionary history of the genus
565 *Nassella*, which is thought to have originated from a LD-flowering ancestor (Preston and
566 Fjellheim 2020, Fjellheim *et al.* 2022).

567 **Photoperiod signal processing is largely conserved, but perception and integration seem**
568 **to have diverged**

569 Floral induction by photoperiodic cues involves a series of sequential events, starting with the
570 perception of light signals by photoreceptors. These cues are then relayed to and processed by
571 the circadian clock, leading to the activation of floral integrators. Ultimately, the expression of

572 specific genes responsible for modulating meristem identity is triggered, resulting in the
573 initiation of flowering (Cao *et al.* 2021). We observed a largely conserved systemic response
574 of circadian clock genes to daylength signals between *O. miliaceum* and *N. pubiflora* (Fig. 5).
575 This suggests that reversion to SD-flowering in *Nassella* happened via reprogramming of the
576 photosensory system or specific flowering-time genes outside the endogenous time-keeping
577 system rather than the core circadian circuitry itself. This is supported by the occurrence of
578 light-signalling genes such as *LIGHT-INDUCED, RICE 1* (*LIR1*), *ULTRAVIOLET*
579 *RESISTANCE LOCUS 8* (*UVR8*), and the PHYB-interacting factor *VASCULAR PLANT ONE-*
580 *ZINC FINGER 1* (*VOZ1*) among the orthologues exhibiting the most species-specific SD
581 expression (Table 1, Fig. 5). It is reported that at least *LIR1* and *VOZ1* play minor, but
582 significant roles in promoting of non-reproductive growth in *Lolium perenne* and stabilising
583 CO in *Arabidopsis*, respectively (Ciannamea *et al.* 2007, Yasui *et al.* 2012, Kumar *et al.* 2018).
584 While *UVR8* is not directly implicated in the floral transition, its involvement in UV-B-induced
585 photomorphogenesis and the observed species-specific expression patterns further strengthens
586 the hypothesis that light perception happens through different mechanisms in *Nassella* and
587 *Oloptum* (Favory *et al.* 2009, Chen *et al.* 2023). Additional means of differential integration of
588 photoperiod signals between our study species may include distinct regulation of chromatin
589 structure and post-transcriptional modifications, as evidenced by the species-specific
590 expression of the histone methyltransferase gene *JUMONJI 706* (*JMJ706*) (Sun and Zhou
591 2008), and *SUPPRESSOR OF GENE SILENCING 3* (*SGS3*) involved in post-translational gene
592 silencing under LDs and SDs, respectively (Peragine *et al.* 2004).

593 **Divergent regulation of floral integrators**

594 Due to the pivotal role of *FLOWERING LOCUS T* (*FT*) and *CENTRORADIALIS*/*TERMINAL*
595 *FLOWER 1* (*CEN*/*TFL1*) genes in the floral transition, their identification as possible
596 determinants of reversible photoperiodic flowering behaviour deserves particular attention.
597 *FT*/*TFL1*-like genes, represented by *CEN*/*TFL1* in our species, play a crucial role in floral
598 transition and are important determinants of flowering behaviour (Shannon and Meeks-Wagner
599 1991, Bradley *et al.* 1996, Pnueli *et al.* 1998, Banfield and Brady 2000, Comadran *et al.* 2012,
600 Li *et al.* 2015, Bi *et al.* 2019, Périlleux *et al.* 2019). While CEN/TFL1 acts as a floral repressor,
601 antagonising the function of its close homologue FT1 in many species, its role in grasses is
602 more versatile and context-dependent. In rice, for instance, CEN/TFL1-like competes with the
603 FT1 orthologue HEADING DATE 3a (HD3a) during the polymerisation of the florigen
604 compound which leads to the assembly of FRCs mitigating the floral transition (Kaneko-Suzuki

605 *et al.* 2018). Cereal *CEN*/*TFL1* genes are well-characterised, and allelic variation in *CEN*/*TFL1*
606 loci is known to fine-tune phenological adaptation along latitudinal daylength clines in both
607 rice and barley (Fernández-Calleja *et al.* 2021, Zhou *et al.* 2021). Interestingly, the role of
608 CEN/TFL1 as a floral repressor is not universally conserved in grasses, as observed in the case
609 of the *Chionochloa pallens* (Danthonioideae), where flowering is promoted by *CpCEN*/*TFL1*
610 in response to specific endogenous signals (Samarth *et al.* 2022). In case of Stipeae, regulatory
611 divergence of *CEN*/*TFL1* was most pronounced under SDs. Although FT/TFL1-like primarily
612 regulate flowering through successive accumulation at the SAM (Corbesier *et al.* 2007, Faure
613 *et al.* 2007, Gauley and Boden 2020), *FT/TFL1*-like expression follows the diurnal oscillations
614 of their regulators (e.g., Kikuchi *et al.* 2009). Thus, the intriguing SD expression pattern of
615 *NpCEN*/*TFL1*, characterised by a trough coinciding with the onset of the light period and
616 gradually increasing expression throughout the day, indicates its responsiveness to SDs in
617 *Nassella*. Conversely, its ortholog in *O. miliaceum* did not exhibit a tightly coupled response to
618 alternating light and dark periods. This suggests that *NpCEN*/*TFL1* functions distinctly from its
619 *O. miliaceum* counterpart under SDs, making it a potential candidate responsible for SD-
620 flowering in *Nassella*. Due to their close ties to photoperiod, early flowering, and their emerging
621 role as a flowering promoters, it is tempting to conclude that functional and regulatory
622 diversification of *CEN*/*TFL1* genes have been important for the photoperiodic calibration of
623 flowering time (Gaudinier and Blackman 2020), thereby aiding range expansions in wild
624 Pooideae. Interactions between *CEN*/*TFL1* and other rhythmically expressed genes transmitting
625 photoperiodic signals deserves further attention to elucidate their capacity to foster promote
626 shifts between LD, SD, and day-neutral flowering.

627 In addition to *CEN*/*TFL1* genes, we detected species-specific regulatory patterns of
628 flowering genes known to be upstream of *VRN3*/*FT*, possibly contributing to the generation of
629 the observed opposite photoperiodic flowering responses. For instance, *ELF3*, a central
630 constituent of the evening complex in the circadian clock, acts as a gatekeeper of light-
631 dependent flowering and is involved in transmitting photoperiodic cues into the flowering
632 pathway (Huang *et al.* 2017, Woods *et al.* 2019, 2023, Anwer *et al.* 2020, Müller *et al.* 2020,
633 Bouché *et al.* 2022, Alvarez *et al.* 2023, Wittern *et al.* 2023). It interacts with PPD1, the primary
634 target of ELF3-mediated flowering repression (Woods *et al.* 2023). Although directly
635 repressing *PPD1* transcription (Gao *et al.* 2019, Andrade *et al.* 2022, Alvarez *et al.* 2023), ELF3
636 has no known DNA-binding activity and likely acts via PCL1/LUX transcription factors that
637 can recognise *cis*-regulatory motifs in the *PPD1* promoter (Woods *et al.* 2019, 2023). The
638 simultaneous downregulation of PPD1 and peak expression of *ELF3* and *PCL1*/*LUX* in both of

our focal species supports this model. However, transcriptional deactivation of *OmPPD1* is less pronounced than anticipated, suggesting that the prolonged and shifted peaks in *OmELF3* and *OmPCL1/LUX* expression attenuate *OmPPD1* transcription far into the light period. However, considering the substantial impact of non-functional *ppd1* alleles on the timing of *CO1* and *CO2* expression in barley (Turner *et al.* 2005), and the absence of differential timing of *CO1/2* between our focal species, the aberrant *OmPPD1* pattern should be verified to rule-out technical artifacts due to low gene expression and read-count normalisation filtering in *O. miliaceum* (Gao *et al.* 2019, Woods *et al.* 2019, 2023, Andrade *et al.* 2022, Alvarez *et al.* 2023).

Another interesting candidate warranting further investigation is *EARLY HEADING DATE 3* (*EHD3*), a grass-specific transcription factor (Zhang and Yuan 2014) and part of the flowering pathway unique to rice. Notably, under SDs, *NpEHD3* and *NpCEN/TFL1* demonstrate markedly opposing expression patterns. The unique peak/trough expression that differentiates *NpCEN/TFL1* in LDs versus SDs coincides with the lowest point of *NpCO1/2* expression. This pattern suggests a potential connection between *EHD3* and *CEN/TFL1*, possibly through an undiscovered regulatory mechanism involving *OsHD1* orthologues *CO1* and *CO2*. Similar to *N. pubiflora*, rice is a facultative SD plant that experiences accelerated flowering under SDs but also flowers under LD, albeit significantly later (Brambilla and Fornara 2013). In rice, *EHD3* is part of the alternative regulatory pathway supporting flowering under LDs where it acts as the transcriptional repressor of *GHD7*. Contrary to the Pooideae orthologue VRN2, GHD7 does not directly repress transcription of the rice *FT1* orthologue *HD3a*. Rather, GHD7 acts via repression of the B-type response regulator *EARLY HEADING DATE 1* (*EHD1*) which promotes *HD3a* expression (Doi *et al.* 2004, Zhao *et al.* 2015). The function of *EHD1* is exclusive to rice and it does not appear to have any immediate, functionally conserved orthologues in Pooideae (Vicentini *et al.* 2023). Rice *EHD3* triggers flowering through the downregulation of the floral repressor *GHD7* and upregulation of *EHD1* (Matsubara *et al.* 2011). Although *EHD3* orthologues are present in *B. distachyon* and our study species, their functions have not yet been characterised due to the absence of their main target gene in Pooideae. Interestingly, there is an indirect link between *EHD3* and rice *CEN/TFL1* (*RCN*). In rice plants with a non-functional *HD1a* (orthologue of Pooideae *CO1/2*) and non-functional *EHD1*, expression of rice *CEN/TFL1* orthologues *RCN1* and *RCN2* was significantly elevated, although this was tested only after floral transition (Endo-Higashi and Izawa 2011). This suggests the presence of a regulatory module involving *EHD3* and *CEN/TFL1*-like florigen antagonists awaiting further characterisation.

Conclusions

In this study, we use a well-established statistical framework in a novel context and highlight its feasibility for the detection of rhythmically divergent gene expression in whole-transcriptome data across species and photoperiods. FPCA is a convenient tool for dimensionality reduction of large, time-dependent gene expression data sets and can condense complex temporal regulatory processes into variables with direct biological interpretability. Using this approach, our data support strong conservation of core circadian clock gene expression, even between species with opposite flowering behaviours. We find notable interspecific shifts in the diurnal expression patterns of at least three major flowering genes and several photoreceptors. Collectively, these findings demonstrate that the evolution of flowering time is intimately tied to shifts in diurnal expression of relatively few, but central genes that convey daylength cues into important developmental pathways.

Author Contributions

S.F. conceived and designed the experiment; M.P. conducted the growth experiment, isolated RNA, assembled and annotated the transcriptomes with input from M.S. and T.R.H.; M.P. carried out statistical analyses with help from T.R.H., M.S., S.F., and K.F.F.; S.F. received the funding; M.P. interpreted the results with input from S.F. and J.C.P.; M.P. wrote the paper with input from all authors.

Funding

The work carried out in this study was part a PhD project funded by the Faculty of Biosciences (BIOVIT) at the Norwegian University of Life Sciences (NMBU). Growth experiments and RNA-sequencing were funded by the Norwegian Research Council (grant number 231009 to Siri Fjellheim).

Acknowledgements

We thank Ane Charlotte Hjertaas and Øyvind Jørgensen for plant care and assistance during the growth experiment, Erica Helen Leder for provision of scripts for the annotation pipeline, and Camilla Lorange Lindberg, Felix Hernandez Nohr and Akhil Reddy Pashapu for helpful discussions. Computational analyses were performed on the Orion high-performance computing cluster at the Norwegian University of Life Sciences (NMBU).

References

Ahn, J.H., Miller, D., Winter, V.J., Banfield, M.J., Lee, J.H., Yoo, S.Y., Henz, S.R., Brady, R.L., and Weigel, D., 2006. A divergent external loop confers antagonistic activity on floral regulators FT and TFL1. *The EMBO Journal*, 25 (3), 605–614.

Alexa, A., Rahnenführer, J., and Lengauer, T., 2006. Improved scoring of functional groups from gene expression data by decorrelating GO graph structure. *Bioinformatics*, 22 (13), 1600–1607.

Altschul, S.F., Gish, W., Miller, W., Myers, E.W., and Lipman, D.J., 1990. Basic local alignment search tool. *Journal of Molecular Biology*, 215 (3), 403–410.

Alvarez, M.A., Li, C., Lin, H., Joe, A., Padilla, M., Woods, D.P., and Dubcovsky, J., 2023. EARLY FLOWERING 3 interactions with PHYTOCHROME B and PHOTOPERIOD1 are critical for the photoperiodic regulation of wheat heading time. *PLOS Genetics*, 19 (5), e1010655.

Amasino, R. and Michaels, S.D., 2010. The timing of flowering. *Plant Physiology*, 154 (2), 516–520.

Andrade, L., Lu, Y., Cordeiro, A., Costa, J.M.F., Wigge, P.A., Saibo, N.J.M., and Jaeger, K.E., 2022. The evening complex integrates photoperiod signals to control flowering in rice. *Proceedings of the National Academy of Sciences of the United States of America*, 119 (26), e2122582119.

Andrés, F. and Coupland, G., 2012. The genetic basis of flowering responses to seasonal cues. *Nature Reviews Genetics*, 13 (9), 627–639.

Andrews, S., 2010. *A quality control tool for high throughput sequence data*.

Anwer, M.U., Davis, A., Davis, S.J., and Quint, M., 2020. Photoperiod sensing of the circadian clock is controlled by EARLY FLOWERING 3 and GIGANTEA. *The Plant Journal*, 101 (6), 1397–1410.

Banfield, M.J. and Brady, R.L., 2000. The structure of Antirrhinum centroradialis protein (CEN) suggests a role as a kinase regulator11Edited by I. A. Wilson. *Journal of Molecular Biology*, 297 (5), 1159–1170.

Barkworth, M.E. and Torres, M.A., 2001. Distribution and diagnostic characters of Nassella (Poaceae: Stipeae). *Taxon*, 50 (2), 439–468.

Bäurle, I. and Dean, C., 2006. The timing of developmental transitions in plants. *Cell*, 125 (4), 655–664.

735 Bennett, T. and Dixon, L.E., 2021. Asymmetric expansions of FT and TFL1 lineages
736 characterize differential evolution of the EuPEBP family in the major angiosperm lineages.
737 *BMC Biology*, 19 (1), 181.

738 Benson, D.A., Cavanaugh, M., Clark, K., Karsch-Mizrachi, I., Lipman, D.J., Ostell, J., and
739 Sayers, E.W., 2013. GenBank. *Nucleic Acids Research*, 41 (D1), D36–D42.

740 Bettgenhaeuser, J., Corke, F.M., Opanowicz, M., Green, P., Hernández-Pinzón, I., Doonan,
741 J.H., and Moscou, M.J., 2017. Natural variation in Brachypodium links vernalization and
742 flowering time loci as major flowering determinants. *Plant Physiology*, 173 (1), 256 268.

743 Bi, X., van Esse, W., Mulki, M.A., Kirschner, G., Zhong, J., Simon, R., and von Korff, M.,
744 2019. CENTRORADIALIS interacts with FLOWERING LOCUS T-like genes to control
745 floret development and grain number. *Plant Physiology*, 180 (2), 1013–1030.

746 Bolger, A.M., Lohse, M., and Usadel, B., 2014. Trimmomatic: a flexible trimmer for Illumina
747 sequence data. *Bioinformatics*, 30 (15), 2114–2120.

748 Bouché, F., Woods, D.P., Linden, J., Li, W., Mayer, K.S., Amasino, R.M., and Périlleux, C.,
749 2022. EARLY FLOWERING 3 and photoperiod sensing in Brachypodium distachyon.
750 *Frontiers in Plant Science*, 12, 769194.

751 Bradley, D., Carpenter, R., Copsey, L., Vincent, C., Rothstein, S., and Coen, E., 1996.
752 Control of inflorescence architecture in Antirrhinum. *Nature*, 379 (6568), 791–797.

753 Brambilla, V. and Fornara, F., 2013. Molecular control of flowering in response to day length
754 in rice. *Journal of Integrative Plant Biology*, 55 (5), 410–418.

755 Brambilla, V. and Fornara, F., 2017. Y flowering? Regulation and activity of CONSTANS
756 and CCT-domain proteins in Arabidopsis and crop species. *Biochimica et Biophysica Acta*,
757 1860 (5), 655–660.

758 Brambilla, V., Martignago, D., Goretti, D., Cerise, M., Somssich, M., de Rosa, M., Galbiati,
759 F., Shrestha, R., Lazzaro, F., Simon, R., and Fornara, F., 2017. Antagonistic transcription
760 factor complexes modulate the floral transition in rice. *The Plant Cell*, 29 (11), 2801–2816.

761 Brereton, R.G., 2015. The Mahalanobis distance and its relationship to principal component
762 scores. *Journal of Chemometrics*, 29 (3), 143–145.

763 Buchfink, B., Xie, C., and Huson, D.H., 2015. Fast and sensitive protein alignment using
764 DIAMOND. *Nature Methods*, 12 (1), 59–60.

765 Calixto, C.P.G., Waugh, R., and Brown, J.W.S., 2015. Evolutionary relationships among
766 barley and Arabidopsis core circadian clock and clock-associated genes. *Journal of*
767 *Molecular Evolution*, 80 (2), 108–119.

768 Camacho, C., Coulouris, G., Avagyan, V., Ma, N., Papadopoulos, J., Bealer, K., and Madden,
769 T.L., 2009. BLAST+: architecture and applications. *BMC Bioinformatics*, 10 (1), 421.

770 Cao, S., Luo, X., Xu, D., Tian, X., Song, J., Xia, X., Chu, C., and He, Z., 2021. Genetic
771 architecture underlying light and temperature mediated flowering in Arabidopsis, rice, and
772 temperate cereals. *New Phytologist*, 230 (5), 1731–1745.

773 Chardon, F. and Damerval, C., 2005. Phylogenomic analysis of the PEBP gene family in
774 cereals. *Journal of Molecular Evolution*, 61 (5), 579–590.

775 Chen, H., Yin, Y., Niu, J., Kwak, J.M., and Du, M., 2023. Analysis of Brachypodium
776 distachyon UVR8 reveals conservation in UV-B receptors. *Plant Biology*, 25 (5), 750–756.

777 Chen, J., Wang, L., Jin, X., Wan, J., Zhang, L., Je, B.I., Zhao, K., Kong, F., Huang, J., and
778 Tian, M., 2021. Oryza sativa ObgC1 acts as a key regulator of DNA replication and
779 ribosome biogenesis in chloroplast nucleoids. *Rice*, 14 (1), 65.

780 Chong, L., Xu, R., Huang, P., Guo, P., Zhu, M., Du, H., Sun, X., Ku, L., Zhu, J.-K., and Zhu,
781 Y., 2022. The tomato OST1–VOZ1 module regulates drought-mediated flowering. *The*
782 *Plant Cell*, 34 (5), 2001–2018.

783 Cialdella, A.M., Sede, S.M., Romaschenko, K., Peterson, P.M., Soreng, R.J., Zuloaga, F.O.,
784 and Morrone, O., 2014. Phylogeny of Nassella (Stipeae, Pooideae, Poaceae) based on
785 analyses of chloroplast and nuclear ribosomal DNA and morphology. *Systematic Botany*,
786 39 (3), 814–828.

787 Ciannamea, S., Jensen, C.S., Agerskov, H., Petersen, K., Lenk, I., Didion, T., Immink,
788 R.G.H., Angenent, G.C., and Nielsen, K.K., 2007. A new member of the LIR gene family
789 from perennial ryegrass is cold-responsive, and promotes vegetative growth in
790 Arabidopsis. *Plant Science*, 172 (2), 221–227.

791 Cockram, J., Thiel, T., Steuernagel, B., Stein, N., Taudien, S., Bailey, P.C., and O'Sullivan,
792 D.M., 2012. Genome dynamics explain the evolution of flowering time CCT domain gene
793 families in the Poaceae. *PLOS One*, 7 (9), e45307.

794 Colasanti, J. and Coneva, V., 2009. Mechanisms of floral induction in grasses: something
795 borrowed, something new. *Plant Physiology*, 149 (1), 56 62.

796 Comadran, J., Kilian, B., Russell, J., Ramsay, L., Stein, N., Ganal, M., Shaw, P., Bayer, M.,
797 Thomas, W., Marshall, D., Hedley, P., Tondelli, A., Pecchioni, N., Francia, E., Korzun, V.,
798 Walther, A., and Waugh, R., 2012. Natural variation in a homolog of Antirrhinum
799 CENTRORADIALIS contributed to spring growth habit and environmental adaptation in
800 cultivated barley. *Nature Genetics*, 44 (12), 1388–1392.

801 Conti, L. and Bradley, D., 2007. TERMINAL FLOWER1 is a mobile signal controlling
802 Arabidopsis architecture. *The Plant Cell*, 19 (3), 767–778.

803 Corbesier, L., Vincent, C., Jang, S., Fornara, F., Fan, Q., Searle, I., Giakountis, A., Farrona,
804 S., Gissot, L., Turnbull, C., and Coupland, G., 2007. FT protein movement contributes to
805 long-distance signaling in floral induction of Arabidopsis. *Science*, 316 (5827), 1030–
806 1033.

807 Covington, M.F., Maloof, J.N., Straume, M., Kay, S.A., and Harmer, S.L., 2008. Global
808 transcriptome analysis reveals circadian regulation of key pathways in plant growth and
809 development. *Genome Biology*, 9 (8), R130.

810 Covington, M.F., Panda, S., Liu, X.L., Strayer, C.A., Wagner, D.R., and Kay, S.A., 2001.
811 ELF3 modulates resetting of the circadian clock in Arabidopsis. *The Plant Cell*, 13 (6),
812 1305–1316.

813 Creux, N. and Harmer, S., 2019. Circadian rhythms in plants. *Cold Spring Harbor*
814 *Perspectives in Biology*, 11 (9), a034611.

815 Dalchau, N., Hubbard, K.E., Robertson, F.C., Hotta, C.T., Briggs, H.M., Stan, G.-B.,
816 Gonçalves, J.M., and Webb, A.A.R., 2010. Correct biological timing in Arabidopsis
817 requires multiple light-signaling pathways. *Proceedings of the National Academy of*
818 *Sciences of the United States of America*, 107 (29), 13171 13176.

819 Danilevskaya, O.N., Meng, X., and Ananiev, E.V., 2010. Concerted modification of flowering
820 time and inflorescence architecture by ectopic expression of TFL1-like genes in maize.
821 *Plant Physiology*, 153 (1), 238–251.

822 Davidson, N.M. and Oshlack, A., 2014. Corset: enabling differential gene expression analysis
823 for de novo assembled transcriptomes. *Genome Biology*, 15 (7), 410.

824 de los Reyes, P., Romero-Campero, F.J., Ruiz, M.T., Romero, J.M., and Valverde, F., 2017.
825 Evolution of daily gene co-expression patterns from algae to plants. *Frontiers in Plant*
826 *Science*, 8, 1217.

827 Desvaux, É.-É., 1853. Gramineæ Chilenses. *In*: C. Gay, ed. *Flora Chilena*. Paris, Chile, 233–
828 469.

829 Doi, K., Izawa, T., Fuse, T., Yamanouchi, U., Kubo, T., Shimatani, Z., Yano, M., and
830 Yoshimura, A., 2004. Ehd1, a B-type response regulator in rice, confers short-day
831 promotion of flowering and controls FT-like gene expression independently of Hd1. *Genes*
832 *& Development*, 18 (8), 926–936.

833 Durinck, S., Moreau, Y., Kasprzyk, A., Davis, S., Moor, B.D., Brazma, A., and Huber, W.,
834 2005. BioMart and Bioconductor: a powerful link between biological databases and
835 microarray data analysis. *Bioinformatics*, 21 (16), 3439–3440.

836 Emms, D.M. and Kelly, S., 2015. OrthoFinder: solving fundamental biases in whole genome
837 comparisons dramatically improves orthogroup inference accuracy. *Genome Biology*, 16
838 (1), 157.

839 Emms, D.M. and Kelly, S., 2019. OrthoFinder: phylogenetic orthology inference for
840 comparative genomics. *Genome Biology*, 20 (1), 238.

841 Endo-Higashi, N. and Izawa, T., 2011. Flowering time genes Heading date 1 and Early
842 heading date 1 together control panicle development in rice. *Plant and Cell Physiology*, 52
843 (6), 1083–1094.

Faure, S., Higgins, J., Turner, A., and Laurie, D.A., 2007. The FLOWERING LOCUS T-like gene family in barley (Hordeum vulgare). *Genetics*, 176 (1), 599–609.

Favory, J., Stec, A., Gruber, H., Rizzini, L., Oravecz, A., Funk, M., Albert, A., Cloix, C., Jenkins, G.I., Oakeley, E.J., Seidlitz, H.K., Nagy, F., and Ulm, R., 2009. Interaction of COP1 and UVR8 regulates UV-B-induced photomorphogenesis and stress acclimation in Arabidopsis. *The EMBO Journal*, 28 (5), 591–601.

Fernández-Calleja, M., Casas, A.M., and Igartua, E., 2021. Major flowering time genes of barley: allelic diversity, effects, and comparison with wheat. *Theoretical and Applied Genetics*, 134 (7), 1867–1897.

Ferrari, C., Proost, S., Janowski, M., Becker, J., Nikoloski, Z., Bhattacharya, D., Price, D., Tohge, T., Bar-Even, A., Fernie, A., Stitt, M., and Mutwil, M., 2019. Kingdom-wide comparison reveals the evolution of diurnal gene expression in Archaeplastida. *Nature Communications*, 10 (1), 737.

Filichkin, S.A., Breton, G., Priest, H.D., Dharmawardhana, P., Jaiswal, P., Fox, S.E., Michael, T.P., Chory, J., Kay, S.A., and Mockler, T.C., 2011. Global profiling of rice and poplar transcriptomes highlights key conserved circadian-controlled pathways and cis-regulatory modules. *PLOS ONE*, 6 (6), e16907.

Fisher, R.A., 1922. On the interpretation of χ^2 from contingency tables, and the calculation of P. *Journal of the Royal Statistical Society*, 85 (1), 87.

Fjellheim, S., Boden, S., and Trevaskis, B., 2014. The role of seasonal flowering responses in adaptation of grasses to temperate climates. *Frontiers in Plant Science*, 5, 431.

Fjellheim, S., Young, D.A., Paliocha, M., Johnsen, S.S., Schubert, M., and Preston, J.C., 2022. Major niche transitions in Pooideae correlate with variation in photoperiodic flowering and evolution of CCT domain genes. *Journal of Experimental Botany*, 73 (12), 4079–4093.

Gallaher, T.J., Adams, D.C., Attigala, L., Burke, S.V., Craine, J.M., Duvall, M.R., Klahs, P.C., Sherratt, E., Wysocki, W.P., and Clark, L.G., 2019. Leaf shape and size track habitat transitions across forest–grassland boundaries in the grass family (Poaceae). *Evolution*, 63 (5), 685.

Gallaher, T.J., Peterson, P.M., Soreng, R.J., Zuloaga, F.O., Li, D., Clark, L.G., Tyrrell, C.D., Welker, C.A.D., Kellogg, E.A., and Teisher, J.K., 2022. Grasses through space and time: An overview of the biogeographical and macroevolutionary history of Poaceae. *Journal of Systematics and Evolution*, 60 (3), 522–569.

Gao, M., Geng, F., Klose, C., Staudt, A.-M., Huang, H., Nguyen, D., Lan, H., Mockler, T.C., Nusinow, D.A., Hiltbrunner, A., Schäfer, E., Wigge, P.A., and Jaeger, K.E., 2019. Phytochromes measure photoperiod in Brachypodium. *bioRxiv*, 697169.

Garner, W.W. and Allard, H.A., 1920. Effect of the relative length of day and night and other factors of the environment on growth and reproduction in plants. *Journal of Agricultural Research*, 18 (11), 553–606.

883 Gaudinier, A. and Blackman, B.K., 2020. Evolutionary processes from the perspective of
884 flowering time diversity. *New Phytologist*, 225 (5), 1883–1898.

885 Gauley, A. and Boden, S.A., 2020. Step-wise increases in FT1 expression regulate seasonal
886 progression of flowering in wheat (Triticum aestivum). *New Phytologist*, 229 (2), 1163–
887 1176.

888 Gene Ontology Consortium, 2004. The Gene Ontology (GO) database and informatics
889 resource. *Nucleic Acids Research*, 32 (S1), D258–D261.

890 Giaume, F., Bono, G.A., Martignago, D., Miao, Y., Vicentini, G., Toriba, T., Wang, R.,
891 Kong, D., Cerise, M., Chirivì, D., Biancucci, M., Khahani, B., Morandini, P., Tameling,
892 W., Martinotti, M., Goretti, D., Coupland, G., Kater, M., Brambilla, V., Miki, D.,
893 Kyozuka, J., and Fornara, F., 2023. Two florigens and a florigen-like protein form a triple
894 regulatory module at the shoot apical meristem to promote reproductive transitions in rice.
895 *Nature Plants*, 1–10.

896 Grabherr, M.G., Haas, B.J., Yassour, M., Levin, J.Z., Thompson, D.A., Amit, I., Adiconis, X.,
897 Fan, L., Raychowdhury, R., Zeng, Q., Chen, Z., Mauceli, E., Hacohen, N., Gnirke, A.,
898 Rhind, N., di Palma, F., Birren, B.W., Nusbaum, C., Lindblad-Toh, K., Friedman, N., and
899 Regev, A., 2011. Full-length transcriptome assembly from RNA-seq data without a
900 reference genome. *Nature Biotechnology*, 29 (7), 644–652.

901 Gu, Z., Eils, R., and Schlesner, M., 2016. Complex heatmaps reveal patterns and correlations
902 in multidimensional genomic data. *Bioinformatics*, 32 (18), 2847–2849.

903 Haas, B.J., Papanicolaou, A., Yassour, M., Grabherr, M., Blood, P.D., Bowden, J., Couger,
904 M.B., Eccles, D., Li, B., Lieber, M., MacManes, M.D., Ott, M., Orvis, J., Pochet, N.,
905 Strozzi, F., Weeks, N., Westerman, R., William, T., Dewey, C.N., Henschel, R., LeDuc,
906 R.D., Friedman, N., and Regev, A., 2013. De novo transcript sequence reconstruction from
907 RNA-seq using the Trinity platform for reference generation and analysis. *Nature*
908 *Protocols*, 8 (8), 1494–1512.

909 Hamasha, H.R., von Hagen, K.B., and Röser, M., 2012. Stipa (Poaceae) and allies in the Old
910 World: molecular phylogenetics realigns genus circumscription and gives evidence on the
911 origin of American and Australian lineages. *Plant Systematics and Evolution*, 298 (2),
912 351–367.

913 Hanano, S. and Goto, K., 2011. Arabidopsis TERMINAL FLOWER1 is involved in the
914 regulation of flowering time and inflorescence development through transcriptional
915 repression. *The Plant Cell*, 23 (9), 3172–3184.

916 Hanzawa, Y., Money, T., and Bradley, D., 2005. A single amino acid converts a repressor to
917 an activator of flowering. *Proceedings of the National Academy of Sciences of the United*
918 *States of America*, 102 (21), 7748–7753.

919 Harmer, S.L., Hogenesch, J.B., Straume, M., Chang, H.-S., Han, B., Zhu, T., Wang, X.,
920 Kreps, J.A., and Kay, S.A., 2000. Orchestrated transcription of key pathways in
921 Arabidopsis by the circadian clock. *Science*, 290 (5499), 2110–2113.

Hartley, W., 1973. Studies on the origin, evolution, and distribution of the Gramineae. V. The subfamily Festucoideae. *Australian Journal of Botany*, 21 (2), 201–234.

Hartung, F. and Puchta, H., 2006. The RecQ gene family in plants. *Journal of Plant Physiology*, 163 (3), 287–296.

Heide, O.M., 1994. Control of flowering and reproduction in temperate grasses. *New Phytologist*, 128 (2), 347–362.

Helfer, A., Nusinow, D.A., Chow, B.Y., Gehrke, A.R., Bulyk, M.L., and Kay, S.A., 2011. LUX ARRHYTHMO encodes a nighttime repressor of circadian gene expression in the Arabidopsis core clock. *Current Biology*, 21 (2), 126–133.

Herath, V., 2019. The architecture of the GhD7 promoter reveals the roles of GhD7 in growth, development and the abiotic stress response in rice. *Computational Biology and Chemistry*, 82, 1–8.

Higgins, J.A., Bailey, P.C., and Laurie, D.A., 2010. Comparative genomics of flowering time pathways using Brachypodium distachyon as a model for the temperate grasses. *PLOS One*, 5 (4), e10065.

Hotta, C.T., Gardner, M.J., Hubbard, K.E., Baek, S.J., Dalchau, N., Suhita, D., Dodd, A.N., and Webb, A.A.R., 2007. Modulation of environmental responses of plants by circadian clocks. *Plant, Cell & Environment*, 30 (3), 333–349.

Howe, K.L., Achuthan, P., Allen, J., Allen, J., Alvarez-Jarreta, J., Amode, M.R., Armean, I.M., Azov, A.G., Bennett, R., Bhai, J., Billis, K., Boddu, S., Charkhchi, M., Cummins, C., Da Rin Fioretto, L., Davidson, C., Dodiya, K., El Houdaigui, B., Fatima, R., Gall, A., Garcia Giron, C., Grego, T., Guijarro-Clarke, C., Haggerty, L., Hemrom, A., Hourlier, T., Izuogu, O.G., Juettemann, T., Kaikala, V., Kay, M., Lavidas, I., Le, T., Lemos, D., Gonzalez Martinez, J., Marugán, J.C., Maurel, T., McMahon, A.C., Mohanan, S., Moore, B., Muffato, M., Oheh, D.N., Paraschas, D., Parker, A., Parton, A., Prosovetskaia, I., Sakthivel, M.P., Salam, A.I.A., Schmitt, B.M., Schuilenburg, H., Sheppard, D., Steed, E., Szpak, M., Szuba, M., Taylor, K., Thormann, A., Threadgold, G., Walts, B., Winterbottom, A., Chakiachvili, M., Chaubal, A., De Silva, N., Flint, B., Frankish, A., Hunt, S.E., IIsley, G.R., Langridge, N., Loveland, J.E., Martin, F.J., Mudge, J.M., Morales, J., Perry, E., Ruffier, M., Tate, J., Thybert, D., Trevanion, S.J., Cunningham, F., Yates, A.D., Zerbino, D.R., and Flicek, P., 2021. Ensembl 2021. *Nucleic Acids Research*, 49 (D1), D884–D891.

Howe, K.L., Contreras-Moreira, B., Silva, N.D., Maslen, G., Akanni, W., Allen, J., Alvarez-Jarreta, J., Barba, M., Bolser, D.M., Cambell, L., Carbajo, M., Chakiachvili, M., Christensen, M., Cummins, C., Cuzick, A., Davis, P., Fexova, S., Gall, A., George, N., Gil, L., Gupta, P., Hammond-Kosack, K.E., Haskell, E., Hunt, S.E., Jaiswal, P., Janacek, S.H., Kersey, P.J., Langridge, N., Maheswari, U., Maurel, T., McDowall, M.D., Moore, B., Muffato, M., Naamati, G., Naithani, S., Olson, A., Papatheodorou, I., Patricio, M., Paulini, M., Pedro, H., Perry, E., Preece, J., Rosello, M., Russell, M., Sitnik, V., Staines, D.M., Stein, J., Tello-Ruiz, M.K., Trevanion, S.J., Urban, M., Wei, S., Ware, D., Williams, G., Yates, A.D., and Flicek, P., 2020. Ensembl Genomes 2020—enabling non-vertebrate genomic research. *Nucleic Acids Research*, 48 (D1), D689–D695.

964 Hu, L., Liang, W., Yin, C., Cui, X., Zong, J., Wang, X., Hu, J., and Zhang, D., 2011. Rice
965 MADS3 regulates ROS homeostasis during late anther development. *The Plant Cell*, 23
966 (2), 515–533.

967 Huang, H., Gehan, M.A., Huss, S.E., Alvarez, S., Lizarraga, C., Gruebbling, E.L., Gierer, J.,
968 Naldrett, M.J., Bindbeutel, R.K., Evans, B.S., Mockler, T.C., and Nusinow, D.A., 2017.
969 Cross-species complementation reveals conserved functions for EARLY FLOWERING 3
970 between monocots and dicots. *Plant Direct*, 1 (4), e00018.

971 Huang, H. and Nusinow, D.A., 2016. Into the Evening: Complex interactions in the
972 Arabidopsis circadian clock. *Trends in Genetics*, 32 (10), 674–686.

973 Humphreys, A.M. and Linder, H.P., 2013. Evidence for recent evolution of cold tolerance in
974 grasses suggests current distribution is not limited by (low) temperature. *New Phytologist*,
975 198 (4), 1261 1273.

976 Jaeger, K.E. and Wigge, P.A., 2007. FT protein acts as a long-range signal in Arabidopsis.
977 *Current Biology*, 17 (12), 1050–1054.

978 Jensen, C.S., Salchert, K., Gao, C., Andersen, C., Didion, T., and Nielsen, K.K., 2004. Floral
979 inhibition in red fescue (Festuca rubra L.) through expression of a heterologous flowering
980 repressor from Lolium. *Molecular Breeding*, 13 (1), 37–48.

981 Jensen, C.S., Salchert, K., and Nielsen, K.K., 2001. A TERMINAL FLOWER1-like gene
982 from perennial ryegrass involved in floral transition and axillary meristem identity. *Plant*
983 *Physiology*, 125 (3), 1517–1528.

984 Jiang, Q., Hua, X., Shi, H., Liu, J., Yuan, Y., Li, Z., Li, S., Zhou, M., Yin, C., Dou, M., Qi,
985 N., Wang, Y., Zhang, M., Ming, R., Tang, H., and Zhang, J., 2023. Transcriptome
986 dynamics provides insights into divergences of the photosynthesis pathway between
987 Saccharum officinarum and Saccharum spontaneum. *The Plant Journal*, 113 (6), 1278–
988 1294.

989 Jin, S., Nasim, Z., Susila, H., and Ahn, J.H., 2021. Evolution and functional diversification of
990 FLOWERING LOCUS T/TERMINAL FLOWER 1 family genes in plants. *Seminars in*
991 *Cell & Developmental Biology*, 109, 20–30.

992 Johansson, M. and Staiger, D., 2014. Time to flower: interplay between photoperiod and the
993 circadian clock. *Journal of Experimental Botany*, 66 (3), 719 730.

994 Kaneko-Suzuki, M., Kurihara-Ishikawa, R., Okushita-Terakawa, C., Kojima, C., Nagano-
995 Fujiwara, M., Ohki, I., Tsuji, H., Shimamoto, K., and Taoka, K.-I., 2018. TFL1-like
996 proteins in rice antagonize rice FT-like protein in inflorescence development by
997 competition for complex formation with 14-3-3 and FD. *Plant and Cell Physiology*, 59 (3),
998 458–468.

999 Kikuchi, R., Kawahigashi, H., Ando, T., Tonooka, T., and Handa, H., 2009. Molecular and
1000 functional characterization of PEBP genes in barley reveal the diversification of their roles
1001 in flowering. *Plant Physiology*, 149 (3), 1341–1353.

1002 Kikuchi, R., Kawahigashi, H., Oshima, M., Ando, T., and Handa, H., 2011. The differential
1003 expression of HvCO9, a member of the CONSTANS-like gene family, contributes to the
1004 control of flowering under short-day conditions in barley. *Journal of Experimental Botany*,
1005 63 (2), 773–84.

1006 King, R.W. and Heide, O.M., 2009. Seasonal flowering and evolution: the heritage from
1007 Charles Darwin. *Functional Plant Biology*, 36 (12), 1027 1036.

1008 Kobayashi, Y., Kaya, H., Goto, K., Iwabuchi, M., and Araki, T., 1999. A pair of related genes
1009 with antagonistic roles in mediating flowering signals. *Science*, 286 (5446), 1960–1962.

1010 Koo, B.-H., Yoo, S.-C., Park, J.-W., Kwon, C.-T., Lee, B.-D., An, G., Zhang, Z., Li, J., Li, Z.,
1011 and Paek, N.-C., 2013. Natural variation in OsPRR37 regulates heading date and
1012 contributes to rice cultivation at a wide range of latitudes. *Molecular Plant*, 6 (6), 1877–
1013 1888.

1014 Kriventseva, E.V., Kuznetsov, D., Tegenfeldt, F., Manni, M., Dias, R., Simão, F.A., and
1015 Zdobnov, E.M., 2019. OrthoDB v10: sampling the diversity of animal, plant, fungal,
1016 protist, bacterial and viral genomes for evolutionary and functional annotations of
1017 orthologs. *Nucleic Acids Research*, 47 (D1), D807–D811.

1018 Kumar, S., Choudhary, P., Gupta, M., and Nath, U., 2018. VASCULAR PLANT ONE-ZINC
1019 FINGER1 (VOZ1) and VOZ2 interact with CONSTANS and promote photoperiodic
1020 flowering transition. *Plant Physiology*, 176 (4), 2917–2930.

1021 Langfelder, P., Zhang, B., and Horvath, S., 2007. Defining clusters from a hierarchical cluster
1022 tree: the Dynamic Tree Cut package for R. *Bioinformatics*, 24 (5), 719–720.

1023 Langmead, B. and Salzberg, S.L., 2012. Fast gapped-read alignment with Bowtie 2. *Nature*
1024 *Methods*, 9 (4), 357–359.

1025 Leder, E.H., André, C., Alan, L.M., Töpel, M., Blomberg, A., Havenhand, J.N., Lindström,
1026 K., Volckaert, F.A.M., Kvarnemo, C., Johannesson, K., and Svensson, O., 2021. Post-
1027 glacial establishment of locally adapted fish populations over a steep salinity gradient.
1028 *Journal of Evolutionary Biology*, 34 (1), 138–156.

1029 Leemis, L.M., 1986. Relationships among common univariate distributions. *The American*
1030 *Statistician*, 40 (2), 143 146.

1031 Li, C., Distelfeld, A., Comis, A., and Dubcovsky, J., 2011. Wheat flowering repressor VRN2
1032 and promoter CO2 compete for interactions with NUCLEAR FACTOR-Y complexes. *The*
1033 *Plant Journal*, 67 (5), 763–773.

1034 Li, C. and Dubcovsky, J., 2008. Wheat FT protein regulates VRN1 transcription through
1035 interactions with FDL2. *The Plant Journal*, 55 (4), 543–554.

1036 Li, C., Lin, H., and Dubcovsky, J., 2015. Factorial combinations of protein interactions
1037 generate a multiplicity of florigen activation complexes in wheat and barley. *The Plant*
1038 *Journal*, 84 (1), 70–82.

1039 Li, H., Handsaker, B., Wysoker, A., Fennell, T., Ruan, J., Homer, N., Marth, G., Abecasis, G.,
1040 Durbin, R., and 1000 Genome Project Data Processing Subgroup, 2009. The Sequence
1041 Alignment/Map format and SAMtools. *Bioinformatics*, 25 (16), 2078–2079.

1042 Li, S., Zhou, B., Peng, X., Kuang, Q., Huang, X., Yao, J., Du, B., and Sun, M., 2014. OsFIE2
1043 plays an essential role in the regulation of rice vegetative and reproductive development.
1044 *New Phytologist*, 201 (1), 66–79.

1045 Lin, C., 2000. Photoreceptors and regulation of flowering time. *Plant Physiology*, 123 (1),
1046 39–50.

1047 Linhares-Neto, M.V., Schumacher, P.V., Ribeiro, T.H.C., Cardon, C.H., Resende, P.M.,
1048 Colasanti, J., and Chalfun-Junior, A., 2023. Molecular screening reveals a photoperiod
1049 responsive floral regulator in sugarcane. *Theoretical and Experimental Plant Physiology*,
1050 1–16.

1051 Liu, H., Zhou, X., Li, Q., Wang, L., and Xing, Y., 2020. CCT domain-containing genes in
1052 cereal crops: flowering time and beyond. *Theoretical and Applied Genetics*, 133 (5), 1385–
1053 1396.

1054 Lu, L., Yan, W., Xue, W., Shao, D., and Xing, Y., 2012. Evolution and association analysis of
1055 Ghd7 in rice. *PLOS One*, 7 (5), e34021.

1056 Lu, Q., Xu, Z., and Song, R., 2006. OsFY, a homolog of AtFY, encodes a protein that can
1057 interact with OsFCA-γ in rice (Oryza sativa L.). *Acta Biochimica et Biophysica Sinica*, 38
1058 (7), 492–499.

1059 Lv, B., Nitcher, R., Han, X., Wang, S., Ni, F., Li, K., Pearce, S., Wu, J., Dubcovsky, J., and
1060 Fu, D., 2014. Characterization of FLOWERING LOCUS T1 (FT1) gene in Brachypodium
1061 and wheat. *PLOS One*, 9 (4), e94171.

1062 Mahalanobis, P.C., 1936. On the generalised distance in statistics. *Proceedings of the*
1063 *National Institute of Sciences of India*, 2 (1), 49–55.

1064 Martin-Tryon, E.L. and Harmer, S.L., 2008. XAP5 CIRCADIAN TIMEKEEPER coordinates
1065 light signals for proper timing of photomorphogenesis and the circadian clock in
1066 Arabidopsis. *The Plant Cell*, 20 (5), 1244–1259.

1067 Maruta, T., Yoshimoto, T., Ito, D., Ogawa, T., Tamoi, M., Yoshimura, K., and Shigeoka, S.,
1068 2012. An Arabidopsis FAD pyrophosphohydrolase, AtNUDX23, is involved in flavin
1069 homeostasis. *Plant and Cell Physiology*, 53 (6), 1106–1116.

1070 Matsubara, K., Yamanouchi, U., Nonoue, Y., Sugimoto, K., Wang, Z.-X., Minobe, Y., and
1071 Yano, M., 2011. Ehd3, encoding a plant homeodomain finger-containing protein, is a
1072 critical promoter of rice flowering: Ehd3 is critical promoter of rice flowering. *The Plant*
1073 *Journal*, 66 (4), 603–612.

1074 McKeown, M., Schubert, M., Marcussen, T., Fjellheim, S., and Preston, J.C., 2016. Evidence
1075 for an early origin of vernalization responsiveness in temperate Pooideae grasses. *Plant*
1076 *Physiology*, 172 (1), 416–426.

1077 Michael, T.P., Mockler, T.C., Breton, G., McEntee, C., Byer, A., Trout, J.D., Hazen, S.P.,
1078 Shen, R., Priest, H.D., Sullivan, C.M., Givan, S.A., Yanovsky, M., Hong, F., Kay, S.A.,
1079 and Chory, J., 2008. Network discovery pipeline elucidates conserved time-of-day–
1080 specific cis-regulatory modules. *PLOS Genetics*, 4 (2), e14.

1081 Minh, B.Q., Schmidt, H.A., Chernomor, O., Schrempf, D., Woodhams, M.D., von Haeseler,
1082 A., and Lanfear, R., 2020. IQ-TREE 2: New models and efficient methods for
1083 phylogenetic inference in the genomic era. *Molecular Biology and Evolution*, 37 (5),
1084 1530–1534.

1085 Mizuno, T. and Nakamichi, N., 2005. Pseudo-response regulators (PRRs) or true oscillator
1086 components (TOCs). *Plant and Cell Physiology*, 46 (5), 677–685.

1087 Müller, L.M., Mombaerts, L., Pankin, A., Davis, S.J., Webb, A.A.R., Goncalves, J., and
1088 Korff, M. von, 2020. Differential effects of day/night cues and the circadian clock on the
1089 barley transcriptome. *Plant Physiology*, 183 (2), 765–779.

1090 Murfet, I.C., 1977. Environmental interaction and the genetics of flowering. *Annual Review of*
1091 *Plant Physiology*, 28 (1), 253–278.

1092 Murtagh, F. and Legendre, P., 2014. Ward's hierarchical agglomerative clustering method:
1093 Which algorithms implement Ward's criterion? *Journal of Classification*, 31 (3), 274–295.

1094 NCBI Resource Coordinators, 2017. Database resources of the National Center for
1095 Biotechnology Information. *Nucleic Acids Research*, 45 (D1), D12–D17.

1096 Ng, H.H., Dole, S., and Struhl, K., 2003. The Rtf1 component of the Paf1 transcriptional
1097 elongation complex is required for ubiquitination of histone H2B. *Journal of Biological*
1098 *Chemistry*, 278 (36), 33625–33628.

1099 Nusinow, D.A., Helfer, A., Hamilton, E.E., King, J.J., Imaizumi, T., Schultz, T.F., Farré,
1100 E.M., and Kay, S.A., 2011. The ELF4–ELF3–LUX complex links the circadian clock to
1101 diurnal control of hypocotyl growth. *Nature*, 475 (7356), 398–402.

1102 Okada, R., Nemoto, Y., Endo-Higashi, N., and Izawa, T., 2017. Synthetic control of flowering
1103 in rice independent of the cultivation environment. *Nature Plants*, 3 (4), 17039.

1104 Olsen, P., Lenk, I., Jensen, C.S., Petersen, K., Andersen, C.H., Didion, T., and Nielsen, K.K.,
1105 2006. Analysis of two heterologous flowering genes in Brachypodium distachyon
1106 demonstrates its potential as a grass model plant. *Plant Science*, 170 (5), 1020–1025.

1107 Paliocha, M., Schubert, M., Hvidsten, T.R., Aunbakk, N.B., Preston, J.C., Frøslie, K.F., and
1108 Fjellheim, S., 2023. Modulation of diurnal gene expression under contrasting photoperiods
1109 in the early-diverging Pooideae grass Melica ciliata. *Manuscript*.

1110 Paliocha, M., Schubert, M., Preston, J.C., and Fjellheim, S., 2023. Independent recruitment of
1111 FRUITFULL-like transcription factors in the convergent origins of vernalization-
1112 responsive grass flowering. *Molecular Phylogenetics and Evolution*, 179, 107678.

Peragine, A., Yoshikawa, M., Wu, G., Albrecht, H.L., and Poethig, R.S., 2004. SGS3 and SGS2/SDE1/RDR6 are required for juvenile development and the production of trans-acting siRNAs in Arabidopsis. *Genes & Development*, 18 (19), 2368–2379.

Périlleux, C., Bouché, F., Randoux, M., and Orman-Ligeza, B., 2019. Turning meristems into fortresses. *Trends in Plant Science*, 24 (Mol. Plant 8 2015).

Pertea, G. and Pertea, M., 2020. GFF Utilities: GffRead and GffCompare. *F1000Research*, 9, 304.

Pieck, M., Yuan, Y., Godfrey, J., Fisher, C., Zolj, S., Vaughan, D., Thomas, N., Wu, C., Ramos, J., Lee, N., Normanly, J., and Celenza, J.L., 2015. Auxin and tryptophan homeostasis are facilitated by the ISS1/VAS1 aromatic aminotransferase in Arabidopsis. *Genetics*, 201 (1), 185–199.

Pnueli, L., Carmel-Goren, L., Hareven, D., Gutfinger, T., Alvarez, J., Ganal, M., Zamir, D., and Lifschitz, E., 1998. The SELF-PRUNING gene of tomato regulates vegetative to reproductive switching of sympodial meristems and is the ortholog of CEN and TFL1. *Development*, 125 (11), 1979–1989.

Preston, J.C. and Fjellheim, S., 2020. Understanding past, and predicting future, niche transitions based on grass flowering time variation. *Plant Physiology*, 183 (3), 822–839.

R Core Team, 2022. *R: A language and environment for statistical computing*.

Ramsay, J.O., Graves, S., and Hooker, G., 2022. *fda: Functional Data Analysis*.

Ramsay, J.O., Hooker, G., and Graves, S., 2009. *Functional Data Analysis with R and MATLAB*. 1st ed. New York, NY, USA: Springer.

Reimmann, C. and Dudler, R., 1993. Circadian rhythmicity in the expression of a novel light-regulated rice gene. *Plant Molecular Biology*, 22 (1), 165–170.

Robinson, M.D., McCarthy, D.J., and Smyth, G.K., 2010. edgeR: a Bioconductor package for differential expression analysis of digital gene expression data. *Bioinformatics*, 26 (1), 139–140.

Romaschenko, K., Peterson, P.M., Soreng, R.J., Garcia-Jacas, N., Futorna, O., and Susanna, A., 2012. Systematics and evolution of the needle grasses (Poaceae: Pooideae: Stipeae) based on analysis of multiple chloroplast loci, ITS, and lemma micromorphology. *Taxon*, 61 (1), 18–44.

Samarth, Lee, R., Kelly, D., Turnbull, M.H., Macknight, R., Poole, A.M., and Jameson, P.E., 2022. A novel TFL1 gene induces flowering in the mast seeding alpine snow tussock, Chionochloa pallens (Poaceae). *Molecular Ecology*, 31 (3), 822–838.

Sanchez, S.E., Cagnola, J.I., Crepy, M., Yanovsky, M.J., and Casal, J.J., 2011. Balancing forces in the photoperiodic control of flowering. *Photochemical & Photobiological Sciences*, 10 (4), 451–460.

1149 Sanchez, S.E., Rugnone, M.L., and Kay, S.A., 2020. Light perception: A matter of time.
1150 *Molecular Plant*, 13 (3), 363–385.

1151 Schubert, M., Grønvold, L., Sandve, S.R., Hvidsten, T.R., and Fjellheim, S., 2019. Evolution
1152 of cold acclimation and its role in niche transition in the temperate grass subfamily
1153 Pooideae. *Plant Physiology*, 180 (1), 404–419.

1154 Schubert, M., Humphreys, A.M., Lindberg, C.L., Preston, J.C., and Fjellheim, S., 2020. To
1155 coldly go where no grass has gone before: A multidisciplinary review of cold adaptation in
1156 Poaceae. *Annual Plant Reviews*, 3 (4), 523–562.

1157 Schubert, M., Marcussen, T., Meseguer, A.S., and Fjellheim, S., 2019. The grass subfamily
1158 Pooideae: Cretaceous–Palaeocene origin and climate-driven Cenozoic diversification.
1159 *Global Ecology and Biogeography*, 28 (8), 1168–1182.

1160 Serrano-Bueno, G., Romero-Campero, F.J., Lucas-Reina, E., Romero, J.M., and Valverde, F.,
1161 2017. Evolution of photoperiod sensing in plants and algae. *Current Opinion in Plant*
1162 *Biology*, 37, 10–17.

1163 Shannon, S. and Meeks-Wagner, D.R., 1991. A mutation in the Arabidopsis TFL1 gene
1164 affects inflorescence meristem development. *The Plant Cell*, 3 (9), 877–892.

1165 Shaw, L.M., Li, C., Woods, D.P., Alvarez, M.A., Lin, H., Lau, M.Y., Chen, A., and
1166 Dubcovsky, J., 2020. Epistatic interactions between PHOTOPERIOD1, CONSTANS1 and
1167 CONSTANS2 modulate the photoperiodic response in wheat. *PLOS Genetics*, 16 (7),
1168 e1008812.

1169 Sherrill-Mix, S., 2019. *taxonomizr: Functions to work with NCBI accessions and taxonomy*.

1170 Simão, F.A., Waterhouse, R.M., Ioannidis, P., Kriventseva, E.V., and Zdobnov, E.M., 2015.
1171 BUSCO: assessing genome assembly and annotation completeness with single-copy
1172 orthologs. *Bioinformatics*, 31 (19), 3210–3212.

1173 Slater, G.S.C. and Birney, E., 2005. Automated generation of heuristics for biological
1174 sequence comparison. *BMC Bioinformatics*, 6 (1), 31.

1175 Soreng, R.J., Peterson, P.M., Zuloaga, F.O., Romaschenko, K., Clark, L.G., Teisher, J.K.,
1176 Gillespie, L.J., Barberá, P., Welker, C.A.D., Kellogg, E.A., Li, D., and Davidse, G., 2022.
1177 A worldwide phylogenetic classification of the Poaceae (Gramineae) III: An update.
1178 *Journal of Systematics and Evolution*, 60 (3), 476–521.

1179 Stolinski, L.A., Eisenmann, D.M., and Arndt, K.M., 1997. Identification of RTF1, a novel
1180 gene important for TATA site selection by TATA box-binding protein in Saccharomyces
1181 cerevisiae. *Molecular and Cellular Biology*, 17 (8), 4490–4500.

1182 Strayer, C., Oyama, T., Schultz, T.F., Raman, R., Somers, D.E., Más, P., Panda, S., Kreps,
1183 J.A., and Kay, S.A., 2000. Cloning of the Arabidopsis clock gene TOC1, an autoregulatory
1184 response regulator homolog. *Science*, 289 (5480), 768–771.

1185 Sun, Q. and Zhou, D.-X., 2008. Rice jmjC domain-containing gene JMJ706 encodes H3K9
1186 demethylase required for floral organ development. *Proceedings of the National Academy*
1187 *of Sciences*, 105 (36), 13679–13684.

1188 Takahashi, Y., Teshima, K.M., Yokoi, S., Innan, H., and Shimamoto, K., 2009. Variations in
1189 Hd1 proteins, Hd3a promoters, and Ehd1 expression levels contribute to diversity of
1190 flowering time in cultivated rice. *Proceedings of the National Academy of Sciences of the*
1191 *United States of America*, 106 (11), 4555–4560.

1192 Trevaskis, B., Hemming, M.N., Dennis, E.S., and Peacock, W.J., 2007. The molecular basis
1193 of vernalization-induced flowering in cereals. *Trends in Plant Science*, 12 (8), 352–357.

1194 Trevaskis, B., Hemming, M.N., Peacock, W.J., and Dennis, E.S., 2006. HvVRN2 responds to
1195 daylength, whereas HvVRN1 is regulated by vernalization and developmental status. *Plant*
1196 *Physiology*, 140 (4), 1397–1405.

1197 Turner, A., Beales, J., Faure, S., Dunford, R.P., and Laurie, D.A., 2005. The pseudo-response
1198 regulator Ppd-H1 provides adaptation to photoperiod in barley. *Science*, 310 (5750), 1031–
1199 1034.

1200 Valverde, F., Mouradov, A., Soppe, W., Ravenscroft, D., Samach, A., and Coupland, G.,
1201 2004. Photoreceptor regulation of CONSTANS protein in photoperiodic flowering.
1202 *Science*, 303 (5660), 1003–1006.

1203 Vicentini, G., Biancucci, M., Mineri, L., Chirivì, D., Giaume, F., Miao, Y., Kyozuka, J.,
1204 Brambilla, V., Betti, C., and Fornara, F., 2023. Environmental control of rice flowering
1205 time. *Plant Communications*, 100610.

1206 Vigeland, M.D., Spannagl, M., Asp, T., Paina, C., Rudi, H., Rognli, O.A., Fjellheim, S., and
1207 Sandve, S.R., 2013. Evidence for adaptive evolution of low-temperature stress response
1208 genes in a Pooideae grass ancestor. *New Phytologist*, 199 (4), 1060–1068.

1209 Wang, S., Zhang, S., Sun, C., Xu, Y., Chen, Y., Yu, C., Qian, Q., Jiang, D., and Qi, Y., 2014.
1210 Auxin response factor (OsARF12), a novel regulator for phosphate homeostasis in rice
1211 (Oryza sativa). *New Phytologist*, 201 (1), 91–103.

1212 Wang, Z.Y., Kenigsbuch, D., Sun, L., Harel, E., Ong, M.S., and Tobin, E.M., 1997. A Myb-
1213 related transcription factor is involved in the phytochrome regulation of an Arabidopsis
1214 Lhcb gene. *The Plant Cell*, 9 (4), 491–507.

1215 Ward, J.H., 1963. Hierarchical grouping to optimize an objective function. *Journal of the*
1216 *American Statistical Association*, 58 (301), 236–244.

1217 Waterhouse, R.M., Seppey, M., Simão, F.A., Manni, M., Ioannidis, P., Klioutchnikov, G.,
1218 Kriventseva, E.V., and Zdobnov, E.M., 2017. BUSCO applications from quality
1219 assessments to gene prediction and phylogenomics. *Molecular Biology and Evolution*, 35
1220 (3), 543–548.

1221 Wittern, L., Steed, G., Taylor, L.J., Ramirez, D.C., Pingarron-Cardenas, G., Gardner, K.,
1222 Greenland, A., Hannah, M.A., and Webb, A.A.R., 2023. Wheat EARLY FLOWERING 3

affects heading date without disrupting circadian oscillations. *Plant Physiology*, 191 (2), 1383–403.

Woods, D., Dong, Y., Bouché, F., Bednarek, R., Rowe, M., Ream, T., and Amasino, R., 2019. A florigen paralog is required for short-day vernalization in a pooid grass. *eLife*, 8, 27.

Woods, D.P., Li, W., Sibout, R., Shao, M., Laudencia-Chingcuanco, D., Vogel, J.P., Dubcovsky, J., and Amasino, R.M., 2023. PHYTOCHROME C regulation of photoperiodic flowering via PHOTOPERIOD1 is mediated by EARLY FLOWERING 3 in Brachypodium distachyon. *PLOS Genetics*, 19 (5), e1010706.

Woods, D.P., McKeown, M., Dong, Y., Preston, J.C., and Amasino, R., 2016. Evolution of VRN2/Ghd7-like genes in vernalization-mediated repression of grass flowering. *Plant Physiology*, 170 (4), 2124–2135.

Wu, T.D. and Watanabe, C.K., 2005. GMAP: a genomic mapping and alignment program for mRNA and EST sequences. *Bioinformatics*, 21 (9), 1859–1875.

Yamaguchi, T., Lee, D.Y., Miyao, A., Hirochika, H., An, G., and Hirano, H.-Y., 2006. Functional diversification of the two C-class MADS box genes OSMADS3 and OSMADS58 in Oryza sativa. *The Plant Cell*, 18 (1), 15 28.

Yan, L., Fu, D., Li, C., Blechl, A., Tranquilli, G., Bonafede, M., Sanchez, A., Valarik, M., Yasuda, S., and Dubcovsky, J., 2006. The wheat and barley vernalization gene VRN3 is an orthologue of FT. *Proceedings of the National Academy of Sciences of the United States of America*, 103 (51), 19581 19586.

Yasui, Y. and Kohchi, T., 2014. VASCULAR PLANT ONE-ZINC FINGER1 and VOZ2 repress the FLOWERING LOCUS C clade members to control flowering time in Arabidopsis. *Bioscience, Biotechnology, and Biochemistry*, 78 (11), 1850–1855.

Yasui, Y., Mukougawa, K., Uemoto, M., Yokofuji, A., Suzuri, R., Nishitani, A., and Kohchi, T., 2012. The phytochrome-interacting VASCULAR PLANT ONE–ZINC FINGER1 and VOZ2 redundantly regulate flowering in Arabidopsis. *The Plant Cell*, 24 (8), 3248–3263.

Yates, A.D., Achuthan, P., Akanni, W., Allen, J., Allen, J., Alvarez-Jarreta, J., Amode, M.R., Armean, I.M., Azov, A.G., Bennett, R., Bhai, J., Billis, K., Boddu, S., Marugán, J.C., Cummins, C., Davidson, C., Dodiya, K., Fatima, R., Gall, A., Giron, C.G., Gil, L., Grego, T., Haggerty, L., Haskell, E., Hourlier, T., Izuogu, O.G., Janacek, S.H., Juettemann, T., Kay, M., Lavidas, I., Le, T., Lemos, D., Martinez, J.G., Maurel, T., McDowall, M., McMahon, A., Mohanan, S., Moore, B., Nuhn, M., Oheh, D.N., Parker, A., Parton, A., Patricio, M., Sakthivel, M.P., Abdul Salam, A.I., Schmitt, B.M., Schuilenburg, H., Sheppard, D., Sycheva, M., Szuba, M., Taylor, K., Thormann, A., Threadgold, G., Vullo, A., Walts, B., Winterbottom, A., Zadissa, A., Chakiachvili, M., Flint, B., Frankish, A., Hunt, S.E., IIsley, G., Kostadima, M., Langridge, N., Loveland, J.E., Martin, F.J., Morales, J., Mudge, J.M., Muffato, M., Perry, E., Ruffier, M., Trevanion, S.J., Cunningham, F., Howe, K.L., Zerbino, D.R., and Flicek, P., 2020. Ensembl 2020. *Nucleic Acids Research*, 48 (D1), D682–D688.

1262 You, C., Dai, X., Li, X., Wang, L., Chen, G., Xiao, J., and Wu, C., 2010. Molecular
1263 characterization, expression pattern, and functional analysis of the OsIRL gene family
1264 encoding intracellular Ras-group-related LRR proteins in rice. *Plant Molecular Biology*,
1265 74 (6), 617–629.

1266 Zeevaart, J.A., 2008. Leaf-produced floral signals. *Current Opinion in Plant Biology*, 11 (5),
1267 541 547.

1268 Zhang, D. and Yuan, Z., 2014. Molecular control of grass inflorescence development. *Annual*
1269 *Review of Plant Biology*, 65 (1), 553–578.

1270 Zhang, Z., Hu, W., Shen, G., Liu, H., Hu, Y., Zhou, X., Liu, T., and Xing, Y., 2017.
1271 Alternative functions of Hd1 in repressing or promoting heading are determined by Ghd7
1272 status under long-day conditions. *Scientific Reports*, 7 (1), 5388.

1273 Zhao, J., Chen, H., Ren, D., Tang, H., Qiu, R., Feng, J., Long, Y., Niu, B., Chen, D., Zhong,
1274 T., Liu, Y., and Guo, J., 2015. Genetic interactions between diverged alleles of Early
1275 heading date 1 (Ehd1) and Heading date 3a (Hd3a)/ RICE FLOWERING LOCUS T1
1276 (RFT1) control differential heading and contribute to regional adaptation in rice (Oryza
1277 sativa). *New Phytologist*, 208 (3), 936–948.

1278 Zheng, X., Feng, L., Wang, J., Qiao, W., Zhang, L., Cheng, Y., and Yang, Q., 2016.
1279 Nonfunctional alleles of long-day suppressor genes independently regulate flowering time.
1280 *Journal of Integrative Plant Biology*, 58 (6), 540–548.

1281 Zhong, J., Robbett, M., Poire, A., and Preston, J.C., 2018. Successive evolutionary steps
1282 drove Pooideae grasses from tropical to temperate regions. *New Phytologist*, 217 (2), 925–
1283 938.

1284 Zhou, S., Zhu, S., Cui, S., Hou, H., Wu, H., Hao, B., Cai, L., Xu, Z., Liu, L., Jiang, L., Wang,
1285 H., and Wan, J., 2021. Transcriptional and post-transcriptional regulation of heading date
1286 in rice. *New Phytologist*, 230 (3), 943–956.

1287

1288

1289

Table 2: Most divergently expressed orthologues involved in flowering, light-signalling and circadian clock functions. These genes exhibited strongest diurnal rhythmicity in both species and photoperiods and were deemed to have the most divergent expression pattern between species in either long day (LD) or short day (SD). Transcript identifiers refer to Brachypodium_distachyon_v3.0 and IRGSP-1.0 annotations from Ensembl Plants. Gene ontology biological process annotation: **CR**: Circadian rhythm (GO:0007623); **FD**: Flower development (GO:0009908); **LR**: Response to light stimulus (GO:0009416).

Symbol	*Brachypodium* ID	Rice ID	Description	Photoperiod	FD	CR	LR	References
ARF12	BRADI_5g25767v3	Os04t0671900	*AUXIN RESPONSE FACTOR 12*, regulates stress response and phosphate homeostasis in rice	LD	×			(Wang *et al.* 2014)
CEN/TFL1	BRADI_4g42400v3 BRADI_3g44860v3	Os02g0531600 Os12g0152000 Os11g0152500	*CENTRORADIALIS/TERMINAL FLOWER 1*; close *VRN3/FT1* homologue; also called 'antiflorigen', antagonises FT1 in the shoot apical meristem and represses flowering in most angiosperms; flowering promoter in *Chionochloa pallens* (Danthonioideae)	SD	×			(Kobayashi *et al.* 1999, Olsen *et al.* 2006, Kaneko-Suzuki *et al.* 2018, Bi *et al.* 2019, Samarth *et al.* 2022)
EHD3	BRADI_3g13210v3	Os08g0105000	*EARLY HEADING DATE 3* downregulates the rice orthologue of *VRN2* (*GHD7*) under SDs; not characterised in Pooideae grasses	SD	×		×	(Matsubara *et al.* 2011)
ELF3	BRADI_2g14290v3	Os06g0142600 Os01g0566100	*EARLY FLOWERING 3* represses flowering under uninductive photoperiods (SDs) and mediates flowering under ambient temperatures in *Brachypodium distachyon*; interacts with PHYB in wheat and represses *PPD1*	SD	×		×	(Bouché *et al.* 2022, Alvarez *et al.* 2023)
FIE2	BRADI_2g07820v3 BRADI_3g14520v3 BRADI_3g17417v3 BRADI_3g14510v3	Os08g0137100 Os08g0137250	Polycomb group protein FERTILIZATION-INDEPENDENT ENDOSPERM 2; involved in endosperm formation and root development	SD				(Li *et al.* 2014)
FY	BRADI_2g60817v3	Os01g0951000	Part of the autonomous flowering pathway in rice; minor effect on flowering time in *Brachypodium distachyon*	SD	×			(Lu *et al.* 2006, Bettgenhaeuser *et al.* 2017)
IRL5	BRADI_3g33990v3	Os10g0572300	*INTRACELLULAR LEUCINE-RICH REPEAT 5*, expression induced by light in rice	SD			×	(You *et al.* 2010)
ISS1	BRADI_2g04860v3	Os01g0178000	INDOLE SEVERE SENSITIVE 1 aromatic aminotransferase; facilitates auxin and tryptophan homeostasis om *Arabidopsis thaliana*	SD			×	(Pieck *et al.* 2015)
JMJ706	BRADI_3g34240v3	Os10g0577600	Histone H3K9 demethylase involved in floral organogenesis in rice	LD	×			(Sun and Zhou 2008)
LHCA4	BRADI_3g36760v3 BRADI_4g30060v3	Os08g0435900	LIGHT-HARVESTING COMPLEX A4, subunit of light-harvesting peripheral antenna complex of photosystem I; cyclic expression in *Arabidopsis thaliana*	LD			×	(Harmer *et al.* 2000)
LHCB7	BRADI_4g27480v3	Os09g0296800	LIGHT-HARVESTING COMPLEX B7 subunit of light-harvesting peripheral antenna complex of photosystem II; cyclic expression in *Arabidopsis thaliana*	SD			×	(Harmer *et al.* 2000)
LIR1	BRADI_2g03610v3	Os01g0102900	*LIGHT-INDUCED, RICE 1* shows strong diurnal oscillations in rice and is induced by light; delays flowering under SDs after vernalisation in *Lolium perenne*, expressed in vegetative tissue in *L. perenne* (leaves), peaks before dusk and decreases during night	SD		×	×	(Reimmann and Dudler 1993, Ciannamea *et al.* 2007)
MADS3	BRADI_2g32910v3 BRADI_2g06330v3	Os05g0203800 Os01g0201700	*AGAMOUS*-like (*AG*-like) floral homeotic transcription factor with C-class function in carpel, stamen development; ROS homeostasis in anther development	SD	×			(Yamaguchi *et al.* 2006, Hu *et al.* 2011)
NUDX23	BRADI_4g37360v3	Os09g0553300	Flavin adenine dinucleotide (FAD) pyrophosphohydrolase involved in flavin homeostasis in *Arabidopsis thaliana*	SD			×	(Maruta *et al.* 2012)
OBGC1	BRADI_1g18570v3	Os07g0669200 Os07g0669250	Regulates DNA replication and ribosome biogenesis in chloroplasts	LD			×	(Chen *et al.* 2021)
RECQ	BRADI_1g17580v3 BRADI_4g03880v3	Os07g0681600	ATP-dependent DNA helicase involved in DNA repair and recombination	SD			×	(Hartung and Puchta 2006)
RTF1	BRADI_4g05840v3	Os12g0535900	Component of PAF1 elongation complex required for histone H2B ubiquitination	SD	×			(Stolinski *et al.* 1997, Ng *et al.* 2003)
SGS3	BRADI_4g40517v3 BRADI_4g05850v3	Os12g0197500	*SUPPRESSOR OF GENE SILENCING 3* involved in juvenile to adult phase change of vegetative development prior to flowering in *Arabidopsis thaliana*	SD			×	(Peragine *et al.* 2004)
UVR8	BRADI_1g15060v3	Os03g0599600	*ULTRAVIOLET RESISTANCE LOCUS 8*, involved in UV-B perception in *Brachypodium*; interacts with CONSTITUTIVELY PHOTOMORPHOGENIC 1 (COP1) in *Arabidopsis*	LD			×	(Favory *et al.* 2009, Chen *et al.* 2023)
VOZ1	BRADI_2g50070v3	Os01g0753000	VASCULAR PLANT ONE-ZINC FINGER 1 interacts physically with *Arabidopsis thaliana* CO together with CO in Arabidopsis where it promotes photoperiodic flowering; regulates drought-mediated flowering in tomato	SD			×	(Yasui *et al.* 2012, Yasui and Kohchi 2014, Kumar *et al.* 2018, Chong *et al.* 2022)
XCT	BRADI_4g36330v3	Os09g0535300	Coordinates circadian clock and light signalling pathways in *Arabidopsis*	SD		×		(Martin-Tryon and Harmer 2008)

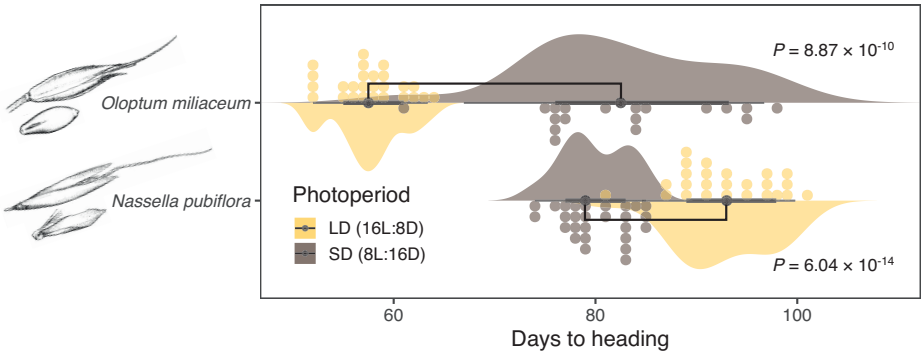

Figure 1: Flowering responses of two Stipeae grasses with opposite flowering phenotypes. Long day (LD) promotes rapid flowering in *Oloptum miliaceum* but has a negative effect on heading date in *Nassella pubiflora*. Conversely, emergence of inflorescences is promoted by short day (SD) in *N. pubiflora* but delayed in *O. miliaceum*. Coloured dots indicate heading individuals under each photoperiod. Black dot represents median heading date under each photoperiod, black bar indicates interquartile range, and black line indicates range between minimum and maximum. *P* values obtained with Student's *t*-test, two-tailed.

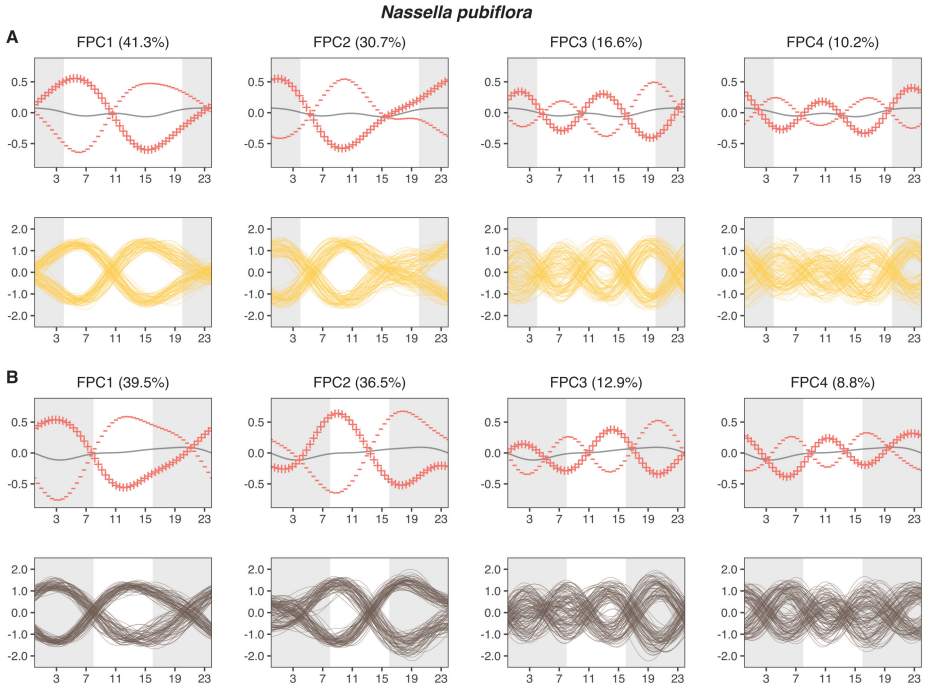

Figure 2: Temporal variation of the *Nassella pubiflora* transcriptomes under **A)** long days (LD, yellow lines) and **B)** short days (SD, grey lines) described by functional principal component analysis (FPCA). Upper panel visualises the effect of the standard deviations of the first four functional principal components visualised as perturbations from the mean (mean ± 1 SD). Lower panel shows expression profiles of transcripts with the 0.5% highest/lowest score on the corresponding FPC.

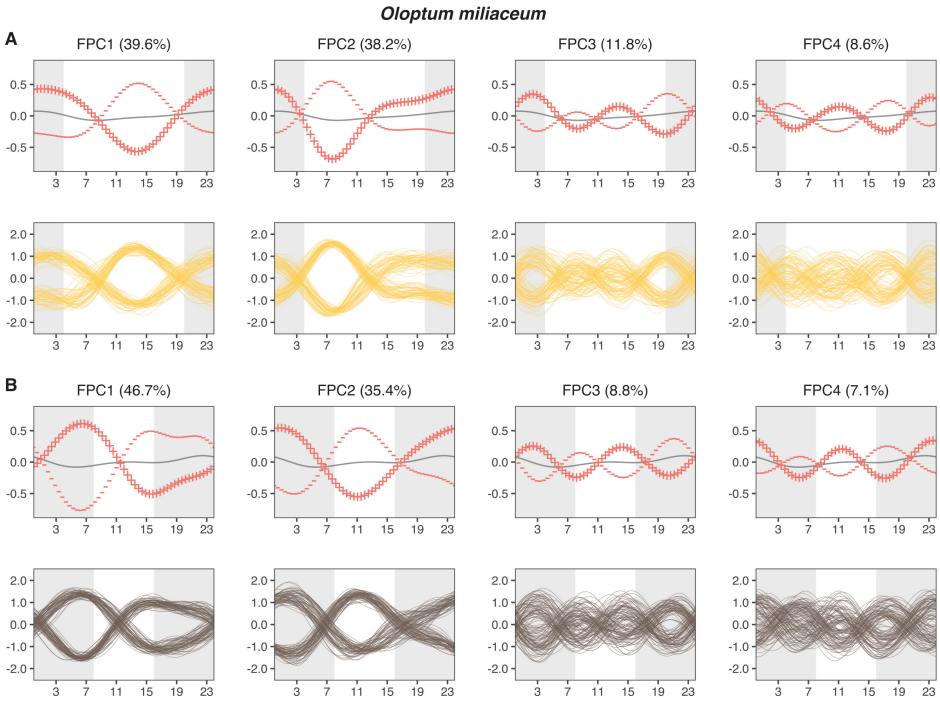

Figure 3: Temporal variation of the *Oloptum miliaceum* transcriptomes under **A)** long days (LD, yellow lines) and **B)** short days (SD, grey lines) described by functional principal components analysis (FPCA). Upper panel visualises the effect of the standard deviations of the first four functional principal components visualised as perturbations from the mean (mean ± 1 SD). Lower panel shows diurnal expression profiles of transcripts with the 0.5% highest/lowest score on the corresponding FPC.

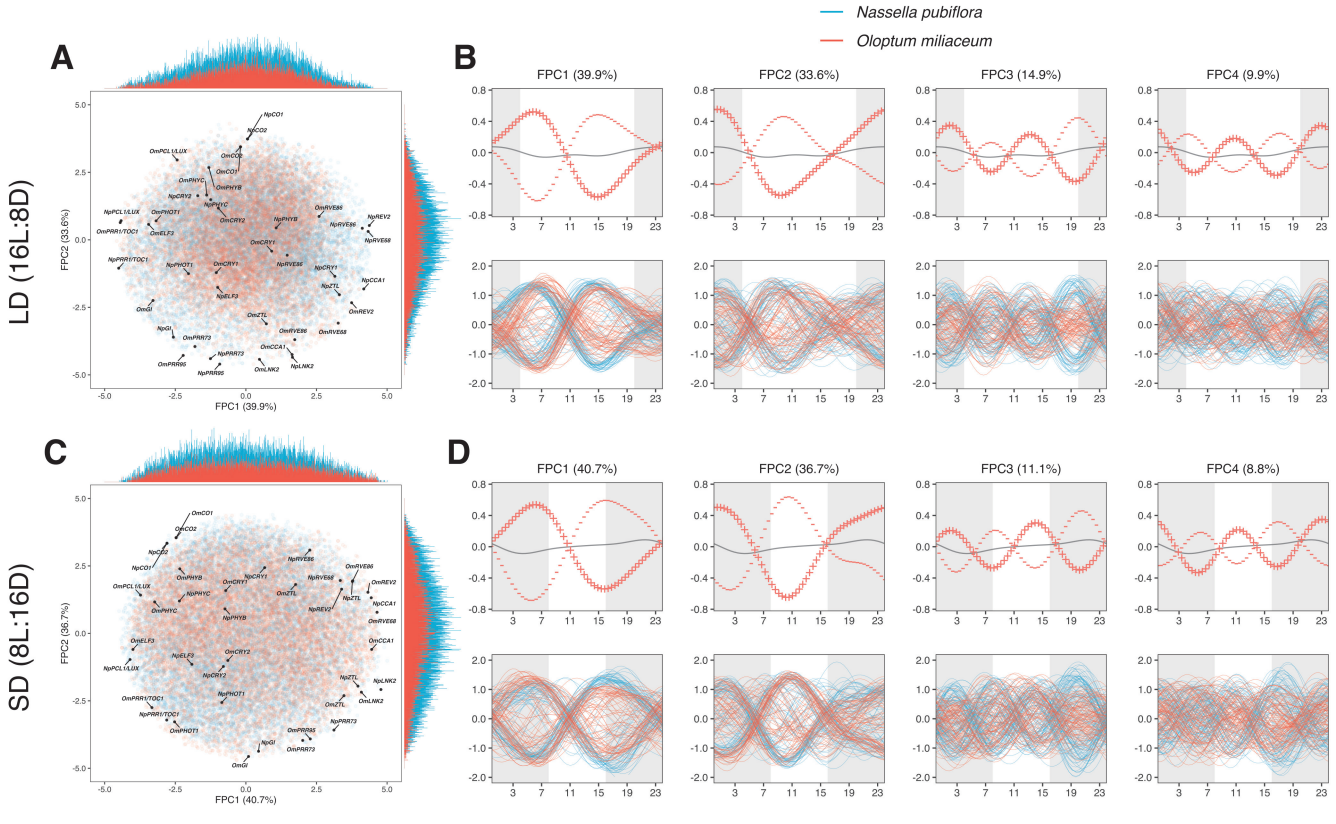

Figure 4: Main modes of variation in the scaled circadian transcriptomes of *Nassella pubiflora* (blue) and *Oloptum miliaceum* (red) identified by functional principal components analysis (FPCA). **A)** Scores plot of long day (LD) gene expression with placement of exemplary photoperiod and circadian clock genes. **B)** Effects of the first four FPC functions as deviations from the mean function (mean ± 1 SD) in LD (upper row) and profiles of transcripts represented in the top and bottom 0.5% scores on the respective FPC (lower panel). **C)** Scores plot of short day (SD) gene expression with placement of exemplary photoperiod and circadian clock genes. **D)** Effects of the first four FPCs as deviations from the mean function (mean ± 1 SD) in SD (upper row) and profiles of transcripts represented in the top and bottom 0.5% scores on the respective FPC (lower panel).

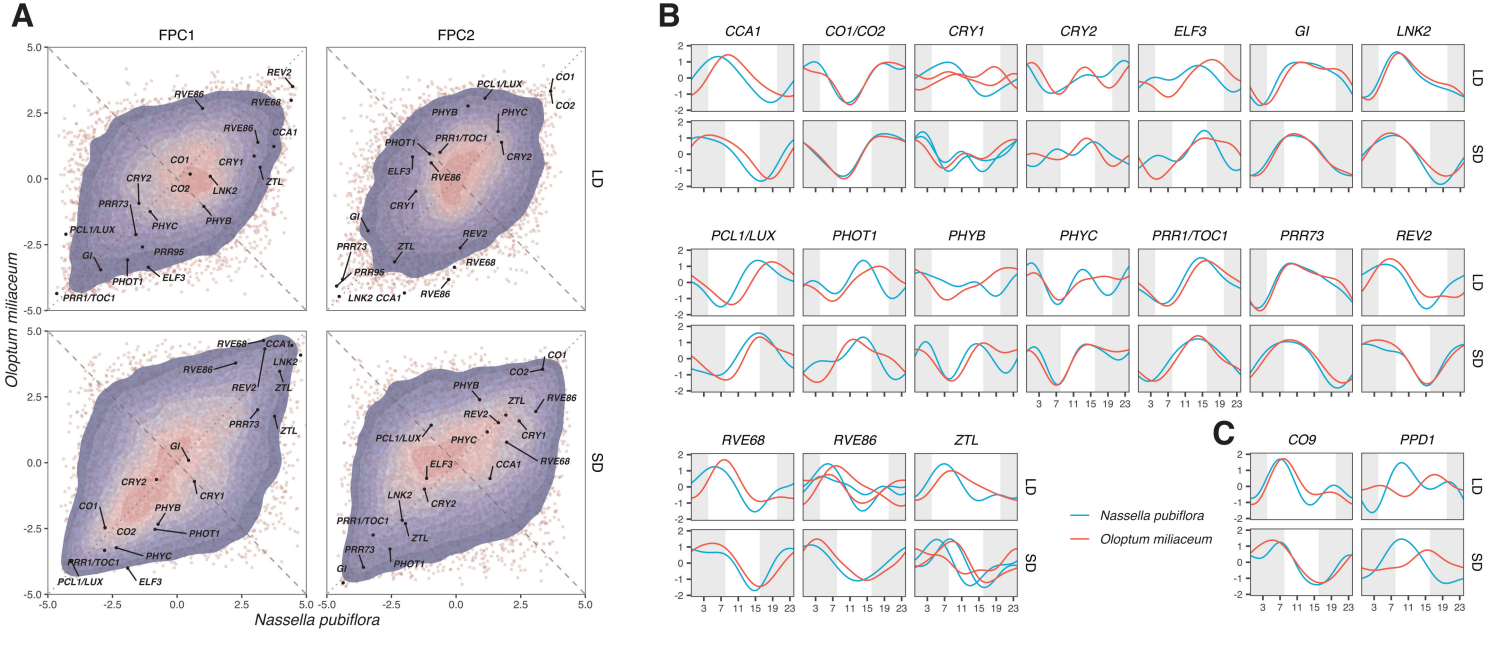

Figure 5: Functional principal component analysis (FPCA) is a useful tool for the detection of (differential) oscillatory gene expression. **A)** Similarity of global gene expression in the LD and SD transcriptomes of *Oloptum miliaceum* (LD plant) and *Nassella pubiflora* (SD plant). Position of core circadian clock and photoreceptor genes within the score distributions of the first two functional principal components (FPCs) in long day (LD) and short day (SD) with respect to the study species is highlighted. LD and SD expression is conserved across species when genes are located on the diagonal (dotted line). If gene regulation is different between *N. pubiflora* and *O. miliaceum*, genes are dispersed along the off-diagonal (dashed line). Purple area indicates density of FPC scores in 10% increments. For orthologue pairs with mismatching number of paralogues/transcripts, the lowest score is shown. **B)** Diurnal expression profiles of selected photoreceptor and circadian clock genes highlighted in **A)** under LD and SD in the two study species. **C)** Expression profiles of *CO9* and *PRR37* (*PPD1*) not included in the FPCAs. Grey areas indicate darkness.

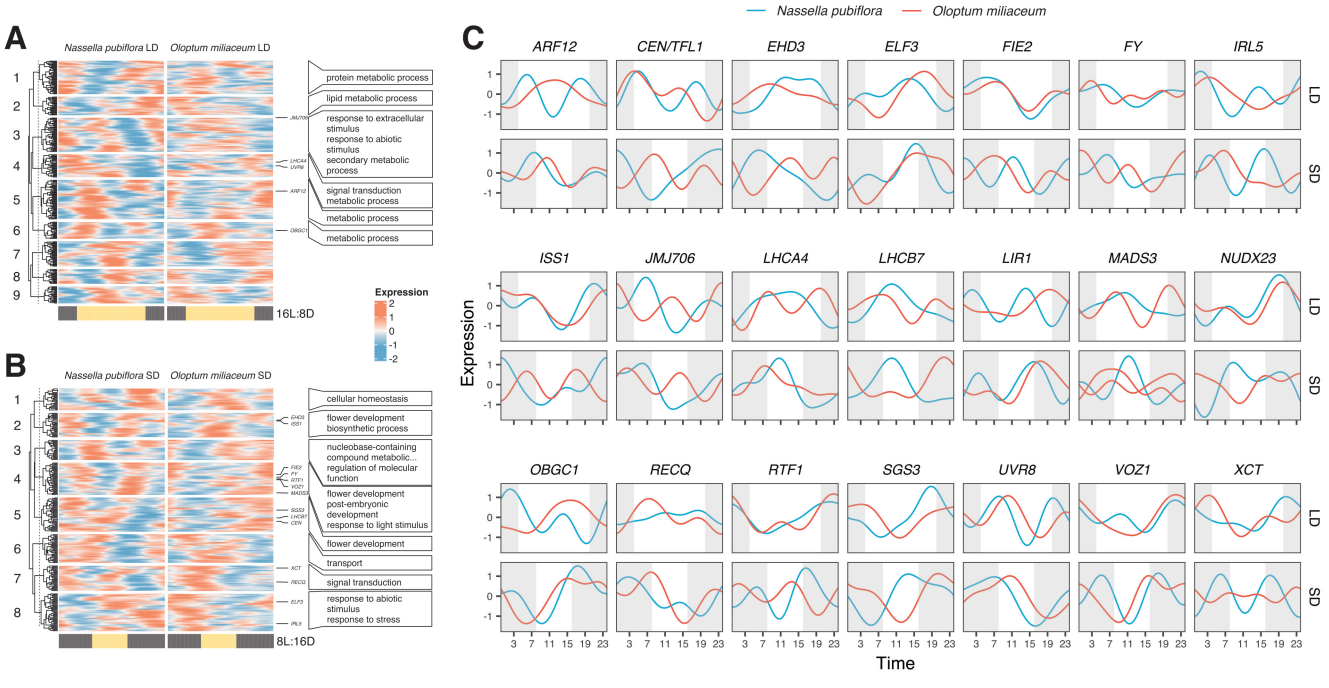

Figure 6: Significant enrichment of between biological processes and orthologous *Nassella pubiflora* and *Oloptum miliaceum* genes with divergent diurnal expression under **A)** short day (SD, n = 257) and **B)** long day (LD, n = 300). Expression profiles are clustered by expression dissimilarity (1 - ρ). Genes with divergent, daylength-specific diurnal expression between species annotated with 'flowering development' (GO:0009908), 'circadian rhythm' (GO:0007623), and 'response to light stimulus' (GO:0009416) are highlighted and their profiles visualised in **(C)**.

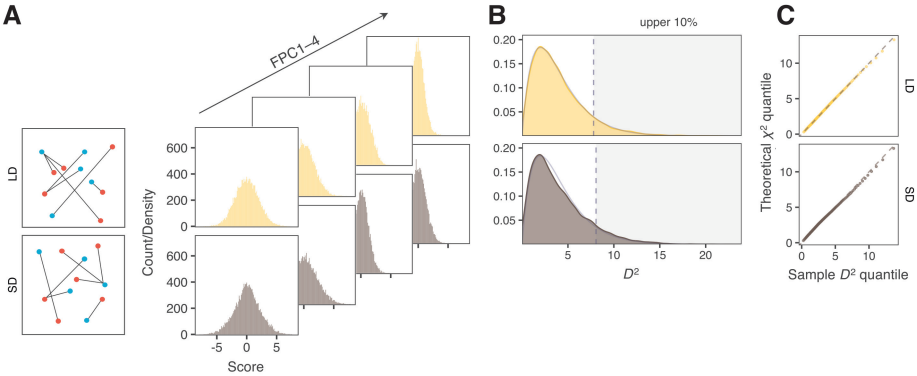

Supplementary Figure S1: Determination of expression dissimilarity and divergence using functional principal component (FPC) scores and squared Mahalanobis distance (D^2). **A)** Calculation of interspecific score differences on FPC axis 1–4. **B)** Approximation of pairwise D^2 between ortholog expression in long (LD, yellow) and short day (SD, grey). **C)** Quantile comparison of estimated D^2 values and a χ^2 distribution.

ISBN: 978-82-575-2093-9
ISSN: 1894-6402

Norwegian University
of Life Sciences

Postboks 5003
NO-1432 Ås, Norway
+47 67 23 00 00
www.nmbu.no

118428 / ANDVORDGRAFISK.NO